THE UNIVERSITY OF QUEENSLAND

AUSTRALIA

The Antitumor Activity of a Novel Diterpene Ester

Maria-Anna Marjorie Agnela D'Souza

Master of Science (MSc)

A thesis submitted for the degree of Doctor of Philosophy at

The University of Queensland in 2014

School of Medicine

Abstract

Previous work in this laboratory has shown that topical application of a protein kinase C (PKC) activator (the ingenol ester PEP005) cured subcutaneous tumors in mice with a favourable cosmetic outcome. Efficacy involved a neutrophil-dependent host inflammatory response; characteristic of diterpene esters that activate PKC. The aim of this study was to explore the antitumor efficacy and mechanism of action of EBC-46, a novel diterpene ester of the tigliane (phorbol) class, isolated by QBiotics Pty Ltd from a native rainforest plant in North Queensland, Australia, when given by intratumoral injection rather than by topical application.

Preliminary work with EBC-46 *in vivo* resulted in successful treatment of tumors via intratumoral injection, showing outcomes similar to topical application of PEP005. Intralesional therapy bypasses the barrier zone and establishes a sub-epidermal depot, and, depending on the mode of action, may minimize the circulating level of the drug.

EBC-46 activated protein kinase C (PKC), as shown by the translocation of PKC isoforms to the plasma membrane of HeLa. Here, PKC can phosphorylate other proteins involved in signal transduction of cellular activities such as growth, differentiation, migration, proliferation and inflammatory responses. TPA, a prototype PKC activator, was used for *in vitro* and *in vivo* experiments as a positive control. A single intratumoral injection of EBC-46 resulted in a local inflammatory response and ablation of tumors in human xenograft (melanoma, HNSCC) and mouse tumors (B16-F0, MC38) in immunocompromised (BALB/c *Foxn1*^{nu}) and immunocompetent (C57BL6/J) mice respectively. The cure rate was > 75% and there were no recurrences over a period of up to 12 months. Compared with the sub-microgram per ml IC_{50} levels of current anticancer drugs, the cytotoxic effect of EBC-46 was minimal in most tumor lines *in vitro*, requiring doses of 100-300 µg/ml to stop growth. IC_{50} levels in the region of 100 ng/ml however could be achieved in the same cell lines by over-expression of PKC-α and -δ. EBC-46 had minimal effect on the cell cycle, but caused phosphorylation of ERK 1/2.

It was inferred that the mechanism of action was co-dependent on the host response to the drug, thus further studies focused on the host.

Tumors exhibited an inflamed appearance within 1-2 hr of injection, changing to greenish black color by 24 hr, typical of a severe bruise. Indurations were formed at the now-flattened site, and

resolved over the next 2 weeks with sloughing of the scab, resulting in cure and excellent healing of the skin. A key finding in this project, emerging from the novel approach of *ex vivo* culture of treated tumor sites, was that no clonogenic tumor cells remained by 4 hr after injection of EBC-46; and significant loss of such cells even within 1 hr. This established a short time window for drug action and cell kill, and focused subsequent studies of mechanism.

Immunohistochemical analysis confirmed the clinical observations, revealing loss of capillaries and the endothelial cell marker PECAM, tumor cell necrosis, and presence of neutrophils. EBC-46 induced the production of the pro-inflammatory cytokines IL-1β, TNF-α and IL-8 in tumor cells, dependent on activation of PKC isoforms. Global gene expression of treated tumor sites showed rapidly changing profiles but no dominant cell signaling pathway, with no RNA recoverable after 8 hr. The target tumor cells, analyzed with human-specific chips, showed .>10-fold elevation of 3 *SNORD* RNA sequences at the early time points, non-coding RNA sequences involved in regulation of gene expression. The antitumor role of this striking finding, if any, is yet to be determined but may reflect a novel, possibly EBC-46-specific cellular response to hemorrhagic necrosis. Such changes were not found using TPA, and numerous other differences in gene expression caused by the two drugs *in vivo* were observed. The host response at tumor sites, analyzed with murine-specific chips, also showed no single significant signaling pathway but induction of some proinflammatory markers was found. A more controlled *in vitro* expression profiling of human lymphocytes also revealed induction of proinflammatory markers by EBC-46, some but not all of which were paralleled by release of cytokine proteins.

EBC-46 was therefore distinguished from most current anticancer agents by triggering a rapid and tumor-destructive host response at and around the tumor site, with no discernible adverse effects. Tumor ablation was associated with local inflammation, hemorrhagic necrosis, and cellular effects consistent with PKC activation in both tumor and host cells.

Intratumoral injection of EBC-46 has been successfully trialed by QBiotics in a range of cutaneous and subcutaneous tumors in more than 250 companion animals (dogs, cats and horses). The macroscopic changes at the tumor site were similar to those found in mouse tumors in this study. The evidence overall suggests that EBC-46 may find use as a palliative treatment, local disease control or adjuvant therapy preceding surgery or radiation. Ongoing advances in drug delivery and imaging technologies may facilitate intratumoral administration to less accessible sites.

Declaration by Author

This thesis is composed of my original work, and contains no material previously published or written by another person except where due reference has been made in the text. I have clearly stated the contribution by others to jointly-authored works that I have included in my thesis.

I have clearly stated the contribution of others to my thesis as a whole, including statistical assistance, survey design, data analysis, significant technical procedures, professional editorial advice, and any other original research work used or reported in my thesis. The content of my thesis is the result of work I have carried out since the commencement of my research higher degree candidature and does not include a substantial part of work that has been submitted to qualify for the award of any other degree or diploma in any university or other tertiary institution. I have clearly stated which parts of my thesis, if any, have been submitted to qualify for another award.

I acknowledge that an electronic copy of my thesis must be lodged with the University Library and, subject to the General Award Rules of The University of Queensland, immediately made available for research and study in accordance with the *Copyright Act 1968*.

I acknowledge that copyright of all material contained in my thesis resides with the copyright holder(s) of that material. Where appropriate I have obtained copyright permission from the copyright holder to reproduce material in this thesis.

Publications during candidature

Boyle, G.M*., **D'Souza, M.M.A*.,** Pierce, C.J., Adams, R.A., Cantor, A.S., Johns, J.P., Maslovskaya, L., Gordon, V.A., Reddell, P.W. and Parsons, P.G. (2014) "Intra-lesional injection of the novel PKC activator EBC-46 rapidly ablates tumors in mouse models." *PLoS One.* *DOI:10.1371/journal.pone.0108887*

**equal contribution*

Publications included in this thesis:

No publications.

Contributions by others to this thesis

Dr. Glen Boyle provided the melanoma cell lines over-expressing PKC isoforms –α and –δ and empty vector control *lacZ* used in *Chapters Three* and *Four* and gave guidance on microarray analysis in *Chapter Six*.

Carly Chapman transiently transfected HeLa cells with EGFP-tagged PKC isoforms for PKC isoforms translocation studies in *Chapter Three*.

Jenny Johns and Lidia Maslovskaya isolated and purified EBC-46 from the kernel of the Blushwood plant.

Statement of parts of the thesis submitted to qualify for the award of another degree

None

Acknowledgements

Over the period of my PhD research years, there have been several people who have immensely contributed to the completion of my thesis.

In the first place, I owe a debt of gratitude to my principle supervisor Professor Peter Parsons for his scholarly guidance, his diligent supervision and his constant support, without which this thesis would have not materialized.

My heartfelt thanks to my associate supervisor Dr. Glen Boyle who so generously beyond his call of duty provided me with his expertise, support, guidance and patiently answered every question I posed.

Both have been excellent supervisors. Thank you for your valuable time invested in me and the encouragement you have offered.

I am indebted to Clay Winterford, Rita Collins, Glynn Reese, Sang-Hee Park and Anthony Chan for processing the innumerable histological samples and the informative discussions on cells and stains. My profound thanks to Paula Hall and Dr. Viviana Lutzky for their help with FACS instrumentation and analysis.

To my colleagues in the Drug Discovery Group; Carly, Jenny, Lidia, Julie, Tim and Jacinta. A big thank you for making it possible for me to sail smoothly through these years. You indeed contributed in more than one way in lightening my research work.

Thank you Graeme (Walker) for continually stimulating my interest in this area of research during our conversations, for your advice and proof-reading documents.

My gratitude to Dr. Victoria Gordon and Dr. Paul Reddell at QBiotics for giving me the opportunity to work on EBC-46.

I would like to express my personal thanks to my friends and family without whom survival through the ups and downs of my research and the writing process would not have been possible. In particular, thanks to Jyothy (Jo), Ritu (Jaiswal), Herlina, Yenni (Pedra) and Shirley who have either proof-read, provided technical support, patiently given a listening ear to my presentation rehearsals or to my woes on doing a PhD. Thank you Jyothy once again for always being there, so supportive

and understanding. Lastly, my deep thanks to Mama, Papa and sis for your love and constant support and for patiently co-operating with me in so many ways even from miles away.

Keywords

melanoma, diterpene ester. ebc-46, tpa, intratumoral injection, protein kinase c, innate immune response.

Australian and New Zealand Standard Research Classifications (ANZSRC)

ANZSRC code: 111201, Cancer Cell Biology, 40%

ANZSRC code: 111205, Chemotherapy, 40%

ANZSRC code: 110709, Tumor Immunology, 20%

Fields of Research (FoR) Classification

FoR code: 1112, Oncology and Carcinogenesis, 80%

FoR code: 1107, Immunology, 20%

Table of Contents

List of Figures

Chapter One

Chapter Two

Chapter Three

Chapter Four

Chapter Six

Chapter Seven

List of Tables

Chapter One

Chapter Two

Chapter Five

Chapter Six

List of Abbreviations

µg	microgram
aPKC	atypical PKC
cPKC	classical PKC
DMSO	dimethyl sulfoxide
EBC-46	12-tigloyl/angeloyl-13(2-methylbutanoyl)-6,7-epoxy-4,5,9,12,13,20-hexahydroxy-1-tigliaen-3-one
ERK	extracelluar signal-regulated kinase
FBS/FCS	fetal bovine serum/fetal calf serum
h / hr	hour
H&E	hematoxylin and eosin stain
JAK/STAT	Janus kinase/Signal transducer and activator transcription
JNK/SAPK	Jun amino-terminal kinases/Stress-activated protei kinases
MAPK	mitogen-activated protein kinase
MPO	myeloperoxidase
nPKC	novel PKC
PEG	polyethylene glycol
Pen/Strep	Penicillin/Streptomycin
PG	propylene glycol
PH	pleckstrin homology
PKC	protein kinase C

PseudoS	autoinhibitory pseudosubstrate
RNA	ribonucleic acid
RPMI-1640	Roswell Park Memorial Institute-1640 medium
RTemp; RT	room temperature
TPA	12-O-tetradecanoylphorbol-13-acetate

Chapter One

General Introduction

1.1 PREFACE

Cancer is described as a class of diseases, where an abnormal growth of cells caused by multiple changes in gene expression or mutations lead to a dysregulated balance in cell proliferation and death. Such cells can ultimately invade locally and metastasize to distant sites in the body.

From a clinical point of view, cancer is a large group of complex diseases that vary in their age of onset, state of cellular differentiation, rate of growth, invasiveness, metastatic potential, diagnostic detectability, prognosis and treatment response. From a molecular and cell biological point of view, however, cancer may be a relatively small number of diseases caused by similar molecular defects in cell function resulting from common types of alterations to specific genes. Ultimately, cancer is a disease of abnormal gene expression. There are a number of mechanisms associated with alteration of gene expression; which may occur via a direct insult to DNA, such as gene mutation, translocation, amplification, deletion, loss of heterozygosity, or via a mechanism resulting from abnormal gene transcription or translation. The overall result is an imbalance in cell replication and cell death in tumor cell population that leads to an expansion of tumor tissue. In normal tissues, cell proliferation and cell loss are in a state of equilibrium.

In addition to mutations, epigenetic events such as abnormal DNA methylation can also lead to silencing of tumor suppressor genes or result in the activation of oncogenes, thus compromising the genetic balance and leading to malignant transformation.

Cancer is a leading cause of death in Australia with 1 in 3 Australians being affected in their lifetime. It is estimated that an approximate 120,710 new cases of cancer were diagnosed in 2012 with more than 43,000 cases resulting in mortality in spite of a 30% improvement in survival over the last two decades (AIHW, 2012). The National Health Priority Area cancers include prostate, lung, and colorectal cancers in males and breast, lung and colorectal in women; accounting for 59% of all cancers. The age group below 15 years is commonly affected by lymphoid, brain and central nervous system neoplasms, while melanoma and breast cancers are predominant in the 15 – 44 age groups.

1.1.1 Skin Cancer

The three most common forms of skin cancer are basal cell carcinoma (BCC), squamous cell carcinoma (SCC) and melanoma, each of which is named after the type of cell from which it originates. Melanoma is less common than basal and squamous cell carcinomas, however it is the most serious, being responsible for ~75% of all skin cancer – related deaths. The primary cause of skin cancers is over-exposure to UV-radiation via direct or indirect DNA damage. Smoking tobacco and related products (Morita, 2007, Tanaka *et al.*, 2007), genetic predisposition (Halpern and Altman, 1999) and human papilloma virus (HPV) (Pfister, 2003) are some of the factors that can increase the risk of skin cancer.

Basal cell carcinomas originate in the basal cell layer of the epidermis, where they begin as a papule and develop into a crater that erodes and bleeds. Metastasis is rare, but BCC cells can locally invade into adjacent tissues (Hauben *et al.*, 1982). A mutant of the human homologue of the *Drosophila* gene, *PTCH (PATCHED)*, has been identified in the development of basal cell carcinoma (Gailani *et al.*, 1996, Unden *et al.*, 1996).

Squamous cell carcinomas are the second most common form of non-melanoma skin cancer. They originate in the epidermis, squamous mucosa or areas of squamous metaplasia. Their clinical appearance is highly variable, where the tumor is often elevated, or may be ulcerated with irregular borders. Squamous cell carcinomas spread faster than BCCs, but are still relatively slow. Rarely, they can metastasize to other locations including internal organs (Alam and Ratner, 2001). Actinic keratosis is a precancerous lesion that can develop into a squamous cell carcinoma (Leffell, 2000). UV-induced mutations in *p53* have been observed in basal cell carcinomas, as well as squamous cell carcinomas (Brash *et al.*, 1991, Quinn *et al.*, 1994, Rady *et al.*, 1992). In addition, EGFR-1 and HER2 mutations have been detected in squamous cell carcinomas of the head and neck (Lee *et al.*, 2005, Willmore-Payne *et al.*, 2006).

Melanoma results from the uncontrolled proliferation of melanocytes giving rise to the formation of malignant melanoma. Melanoma may arise *de novo* or from a precursor lesion. Melanoma is less common than the other forms of skin cancer; however it is more often fatal, resulting in 75 – 80% mortality if it has progressed to stage II. The strongest risk factors for melanoma are exposure to UV-radiation, multiple nevi, a previous incidence of melanoma and a family history of the cancer

(Elder, 2006, Miller and Mihm, 2006). A number of genes have been identified in the development of the various types of melanoma, some of which are *BRAF*, *NRAS*, *c-kit*, *PTEN*, *CDKN2A* and *CDK4* (Herlyn, 2009, Miller and Mihm, 2006, Willmore-Payne *et al.*, 2005).

1.1.2 Breast Cancer

Breast cancers originate from breast tissue, most commonly from the inner lining of milk ducts or the lobules that supply the ducts with milk. Depending on their origin, breast cancer can be broadly classified into ductal carcinomas (originating from the ducts) and lobular carcinomas (originating from the lobules) (Perry and Phillips, 2002). Many breast cancers develop from a progression sequence that begins with an increase in the number of breast cancer precursor cells (known as hyperplasia) followed by the emergence of atypical breast cells (called atypical hyperplasia). This stage is followed by carcinoma *in situ*, a non-invasive cancer which may finally develop into an invasive cancer.

Mutations in either of two major susceptibility genes *BRCA1* (breast cancer susceptibility gene 1) and *BRCA2* (breast cancer susceptibility gene 2), confer a lifetime risk for breast cancer and ovarian cancer, respectively (Thompson *et al.*, 2002, The Breast Cancer Linkage Consortium, 1999).

1.1.3 Colon Cancer

Colon cancer, also called colorectal cancer, includes cancerous growths in the colon, rectum and appendix. It is the third most common cause of cancer – related deaths in the Western world. Colon cancers arise from epithelial cells lining the colon and rectum, which grow into an adenoma with high-grade dysplasia and then progress to invasive cancer (Kinzler and Vogelstein, 2002).

Colon cancer is associated with genetic alterations, environmental exposures including diet and inflammatory conditions of the digestive tract. At the cellular and molecular level, colorectal cancer begins with a mutation in the *Wnt* signaling pathway. When Wnt binds to a receptor, it activates a chain of molecular events that ends with β-catenin entering the nucleus and interacting with TCF/LEF family of transcription factors that are bound to DNA via a high mobility group domain. The early event of colon cancer is the result of a mutation of APC (adenomatous polyposis gene). The protein encoded by APC is important in the activation of an oncogene *c-myc* and cyclin D1 which initiates a malignant progression (Cancer Council NSW, 2007). Other changes featuring in

colon carcinogenesis include *KRAS* mutation, chromosomal abnormalities such as in chromosome 18 (loss of heterozygosity – LOH), chromosome 17p deletion and mutations in the *p53* tumor suppressor gene (Lea *et al.*, 2009, Vogelstein *et al.*, 1988).

1.1.4 Treatment Modalities

Treatment of cancer is dependent on the type, location of the cancer, age of the patient, and whether the cancer is a primary tumor or a recurrence. Surgery and radiation have been the most common modes for treatment of cancers, with the choice of technique being dictated by the size and location of the disease. Immunotherapy, or biological therapy, is a relatively new addition to the group of cancer treatments. Topical therapy might also be indicated for accessible tumors for a good cosmetic outcome.

Radiation is an adjuvant treatment, usually administered in association with other forms of cancer therapies. It is also used as a palliative treatment aiming for local disease control. Radiotherapy works by damaging DNA in cells which is triggered by radioisotopes. Unlike their healthy differentiated counterparts, cancer cells are generally undifferentiated and have diminished ability to repair damaged DNA (Camphausen and Lawrence, 2008). Oxygen acts as a potent radiosensitizer. One of the limitations of radiotherapy is that solid tumor cells become deficient in oxygen, and thus create a hypoxic environment. This makes solid tumor cells resistant to radiation damage compared to those in a normal oxygen environment.

Chemotherapy involves the use of toxic drugs to kill cancer cells. In a broad sense, chemotherapeutic drugs effectively target fast-dividing cells by impairing mitosis or other events associated with proliferation. Tumors with higher growth rates therefore tend to be more sensitive as a larger proportion of cells are undergoing cell division. On the other hand, tumors with a slower growth rate respond moderately (Skeel, 2003). Depending on the medications used, a range of side effects is observed such as depression of the immune system, fatigue, tendency to bleed easily, hair loss, erythema, and dry skin. More recently, targeted therapies such as B-raf inhibitors have induced spectacular remission in some melanoma patients (Flaherty *et al.*, 2010, Sosman *et al.*, 2012)but resistance eventually emerges.

Immunotherapy uses the body's immune system to fight cancer or to minimize the adverse effects that may be caused by chemotherapy or radiation. Biological response modifiers such as cytokines,

antibodies, growth factors, peptides, nucleic acids and dendritic cells are being used in the development of vaccines (Agarwala, 2010, Dunn *et al.*, 2004).

Although there have been vast improvements in the currently available techniques, there still are limitations with respect to safety, side effects and long-term efficacy. This suggests the need for new and improved treatments.

1.2 PROTEIN KINASE C

First identified in the late 1970s (Takai *et al.*, 1977), protein kinase C enzymes were described to be a product of limited proteolysis by a calcium-dependent protease (Inoue *et al.*, 1977). However shortly after, it was reported that PKC was activated by Ca^{2+} and phospholipids with no proteolysis (Takai *et al.*, 1979); and the significant activation of PKC by diacylglycerol was also independent of proteolysis (Kishimoto *et al.*, 1980). Protein Kinase C consists of a family of serine/threonine protein kinases that are physiologically activated by 1,2-diacylglycerol (DAG) and other lipids. When an external stimulus activates a G-protein coupled receptor (GPCR), it in turn stimulates a G-protein. The G-protein activates phospholipase C (PLC), which cleaves phosphoinositol-4,5-biphosphate (PIP_2) into 1,2-diacylglycerol and inositol-1,4,5-triphosphate (IP_3). The IP_3 interacts with a calcium-ion channel in the endoplasmic reticulum (ER), releasing Ca^{2+} into the cytoplasm. Increase of Ca^{2+} activates PKC by binding to the C2 domain of the PKC complex and translocates to the membrane, anchoring the PKC to DAG and phosphatidylserine (Newton, 1995, Newton, 1997). Importantly, phorbol esters were found to activate PKC directly in a manner analogous to diacylglycerol (Castagna *et al.*, 1982). From molecular cloning studies, a family of 12 distinct members of mammalian PKCs have been identified, not all of which are activated by DAG or phorbol esters (Nishizuka, 1995). They are subdivided based on their sequence similarities and their modes of activation. The 'conventional' PKCs (cPKC) which include α; β_1 and β_2 (alternative splice variants from the same gene); and γ, are activated by phosphatidylserine, diacylglycerol or phorbol esters and Ca^{2+} (Table 1.1). Members of the 'novel' PKC subfamily (nPKC), δ, ε, η, and θ, rely on DAG/phorbol esters for activation but are independent of calcium. Though structurally similar to conventional PKCs, the activation requirement of this subfamily may be explained by the

Table 1.1 Basic structures of members of the PKC family.

PKC subfamily	Isoforms	Domains present	Mode of activation
Conventional PKC	α	PseudoS – C1A-C1B – C2 – C3 – C4	DAG/phorbol esters + Ca^{2+} + PS
	β_1	PseudoS – C1A-C1B – C2 – C3 – C4	
	β_2	PseudoS – C1A-C1B – C2 – C3 – C4	
	γ	PseudoS – C1A-C1B – C2 – C3 – C4	
Novel PKC	δ	C2 – PseudoS – C1A-C1B – C3 – C4	DAG/Phorbol esters
	ε	C2 – PseudoS – C1A-C1B – C3 – C4	
	η	C2 – PseudoS – C1A-C1B – C3 – C4	
	θ	C2 – PseudoS – C1A-C1B – C3 – C4	
Atypical PKC	ι	PseudoS – C1 – C3 – C4	phospholipids
	ζ	PseudoS – C1 – C3 – C4	
	μ	PTD – PseudoS – C1 – PH – C3 – C4	DAG/Phorbol esters + phospholipids
	ν	PseudoS – C1 – PH – C3 – C4	

Abbreviations: PseudoS – pseudosubstrate; PH – pleckstrin homology, PTD – putative transmembrane domain.

difference in the peptide sequence (Sutton *et al.*, 1995). A third subfamily, termed 'atypical' PKC

(aPKC) and including *ι* (which is a homolog of the murine isotype *λ*) and *ζ*, are independent of activation by DAG/phorbol esters and calcium, but have been found to be activated by cis-unsaturated fatty acids. The distant relatives of this subfamily include PKC*μ*/PKD (the mouse homolog) and PKC- *v*, and are found to be activated by diacylglycerol or phorbol esters and L-α-phosphatidyl-D-myo-inositol-4,5-bisphosphate (Hayashi *et al.*, 1999, Johannes *et al.*, 1994, Valverde *et al.*, 1994). These kinases have common structural features which suggests that they belong to the same family (Hofmann, 2001).

1.2.1 Structure

The members of the PKC family are monomeric enzymes, with an N-terminal regulatory region (20 – 70 kDa) and a C-terminal catalytic region (~45 kDa); where each isozyme is a product of a separate gene, except for β_1 and β_2 which are splice variants of the same gene. Four conserved domains have been revealed by molecular cloning: C1 – C4 (Figure 1.1); with alternating variable regions V1 – V4. The regulatory region of PKCs comprises an autoinhibitory pseudosubstrate domain and a membrane-targeting motif, the C1 domain, which is present in duplicate in conventional and novel PKCs, and singly in the atypical PKCs. These are cysteine-rich motifs and are specific for the diacylglycerol/phorbol ester binding. The C2 domain, also grouped within the regulatory region, is present in conventional and novel protein kinase Cs; provides the binding site for the Ca^{2+}, and in some isozymes, for acidic lipids. In the catalytic region, the C3 and C4 domains (present in all PKC isoforms) form the ATP- and substrate-binding regions. The regulatory and catalytic regions are separated by a hinge region that becomes proteolytically unstable when the enzyme is bound to a membrane (Gomperts *et al.*, 2003, Newton, 1995).

The atypical protein kinase Cs differ considerably from the other classes, in that, the C1 domain contains only a single Cys-rich sequence and also the key residues that maintain the C2 fold, appear to be absent. More importantly, these isozymes cannot respond to phorbol esters either *in vivo* or *in vitro* (Nishizuka, 1995). Between the distant members of this subfamily – PKC-*μ* and PKC-*v*, there exists ~80% structural homology. A single Cys-rich sequence (C1 domain), catalytic region with the C3 and C4 domains and a pleckstrin homology between the C1 domain and catalytic region

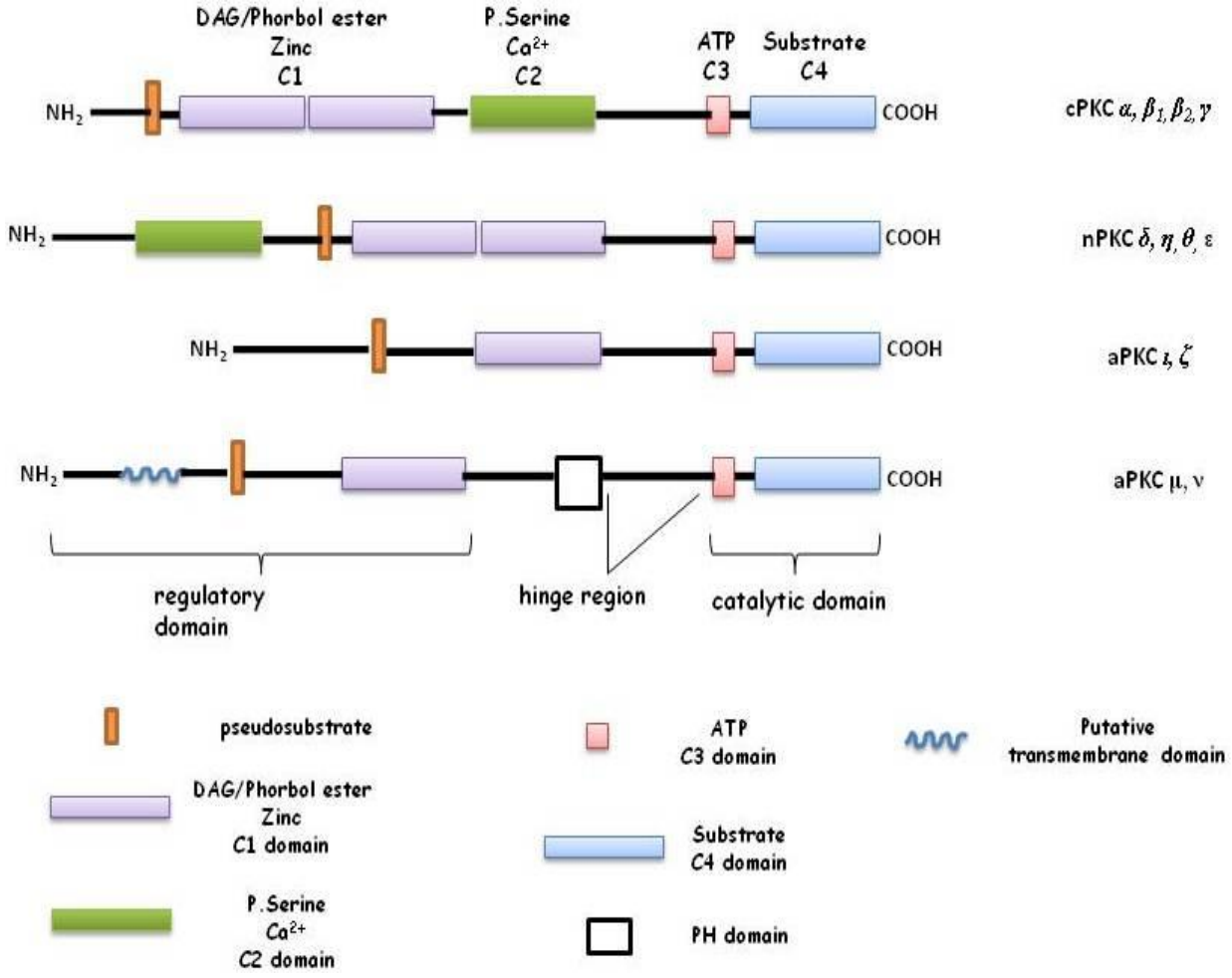

Figure 1.1 Schematic diagram of the primary structure of Protein Kinase C isozymes.

Protein kinase Cs comprise of four conserved domains have been revealed by molecular cloning: C1 – C4 with alternating variable regions V1 – V4. The regulatory region of PKCs consist of an autoinhibitory pseudosubstrate domain and a membrane-targeting motif, the C1 domain, which is present in duplicate in conventional and novel PKCs, and singly in the atypical PKCs. cPKC; conventional PKCs include α, β and γ. nPKC; novel PKCs include δ, ε, η and θ. aPKC; atypical PKCs include ι, ζ, μ and ν.(Gomperts et al., 2003, Hayashi et al., 1999, Johannes et al., 1994, Newton, 1995).

are found to be conserved among the two enzymes (Hayashi *et al.*, 1999, Johannes *et al.*, 1994). PKC-μ was also reported to harbour a putative transmembrane domain in the regulatory region which is absent in PKC-ν (Johannes *et al.*, 1994).

1.2.2 Regulation

Newly synthesized PKC is present in an inactive state in the cytosol, with the autoinhibitory pseudosubstrate domain bound to the catalytic domain (C4 domain). This conformation restricts the ability of the PKC to bind to substrates. The main regulatory inputs that control PKC activity are: 1) phosphorylation signals, 2) cofactor binding and 3) protein – protein interactions.

1.2.2.1 Regulation by Phosphorylation

Phosphorylation of Serine/Threonine and Tyrosine residues is essential for the maturation and activation of PKC. In the initial phosphorylation step, all PKC isozymes are *trans*-phosphorylated by phosphoinositol-dependent protein kinase – 1 (PDK-1) on the Ser/Thr and Tyr residues in the activation segment of the catalytic domain (Chou et al., 1998, Dutil et al., 1998, Krauss, 2003d, Le Good et al., 1998). As a consequence of PDK-catalyzed phosphorylation, auto-phosphorylation on two sites near the C-terminus is triggered (Figure 1.2). Overall, the *trans*- and *auto*-phosphorylation events are important for regulating the catalytic activity of PKCs and their subcellular distribution.

The two auto-phosphorylation events have been observed both *in vivo* and *in vitro* (Keranen *et al.*, 1995). The first phosphorylation is essential for membrane translocation of PKC to the plasma membrane. The second phosphorylation increases the thermal and proteolytic stability of PKC, thereby, increasing the enzymatic affinity towards cofactor binding, such as ATP, peptide substrate and Ca^{2+} (Edwards *et al.*, 1999, Edwards and Newton, 1997, Keranen *et al.*, 1995) (Table 1.2).

1.2.2.2 Regulation by Membrane Association

The first steps of signal transduction often take place in close association with the plasma membrane, before the signal is directed towards the cell interior. The cell mainly uses two mechanisms for transmission of signals at the cytosolic site of the membrane and the cell interior.

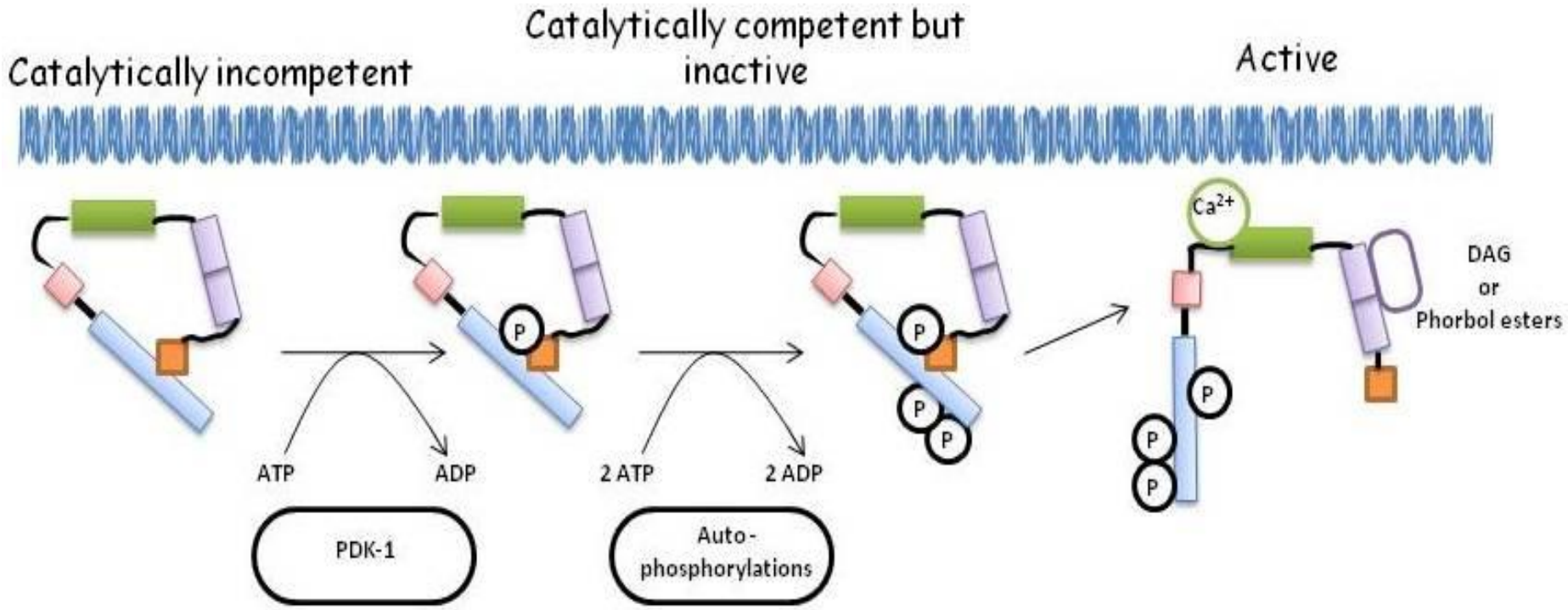

Figure 1.2 Regulation of Protein Kinase C

Regulation of protein kinase C involves three main regulatory steps 1) phosphorylation signals, 2) cofactor binding and 3) protein – protein interactions (Keranen *et al.*, 1995).

Table 1.2 Alignment of phosphorylation sites on members of the PKC family

Isoform	In activation loop		In C-terminus 1		In C-terminus 2	
hPKC-α	GVTTRTFCGTPDYIAPE	T497	RGQPVLTPPDQLVI	T638	QSDFEFGSYVNPQ	S657
hPKC-β_1	GVTTKTFCGTPDYIAPE	T500	RQPVELTPTDKLFI	T642	QNEFAGFSYTNPE	S661
hPKC-β_2	GVTTKTPCGTPDYIAPE	T500	RHPPVLTPPDQEVI	T641	QSEFEGFSFVNSE	S660
hPKC-γ	GTTTRTFCGTPDYIAPE	T514	RAAPAVTPPDRLVL	T655	QADFQGFTYVNPD	T674
hPKC-δ	ESRASTFCGTPDYIAPE	T507	NEKARLSYSDKNLI	S645	QSAFAGFSFVNPK	S664
hPKC-ι	GVTTTTFCGTPDYIAPE	T566	REEPVLTLVDEAIV	T710	QEEFKGFSYFGED	S729
hPKC-η	GVTTATFCGTPDYIAPE	T510	KEEPVLTPIDEGHL	T650	QDEFRNFSYVSPE	S672
hPKC-θ	DAKTNTFCGTPDYIAPE	T538	NEKPRLSPADRALI	S676	QNMFRNFSFMNPG	S695
hPKC-ζ	GDTTSTFCGTPNYIAPE	T410	SEPVQLTPDDEDAI	T552	QSEFEGFEYINPL	E579
hPKC-λ	GDTTSTFCGTPNYIAPE	T411	NEPVQLTPDDDDIV	T563	QSEFEGFEYINPL	E582
hPKC-μ	KSFRRSVVGTPAYLAPE	S742	Absent		Absent	

The first phosphorylation occurs in the activation loop near the APE sequence (targets indicated in red). This is brought about by phosphoinositide-dependent protein kinase-1 (PDK-1). The subsequent autophosphorylations targets at the C-terminus of the catalytic domain are indicated in yellow and green respectively. Adapted from Toker, A. (Toker, 1998).

Signals may be transmitted with the help of low-molecular-weight messenger substances known as "*second messengers*" (Newton, 1993). The intracellular messenger substances are products of specific enzyme reactions. They are *diffusible signal molecules* and reach their target mostly by diffusion.

The second messengers can be differentiated into:

Hydrophilic messengers with good aqueous solubility and are localized in the cytosol, such as inositol phosphates and Ca^{2+}.

Hydrophobic messengers such as diacylglycerol and the phosphatidyl inositol derivatives which are membrane localized. They reach their targets by diffusing through the plasma membrane and regulate their activity.

These cofactors are products of enzyme reactions, namely, G-protein-dependent pathways and Receptor Tyrosine Kinase pathways. Upon binding with Ca^{2+}, there is an increase in membrane association and activation by the release of the autoinhibitory pseudosubstrate from the catalytic domain of the protein kinase C. Further activation takes place by the binding of DAG to the C1 domain, which directly favors membrane association and enhances binding of PS to the C2 domain (Griner and Kazanietz, 2007, Newton, 1995, Newton, 1997).

Multiple Sources of DAG

Considering the requirement for DAG, the regulation of PKC is linked to PLC (Berridge and Irvine, 1984). The hydrophobicity and small size of DAG, enables it to diffuse laterally in membranes. It is also short-lived as it is either broken down by DAG lipase or converted to phosphatidate by the action of DAG kinase. Virtually all ligands, growth factors, hormones or neurotransmitters promote the production of DAG (and IP_3), which means PKC is implicated in a large number of cellular responses.

Several other lipid second messengers and mediators either potentiate the effect of DAG and Ca^{2+} or directly activate PKC. 3-phosphorylated inositol lipids $PI(3,4)P_2$, and products of the phosphoinositide-3-kinases $PI(3,4,5)P_3$; activate both the novel (δ, ε and θ) and atypical (ζ) PKCs in a phosphatidylserine environment (Toker *et al.*, 1994). Unsaturated fatty acids, particularly arachidonic acid, lysophosphatidic acid (LPA) and lyso-phosphatidylcholine (lysoPC), can enhance

the activity of PKC (Sando and Chertihin, 1996). Breakdown products of sphingolipids, such a sphingosine and lysosphingolipids, inhibit the conventional PKCs most likely by masking their interaction with phosphatidylserine (Hannun and Bell, 1989).

1.2.2.3 Regulation by Localization and Protein-Protein Interaction

A major regulatory aspect of protein kinase C is the localization of the enzymes to distinct subcellular compartments mediated by protein-protein interactions (Jaken, 1996). PKC enzymes have been found to interact with a range of proteins of diverse functions such as scaffolding, adaptor or membrane-targeting, inhibitory functions and also substrate proteins. Examples of membrane-targeting proteins are the receptors for activated C kinase, the RACK proteins; a group of proteins that bind to the active conformation of PKC and anchor them to the membrane, providing access to membrane-localized substrates (Mochly-Rosen, 1995). Members of the A kinase-anchoring protein, AKAPs, have also been identified as binding partners of PKC enzymes that assemble PKC into protein signaling complexes, keeping it in an inactive state. Upon receipt of Ca^{2+}/DAG signals, PKC is released from this inhibitory state (Klauck *et al.*, 1996).

The regulation of PKC by phorbols and DAG occur by the same mechanism; with some differences is the strength of the reaction. Upon activation, PKC isoforms translocate to the particulate fraction where they interact with the substrates, such as the mitogen activated protein kinase (MAP kinase); after which they are proteolytically degraded. TPA can both activate PKC and after longer incubation, down-regulate the enzyme (Silinsky and Searl, 2003), via the ubiquitin – proteosome pathway (Hofmann, 2001, Lu *et al.*, 1998). Diacylglycerol, the physiological activator of PKC, also demonstrated the degradation of PKC, thus suggesting that ubiquitination is a physiological response to PKC activation (Lu *et al.*, 1998).

1.3 PROTEIN KINASE C ACTIVATION BY PHORBOL ESTERS

The protein kinase C family of phospholipid-dependent protein kinases plays a key role in signal transduction. The PKC isozymes are activated by diacylglycerol, one of the products of the receptor-mediated hydrolysis of inositol phospholipids, and also by certain drugs, such as phorbol esters. PKC activators have been previously studied as chemotherapeutic agents (Section 1.3.1).

It has been suggested that the cysteine-rich regions in PKC are essential for phorbol ester binding (Ono *et al.*, 1989). The PKC activators form hydrogen-bonds with main-chain groups forming a hydrophobic surface over one-third of the C1 domain, thereby stabilizing the membrane-inserted state of the PKC (Zhang *et al.*, 1995).

1.3.1 Phorbol Esters

Phorbol esters are naturally occurring compounds and are found to mimic the action of diacylglycerol in the activation of PKC, which regulates different signal transduction pathways and other cellular metabolic activities. Their structure is dependent on the tetracyclic diterpene carbon skeleton known as *tigliane* (Figure 1.3). A tigliane contains four rings; A, B, C and D. Hydroxylation of this basic structure at different positions followed by ester bonding to various acid moieties results in the formation of a number of different phorbol ester compounds. The widely active phorbol 12-O-tetradecanoylphorbol-13-acetate (TPA) is accepted as the prototype of phorbol ester (Figure 1.3). It is obtained from the latex of *Croton tiglium*, a leafy shrub member of the *Euphorbia* family that is native to Southeastern Asia (Goel *et al.*, 2007).

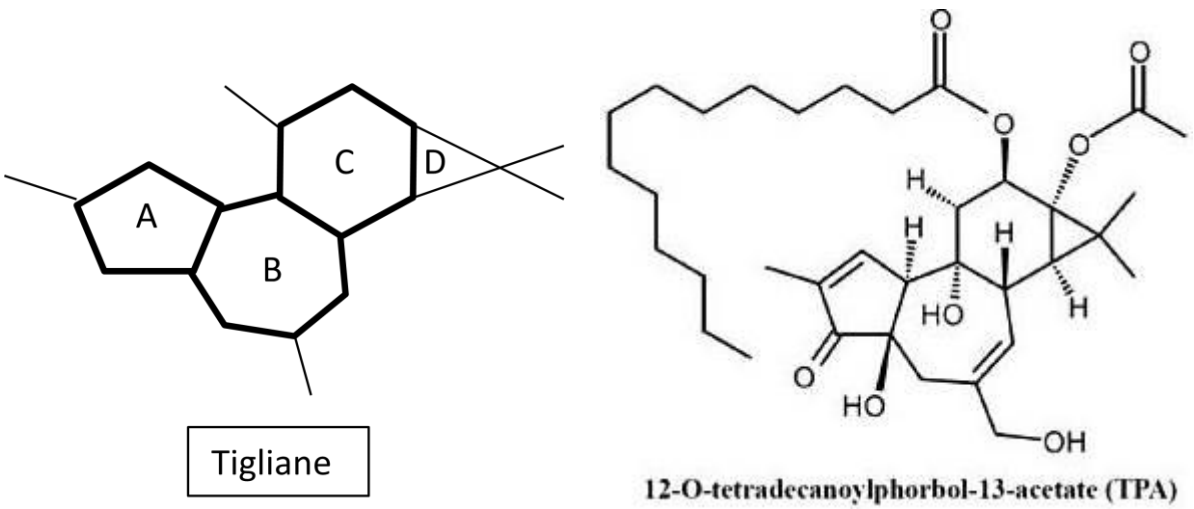

Figure 1.3 Structure of Phorbol Ester 12-O-tetradecanoyl-13-acetate (TPA) (Evans, 1986, Goel *et al.*, 2007, Zucker *et al.*, 1974)

Phorbol esters are amphiphillic molecules and tend to bind to phospholipid membrane receptors. The phorbol acts as an analogue for DAG (Castagna *et al.*, 1982); though, unlike DAG, phorbol esters are not readily metabolized (Asaoka *et al.*, 1992, Nishizuka, 1992, Nishizuka, 1995).

Though graded as a tumor-promoter in carcinogenic experiments performed on normal mouse skin and xenograft human foreskins (Yuspa *et al.*, 1979), TPA has also been established to induce cytostatic, cytotoxic and differentiation end points in cancer cells (Hofmann, 2001).

Studies of TPA as a therapeutic agent indicated an effect upon systemic administration in myelocytic leukaemia patients; though there was a decrease in myeloblasts in bone marrow and peripheral blood as well as temporary remissions (Han *et al.*, 1998 (i)). It was also observed that TPA induced an increase in depressed white blood cell counts and neutrophils towards the normal range, when administered to patients treated with cytotoxic cancer chemotherapeutic drugs (Han *et al.*, 1998 (ii)). These findings broaden the therapeutic potential of phorbol esters towards treatment of solid tumors.

The compound PEP005 (ingenol-3-angelate) is a novel anticancer drug (Kedei *et al.*, 2004) that is an activator of protein kinase C. Topical application of a high-dose of the diterpene ester, has been shown to cure ~80% of subcutaneous tumors in mice. *In vitro*, PEP005 was found to be highly toxic to cells when treated with high concentrations (Ogbourne *et al.*, 2004). Treatment of melanoma cell lines with TPA or PEP005 indicated irreversible growth arrest, with no adverse effects observed in normal melanocytes and normal fibroblasts (Cozzi *et al.*, 2006). Phase IIa trials of topically applied PEP005, indicated that it was safe and efficient in treating basal cell carcinomas and the squamous cell carcinoma precursor, actinic keratosis (AK) (Siller *et al.*, 2009, Siller *et al.*, 2010). Phase III trials of PEP005 in a gel formulation successfully reached a primary clinical endpoint of complete clearance of actinic keratosis in non-head locations (www.leo-pharma.com, 2010).

1.4 PROTEIN KINASE C AND SIGNAL TRANSDUCTION

Protein kinase C is an enzyme activated by diacylglycerol or phorbol esters and relays information via a variety of extracellular signals across the cell membrane to regulate many intracellular

processes. PKCs have been largely implicated in the regulation of gene expression with its ability to translocate and enter the cell nucleus (Nishizuka, 1992, Nishizuka, 1989, Nishizuka, 1984).

Phosphorylation by protein kinases to side chains of either serine or threonine specific protein substrates inside cells, can control their interaction with other proteins and molecules, their enzymatic activity and their predisposition to degradation by proteases. The family of mitogen-activated protein kinases is an example of such protein kinases. Phosphorylation of substrate proteins by mitogens functions as a switch to turn on or off the activity of the protein. Substrate proteins include other protein kinases, phospholipases, transcription factors and cytoskeletal proteins (Johnson and Lapadat, 2002). Protein Kinase C is known to phosphorylate members of the mitogen – activated protein kinase pathways (MAPK) (Section 1.4.1).

1.4.1 MAPK Pathways:

In general, an intracellular signaling pathway involves an extracellular signal that activates a transmembrane receptor. This activation transmits signals to downstream effector molecules via a sequential cascade. Among such pathways are the highly conserved mitogen-activated protein kinase (MAPK) modules and are found in all eukaryotic organisms. The mitogenic activated protein kinase pathways are organized in modules containing a core of three protein kinases. A multitude of signals have been found to activate MAPK modules. Initially, the activation of Raf kinase the by Ras family were discovered as the entry point into the MAPK signaling cascade. Later on it was established that the signal – transducing function of a MAPK pathway is determined by the nature of the MAPK module involved, this in turn depends on the properties of the protein kinases it contains, which differ in regulation and substrate specificity. Furthermore, the modules can share a common protein kinase but regulate different biological processes. The signal is passed on by the terminal member in the phosphorylation cascade in the form of phosphorylated substrate proteins. In many cases, this process is linked to translocation of the protein kinase into the nucleus, where nuclear localized substrates, particularly transcription factors, are phosphorylated. The various modules are not strictly independent; rather they mutually influence each other (Krauss, 2003a).

One of the first and best characterized MAPK pathways consists of Raf isoforms that activate two MEKs; MEK1 and MEK2, which in turn activate protein kinases known as ERK1 and ERK2. This pathway is known as the *ERK pathway* and is linked to cell proliferation and survival. Two other

mammalian pathways that stand out are the *c-Jun amino-terminal kinase/stress-activated protein kinase (JNK/SAPK)* and *p38* pathways, which mediate responses to cellular stress, such as cell-cell interaction, U.V. radiation and heat-stress and are associated with apoptosis (Figure 1.4).

Components of the MAPK pathways:

MAPK pathways comprise of a core module of three protein kinases that are organized as functional units with the aid of scaffolding proteins. The MAPK proteins are at the lower end of the signal transduction within a MAPK module and are generally preceded by two other protein kinases; MAPK kinase (MAP2K or MAPKK) and MAPK kinase kinase (MAP3K or MAPKKK). Generally, the ERK pathway starting from Ras protein activation is used to represent other MAPK pathways with similar structure.

1.4.1.1 Small molecular weight GTPases:

Small molecular weight GTP binding proteins (GTPases) comprise a superfamily of regulatory proteins that control a diverse array of intracellular signaling pathways. Diverse external stimuli activate the MAPK pathways via interactions with small molecular weight GTPases such as the Rho family proteins, Ras, ARF. Rac and CDC42 are members of the Rho family and are found to couple different stimuli and receptors to intracellular signaling pathways, such as the JNK/SAPK pathway (Price and Collard, 2001, Takai *et al.*, 2001). They have been known to regulate the organization of the actin cytoskeleton where Rac regulates lamellipodia and CDC42 regulates the filopodia in cells. Activation of the signaling pathway involves a guanine nucleotide exchange in Rac or CDC42 where the GTPases function as molecular switches that cycle between a GDP bound inactive state and a GTP bound active state. This cycle is controlled by GTPase Activating Proteins (GAPs) (Scheffzek *et al.*, 1997), which stimulate the slow intrinsic rate of GTP hydrolysis and Guanine Nucleotide Exchange Factors (GEFs), which promote dissociation of GDP and loading of GTP. The GTP-bound Rac or CDC42 bind and stimulate p21 – activated kinases (PAKs) which are the mammalian homologs of Ste20p (Price and Collard, 2001, Reuther and Der, 2000).

1.4.1.2` MAP3Ks, MEKKs (MAPK/ERK kinase kinase):

MAP3Ks (MEKKs) are Ser/Thr-specific protein kinases and are the entry point for signal transduction in a MAPK module. The best characterized representative is the Raf-1 kinase which is

activated by the Ras protein in its GTP-bound form. Other representatives include the Mos kinase and the MEKK1 protein. Signaling proteins that deliver signals to the MAP3Ks comprise mostly small GTPases like members of the Ras and Rho/Rac family. Raf proteins and Mos are perhaps the only MEKKs, which phosphorylate MEKs in a single cascading event. Four mammalian MEKKs have been identified: MEKK1 (Lange-Carter *et al.*, 1993, Xu *et al.*, 1996), MEKK2 and 3 (Blank *et al.*, 1996) and the two splice variants of MEKK4, namely MEKK4α and MEKK4β (Gerwins *et al.*, 1997). MEKK2 and 3 are closely related, sharing a 94% homology in the catalytic region and 65% homology in their N-terminal regions. MEKK1 and 4 both contain a proline-rich sequence that is involved in binding of proteins containing Src-homology 3 (SH3) domains, suggesting a specific regulatory function of these sequences (Gerwins *et al.*, 1997, Xu *et al.*, 1996). The presence of a PH (pleckstrin homology) domain in MEKK1 may partly account for its interaction with membranes of the cell (Xu *et al.*, 1996) and in MEKK4 it may be responsible for the co-localization with Golgi-associated vesicles (Gerwins *et al.*, 1997). Pleckstrin homology domains have been shown to mediate localization of proteins to the plasma membrane (Pawson, 1995). MEKK1 contains a Ras-binding site close to the catalytic region (Russell *et al.*, 1995) while MEKK4 has a cdc42/Rac binding site at a similar position (Gerwins *et al.*, 1997). MEKK2 and 3 have been shown to lack definable domains and are found in the cytoplasm (Hagemann and Blank, 2001). The differential subcellular localization of the MEKK family members, with their potentially divergent interaction motifs, suggests that MEKKs are regulated by distinct extracellular stimuli and intracellular pathways and also implies that they have different functions. MEKK1 preferentially activates JNK/SAPK pathway in transfected cells (Minden *et al.*, 1994, Thorburn *et al.*, 1997, Xu *et al.*, 1996), however, in reconstituted cells, it activates both ERK and JNK/SAPK pathways (Khokhlatchev *et al.*, 1997). MEKK2 and 3 are also both able to activate JNK/SAPK and ERK pathways; however, MEKK2 preferentially activates JNK/SAPK while MEKK3 shows an inclination towards the ERK pathway (Blank *et al.*, 1996). In the ERK pathway, MEKKs appear to phosphorylate only two MEKs; MEK1 and MEK2, thereby placing them exclusively in the MAP/ERK pathway. Activation of MAP3Ks is a complex process requiring the steps of membrane translocation, phosphorylation, oligomerization, and binding to scaffold proteins (Robinson and Cobb, 1997).

Raf proteins: The Raf family of protein kinases was the first known MEKKs and is composed of A-Raf, B-Raf and Raf-1 (or C-Raf). Raf-1 is ubiquitous, while highest expression of A-Raf occurs

in urogenital tissue. B-Raf appears to function primarily in neuronal tissue and testis. Regulation of Raf-1 is complex, involving protein-protein interactions, phosphorylation of serine, threonine and tyrosine residues, and cellular localization (Hagemann and Rapp, 1999, Morrison and Cutler, 1997). There are significant differences in the regulation of Raf isoforms. One notable difference between Raf-1 and B-Raf is the differential regulation by small G-proteins Ras and Rap1a (Erhardt *et al.*, 1995, Seidel *et al.*, 1999, Vossler *et al.*, 1997, Zwartkruis *et al.*, 1998). Raf-1 is activated by H-, K- and N-Ras proteins while B-Raf is activated both by Ras and Rap (Vossler *et al.*, 1997, Zwartkruis *et al.*, 1998). Phosphorylation of Raf-1 is influenced by a number of factors including Src (tyrosine protein kinases), p21-activated protein kinase (PAK), Akt (also called protein kinase B) and most importantly for the current study protein kinase C (PKC) family members (Diaz *et al.*, 1997, Fabian *et al.*, 1993, Morrison *et al.*, 1993).

1.4.1.3 MAP2Ks:

The MAP2K proteins are a special class of proteins as they have a dual specificity characteristic with respect to the nature of the amino acid at the phosphorylation site on the target substrate protein. The *dual specificity kinase* (DSK) that phosphorylates ERK is known as MEK. Thus, MEK1/2 phosphorylates ERK1/2 respectively (Ahn *et al.*, 1991, Crews *et al.*, 1992, Zheng and Guan, 1993). In addition to MEK1/2, there are five other dual specific kinases involved in MAPK modules. MEK3 and 6 phosphorylate and activate the p38/MAPK pathway (Derijard *et al.*, 1995, Han *et al.*, 1996, Moriguchi *et al.*, 1996, Raingeaud *et al.*, 1996). MEK4 and 7 are involved in the phosphorylation of the JNK protein kinases (Derijard *et al.*, 1995, Moriguchi *et al.*, 1997, Tournier *et al.*, 1997, Yao *et al.*, 1997). A less well – characterized MAPK pathway; the ERK5 pathway is activated by MEK5 protein kinase (Zhou *et al.*, 1995). The structural and functional relationships of these kinases have been studied and explained using MEK1/2 as prototypic kinases. MEKs activate the MAPK/ERK proteins by phosphorylation at a Tyr and a Ser/Thr residue in the T-X-Y sequence where 'X' can be Glu, Pro or Gly (Marshall, 1995). Due to this property, the MEKs differ significantly from other protein kinases which are either Tyr or Ser/Thr – specific (Lindberg *et al.*, 1992).

MEK1/2: MEK1 and 2 are 43 – 46 kDa proteins that contain proline – rich sequences in their carboxy – and amino – terminal domains. A deletion of this insert impairs its activation by Raf – 1 (Catling *et al.*, 1995) which is one of the principal upstream kinases that is involved in the

activation of MEKs (Howe *et al.*, 1992, Kyriakis *et al.*, 1992). However, it is worth noting that MEK1/2 can be activated independent of the Ras – Raf pathway where phosphorylation can be achieved by other dual specificity kinases such as cMos (Nebreda *et al.*, 1993, Shibuya and Ruderman, 1993).

MEK3: MEK3 activates p38MAPK through phosphorylation of Thr-180 and Tyr-182 in the TXY motif (Derijard *et al.*, 1995, Raingeaud *et al.*, 1996). Activation of the p38MAPK pathway, leads to the activation of different kinases such as MAPKAP-2 (Rouse *et al.*, 1994, Stokoe *et al.*, 1992) and MAPKAP-3 (Ludwig *et al.*, 1996). Phosphorylated p38MAPK translocates to the nucleus and phosphorylates transcription factors such as ATF2 (Raingeaud *et al.*, 1995), MEF2C (Han *et al.*, 1997) and CREB (Tan *et al.*, 1996).

MEK4: JNK1 (Jun N-terminal kinase-1) was identified as the kinase that phosphorylates transcription factors such as c-Jun at Ser-63 and Ser-73 residues (Derijard *et al.*, 1994), ATF2 (Gupta *et al.*, 1995) and Elk1 (Whitmarsh *et al.*, 1995). Activation of this kinase requires a dual phosphorylation at Thr-183 and Tyr-185 by a dual specificity kinase MEK4 (Derijard *et al.*, 1995).

MEK5: MEK5, the last of the dual specificity kinases to be characterized, is found to regulate a novel downstream enzyme termed as ERK5 (Zhou *et al.*, 1995). Structural analysis of MEK5 suggests a critical role in cytoskeletal organization of the cell. It shares an overall structural similarity with MEKs-1, 2, 3 and 4, with a Raf-1 phosphorylation site similar to MEK1 and the absence of a proline-rich sequence resembling MEK3 and MEK4 (Zhou *et al.*, 1995). There are two distinct alternatively spliced isoforms of MEK5 – MEK5α and MEK5β (English *et al.*, 1995). Activation of the ERK5 pathway by MEK5 leads to phosphorylation of MEF2C transcription factor, belonging to the myocyte enhancer factor – 2 (MEF2) family that have been indicated the expression of several immediate early genes including c-Jun (Kato *et al.*, 1997).

MEK6: MEK6 is a dual specificity kinase that shares close structural similarity to MEK3 and is strongly activated by stress – inducing factors such as U.V. radiation or osmotic shock (Moriguchi *et al.*, 1996, Raingeaud *et al.*, 1996). Expression of MEK6 activates p38MAPK which includes all the four isoforms - p38MAPKα, p38MAPKβ, p38MAPKδ and p38MAPKγ (Raingeaud *et al.*, 1996, Wang *et al.*, 1997). MEK 3 or MEK6 regulates p38MAPK activity and the resultant gene expression mediated by ATF2 and Elk1 (Raingeaud *et al.*, 1996).

MEK7: MEK7 is the mammalian homolog of the *Drosophila* Hep gene product. It is expressed in all adult and embryonic tissue (Moriguchi *et al.*, 1997, Tournier *et al.*, 1997, Yao *et al.*, 1997). MEK7 is activated in response to cellular stress including proinflammatory cytokines, osmotic stress and Fas – induced apoptosis (Finch *et al.*, 1997, Toyoshima *et al.*, 1997). Analysis of mammalian MEK7 has indicated that it is highly specific to JNK regulation (Wu *et al.*, 1997) as is MEK4. However, they appear to be differentially regulated. MEK7 is preferentially activated by TNFα, a proinflammatory cytokine (Moriguchi *et al.*, 1997), whereas MEK4 is not; though other diverse stress stimuli activate both MEK4 and MEK7. MEK7 is specific to JNK, whereas MEK4 can activate both JNK and p38 pathways (Lin *et al.*, 1995, Tournier *et al.*, 1997, Yao *et al.*, 1997).

1.4.1.4 MAPKs:

MAPKs are divided into different subgroups based on their sequence homology, nature of the preceding MEK and the input stimulus. Within these subgroups, further diversification is possible by alternative splicing. Most of the known MAPKs contain a T-X-Y sequence, phosphorylation of which is essential for conduction of signaling of downstream substrate proteins. The T-X-Y motif is found as part of the activation loop. Location of the substrates of the MAPKs can be nuclear or cytoplasmic. Recognition and selection of substrate proteins occurs via specific docking sites on the substrates, which are bound by complementary binding domains on the MAPK (Barsyte-Lovejoy *et al.*, 2002). Till date many MAPKs have been discovered, with ERKs 1/2, p38MAPKs α/β/γ/δ, JNK/SAPK being the well-characterized.

ERK1 and ERK2: These protein kinases, also known as MAPK3 and MAPK1 respectively, are nearly 85% identical with greater identity in the core regions which are involved in binding substrates. Based on their molecular weight they are sometimes referred to as $p44^{ERK1}$ and $p42^{ERK2}$. They were initially isolated and cloned as kinases activated in response to insulin and NGF (Boulton *et al.*, 1991, Boulton *et al.*, 1990). ERK1 and ERK2 are expressed in most, if not all, mammalian tissues. Alternatively spliced isoforms have been reported for ERK1 (ERK1b and ERK1c) (Shaul and Seger, 2006, Yung *et al.*, 2000) and ERK2 (ERK2b) (Gonzalez *et al.*, 1992). Many different stimuli including, cytokines, viral infection, growth factors and activation of G-protein coupled receptors activate the ERKs.

p38MAPKs: There are four p38 kinases: α, β, γ and δ among which p38α enzyme is the best characterized and is expressed in most cell types. The p38MAPKs regulate the expression of many cytokines. They are activated in immune cells by inflammatory cytokines and play an important role in the activation of the immune response (Wang *et al.*, 1997, Jiang *et al.*, 1997, Jiang *et al.*, 1996, Li *et al.*, 1996). The four p38 isoforms are strongly activated by various environmental stimuli such as oxidative stress, UV radiation, hypoxia, and inflammatory cytokines such as interleukins, tumor – necrosis factor alpha (TNFα). P38 isoforms are also activated by G-protein coupled receptors and the Rho family GTPases CDC42 and Rac.

JNKs: Like the p38MAPKs, JNK also responds to stress stimuli, hence the synonym, stress – activated protein kinase (SAPK). There are three known JNK isoforms, JNK-1 (SAPKγ), JNK-2 (SAPKα) and JNK-3 (SAPKβ) (Derijard *et al.*, 1994, Kyriakis *et al.*, 1994). The isoforms are strongly activated by oxidative stress, radiation and cytokines by dual phosphorylation on the Ser/Thr and Tyr residues (Bogoyevitch *et al.*, 2010, Kyriakis and Avruch, 1996, Kyriakis *et al.*, 1991). The JNKs were in turn found to bind and phosphorylates the DNA binding protein c-Jun and increase its transcriptional activity (Kyriakis *et al.*, 1994). Other transcriptional factors regulated by JNKs are ATF2, p53, Elk1, HSF1 and c-Myc (Bogoyevitch *et al.*, 2010, Cargnello and Roux, 2011, Gupta *et al.*, 1995, Raman *et al.*, 2007, Whitmarsh *et al.*, 1995). JNK1 and JNK2 are ubiquitously expressed, whereas JNK3 appears to be localized to neuronal tissues, cardiac myocytes and testis (Bode and Dong, 2007). The isoforms have been indicated in controlling programmed cell death or apoptosis (Tournier *et al.*, 2000). Besides this, they have also been shown to have distinct roles in controlling cell proliferation. Activation of c-Jun by JNKs, promotes the AP-1 complex formation and the transcription of genes containing the AP-1 binding sites, including genes involved in cell cycle such as cyclin D1 (Sabapathy *et al.*, 2004).

Previous studies have shown that activation of PKC with drugs such as PEP005 leads to stimulation of the MAPK signaling pathway particularly the Ras/Raf/MEK/ERK arm (Cozzi *et al.*, 2006) where terminal growth arrest of cancer cells was achieved at doses of TPA which stimulated an increased level of phosphorylation of ERK1/2 of the MAPK pathway.

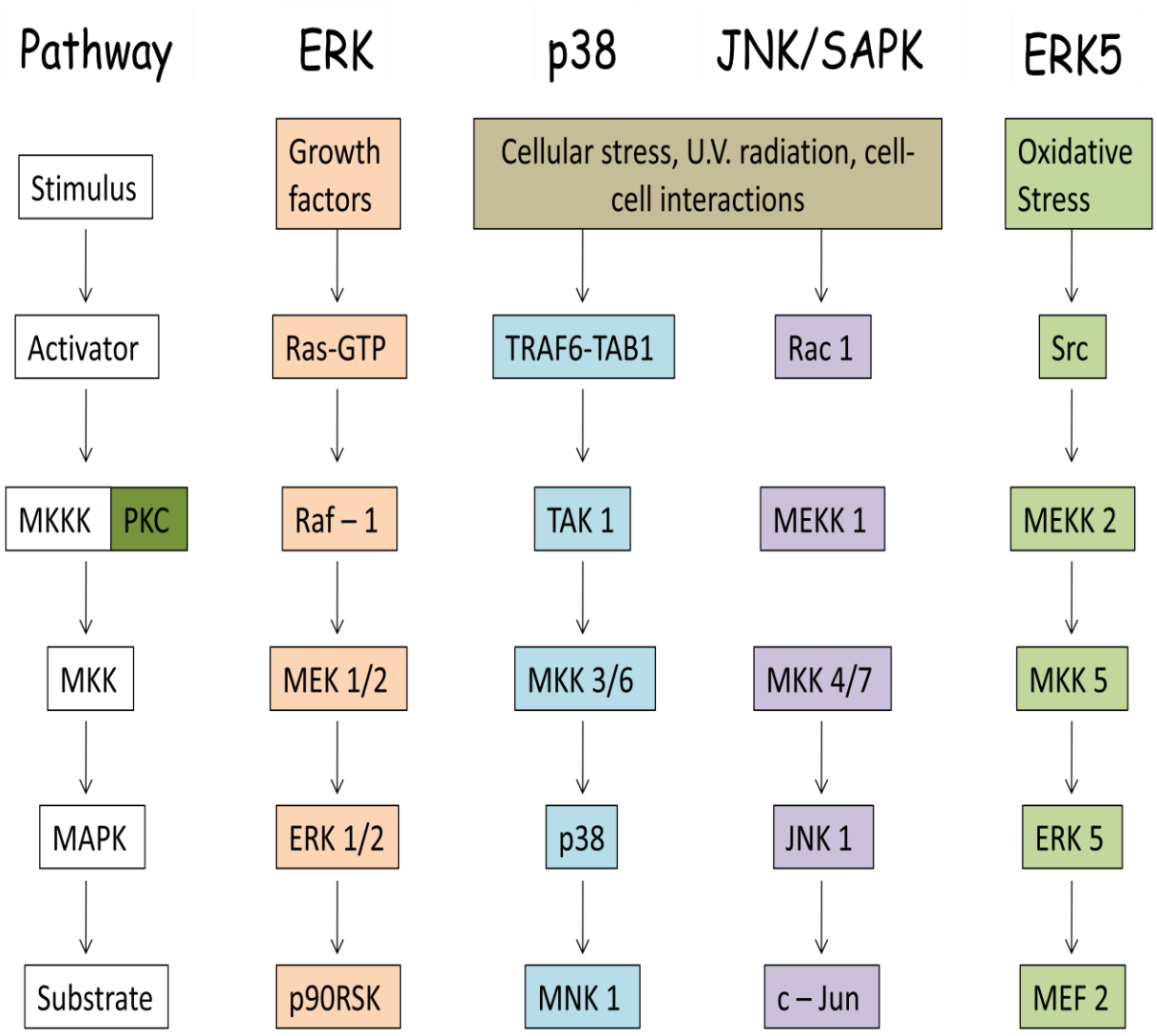

Figure 1. 4 Schematic diagram of the mitogen-activated protein kinase pathways

Activated PKC is considered to bind to Ras/Raf/MEK/ERK arm of the MAPK pathway and increase the level of phosphorylation of ERK1/2 (Cozzi et al., 2006, Technology).

Abbreviations: ERK – Extracellular signal-regulated kinase; JNK/SAPK – c-Jun N-terminal kinase/stress-activated protein kinase

1.5 CELL CYCLE REGULATION

1.5.1 Overview of the Cell Cycle

Eukaryotic cells complete their reproduction in a cyclical process, in which at least two phases, *S phase* and *M phase*, can be differentiated on the basis of biochemical and morphological features. The biochemical characteristic of the S (synthesis) phase is the replication of nuclear DNA and thus doubling of the genetic information. In the M (mitosis) phase, division of the chromosomes between the daughter cells occurs.

In most cell types, two further phases can be distinguished, G_1 and G_2 phase. G_1 phase covers the period between M phase and S phase while G_2 phase covers the period between S phase and M phase. From G_1 phase, the cell may transfer into a quiescent state known as G_0 phase. Appropriate signals (e.g. addition of growth factors) can induce the cell to return from G_0 into G_1 phase and proceed with the cell cycle. The cyclic sequence of G_1, S, G_2 and M phases describes a standard cell cycle (Figure 1.5) (Krauss, 2003c).

1.5.2 Principles of Cell Cycle Control

The different phases of the cell cycle include a number of highly ordered processes that ultimately lead to duplication of the cell. The various cell cycle events are highly coordinated to occur in a defined order and with an exact timing, requiring precise control mechanisms.

The ordered sequence of cell cycle events is ensured by different control loops that have an inhibitory or promoting effect on the progress of the cell cycle. These are monitoring mechanisms that register the completion of important cell cycle events (e.g. complete DNA synthesis) and allow transition to the next event (e.g. entry into mitosis) to occur. The control systems of the cell cycle ensure that the various phases are executed completely and in the correct sequence. Entry into a new phase can only take place when the preceding phase has been completed.

Many of the control mechanisms of the cell cycle are of an *intrinsic* nature and are constitutive, i.e., they are operational in every cell cycle and ensure the ordering of the individual steps. However, other control mechanisms exist that are not active in every cell cycle; these are only induced when defects are detected in central cell cycle events. These control mechanisms are known as

checkpoints. An example is the DNA damage checkpoint, a biochemical pathway that detects DNA damage and creates a signal that slows cells cycle progression or arrests cells in the G_1, S, or G_2 phase. A biochemical pathway is at the centre of the cell cycle, of which the most important players are Ser/Thr-specific protein kinases and regulatory proteins associated with these. In addition to the built-in protection and control mechanisms, the cell is also subject to a number of *external* controls such as growth conditions and mitogenic (e.g. growth factors) and antimitogenic (e.g. TGF-*β*, cell damage) signals during cell-cell communication.

These ensure that cell division occurs in balance with the overall development of the organism and with external growth conditions. This is a kind of social control of cell division that regulates the progress of the cell cycle, with the help of circulating signal molecules or via cell – cell interactions.

The cell cycle contains critical events where the cell switches from one state of biochemical activity to another, in an irreversible manner. These events are called cell cycle transitions. Often, activating and inhibitory signals are received and transmitted at these cell cycle transitions. Key elements of the cell cycle regulation have been identified.

Two processes are central to the cell cycle regulation:

Oscillating changes in the activity of the cell cycle machinery, with protein kinases as the most important component.

Specific proteolysis of the cell cycle regulators

The activity of the cell cycle machinery is controlled by the following proteins:

Cyclin-dependent kinases (CDKs)

Cyclins

Inhibitors of cyclin-dependent kinases (CKIs).

An oscillating system is formed by the interplay of the three protein classes. The activity of the cyclin-dependent kinases (CDKs) is central to the oscillating system. These create a signal that initiates downstream biochemical processes and thus determines the individual phases of the cycle (Krauss, 2003c, Weinberg, 2007a).

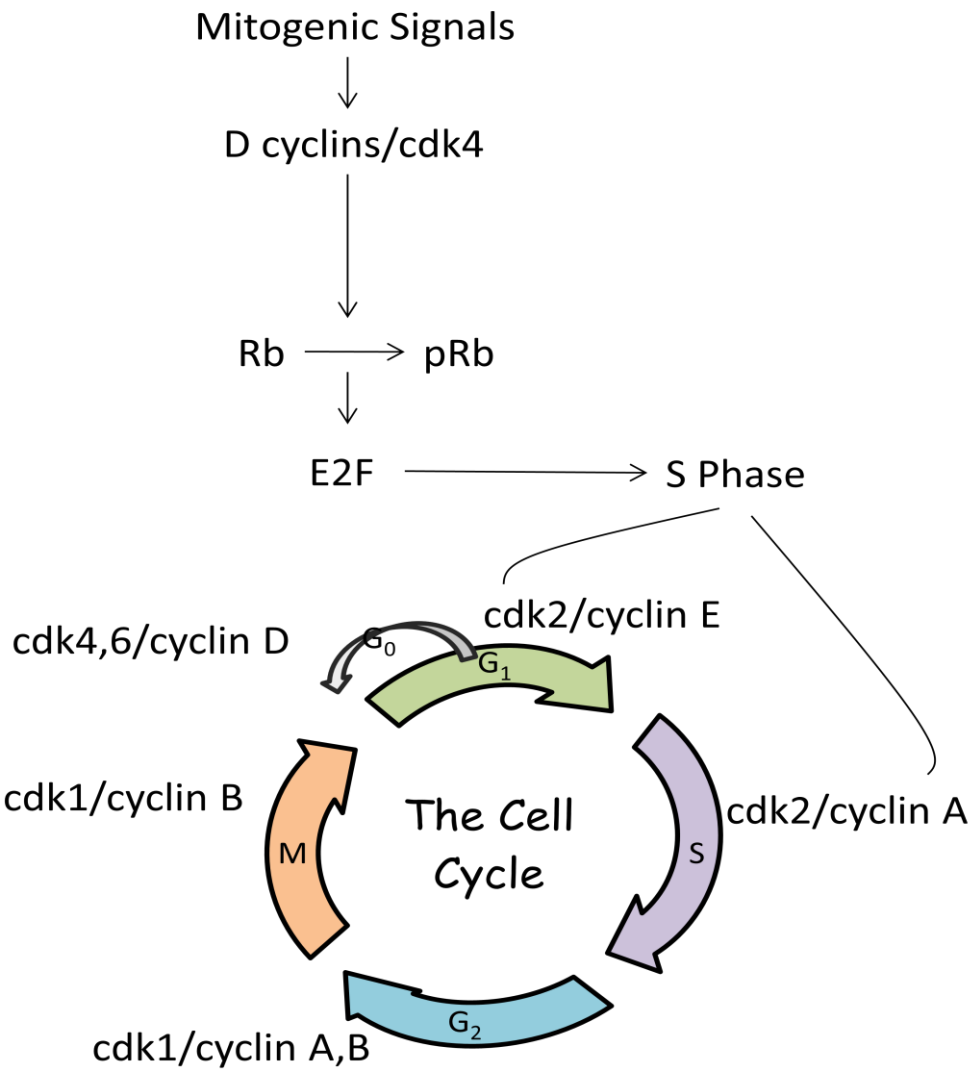

Figure 1. 5 Four Phases of the Cell Cycle in Eukaryotes

The four phases of a typical cycle of a eukaryotic cell. G_1, S and G_2 phases form the interphase, while the cell grows continuously. Cell division occurs in M phase. New synthesis of DNA is limited to S phase. G_1 phase includes the period between M phase and S phase; G_2 phase lies between S phase and M phase (Krauss, 2003c, Weinberg, 2007a).

1.5.3 Mechanisms of Cell Cycle Regulation

Mammalian cell cycle progression is regulated by the activation and inactivation of a conserved family of protein kinases known as cyclin – dependent kinases (CDKs). The CDKs are proteins of 34-40 kDa with Ser/Thr-specific protein kinase activity. The CDKs must associate with the corresponding cyclin (or cyclin-like proteins) to be active. Active cyclin – dependent protein kinases are thus heterodimers in which the CDK subunit carries the catalytic activity and the other subunit, the cyclin, performs an activating and specificity – determining function. In addition to association of the cyclin, most CDKs require phosphorylation in the activation segment for full activation. In mammals, there are at least ten different CDKs, numbered CDK1 to CDK10 (Table 1.3).

Progress of the cell cycle appears to be mainly controlled by CDK1 (also known as CDC2) and CDKs 2, 4 and 6. CDKs 5 and 7-10, are not directly involved in cell cycle control and perform other tasks such as transcription regulation. Particular CDK/cyclin complexes act at different stages of the cell cycle controlling the two key checkpoints, G_1 → S and G_2 → M transitions. Progression through early G_1 depends on CDKs 4 and 6 which are activated by the D-type cyclins (D1, D2, D3). The cyclin D-CDK4/6 complexes to perform a dual task in G_1 phase regulation; one task is to integrate external signals into the cell cycle and the other function is to activate metabolism and promote cell growth. Progression through G_1 and into S phase requires activation of CDK2, which is sequentially regulated by cyclin E and A. CDK2 associates with cyclin E in late G_1 phase and once it enters the S phase, cyclin E is degraded and CDK2 combines with cyclin A. Degradation of cyclin A occurs in early M phase. Transition of the cell cycle from G_2 to M is regulated by CDC2 (CDK1) in association with cyclin A and cyclin B (Figure 1.5).

Activity of the CDK/cyclin complexes is controlled by several mechanisms including the positive and negative phosphorylation events and their interaction with CDK inhibitory proteins. Phosphorylation at Thr161 of CDC2 (CDK1) kinase or the equivalent positions Thr160 of CDK2 and Thr172 of CDK4/6 *activates* the CDK complexes, while phosphorylation at Thr14 and Tyr15 has an *inhibitory* effect. Positive phosphorylation of CDKs is mediated by cyclin H-CDK7 complex, also known as CDK-activating kinase (CAK), which is achieved by the phosphorylation of CDK1 (Fisher and Morgan, 1994, Kaldis, 1999). Negative control of CDK activity in cell cycle is achieved by *cyclin-dependent kinase inhibitors (CKIs)* (Chellappan *et al.*, 1998, Sherr and

Roberts, 1995). They are a heterogenous family of proteins that associate with a CDK or a cyclin-CDK complex and are divided into two groups: CIP/KIP family ($p21^{Waf1/Cip1}$, $p27^{Kip1}$, $p57^{Kip2}$), and INK4 family ($p15^{INK4b}$, $p16^{INK4a}$, $p18^{INK4c}$, $p19^{INK4d}$) (Lee and Yang, 2001). The Cip/Kip family mainly acts on CDK2 complexes, while the inhibitors of the INK family interact with CDK4 and CDK6 complexes.

Important targets of CDK4 and CDK6 include members of the retinoblastoma family which comprise pRb (retinoblastoma protein), p107 and p130. The pRb protein is a nuclear phosphoprotein of 105kDa and belongs to a class of proteins called *pocket proteins* (Grana *et al.*, 1998). These pocket proteins are growth suppressor proteins and are involved in the control of cell cycle progression and differentiation, cell cycle entry and exit, and apoptosis (Grana *et al.*, 1998, Yee *et al.*, 1998). With the characteristics of a *tumor suppressor protein*, loss of pRb functions can result in deregulation of cell division and tumor formation. The pRb protein can be divided into at least three functional regions: an N-terminal region, a central pocket and a C-terminal region. The N-terminal region appears to be required for oligomerization; the pocket region contains binding sites for the transcription factor E2F, for viral oncoproteins TAg, E1A and E7, and for a large number of other cellular proteins. A nonspecific DNA – binding domain is found on the C-terminal region. Numerous Ser/Thr phosphorylation sites have been identified on pRb (Stiegler and Giordano, 2001, Weinberg, 1995).

1.6 PROTEIN KINASE C IN CELL CYCLE REGULATION

Protein Kinase C (PKC) is a family of Ser/Thr kinases which play a central role in cellular processes, including proliferation, and cell cycle progression, differentiation, cytoskeletal remodeling and apoptosis (Dekker *et al.*, 1995, Nishizuka, 1984, Olson *et al.*, 1993). Studies using *in vitro* and *in vivo* systems demonstrate PKC as a key regulator of critical cell cycle regulations. PKC-mediated control of these cell cycle transitions can be either positive or negative; depending on the specific PKC isozymes involved and on the timing of PKC activation during cell cycle. In a vascular endothelial system, short-term application of PKC agonists in the early G_1 phase, potentiated progression of the cell from G_1 → S phase, while PKC activation in mid-to-late G_1 phase, prevented entry into S phase (Zhou et al., 1993, Zhou et al., 1994). The major target of PKC-

Table 1. 3 Functions of the different CDK/Cyclin associations

CDK	CYCLIN	CKI	FUNCTION
CDC2, CDK2	A1	p21, p27, p57	Meiosis
	A2		S, G_1 → S, M phases (Russo *et al.*, 1996)
CDC2	B1, B2, B3		M phase (Krauss, 2003b)
CDK8	C		Transcription repression of RNA polymerase II; phosphorylates cyclin-H thereby inactivating CTD kinase activity of CDK7 (Sano and Schneider, 2003)
CDK2, 4, 5, 6	D1, D2, D3	p15, p16, p18, p19, p21, p27	G_1, Restriction point (Dhavan and Tsai, 2001, Krauss, 2003b)
CDK2	E	p21, p27, p57	G_1/S
	F		G_2, binding to cyclin B
CDK7	H		Phosphorylation of CDC_2; phosphorylation of CTD of RNA polymerase II (Masai and Arai, 2002, Kaldis, 1999)
CDK9	T		Phosphorylation of CTD of RNA polymerase II (Simone and Giordano, 2001)
CDK5	p35, p39		Phosphorylation of structural proteins (Dhavan and Tsai, 2001)
CDK10			Phosphorylation of transcriptional factors (Kasten and Giordano, 2001)

CDK: Cyclin dependent kinase; S phase: Synthesis phase; G_1 phase: growth phase.

mediated cell cycle regulation is a Cip/Kip cyclin-dependent kinase inhibitor, $p21^{waf1/cip1}$. An increase in the expression of $p21^{waf1/cip1}$ blocks the activity of cdk2 in G_1 phase. This leads to hypophosphorylation of the retinoblastoma protein and ultimately results in the inhibition of the cell cycle progression into S phase. Increased expression of $p21^{waf1/cip1}$ during G_2 phase, blocks CDC2/cyclin B activity and prevents progression into M phase (Weinberg, 1995, Weinberg, 2007b). Sustained activation of PKC is a requirement for long-term cellular responses such as differentiation and proliferation. A major step toward understanding the basis for the physiological responses attributed to PKC would involve the recognition of the specific functions of the individual PKC isozymes and their molecular pathways.

Most of the available information relates to the involvement of PKC isozymes in negative control of cell cycle transitions, although limited data is also available regarding positive regulation of PKC-mediated G_2 → M progression. PKC became the subject of intense investigation when it was discovered that it is a key cellular receptor for phorbol esters, which can substitute for diacylglycerol (DAG) in activating the enzyme. Though, unlike DAG, phorbol esters are not rapidly metabolized, hence resulting in a more prolonged activation of PKC by treatment with these agents. Studies with melanoma cells (Coppock *et al.*, 1995) and myelocytic leukemia cells (Millard *et al.*, 1997), treated with DAG analogues or phorbol esters, has been shown to result in accumulation of cells in the G_1 and G_2 phases. This indicates that PKC induces a biphasic block in cell cycle progression in these systems. Cells that are in G_1 when the stimulus is added, are blocked in G_1 (Coppock *et al.*, 1995), while cells which have progressed through G_1 → S transition, complete the S phase and are blocked in G_2 (Kosaka *et al.*, 1996). Notably, inhibition of cell cycle transitions has also been observed as a result of over-expression of PKC isozymes alpha, delta and eta (Black, 2000, Gavrielides *et al.*, 2004, Serova *et al.*, 2008). On the contrary, PKC-β_2 has been shown to be essential in cell proliferation (Duprez *et al.*, 2009).

1.7 PKC FAMILY IN CARCINOGENESIS

Twelve different isozymes have been identified where each isozyme has been implicated in many cellular responses including permeability, contraction, migration, hypertrophy, proliferation, apoptosis and secretion. PKC isozymes are ubiquitously expressed with PKC-α, β and δ found abundantly in various tissue types (Wetsel *et al.*, 1992). Furthermore, opposing effects of PKC

activation on cell growth have been demonstrated within the same cell type, either by stable over-expression of individual PKC isozymes or by the use of PKC agonists that differently activate individual isozymes (Table 1.4)

The role of PKC in carcinogenesis has been recognized for decades. Two-stage mouse carcinogenesis models have demonstrated that application an initiating agent which may be mutagenic to proto-oncogenes such as Ras, followed by the prolonged exposure to a non-mutagenic promoting agent are both needed for cancer development. Variable expression profiles of PKC isozymes have been displayed during cancer progression, depending on a particular cancer type (Table 1.4).

The role of PKC in cancers arises not from mutations in PKC genes but rather the result of their action as receptors for tumor promoting agents and the downstream targets of mitogenic signals. TPA is the strongest known inducer of PKC activation. However, exposure to TPA or closely related genes does not pose a problem in humans, thus it is not considered as an important factor in the contribution towards the development of human tumors. Tobacco smoke contains a number of substances such as catechols, hydroquine and nitrosamines, which are considered as tumor promoters that activate PKC. Particularly, nitrosamines have been shown to increase the expression and activation of PKC-α and β while expression of PKC-δ is lowered (Gopalakrishna *et al.*, 1994, La Porta *et al.*, 1997). High consumption of dietary lipids is carcinogenic as they increase production of bile acids which activate PKC directly (Pickering *et al.*, 1995). Introduction of oncogenic Ras has been shown to up-regulate PKC-α in keratinocytes and colon cancer cells, while it down-regulates PKC-δ in keratinocytes. c-myc and *p53* are also linked to regulation of PKC expression (Denning *et al.*, 1993); while c-myc oncogene induces an increase in PKC-α expression, *p53* mediated signaling displays an up-regulation of PKC-β (Barr *et al.*, 1991). The overall response to PKC activation appears to be dependent on presence or activity of different isozymes in a particular cell. Several cancer initiating factors lead to an increase in activity of PKC-α/β compared to PKC-δ, which in turn is associated with the development of a malignant phenotype.

Table 1. 4 Protein Kinase C expression in Cancers

PKC isoezymes	Expression profile	Cancer types
PKC-*α*	Overexpression	High grade urinary bladder Endometrial Prostate (Fournier *et al.*, 2001, Kamimura *et al.*, 2004, Langzam *et al.*, 2001)
	Down-regulation	Colon Hepatocellular Breast Basal cell cancers (Gokmen-Polar *et al.*, 2001, Kerfoot *et al.*, 2004, Neill *et al.*, 2003, Tsai *et al.*, 2000)
PKC-*β*	Up-regulation	Colon Prostate (Gokmen-Polar *et al.*, 2001, Kamimura *et al.*, 2004)
	Down-regulation	Bladder cancer Melanoma (Gokmen-Polar *et al.*, 2001, Martinez-Gimeno *et al.*, 1995, Neill *et al.*, 2003)
PKC-*δ*	Up-regulation	Hepatocellular cancer (Tsai *et al.*, 2000)
	Down-regulation	Urinary bladder cancer (Langzam *et al.*, 2001)
PKC-ι, ε, λ	Down-regulation	Pancreatic cancers (Evans *et al.*, 2003, Martinez-Gimeno *et al.*, 1995)
PKC-*η*	Up-regulated	Renal cancers (Brenner *et al.*, 2003)
PKC-*λ*	Up-regulated	Ovarian cancers (Fournier *et al.*, 2001, Weichert *et al.*, 2003)
PKC-*ι*	Down-regulation	Ovarian cancers (Fournier *et al.*, 2001, Weichert *et al.*, 2003)
PKC-*γ*	Up-regulated	B-cell lymphoma (Kamimura *et al.*, 2004)

The table summarizes cancer indications where PKC is up or down-regulated.

1.8 PROTEIN KINASE C AS A TARGET IN CANCER THERAPY

A better understanding of the role of individual PKC isozymes in the pathogenesis of a disease can aid in developing a setting where these isozymes will emerge as viable therapeutic targets. The absence of mutations in genes encoding PKCs makes the enzyme a suitable target for cancer therapies with no expected failure of therapy due to mutations in the genes.

Both PKC inhibitors and activators have been extensively studied as potential agents for chemotherapy. Both broad spectrum and isozyme-specific inhibitors have anticancer properties, *in vivo* and *in vitro*; but unfortunately their clinical efficacy has been low.

1.8.1 PKC Inhibitors

Some common inhibitors used in cancer therapy are PKC412 (a broad spectrum inhibitor), Go6976 (a PKCα/β inhibitor), LY317615 (a PKCβ inhibitor), UCN-01/02 (selective inhibitors of the conventional PKCs). These compounds have shown either a decrease in invasion, inhibition of angiogenesis or reduced growth of cancerous cells which demonstrate anti-neoplastic effects. Go6976 and PKC412 have proven to be anti-invasive agents (Koivunen *et al.*, 2004, Masur *et al.*, 2001, Nakamura *et al.*, 2003). A reduction in growth of cancerous cells has been shown to be induced by UCN-01, Go6976 and PKC412 (Biswas et al., 2001, Fabbro et al., 2000, Seynaeve et al., 1993b). The retardation in growth is suggested to be a result of cell cycle arrest i.e. senescence (Mack et al., 1999, Seynaeve et al., 1993b). To some extent this mechanism is also governed by an increase in apoptosis, as demonstrated by Go6976 and UCN-01 in breast and colon cancers respectively (Bhonde *et al.*, 2005, Biswas *et al.*, 2001, Biswas *et al.*, 2003). LY317615, a PKCβ inhibitor, has been shown to inhibit angiogenesis and plasma VEGF-levels in human tumor xenograft-bearing mice (Keyes *et al.*, 2004).

PKC inhibitors PKC412 and UCN-01 have been tested in phases I-III studies of human clinical trials in combination with classical chemotherapeutic drugs. However, due to their strong binding to human plasma proteins, there is limited bioavailability resulting in poor clinical effects. Clinical trials of LY317615 as a single agent in the treatment of gliomas and lymphomas have shown to have minimal effects (www.cancer.gov/clinicaltrials).

1.8.2 PKC Activators

Protein Kinase C rocketed to the forefront of cancer research when it was identified as a target for phorbol esters. Phorbol esters compete with DAG for the binding site in the C1 domain of the regulatory region. A widely accepted phorbol ester is 12-O-tetradecanoylphorbol-13-acetate (TPA). It is obtained from the latex of *Croton tiglium* L., a leafy shrub of the *Euphorbia* family native to Southeastern Asia (Hecker, 1968). Short term exposure of cells to TPA has been shown to bind with greater affinity to PKC compared to diacylglycerol (DAG), leading to a more potent activation of PKC isozymes. Following a long-term exposure of cells to TPA, many PKC isozymes have been found to be down-regulated via the ubiquitin – proteosome pathway (Hofmann, 2001). In experimental studies, TPA is the strongest known inducer of PKC activation. However, exposure to TPA or closely related agents is not a problem for humans and thus, TPA is not considered as an important factor in the development of human cancers (Koivunen *et al.*, 2006). Although graded as a tumor-promoter in carcinogenic experiments performed on normal mouse skin and xenograft human foreskins by Yuspa *et al.* in 1979, TPA has also been established to induce cytostatic, cytotoxic and differentiation end points in cancer cells (Hofmann, 2001). TPA has been indicated as a therapeutic agent in two studies. Systemically administered TPA was used alone or in combination with vitamin D3 and cytosine arabinoside (Ara C) in myelocytic leukaemia patients. In most of the cases, the treatment with TPA resulted in complete or partial remission with improved hematological parameters. Fever, chills and dyspnea were the common side effects of the treatment, although these were shown to be temporary (Han *et al.*, 1998 (i)). In the second study, it was observed that TPA induced an increase in depressed white blood cell counts and neutrophils towards the normal range, when administered to patients treated with cytotoxic cancer chemotherapeutic drugs (Han *et al.*, 1998 (ii)).

Bryostatin-1 is the first of 20 members of a class of naturally occurring macrolides isolated from a marine byrozoan *Bugula neritina* found in the Gulf of Mexico (Mutter and Wills, 2000, Pettit *et al.*, 1982). Bryostatin-1 is a novel antineoplastic agent that binds and activates PKC. It is more potent than TPA for translocating PKC-δ and –ε. Similarly to phorbol esters, short-term exposures of cell to Bryostatin-1 leads to PKC activation while long-term exposure results in protein degradation (Kraft *et al.*, 1988, Kraft *et al.*, 1986). However, the ability of Bryostatin-1 to cause degradation of PKC is influenced by concentration. Low doses have been shown to cause down-regulation of PKC, while high doses have not (Szallasi *et al.*, 1994). Bryostatin-1 has shown the ability to induce only a

subset of the biological functions of TPA. This suggests that it may act as either a PKC agonist or antagonist (Hocevar and Fields, 1991, Kraft *et al.*, 1988, Kraft *et al.*, 1986). In animal models, Bryostatin-1 has shown antineoplastic activity against leukemia (Jones *et al.*, 1990), melanoma (Schuchter *et al.*, 1991) and ovarian cancer (Hornung *et al.*, 1992).

Initial phase I studies of Bryostatin-1 in a broad spectrum of tumors, including malignant melanoma, ovarian cancer and low grade non-Hodgkin's lymphoma produced objective response. This spawned a number of single – agent and combination studies in various tumor types (Varterasian *et al.*, 1998). The first published phase II study of Bryostatin-1 as a single agent failed to demonstrate activity in previously treated patients with metastatic malignant melanoma (Propper *et al.*, 1998). Results from a phase I study of a sequential therapy with Bryostatin-1 and vincristine showed that this combination was feasible and well tolerated. This warranted a phase II study of Bryostatin-1 in combination with other cytotoxic agents (Varterasian *et al.*, 2000). A correlative study of a combination of Bryostatin-1 and vincristine showed significant antitumor activity in relapsed B-cell malignancies (Dowlati *et al.*, 2003). Combinations of bryostatin-1 with chlorodeoxyadenosine and auristatin PE have also resulted in successful treatment of human chronic lymphocytic leukemia (Mohammad *et al.*, 1998a, Mohammad *et al.*, 1998b).

The compound ingenol-3-angelate (PEP005) is a novel anticancer drug (Kedei *et al.*, 2004) that is an activator of protein kinase C. Topical application of a high-dose of PEP005, has been shown to cure ~80% of subcutaneous tumors in mice. Similarly it has been found to be toxic to cells *in vitro* (Ogbourne *et al.*, 2004). Treatment of melanoma cell lines with PEP005 indicated irreversible growth arrest, with no adverse effects observed in normal melanocytes and normal fibroblasts (Cozzi *et al.*, 2006). Three daily topical application of PEP005 cured a series of s.c. mouse and human tumor xenografts in mice. The treatment resulted in a mild short-term erythema (Ogbourne *et al.*, 2004). PEP005 has been shown to be a potent activator of PKC isozymes (Kedei *et al.*, 2004) which are important modulators of a range of biological processes (Nishizuka and Nakamura, 1995). PKC family members have been investigated as important anti-cancer targets, and have been shown to activate or facilitate activation of the innate immune response (Fernandez *et al.*, 2000, Kontny *et al.*, 1999). Topical treatment of PEP005 has been shown to be associated with an acute T cell-independent inflammatory response distinguished by a pronounced neutrophil infiltration (Challacombe *et al.*, 2006). Phase II trials of a topical application indicated PEP005to be safe and

efficient in treating basal cell carcinomas and the squamous cell carcinoma precursor, Actinic Keratosis (AK) (Siller *et al.*, 2009, Siller *et al.*, 2010).

A novel diterpene ester named EBC-46 (formal name 12-tigloyl/angeloyl-13-(2-methylbutanoyl)-6,7-epoxy-4,5,9,12,13,20-hexahydroxy-1-tigliaen-3-one) has been isolated from the seed of the Blushwood tree in Queensland, Australia. It belongs to the tigliane class of naturally occurring products and is structurally similar to TPA (Figure 1.6). Veterinary trials of intratumoral treatments of EBC-46 in animals have been highly successful with a cure rate at more than 80% (data not provided). It is a potential PKC activator and is considered a candidate agent for intralesional therapy (discussed later).

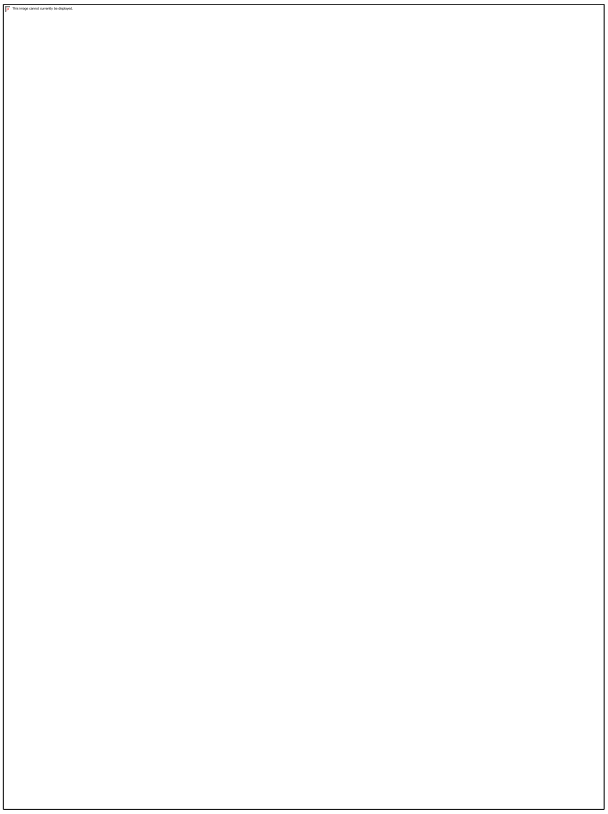

Figure. 1.6 Structure of EBC46 (12-tigloyl/angeloyl-13-(2-methylbutanoyl)-6,7-epoxy-4,5,9,12,13,20-hexahydroxy-1-tigliaen-3-one)

(Structure of EBC-46 obtained from Dr. Paul Reddell and Prof. Peter Parsons; unpublished data).

1.9 PKC AND CELL DEATH

1.9.1 Cell Death:

In general, cell death is a vital process in the development, homeostasis and immune regulation of multicellular organisms. It is often induced upon pathogen infection as part of the defense mechanism. There are two major types of cell death, namely apoptosis and necrosis, defined by their morphological criteria (Duprez *et al.*, 2009).

Until 1971, the term necrosis was used for all types of cell death. Kerr *et al.* in 1971 first observed a form of non-pathologic cell death in certain tissues which they termed shrinkage necrosis (Kerr, 1971). Later shrinkage necrosis became implicated in organ homeostasis and the term "apoptosis" was coined in 1972 by Kerr and colleagues (Kerr *et al.*, 1972) which described a form of cell-intrinsic programmed suicide mechanism associated with cell shrinkage membrane blebbing and chromatin condensation.

Morphologically, apoptosis can be morphologically by pyknosis which is a deep staining of the nuclear mass, nuclear fragmentation, and formation of condensed cell bodies or apoptotic bodies. This is a systematic process which is energy-dependent. On the other hand, necrosis can be defined by electron-lucent cytoplasm, swelling of cellular organelles, and loss of plasma membrane integrity which can be brought about by loss of ATP production. (Zong and Thompson, 2006).

1.9.2 Drug-induced Cell Death:

Many insults induce apoptosis at lower doses and necrosis at higher doses. Even in response to a certain dose of death-inducing agent, features of apoptosis and necrosis may co-exist in the same cell. In addition, if not engulfed by neighbouring phagocytic cells or in cell culture *in vitro* where phagocytosis usually does not occur, dead cells in the late stages of apoptosis may present necrotic features due to loss of cellular energy and plasma membrane integrity. This is known as apoptotic necrosis or secondary necrosis (Majno and Joris, 1995).

Doxorubicin, etoposide, bleomycin and paclitaxel are widely used anticancer drugs in various clinical trials. They induce apoptosis of tumor cells directly linked to their anti-proliferative effects (Fisher, 1994, Skladanowski and Konopa, 1993, Tu *et al.*, 1996). Mailloux and colleagues in 2001

confirmed these findings and showed that doxorubicin and bleomycin resulted in similar cytotoxic effects with cell lysis and detachment which were time-dependent while etoposide and paclitaxel were less cytotoxic (Mailloux *et al.*, 2001). However, the disadvantage of these anticancer agents such as doxorubicin and etoposide was found to be the induction of apoptosis of non cancerous cells such as epithelial cells and thymocytes (Lock and Stribinskiene, 1996, Walker *et al.*, 1991) which could probably be attributed to their toxicities. Similarly, protein kinase C activator Bryostatin 1 was shown to interact in a synergistic manner with cyclin dependent kinase inhibitor flavopiridol (FP) to trigger apoptosis in human leukemia cells. This interaction resulted from enhanced TNF-α production and engagement of the extrinsic apoptotic pathway (Cartee *et al.*, 2003).

1.9.3 Protein Kinase C in Cell Death:

Protein kinase Cs are a family of serine-threonine/tyrosine kinases which are important regulators of cell proliferation and malignant transformation. PKCs are not only able to promote pro-survival responses in cells but are also able to mediate cell growth arrest or lead to cell death through apoptotic mechanisms. Activated PKC isozymes can inhibit the cell cycle both at G1/S and G2/M transitions (Black, 2000, Gavrielides *et al.*, 2004). Nakagawa *et al.* in 2005 determined that TPA-induced PKC activation in lung adenocarcinoma H358 lead to p21 up-regulation, Rb hypophosphorylation and G1 arrest.

Of the twelve isozymes, PKC-δ is known to play a key role in the apoptotic response via activation of the p38 MAPK pathway (Emoto *et al.*, 1995). The majority of studies to date indicate this novel PKC isoform to play a major role in apoptosis in different cellular models. TPA-induced apoptosis was shown to be induced in LNCaP cells via over-expression of the PKC-δ isoform (Fujii *et al.*, 2000).

1.10 PKC AND INFLAMMATION

1.10.1 Phorbol ester and activation of leukocytes and endothelial cells

Phorbol ester TPA is a skin irritant and inflammatory agent. It induces prompt remodelling of the vasculature, resulting in edema formation (Janoff *et al.*, 1970) and this response is enhanced by the induced secretion of histamine from mast cells and blood-borne basophils (Katakami *et al.*, 1984, Schleimer *et al.*, 1981). It activates adhesion molecules present on the surface of the leukocytes

causing them to bind and then to migrate through the vascular endothelial layer into the tissues underlying the skin (Kavanaugh *et al.*, 1991). In the tissues, TPA potentiates antigen-mediated stimulation of T-lymphocytes, enhancing the production of the cytokine interleukin-2 (IL-2) (Rosenstreich and Mizel, 1979). TPA also causes degranulation of neutrophils, releasing pro-inflammatory cytokines and matrix proteases, and activation of oxidative burst (Repine *et al.*, 1974).

Neutrophils are dedicated phagocytic cells and they constitute the first line of defense against invading micro-organisms. Their action can be dissected into 3 distinct processes:

direct migration towards micro-organisms (chemotaxis),

engulfment of the micro-organism (phagocytosis), and

it's killing.

The intracellular killing mechanism is based on two independent but mutually supportive mechanisms, the generation of toxic oxygen metabolites and the release of microbicidal proteins from the storage granules into phagosome (Dale *et al.*, 2008, Segal, 2005). The generation of toxic oxygen metabolites, superoxide anion (O_2^-) and hydrogen peroxide (H_2O_2), is accompanied by a 20 – 30-fold increase in oxygen consumption, called the *respiratory burst* (Dahlgren and Karlsson, 1999, Quinn and Gauss, 2004). The enzyme responsible for oxidative burst is *NADPH oxidase* (nicotinamide adenine dinucleotide phosphate); it transfers electrons from NADPH to O_2, resulting in the formation of superoxide anion. During oxidase activation, cytosolic oxidase proteins translocate to the plasma membrane, where they assemble around a membrane-bound component known as *flavocytochrome b*. This is a highly regulated process involving phosphorylation, translocation and multiple conformational changes (Quinn and Gauss, 2004). The core of the NADPH oxidase enzyme is composed of four oxidase-specific proteins ($p22^{phox}$, $p47^{phox}$, $p67^{phox}$, $gp91^{phox}$) and GTPase (Rac1/2).

1.10.2 Role of PKC in the regulation of the respiratory burst

Infection elicits activation of the serum complement cascade and the binding of specific antibodies (IgG, immunoglobulin G) by microbial antigens. This results in the occupation of neutrophil *Mac-1* and *Fcγ*-receptors which activate phagocytosis and respiratory burst. The binding of Mac-1 and

Fcγ-receptors activates PLCβ, resulting in the generation of DAG and IP_3. A number of kinases have been proposed to participate in $p47^{phox}$ phosphorylation, including protein kinase C (el Benna *et al.*, 1994), p38-mitogen activated protein kinases (MAPK) (El Benna *et al.*, 1996) and extracellular signal-regulated kinases (ERK1/2) (Dewas *et al.*, 2000). PKC plays a vital role in the phosphorylation of $p47^{phox}$ which has been demonstrated by PKCs – α, β_2, δ and ζ (Dang *et al.*, 2001, Fontayne *et al.*, 2002, Reeves *et al.*, 1999). The respiratory burst activity can be induced directly by phorbol ester and in this case the level of phosphorylation of $p47^{phox}$ matches the level of respiratory burst activity. Conversely, compounds that inhibit PKC prevent the respiratory burst (Dekker *et al.*, 2000, Kramer *et al.*, 1989). It is also reduced by 50% in neutrophils obtained from mice that fail to express PKC-$\beta_{(1+2)}$ and PKC-δ (Dekker *et al.*, 2000).

1.11 PROTEIN TARGETS FOR DITERPENE ESTERS OTHER THAN PKC

The traditional view that diterpene esters bind solely to protein kinase C (Section 1.8.2) has been challenged in recent years with the discovery of nonkinase proteins that bind diterpene esters with equal affinity. These receptors include Unc13/Munc13 (mammalian) isoforms (scaffolding proteins involved in exocytosis), chimaerins (a family of RacGTPase activating proteins) and RasGRPs (exchange factors of Ras/Rap1) (Kazanietz, 2002). All of these proteins contain a C1 binding domain similar to protein kinase C and bind to diterpene esters in the presences of phospholipids. It has been shown that PEP005 binds to the C1 domain in a similar manner to phorbol esters and DAG (Pak *et al.*, 2001). Song *et al*, in 2013 reported that the C1 domains of RasGRP1 and RasGRP3 bound PEP005 with higher affinities than they bound to phorbol ester PDBu and similar affinity to PKC-α binding to PEP005.

The RasGRPs are positive regulators of the small GTPase Ras while chimaerins are negative regulators. Increased expression of RasGRP1 ad RasGRP3 show restricted distribution in tissue with prominent expression in lymphocytes with evidence that these proteins play an important role in the function of immune receptors of B- and T-cells (Aiba *et al.*, 2004, Stone, 2011). Stimulation of the immune receptors leads to phospholipase C activation and DAG accumulation in membranes. The C1 domains of RasGRP1 and RasGRP3 bind DAG and phorbol ester (Lorenzo *et al.*, 2000, Lorenzo *et al.*, 2001) leading to their translocation to cellular membranes where they interact with their substrate. Additionally, RasGRPs undergo an activating phosphorylation by PKC which is

itself activated by DAG (Brodie *et al.*, 2004, Ebinu *et al.*, 1998, Roose *et al.*, 2005). Ras activation by RasGRPs is important for thymocyte differentiation, T-cell effector function and lymphocyte homeostatis (Song *et al.*, 2013, Stone, 2011). This raises the possibility of RasGRPs being viable drug targets.

1.12 AIMS and HYPOTHESIS of this THESIS

Topical application of the protein kinase C activator PEP005 was shown to cure subcutaneous tumors in mice (Ogbourne *et al.*, 2004), primarily involving a neutrophil-dependent host inflammatory response. This is an expected reaction considering that one of the biological properties of PKC activators is to cause inflammation at the site of application. This also resulted in cure and a restoration of normal skin (Challacombe *et al.*, 2006, Ogbourne *et al.*, 2004).

The concept of intralesional therapy is to bypass the barrier zone and establish a sub-epidermal depot, thus allowing a higher concentration of the drug to act on the tumor. It eliminates the need for long-term topical treatment, coupled with the fact that it reaches deeply into the tumor tissue where topical medications may not penetrate. Pilot experiments of intralesional injections of PKC activators demonstrated the potential of treating larger tumors with similar outcomes as topical applications.

EBC-46 (formal name 12-tigloyl/angeloyl-13-(2-methylbutanoyl)-6,7-epoxy-4,5,9,12,13,20-hexahydroxy-1-tigliaen-3-one) is a short-chain diterpene ester of the tigliane class, isolated from a rainforest plant *Fontainea picrosperma* in North Queensland, discovered and purified by EcoBiotics Ltd. It is structurally similar to 12-O-13-tetradecanoylphorbol-acetate (TPA/PMA), and is thought to share similar bioactivity.

Hypothesis: intratumoral injections of PKC activating diterpene esters, notably EBC-46, can locally cure tumors by inducing an inflammatory response.

Aim 1. To determine the antitumor efficacy of EBC-46. The initial aim was to compare the antitumor efficacy of EBC46 with other potent PKC activators (e.g., TPA) *in vitro* and *in vivo*. This was achieved by inducing tumor cell arrest *in vitro* in a selection of sensitive and resistant tumor cell lines, and intratumoral injection in mouse tumor models.

Aim 2. To determine the role of the inflammatory response in EBC-46 efficacy. The pro-inflammatory response to the diterpene esters was determined by assessing the respiratory burst in human neutrophils and the tumoricidal activity of treated neutrophils towards tumor cells.

Aim 3. To investigate the role of neutrophils in the antitumor efficacy of EBC-46.

Aim 4. To determine the cellular and molecular responses of tumor and host cells after treatment with EBC-46. Capillary damage, neutrophil density, mode of cell death were inferred from immunohistochemistry and histopathology of tissue sections taken at various time-points. Whole genome arrays were used to follow changes in gene expression in host and tumor cells following treatment with EBC-46.

Chapter Two

Materials and Methods

2.1 Materials

2.1.1 Biologicals & Chemicals:

12-O-tetradecanoylphorbol-13-acetate (TPA)	Sigma Chemicals
Acetic acid	Merck
Agarose	Invitrogen
Ammonium persulfate	Sigma Chemicals
Bisindolylmaleimide-1 (BIS-1)	Sigma Chemicals
Bromophenol blue	Mallinckrodt
CellTitre 96 Aqueous One Solution Assay	Promega
Collagenase A	Roche Applied Science
Deionized formamide	Amresco
Dihydroethidium bromide (DHE)	Sigma Chemicals
Dimethyl sulfoxide (DMSO)	Sigma Life Sciences
Ethanol	BDH Chemicals
Ethidium bromide	Sigma Chemicals
Fetal Calf Serum (FCS)	Gibco Life Technologies
Glycerol	Sigma Chemicals
Glycine	BDH Chemicals
Hank’s balanced salt solution	Gibco Life Technologies
Hydrochloric acid (32% (v/v) HCl)	APS
Isopropanol	BDH Chemicals

Methanol	Merck
Methylated spirits	KCB
MilliQ water	Millipore
Penicillin/Streptomycin	Gibco Life Technologies
Phosphate Buffered Saline	prepared at QIMR Berghofer
Polyacrylamide 30% (mono:bis 29:1)	Bio-Rad Laboratories
Propidium Iodide	Sigma Chemicals
Propylene Glycol (PG)	Sigma Life Sciences
Protease Inhibitor Cocktail (PIC)	Roche Applied Science
RNase	Sigma Chemicals
RPMI-1640	prepared at QIMR Berghofer
Skim Milk powder	Diploma
Sodium chloride (NaCl)	Ajax Finechem
Sodium hydroxide (NaOH)	BDH Chemicals
Sulforhodamine B dye (SRB)	Sigma Life Sciences
TEMED	APS
Tris	Sigma Chemicals
Triton X-100	Sigma Chemicals
Trypsin	Invitrogen
Tween 20	Sigma Chemicals
β-Mercaptoethanol	Sigma Chemicals

2.1.2 Solutions:

1x SDS Running Buffer: 25 mM Tris (unbuffered), 250 mM glycine, 0.1% SDS. Buffer was made up to 1 litre with MilliQ water.

5% (w/v) Blotto: Dissolved 5 g of non-fat dry milk powder in 100 ml 1x PBS-Tween20 solution. For detection of phosphorylated proteins 1x PBS-Tween20 was substituted with 1x TBS-Tween20.

5% SDS-PAGE stacking gel: For 5 ml of stacking gel mix, added 3.4 ml MilliQ water, 830 µl of 30% acrylamide mix, 630 µl of 1.0 mM Tris (pH 6.8), 50 µl 10% SDS, 50 µl 10% ammonium persulfate (AMPS) and 5 µl TEMED.

1× Propidium Iodide Solution: Propidium iodide (50 mg/ml), RNase A (1 mg/ml), 0.01% (v/v) Triton X-100 freshly made-up in PBS just before use.

10x PBS-0.5% Tween20 Wash Buffer: Added 5 ml Tween20 to 1 litre 10x PBS solution.

10% SDS-PAGE resolving gel: For 10 ml of resolving gel mix added 4 ml MilliQ water, 3.3 ml of 30% acrylamide mix, 2.5 ml of 1.5 mM Tris (pH 8.8), 100 µl of 10% SDS, 100 µl of 10% ammonium persulfate (AMPS) and 4 µl TEMED.

10x TBS-1% Tween20 Wash Buffer: Dissolved 80 g NaCl, 24.4 g Ultra-Pure Tris, 10 ml Tween20 in MilliQ water. Adjusted pH to 7.5 with 32% HCl. The buffer was made up to 1 litre with MilliQ water. The TBS-Tween20 wash buffer was used when probing for phosphorylated proteins.

Collagenase A: A working solution of 1 mg/ml of Collagenase A (Roche) was prepared in 1X Hank's solution (Gibco) and sterilized using a 0.20 µm filter unit (Sartorius Stedim Biotech). The sterile Collagenase A solution was diluted to 1:10 in RPMI-1640 and used in *ex vivo* cultures of tumors.

Cell Lysis Buffer: A stock of 20 ml of cell lysis buffer was prepared with 4 ml of 100% glycerol, 2 ml of 10% SDS, 1 ml of 200 mM stock Tris pH 7.4. The solution was made up to desired volume by adding 12.8 ml MilliQ H_2O.

Diterpene Ester Stocks: 10 mg of EBc-46 or TPA was weighed into a 2 ml glass vial and labeled. A stock solution of 10 mg/ml was made up by dissolving the powder in 1 ml of 20% propylene glycol

(PG) (100% PG + Saline) or 1 ml of 100% Ethanol (EtOH). The 10 mg/ml stocks were stored at -20˚C.

Electroblot Buffer: 250 mM glycine, 25 mM Tris (unbuffered), 20% methanol, MilliQ water. Buffer was stored at 4˚C until ready to use for protein transfer.

Formamide Loading Buffer: 50% Glycerol, 40% deionised formamide, 1 mM EDTA, 0.4% Bromophenol Blue.

Sulforhodamine B solution: Dissolved 4.0 g SRB (Sigma) in 1 litre 1% acetic acid (Merck; prepared in MilliQ H_2O and stored at room temperature). The prepared solution was transferred to 4 x 250 ml Schott bottles and stored at 4˚C. The working bottle was stored at RTemp.

2.2 Methods

2.2.1 Cell Lines

The cell lines used in this project were of mouse and human origin and included those described in Table 2.1.

2.2.2 Cell Culture

Cells were cultured at 37 degrees Celsius in a humidified 5% CO_2 incubator in RPMI-1640 culture medium supplemented with 10% v/v fetal calf serum (heat-inactivated at 55˚C for 30 min after thawing in a 37˚C water bath), 50 µg/ml penicillin, 50 µg/ml streptomycin and 3 mM HEPES.

2.2.3 Cryopreservation

Cells were stored at -70˚C when in log phase growth as a source of viable cells for future experiments. Cells were harvested when ~80% confluent, pelleted at 1,500 rpm, 5 min, resuspended in a final concentration of 10% DMSO in RPMI-1640 culture medium and cooled to -80˚C in a Cryo Freezing Container before transferring to liquid nitrogen (-196˚C).

2.2.4 Resuscitation and Maintenance of Cells

Cells stored in liquid nitrogen were transferred to -70˚C, and then thawed to room temperature before culturing. The cells were diluted 1:10 with RPMI-1640 culture medium, centrifuged at 1,500 rpm for 5 min at RTemp, then resuspended in 5 ml of fresh RPMI-1640 medium. The cell suspension was transferred to 25 cm^2 flasks (T25) and incubated at 37˚C. To maintain cells in log phase, cultures were passaged biweekly.

2.3 In Vitro Growth Inhibition

2.3.1 Sulforhodamine B proliferation Assay

The Sulforhodamine B (SRB) assay was developed in 1990 by Skehan *et al.*, to measure drug–induced cytotoxicity with a clonogenic-type assay, whereby cell proliferation was allowed to proceed for an extended period after drug treatment, followed by comparison of cell numbers relative to controls using a quantitative protein stain. Its principle is based on the ability of the pink acidic SRB dye to bind electrostatically to basic cell proteins that had been fixed to tissue–culture plates by trichloroacetic acid.

In the present method, cells sparsely seeded in microtitre plates (3000 cells/well) were treated for 5-6 days. The medium was then tipped off and cells washed with PBS to remove excess FCS protein. Cells were then fixed with 95% ethanol (methylated spirits) for a minimum of 5 min. The fixative was tipped off; cells washed once with tap water and stained with 50 µl/well of 2% SRB solution in 1% acetic acid for 15 min. The SRB stain was tipped off and wells washed twice, rapidly but gently with 1% acetic acid. 100 µl/well of 10 mM Tris base (unbuffered, pH > 9) was added. The absorbance of the wells was read at 564 nm on the ELISA reader (VERSA max microplate reader; Molecular Devices) with 3 second prior shaking to ensure that the released dye was evenly distributed throughout the well. Cell survival was plotted as % control absorbance vs. dose.

2.3.2 MTS Cell Proliferation Assay

The CellTitre 96 Aqueous One Solution Assay from Promega is a colorimetric method for comparing the number of viable cells in proliferation. The solution contains a thiazolium compound

which is bioreduced by cells to a coloured formazan product, and an electron coupling reagent PES. The quantity of formazan product solubilised in the culture medium is measured as absorbance at 490 nm and is directly proportional to the number of viable cells in culture.

10 µl of the MTS reagent was added to each well of a 96–well plate containing 100 µl of cell suspension and the plate incubated at 37˚C for ~2 hr until a dark brown colour developed in wells. 10 µl/well of 10% SDS was added and the plate centrifuged at 2,000 rpm for 15 min. The absorbance was recorded at 490 nm using the ELISA plate reader with 10 second prior shaking. Cell survival was plotted as % control absorbance vs. dose.

2.4 Inoculation of tumor cells into mice

Mice were housed, and all animal work carried out in the QIMR Animal facility. Experiments were approved by the QIMR Animal Ethics Committee (P345). The mice used for *in vivo* experimentation were male immunocompetent C57BL/6J mice and male immunocompromised BALB/c *Foxn1*^{nu} mice. Procedures were carried out in a pathogen-free environment in a laminar flow hood. B16-F0, Sk-Mel-28, MC38 tumor cells were inoculated into mice in different experiments. The tumor cells from serial passaging were trypsinized using trypsin/versene in Dulbecco's solution and suspended in RPMI-1640 media with 10% FCS. A cell count was performed using a haemocytometer and the number of cells required for injection calculated. Listed below are the different cell lines experimented upon, along with the cell densities injected per 50 µl and the respective mice (Table 2.2). The cell suspension was centrifuged at 1,500 rpm for 5 min and the cell pellet resuspended in the required volume of culture media. This cell suspension was taken to the animal house on ice. When C57BL/6J mice were used, their hindquarters were shaved with battery-operated clippers prior to inoculation. Using a Terumo® U-100 Insulin 29G x ½" needle with the bevel facing upwards, 50 µl of the cells were injected subcutaneously into 2 sites on the hindquarter of the mouse. Mice were tagged using an ear punch. Mice were then placed back in their cage and monitored for clinical signs and tumor growth. Tumor volume was determined from the formula length x length x breadth / 2 according to the chart in Appendix Table 1, "Monitoring of Tumor Bearing Mice".

2.5 Intratumoral injections of tumors

Tumor sites were observed until they were at the desired volume range of approximately 100 mm^3 at the start of the treatment. Due to the heterogeneity of the tumor population, occasionally smaller and larger tumors were included in the study. EBC-46 or TPA was dissolved in propylene glycol (PG) solution in varying concentrations, warmed in a 37˚C water bath for 1–2 hr, vortexed for 10 seconds and spun for 5 seconds. The baseline dose of EBC-46 used was 30 µg in 20% PG in a final volume of 50 µl. As a control, 50 µl of 20% PG was injected into tumors. Injections were carried out using a 0.3 ml Terumo® U-100 Insulin syringe with a 29G x ½" needle. The mice were placed back in the cage and monitored daily.

2.6 Monitoring of mice and tumors

Mice were monitored by measuring tumor volume and tissue reaction which was determined by the purplish discolouration and the eventual eschar formation within 5 days after treatment with the diterpene esters EBC-46 or TPA. The tumor sites were measured prior to the first treatment and then underwent regular monitoring 2 – 3 times per week.

Tumor volume: The tumor length (l), width (w) ad height (h) were measured using digital Vernier callipers (Kinachrome) and the tumor volume calculated using the formula (l x w x h) in mm^3.

The raw data for the above measurements was recorded in the Microsoft Excel program and the average calculated and plotted against time with the standard error (SE). A Kaplan-Meier survival curve was prepared in GraphPad Prism 6 with percent survival as a function of time. Mice were monitored for up to 3 months after treatment of tumor. When the tumor load per mouse became too large (approximately 1000 mm^3) the mice were euthanized with carbon dioxide (CO_2) inhalation.

Table 2.1 Cell Lines used in this study

Cell Line Name	Species	Disease	Source
B16-F0	Mouse	Melanoma	ATCC № CRL-6322
MC38	Mouse	Colon Carcinoma	QIMR Berghofer
Sk-Mel-28	Human	Metastatic Melanoma	ATCC № HTB-72
D04	Human	Metastatic Melanoma	QIMR Berghofer
MM649	Human	Metastatic Melanoma	QIMR Berghofer
A549	Human	Lung Carcinoma	ATCC № CCL-185
HOP-62	Human	Non-small Cell Lung Carcinoma	QIMR Berghofer
K562	Human	Leukaemia	QIMR Berghofer

Table 2.2 Table detailing the densities of the tumor cell lines inoculated into mouse models.

Cell Line	Cell Density per site	Mice strain used	№ of sites per mouse
B16-F0	5 x 10^5 cells / 50 µl	C57BL/6J	2 tumor sites
MC38	10^6 cells / 50 µl	C57BL/6J	2 tumor sites
Sk-Mel-28	2 x 10^6 cells / 50 µl	BALB/c *Foxn1*^{nu}	2 tumor sites

2.7 *Ex Vivo* Cell Survival Assessment

An *ex vivo* cell survival was performed to assess the time course for clonogenic survival of tumor cells after treatment with EBC-46. Sk-Mel-28 tumors grown in male BALB/c *Foxn1^{nu}* nude mice were treated with 30 µg of EBC-46 parallel with 20% propylene glycol (PG) injection of controls.

Control and treated tumors were harvested from euthanized mice using sterile disposable surgical instruments. Tumors were briefly washed in 70% ethanol, teased out in 1 ml sterile PBS and pelleted at 1,500 rpm for, 5 min at RT. Cells were resuspended in complete RPMI-1640 with collagenase A (recipe in Section 2.1.2) and incubated at 37˚C for 30 min. Collagenase A was used in *ex vivo* cell cultures for disaggregation of the tissues and preparation of single cell suspensions. The Collagenase A-treated cells were then centrifuged at 1,500 rpm for 5 min, resuspended in complete RPMI-1640 and plated into 24–well plates at 3-fold serial dilutions to achieve varying densities (Figure 2.1). Cells were incubated at 37˚C in a humidified 5% CO_2 incubator and were monitored daily. The dilution that allowed controls to become confluent within 3-5 days was subjected to SRB assay (Section 2.3.1) as a measure of clonogenic survival of cells from the treated tumor.

2.8 Gene Expression Analysis using Microarrays

2.8.1 Total RNA extraction and purification

2.8.1.1 In vivo tumor treatments

Sk-Mel-28 tumors were grown subcutaneously in BALB/c *Foxn1^{nu}* mice with two tumors per mouse. Three individual experimental groups of mice were divided into three treatment groups: vehicle, TPA or EBC-46. Mice in the control vehicle treatment group received a single intratumoral injection (Terumo® U-100 Insulin 29G x ½" syringe) of 50 µl of 20% PG per tumor. The mice in the TPA – and EBC-46 – treatment groups received a single intratumoral injection of 30 µg per tumor of TPA or EBC-46 respectively in 50 µl of 20% PG. To determine/analyze the gene expression profile of tumor and host in response to EBC-46 treatment over a time-frame, tumors were excised at different times, 30 min, 1 hr, 2 hr, 4 hr and 8 hr after treatment and stored at -80˚C.

	0 dilution	1:3 dilution	1:9 dilution	1:27 dilution	1:81 dilution	1:243 dilution
Time 1	1 ml of cell suspension	700 µl RPMI + 300 µl from well 1	700 µl RPMI + 300 µl from well 2	700 µl RPMI + 300 µl from well3	700 µl RPMI + 300 µl from well 4	700 µl RPMI + 300 µl from well 5
	1 ml of cell suspension	‘‘	‘‘	‘‘	‘‘	‘‘
Time 2	1 ml of cell suspension	‘‘	‘‘	‘‘	‘‘	‘‘
	1 ml of cell suspension	‘‘	‘‘	‘‘	‘‘	‘‘

Figure 2.1: Plate format for *ex vivo* cell survival of tumor cells treated with EBC-46 *in vivo*.

2.8.1.2 In vitro cell treatments

Whole blood from a human donor was processed and peripheral blood mononuclear cells (PBMCs) were isolated by Dr. Viviana Lutzky. The PBMCs were cultured in RPMI-1640 10% FCS and treated 4 hr after seeding with the diterpene ester compounds EBC-46 or TPA at 30 ng/ml concentration. Untreated PBMCs were used as the control in this experiment. Cells were harvested at different times following treatment with the compounds, at 4 hr, 24 hr and 96 hr. The cell monolayer was washed once with phosphate buffered saline (PBS) and cells were harvested using sterile cell scrapers. The harvested cells were centrifuged (Eppendorf Centrifuge 5810 R) at 1,500 rpm for 5 min at RTemp. Cell pellets were stored at -80˚ C.

2.8.1.3 Total RNA extraction and purification

Approximately 30 mg of frozen tumor sample was weighed or 1 x 10^7 cells were counted and total RNA extracted using the Qiagen RNeasy Plus Mini Kit, according to manufacturer's instructions. The samples were homogenized using a rotor-stator homogenizer (Polytron) in Buffer RLT Plus containing 10 µl/ml *β*-mercaptoethanol (*β*-MeOH). Supernatant was collected after centrifugation (Eppendorf Centrifuge 5415 D) at maximum speed for 3 min and passed through a gDNA Eliminator spin column with a further centrifugation for 1 min at 10,000 rpm. An equal volume of 70 % ethanol was added to the flow-through and mixed well by pipetting. This was immediately passed through an RNeasy spin column in aliquots and centrifuged for 30 sec (10,000 rpm; RTemp). Columns were washed with 700 µl Buffer RW1 and centrifuged at RTemp for 30 sec (10,000 rpm), followed by two washes with 500 µl Buffer RPE and centrifuged at 10,000 rpm for 30 sec – 2 min. Total RNA was eluted with 50 µl RNase-free water by centrifugation for 1 min at maximum speed.

2.8.1.4 Total RNA quantity and quality determination

The concentration of total RNA extracted was measured on a NanoDrop (NanoDrop® ND-1000 UV-Vis Spectrophotometer) using 1 µl of the RNA sample. RNA integrity was determined by denaturing agarose gel electrophoresis and staining with ethidium bromide (EtBr). An aliquot of 2 µl of the RNA sample was diluted 1:5 in water, and a formamide-based loading buffer was added to denature the RNA. The RNA was heated to 65˚C for 5 min before loading into the gel. The agarose gel was run at 80 V for 45 min to separate the bands for visualization on a UV gel doc. An molecular weight size marker (1 kb Marker, Life Technologies) included in the gel run was not only a good control to ensure the gel was run properly but also facilitated the determination of the size of the bands. Distinct 28S rRNA and 18S rRNA bands indicated intact ribosomal RNA where the ratio should be approximately 2:1. A smear towards the smaller sized RNAs indicated partial degradation of RNA while completely degraded RNA appeared as a low molecular weight smear.

2.8.2 Whole Genome Gene Expression Direct Hybridization Assay

Total RNA extracted from tissues or cells was amplified using the Ambion Illumina® TotalPrep RNA Amplification Kit to produce an amplified amount of biotin-labeled cRNA. The RNA Amplification Kit consists of a first- and second-strand reverse transcription step to produce cDNA

with a T7 site overhang, followed by an *in vitro* transcription amplification step that incorporates biotin-labelled nucleotides. The subsequent steps include array hybridization, washing, blocking and Cy3-Streptavidin staining. The Direct Hybridization gene expression assays were imaged using the iScan System.

2.8.2.1 RNA amplification and labeling

Approximately 500 ng of total unlabelled RNA was adjusted to a final volume of 11 µl with nuclease-free water. The RNA was incubated with 9 µl of the reverse transcriptase master mix (1 µl of T7 Oligo (dT) Primer, 2 µl of 10X first strand buffer, 4 µl of dNTP mix, 1 µl of RNase inhibitor and 1 µl of ArrayScript) at 42 ˚C for 2 hr. This was followed by the second strand cDNA synthesis step which involved a further incubation at 16 ˚C for 2 hr with 80 µl of the second strand master mix (63 µl nuclease-free water, 10 µl 10X second strand buffer, 4 µl dNTP mix, 2 µl DNA polymerase and 1 µl RNase H). The cDNA was purified by filtering through a cDNA Filter Cartridge with 250 µl of cDNA binding buffer and washing with 500 µl of the wash buffer provided in the kit. Purified cDNA was eluted with 20 µl of 55 ˚C nuclease-free water. The next stage involved the synthesis of cRNA by *in vitro* transcription to generate multiple copies of biotinylated cRNA from the double-stranded cDNA templates where each cDNA sample was incubated with 7.5 µl of the IVT master mix (2.5 µl of T7 10X reaction buffer, 2.5 µl of T7 enzyme mix and 2.5 µl biotin-NTP mix) at 37 ˚C for 16 hr. The reaction was stopped with the addition of 75 µl of nuclease-free water to each cRNA sample. The biotinylated, amplified RNA was purified by filtering the cRNA samples through cRNA Filter Cartridges with 350 µl of cRNA binding buffer and 250 µl of 100 % ethanol mixed together prior to loading onto the filters. The cRNA filter cartridges with attached RNA were then washed with 650 µl of wash buffer before eluting purified cRNA with 200 µl of 55 ˚C nuclease-free water.

2.8.2.2 Illumina Expression BeadChip Hybridization

The biotinylated cRNA was quantified on the NanoDrop® ND-1000 UV-Vis Spectrophotometer before hybridization to the Illumina Expression BeadChips. The cRNA samples were heated at 65 ˚C for 5 min and collected by pulse centrifugation. Approximately 750 ng of each biotin-labelled cRNA sample was aliquoted into separate tubes to which were added ~ 5 µl of RNase-free water and 10 µl of Hyb Mix. Approximately 15 µl of the prepared cRNA mix was loaded onto the

Illumina Expression BeadChips. The HumanHT-12 v4 Expression BeadChips provide coverage for more than 47,000 transcripts and known splice variants across the human transcriptome while examination of 12 samples in parallel. The MouseRef-8 v2.0 Expression BeadChips present updated content for the mouse genome targeting approximately 25,600 well-annotated RefSeq (Reference Sequence) transcripts over 19,000 unique genes.

According to the Whole-Genome Gene Expression Direct Hybridization Assay Guide provided by Illumina, the loaded BeadChips with the cRNA samples were inserted into the Hyb Chamber and allowed to hybridize overnight for 16 hr at 58 ˚C. The seals of the BeadChips were removed while submerged in E1BC wash buffer and then washed with 1X High-Temp Wash Buffer in a Hybex waterbath at 55 ˚C for 10 min. The high temperature wash was followed by a room-temp wash in 250 ml of Wash E1BC Buffer on an orbital shaker for 5 min. The rack with the BeadChips was then transferred to a staining dish for another wash with 250 ml 100 % ethanol for 10 min followed by a second room-temp wash in 250 ml of fresh Wash E1BC Buffer for 2 min. The BeadChips were then transferred to wash trays with 4 ml of Block E1 Buffer and placed on a rocker for 10 min. Cy3-Streptavidin (Cy3-SA) fluorescent dye was used to stain the probes. Two ml of Block E1 Buffer with 1:1000 dilution of Cy3-SA was prepared for each BeadChip which was added to new wash trays with the BeadChip. The wash trays were covered from light with a lid and rocked for 10 min at room-temp. Excess stain was washed off the BeadChips with a third room-temp wash in 250 ml of fresh Wash E1BC Buffer for 5 min on the orbital shaker and dried by centrifugation (Eppendorf Centrifuge 5810 R) at 1,400 rpm for 4 min at room temperature.

2.8.2.3 Data Normalization and Analysis

Raw microarray data generated by the iScan System were extracted in GenomeStudio using default settings and were then exported into GeneSpring GX v12.5 (Agilent Technologies, Santa Clara, CA, USA) for processing where the expression values were normalized using quantile normalization with default settings. The entities were filtered based on the detection score calculated by GenomeStudio where $p \leq 0.05$ was considered significant.

2.9 Protein Analysis

2.9.1 Preparation of Protein Samples

Cells were grown in 25 cm^2 or 75 cm^2 flasks and grown to 70% confluence. B16-F0 cells were grown in T25 flasks due to their proliferative growth and Sk-Mel-28 cells were grown in T75 flasks.

The culture medium from the flasks was removed by aspiration. The cell monolayer was washed once with ice-cold PBS and cells were harvested using sterile disposable cell scrappers. Cells were collected by centrifugation at 1,500 rpm for 5 min. The pellets were resuspended in 1 ml ice-cold PBS and transferred to 1.5 ml eppendorf tubes. Cells were collected by spinning at full speed (~13,200 rpm) for 1 min in an Eppendorf Centrifuge 5415 D. The supernatant was discarded and the pellets stored at -20˚C.

The frozen pellets were thawed on ice, and resuspended in cell lysis buffer about 3-4 times the volume of the pellet. The cells were lysed in 200 µl cell lysis buffer (recipe in Section 2.1.2) and were sonicated using a Branson Sonifier 250) for 30-40 pulses at 4˚C with a duty cycle of 30% and output control of 3. The cell lysates were centrifuged at 4˚C for 10 min at 13,200 rpm to isolate the soluble fraction, which was then transferred to a fresh 1.5 ml eppendorf tube for determination of protein quantity. The extracted protein was stored at -70˚C.

2.9.2 Determination of Protein Concentration

Bovine Serum Albumin (BSA) protein standards (Pierce Chemical Corporation) were used to quantify the amount of protein in each sample. This method is based on the well-known reduction of copper Cu^{2+} to cuprous cation Cu^{1+} by protein in an alkaline medium (the biuret reaction) with the highly sensitive and selective colorimetric detection of Cu^{1+} using a unique reagent containing bicinchoninic acid. The purple-coloured end-point of this assay is formed by the chelation of two molecules of BCA with one cuprous ion and exhibits a strong absorbance at 562 nm which is nearly linear with increasing protein concentrations over a broad working range (20-2000 µg/ml) (as explained in the manufacturer's instructions provided in the kit).

Protein samples were diluted 1:10 (v/v) in MilliQ H_2O and 10 µl was plated out in duplicate in a flat-bottom 96-well plate (Costar). A final volume of 100 µl of BSA working reagent (50 parts reagent A: 1 part reagent B) from the BSA protein assay kit was added to each well. The solutions were mixed well by pipetting and the plate was incubated at 37˚C for 30 min before reading at 564 nm using an ELISA plate reader (VERSA max microplate reader; Molecular Devices). The concentration of the protein in the samples was determined by interpolations on the standard curve.

2.9.3 SDS Polyacrylamide Gel Electrophoresis

Depending upon the amount of protein extracted, approximately 15-30 µg of the protein sample was loaded onto SDS-PAGE gel alongside 10 µl of BenchMark™ Prestained Protein Ladder (Gibco Life Technologies). Prior to loading, protein samples were prepared with 2x SDS loading buffer with β-mercaptoethanol and made up to a final concentration (w/v) of 2 µg/µl with cell lysis buffer. Samples were denatured at 65˚C for 5 min. The SDS-PAGE gel was prepared using the minigel system (Bio-Rad Laboratories). A 10% resolving gel was prepared (Section 2.1.2) and allowed to set for 30-40 min at RTemp while overlayed wit water-saturated butanol. Before pouring the 5% stacking gel, the water-saturated butanol was tipped off, the stacking gel poured on top of the resolving gel with a 10-well comb (Bio-Rad Laboratories) and allowed to set for 15 min. Electrophoresis was performed for approximately 45 min or until the dye had run off the bottom of the gel in 1x SDS running buffer (200 V, RTemp).

2.9.4 Western Blotting

Following SDS-PAGE electrophoresis, the gel plates were carefully separated, and the stacking gel transferred to a transblot apparatus. The transfer sandwich was assembled as follows: a porous sponge pre-wet in cold electroblot buffer, a sheet of blotting (Whatmann) paper, Hybond-C nitrocellulose membrane (Amersham Pharmacia), the gel, another sheet of blotting paper, lastly followed by another porous sponge soaked in cold electroblot buffer. This was then inserted into the transfer apparatus with the nitrocellulose membrane closer to the anionic side. Care was taken to prevent any air bubbles during assembly as it would result in inconsistent transfer of proteins. The proteins were transferred at 100 V for 1 hr in ice-cold transfer buffer at 4˚C with an ice-pack and magnetic stirrer added to maintain temperature during transfer.

2.9.5 Immunodetection of Proteins

Once transferred, the nitrocellulose membrane was incubated in 5% (w/v) Blotto at room temperature for 1 hr with gentle orbital shaking (Bioline) to block non-specific binding sites. The primary antibody was diluted as recommended by the manufacturer in 5% (w/v) Blotto to a final volume of 2 ml. A plastic envelope containing the membrane and antibody was prepared and heal-sealed, removing any air bubbles present. The membrane was rotated at 4˚C overnight (approximately 16 hr) on a custom made rotor. A list of antibodies used in this study has been compiled in Table 2.3.

Following the incubation period, the membrane was removed from the bag, placed in a plastic tray with 1x PBS-0.05% Tween20 or 1x TBS-0.1% Tween20 and washed (3 x 2 min; 2 x 5 min) on an orbital shaker and incubated with the appropriate secondary antibody made up in 2 ml 5% Blotto for 1½ hr at RTemp on the rotator. Blots were washed as previously with 0.05% Tween20 in 1x PBS. Antibody detection was performed using the Enhanced Chemilluminescence (ECL) detection kit (Perkin Elmer). Following 1 min of incubation in the chemilluminescence solution (equal volumes of Enhanced Luminol Reagent and Oxidizing Reagent) the blots were dried using blotting paper and imaged using the X-OMAT autoradiography film (Kodak; Rochester, NY).

2.10 Histology

Mice were euthanized by cervical dislocation at various times following a single intratumoral injection of EBC-46 or vehicle to the pre-established tumor. The treated sites were excised using sterile disposable surgical instruments. One tumor each of vehicle – treated and EBC-46 – treated were fixed in 10% phosphate buffered formalin for histological processing. Tumors were processed and stained for H&E, neutrophils, macrophages, mast cells and endothelial cells by Clay Winterford, Rita Collins and Glynn Rees of QIMR Berghofer Histology Facility. Tissue – section slides were scanned at 20x magnification using the Aperio XT Scanscope.

2.11 Cytokine Expression Analysis

2.11.1 Preparation of samples

a. From animal tumors

Mice were treated with 30 µg of EBC-46 per tumor site (maximum of 4 sites per mouse) over a time – course with duplicates at each time. Control and treated tumors were harvested using sterile disposable surgical instruments. Tumors were briefly washed in 70% ethanol, and cells were teased out into 1 ml PBS with a final 1x concentration of protease inhibitor cocktail from Roche. The cell suspension was centrifuged at 1,500 rpm for 5 min at RTemp. The supernatant was stored at -80˚C until ready to assay for cytokines using either the mouse or human inflammation kits depending on the origin of the cell lines. Whole blood from these mice was collected and the serum was assessed for soluble cytokines using the mouse inflammation kit.

b. From cultured cells

Tumor cells of both human and mouse origin were grown in 24 – well cell culture plates (Corning) and treated with varying doses of EBC-46 in the presence of human peripheral blood mononuclear cells (PBMC) at various times. Cells were incubated with RPMI-1640 culture media prepared with 10% v/v FCS and antibiotics. At the different time – points, the medium was transferred to labelled 1.5 ml eppendorf tubes and centrifuged at 10,000 rpm for 2 min. The supernatants were collected in fresh eppendorf tubes and stored at -80˚C until ready to assay for cytokines using either the mouse or human inflammation kits depending on the origin of the cell lines.

2.11.2 Cytokine Expression Analysis

The BD (Becton Dickinson) Cytometric Bead Array assays provide a method for capturing a soluble analyte or set of analytes using beads of known sizes and fluorescence, thus making it possible to detect analytes by flow cytometry. Each supernatant was assayed in duplicate for the presence of soluble cytokines in the host and in the tumor microenvironment using the BD (Becton Dickinson) Inflammation Kits for mice and humans respectively (Table 2.4) and a FACSArray plate reader (BD Biosciences) according to manufacturer’s instructions.

Table 2.3: Antibodies Used in this Study

Antibody	Origin	Dilution	Supplier
Anti-PKC α	Mouse	1:1000	Pharmingen, Becton and Dickinson Biosciences
Anti-PKC β	Mouse	1:250	Pharmingen, Becton and Dickinson Biosciences
Anti-PKC δ	Mouse	1:500	Pharmingen, Becton and Dickinson Biosciences
Anti-Phospho-p44/42 MAPK (Thr202/Tyr204)	Rabbit	1:1000	Cell Signaling
Anti-p44/42 MAPK	Rabbit	1:1000	Cell Signaling
Anti-Phospho-MEK1/2	Rabbit	1:1000	Cell Signaling
Anti- MEK1/2	Rabbit	1:1000	Cell Signaling
Anti-Phospho-PKC (pan)	Rabbit	1:1000	Cell Signaling
Anti-GAPDH	Rabbit	1:10,000	R & D Systems
Anti-Mouse Ig HRP-conjugate	Sheep	1:1000	Chemicon
Anti-Rabbit Ig HRP-conjugate	Sheep	1:1000	Chemicon
Anti-Rabbit Ig HRP-conjugate	Sheep	1:1000	Cell Signaling

Table 2.4: Cytokine Bead Assay kits used in this study

BD CBA Inflammation Kit	Target proteins
Mouse Inflammation Kit	IL-6, IL-10, MCP-1, IFN-γ, TNF, IL-12p70
Human Inflammation Kit	IL-8, IL-1β, IL-6, IL-10, TNF, IL-12p70

2.12 Neutrophil Recruitment

B16-F0 and Sk-Mel-28 cells were injected into male C57BL/6 and BALB/c *Foxn1*^{nu} mice, respectively. Tumors were allowed to grow to approximately 100 mm^3, following which mice were segregated into cages and experimental groups labelled as per table below Table 2.5 Mice were administered with the neutrophil neutralizing anti-Ly-6G antibody or the isotype control IgG_2 antibody via intraperitoneal (IP) injection on days -2, 0 and 2 relative to treatment with EBC-46 (50 µl of 600 µg/ml) or the 50 µl of the control vehicle 20% PG. The neutrophil counts in blood were determined for each of the groups by preparation of blood smears immediately after treatment on SuperFrost® Plus slides from Menzel-Glaser. Mice were regularly monitored until tumors were ablated or mice were culled as a result of tumor burden.

Dried blood smears were fixed with methanol and air dried. Slides were placed in staining racks and submerged in a container with Quick Dip stain I (Fronine/Thermo Fisher Scientific for leukocytes) 1 for 30 sec. The slides were rinsed by dipping into a container with water and were then transferred to a second container with Quick Dip solution II (Fronine/Thermo Fisher Scientific) for 30 sec. The stained slides were placed under gentle running water to wash off excess Quick Dip solution II and were left to dry overnight. Once dried, cover slips were applied onto the slides using 20 – 40 µl of the fixative Kaiser's glycerol gelatine, depending on the area of smear. Slides were allowed to set and dry before observing under 40X magnification.

2.13 Respiratory Burst

Human neutrophils were isolated from fresh blood by lysis of the red blood cell pellet obtained by sedimentation using Ficoll-Plaque. Isolation of the human neutrophils was carried out by Dr. Viviana Lutzky. The neutrophils (~ 4 x 10^6 cells/ml) were incubated with 10 µg/ml dihydroethidium (DHE) (Sigma-Aldrich) in complete culture medium at 37˚C for 15 min alongside an aliquot of unstained cells to be tested as unstained control. This was followed by treatment with EBC-46 or TPA at 0, 1 ng/ml, 10 ng/ml, 100 ng/ml, 1 µg/ml, 10 µg/ml, 100 µg/ml for 15 min. Neutrophils were also treated with BIS-1 (pan-PKC inhibitor) to determine the PKC activating characteristic of EBC-46. For this, neutrophils were treated with a final concentration of 2 µM of BIS-1 for 1 hr prior to diterpene ester treatment with EBC-46 or TPA. Reactive oxygen species generated in the oxidative burst resulted in an increase in fluorescence (emission at 610 nm), measurable immediately on a FACS Canto flow cytometer. The experiment was completed in triplicate.

Table 2.5: Mouse Treatment Groups for Neutrophil Recruitment Study

<table>
<tr><th>Day -2</th><th>Day 0</th><th>Day 2</th></tr>
<tr><td rowspan="4">IgG_2
or
anti-Ly-6G</td><td>IgG_2
or
anti-Ly-6G</td><td rowspan="4">IgG_2
or
anti-Ly-6G</td></tr>
<tr><td>+</td></tr>
<tr><td>30 µg EBC-46
or
20% PG</td></tr>
</table>

2.14 Live uptake of Propidium Iodide

Approximately 3-5 x 10^4 cells/well were seeded in a 96-well microtitre plate. Cells were treated with either EBC-46 or TPA (100 µg/ml, 200 µg/ml and 300 µg/ml) for 30 min and 4 hr, alongside controls which included untreated cells and cells treated with 10 µl of 1% Triton X-100. Propidium iodide solution was added to give a 5 µg/ml final concentration for the last 30 min of treatment. The temperature of the cells was then decreased to zero by placing the plate on ice for about 5 min before imaging using the AMG EvosFl inverted fluorescence microscope at 20x magnification, to stop any further cytotoxic activity of EBC-46

Chapter Three

Activity Profile of EBC-46 versus TPA

3.1 Introduction

PKC activators such as diterpene esters have been extensively studied as potential agents for chemotherapy. Previous research in this laboratory has established that the diterpene ester PEP005 (ingenol-3-angelate) is a PKC activator (Kedei *et al.*, 2004) and is toxic to cancer cells.

Bioactivity-guided fractionation carried out by QBiotics together with the Drug Discovery Group at QIMR Berghofer Medical Research Institute revealed a potential PKC-activating compound in the extracts from the kernel of the Blushwood seed. The extracts were rich in diterpene esters. Preliminary experiments conducted in this laboratory on compounds from the Blushwood kernels established that intralesional injection of a purified compound cured mice bearing tumors of either the human metastatic melanoma MM96L or the murine B16-F0 melanoma cell line, suggesting a role for the compound in the treatment of melanoma.

The purified compound was found to be a novel short chain diterpene ester named EBC-46 (formal name 12-tigloyl/angeloyl-13-(2-methylbutanoyl)-6,7-epoxy-4,5,9,12,13,20-hexahydroxy-1-tigliaen-3-one). Elucidation of the chemical structure of EBC-46 revealed a polycyclic carbon skeleton similar to TPA (Figure 3.1). Hence it was proposed to share similar biological/functional properties with those of TPA.

Diterpene esters such as the phorbol ester TPA are known to target PKC by binding to the C1 domain and inducing the translocation of classical and novel PKC isoforms from the cytoplasm to the membranous fractions (Section 3.2.1). Given the structural similarity between TPA and EBC-46, a potential role of PKC as a target for this compound was explored.

The aim of the following studies was to characterize the PKC activity profile of EBC-46 and to compare it to that of the phorbol ester TPA. The studies focused on: (1) determining the ability of EBC-46 to selectively induce translocation of PKC isoforms possessing a C1 DAG-binding domain to the plasma membrane; (2) comparing the effects of EBC-46 to TPA on activation of MAPK signaling, a process known to be modulated by PKC activity; (3) establishing the potency of the diterpene esters in inducing human leukocytes into respiratory burst, a process reported to the dependent on PKC activity; and (4) testing the effect of EBC-46 on the cell cycle.

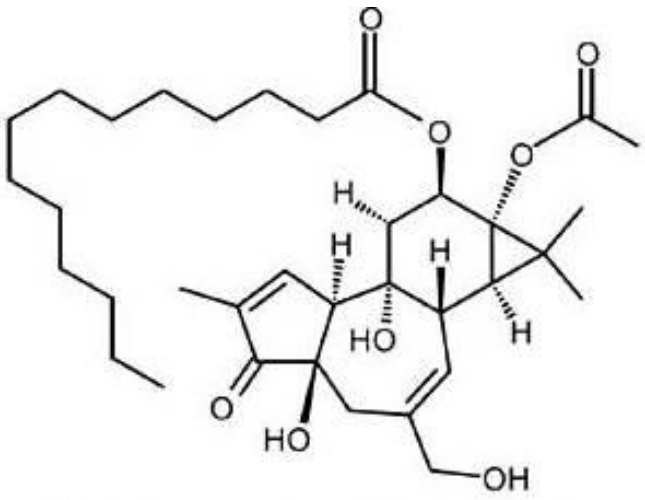

12-O-tetradecanoylphorbol-13-acetate (TPA)

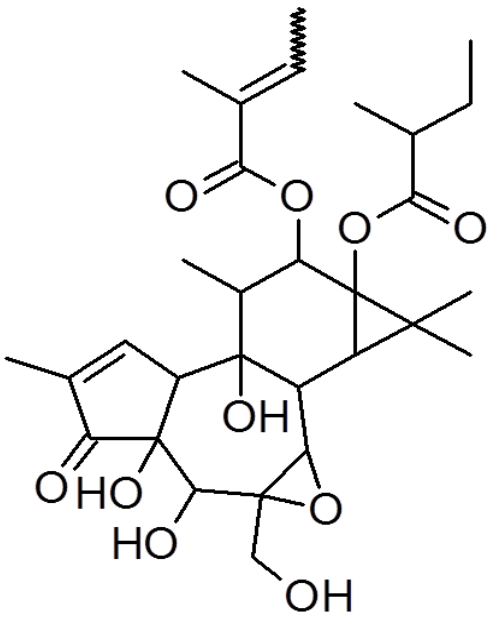

EBC-46

Figure 3.1: Structures of diterpene esters TPA and EBC-46 used in this study

(Evans, 1986, Goel *et al.*, 2007, Zucker *et al.*, 1974).

(Structure of EBC-46 obtained from Dr. Paul Reddell and Prof.Peter Parsons; unpublished data).

3.2 Results

3.2.1 Translocation of PKC Isoforms by EBC-46 and TPA

To determine whether EBC-46 was an activator of PKC, initial experiments aimed to establish the ability of EBC-46 to cause translocation of classical and novel PKC isoforms in HeLa cells transiently transfected with EGFP-tagged PKC vectors. The isoforms examined were α, β_1, β_2 and γ, and θ, and ζ of the classical, novel and atypical subfamilies respectively. Cells were treated with either 10 ng/ml, 30 ng/ml or 100 ng/ml of EBC-46 or TPA for 1 hour, a day following transient transfection of the tagged PKC isoforms. Control cells treated with the vehicle alone showed PKC isoforms to be localized in the cytosol, while cells treated with EBC-46 or TPA demonstrated differences in subcellular localization of the activated PKC isoforms. TPA resulted in efficient translocation of PKC-α, -β_1, -β_2, γ and θ. As expected, neither compound led to translocation of atypical PKC-ζ which lacks the C1 domain required for binding of phorbol esters (Figure 3.2). EBC-46 resulted in complete translocation of PKC isoforms -β_1 and -β_2 and less translocation of –α and –γ isoforms (Figure 3.2). Fluorescence microscopy showed PKC-β to be translocated to the plasma membrane following treatment with EBC-46 similar to that of TPA in comparison to control PKC β_1 localized in the cytosol of tested HeLa cells (Figure 3.3). TPA translocated PKC-θ from the cytoplasm to the plasma membrane and other organelles such as the Golgi, and nucleus. In contrast, treatment of HeLa cells transiently transfected with EGFP tagged PKC-θ with EBC-46 led to no translocation of this isoform to the plasma membrane (Figure 3.2). Fluorescence microscopy images of HeLa cells showing translocation of PKC isoforms α, γ, θ and ζ after treatment with the diterpene esters, correlated with the data plotted in Figure 3.2. Among the isoforms tested, PKC-α, -γ and -θ demonstrated differential translocation patterns when stimulated with TPA or EBC-46. Photographs of the critical findings are shown in Figure 3.3. No work was done with inhibitors using this technique.

3.2.2 Comparison of EBC-46 and TPA in activating the MAPK pathway

PKC isoforms are present in varying combinations and concentrations in different cell types. In addition, PKC isoforms play an important role as tumor suppressors in cancer development. The spatial regulation of PKC isoforms may be dependent on the phosphorylation of substrates which

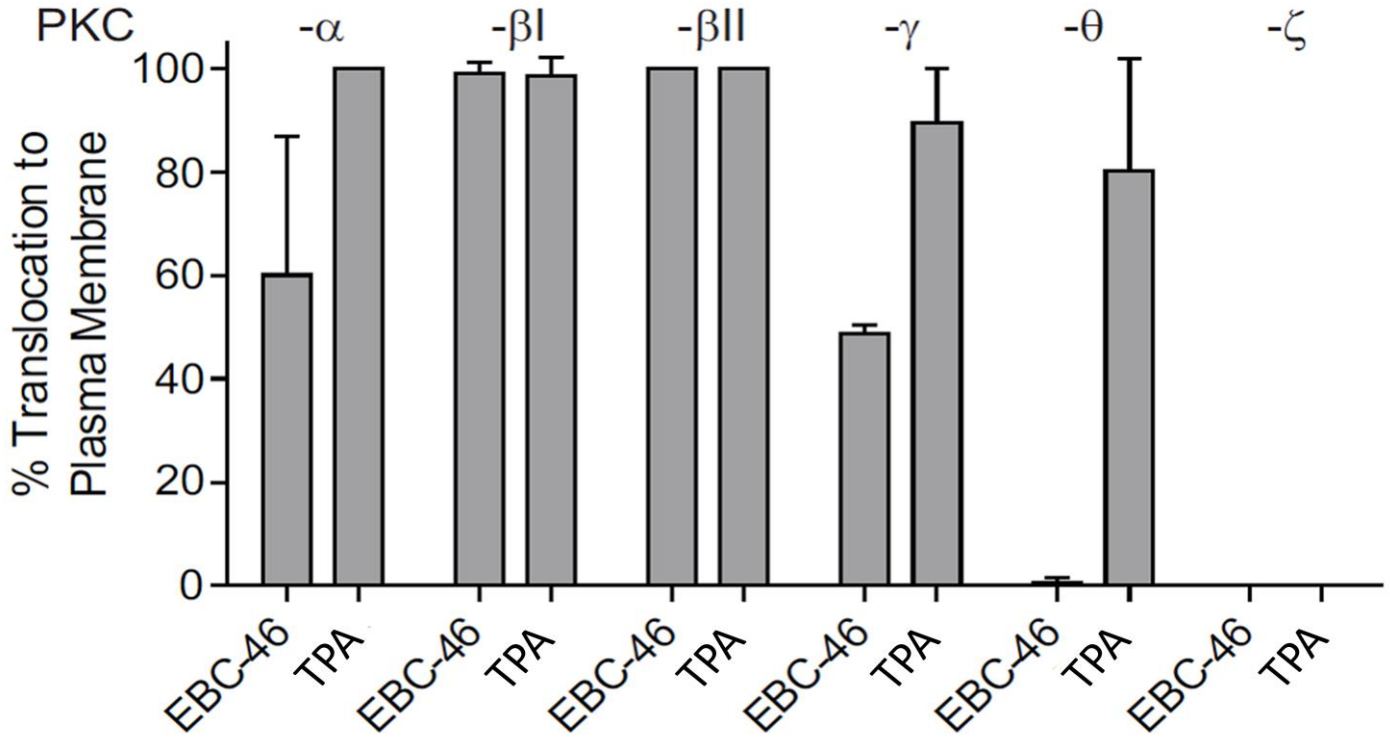

Figure 3.2: EGFP-tagged PKC isoform translocation in transiently-transfected HeLa cells following 1 hr treatment with 100 ng/ml of TPA or EBC-46.

EGFP-tagged PKC- isoform translocation in transiently transfected HeLa cells following 1 hr of treatment with either 100 ng/ml of EBC-46 or TPA. Data is from assessment of at least 50 cells per well from each of triplicate transient-transfection experiments. The error bars indicate standard deviation.

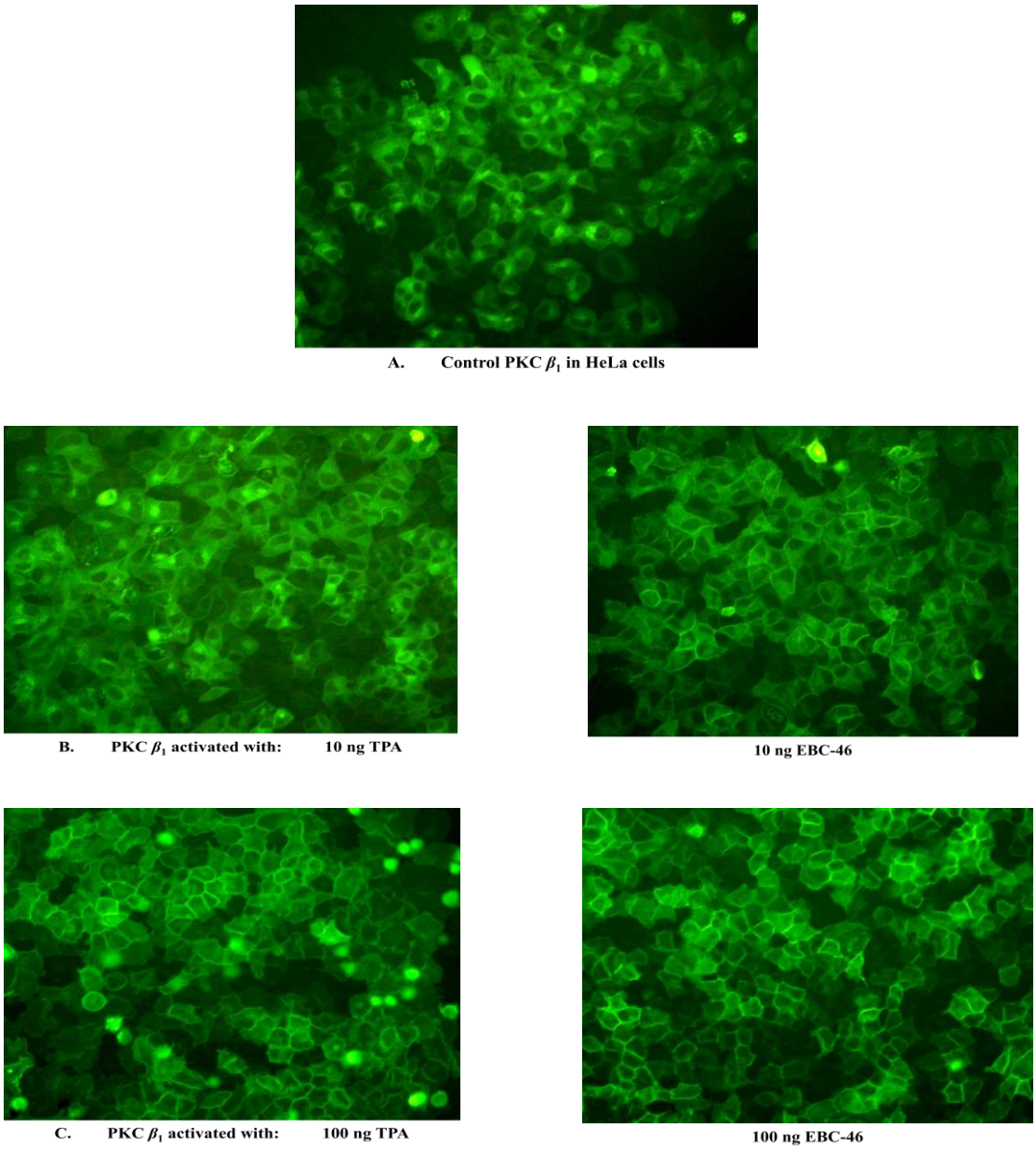

Figure 3.3: Translocation of PKC-β_1 in HeLa cells achieved through treatment with EBC-46 or TPA and visualized by fluorescence microscopy

Representative fluorescence images of translocation of PKC-β_1 transiently-transfected HeLa cells treated with 10 ng/ml or 100 ng/ml of EBC-46 or TPA for 1 hour.

A. Control PKC β_1 in vehicle-treated HeLa cells.
B. PKC β_1 translocated to the plasma membrane in HeLa cells treated with 10 ng/ml of EBC-46 or TPA.
C. PKC β_1 translocated to the plasma membrane in HeLa cells treated with 100 ng/ml of EBC-46 or TPA.

facilitate intracellular localization. For instance, PKC-*δ* was shown to translocate differently to the Golgi or mitochondrion, the nucleus, or membrane based on the regulatory molecule(s) it bound to, namely ceramide, DAG or RACKs (Steinberg, 2005). Activated PKC participates in different cellular signaling pathways. Studies have shown phorbol ester TPA to be involved in the regulation of the MAPK pathways (Joppich et al., 1967). Activated/phosphorylated PKC is translocated to membranous fractions with the aid of the cytosolic receptor for activated C kinases (RACK) (Buensuceso *et al.*, 2001) where they participate in down-stream signal transduction pathways.

As outlined in the *Introductory Chapter* of this thesis, prolonged exposure of cells to PKC activators such as TPA resulted in activation of PKC isoforms followed by proteolytic degradation of the isoforms via the ubiquitin-proteosome pathway (Lu *et al.*, 1998). Western blot analysis was conducted to confirm the ability of EBC-46: (1) to activate PKC and its specificity for certain isoforms, and (2) to modulate the MAPK pathway where phospho-specific antibodies were used against ERK1/2 which is the target substrate of the Ras/Raf/MEK/ERK signaling pathway.

B16-F0 and Sk-Mel-28 cells were grown in 25 cm^2 and 75 cm^2 flasks respectively at an appropriate sub-cultivation ratio to ensure ~ 70% confluence in growth by the end of treatment duration which extended to a maximum of 48 hr. Cells were pre-treated with the PKC inhibitor at a final concentration of 5 µM BIS-1 for 1 hr prior to treatment with 1 µg/ml of EBC-46 or TPA for 6 hr, 24 hr, and 24 hr recovery in fresh media after 24 hr of treatment. At the end of the treatment duration, cells were washed with ice-cold PBS and harvested for extraction of proteins for western blotting analysis. Western blots of B16-F0 and Sk-Mel-28 cell lysates were probed for PKC-*α*, -*β*, -*γ*, -*δ*, -*ε*, -*θ* and -*ι* which represent the classical, novel and atypical isoforms, and the house-keeping gene GAPDH which was probed to ensure equal loading of protein samples into wells of the gel (Figure 3.4).

The protein levels of the classical isoform PKC-*α* appeared to be similar in both melanoma cell lines, B16-F0 and Sk-Mel-28. Further, protein levels of PKC-*α* following 6-24 hr of either EBC-46 or TPA treatment were also similar. However there was a difference observed in the protein expression levels, when comparing the two diterpene esters EBC-46 and TPA compared to the controls.

There was a slight decrease in expression noted between 6 hr to 24 hr after treatment of B16-F0 cells with TPA but not with EBC-46 which indicated a more sustained expression efficiency with the latter (Figure 3.4; Panel A). Expression of PKC-*α* after 24 hr of treatment with either diterpene ester followed by 24 hr of recovery in fresh media does not change when treated with either 1 µg/ml of EBC-46 or TPA indicating sustained depletion of the PKC isoform up to 24 hr (Figure 3.4; Panel A). PKC-*β* and –*γ* were absent in both cell types (data not shown). Among the other PKC isoforms probed for, the western blot analysis showed no expression of PKC-*δ*, -*ε*, -*θ*, and –*ι* in B16-F0 cells (data not shown).

In Sk-Mel-28 cells, PKC-*δ* showed a similar expression profile upon treatment with TPA and EBC-46 as seen with PKC-*α* (Figure 3.4; Panel B). No striking changes were noticed in the expression levels among the other isoforms tested, namely PKC-*ε*, -*θ*, -*ι*. Immunodetection with PKC-*ε* antibody showed low expression of the isoform through all of the protein samples extracted from Sk-Mel-28 cells indicating a slight decreased in expression by 24 hr after treatment. The expression of this isoform following recovery in fresh media showed a further decline in intensity. The overall expression of PKC-*θ* was low and as with PKC-*ι*, the expression of both isoforms appeared unaffected by exposure to EBC-46 or TPA (Figure 3.4; Panel B).

Activation of the MAPK pathway by phorbol ester TPA has been reported in several studies (Krumhaar and Hecker, 1967, Joppich et al., 1967, Wen-Sheng, 2003). MAPKs are the final components of a three-tier protein kinase cascade (as explained in *Chapter One*; Section 1.4.1). Considerable evidence shows that PKC activates the MAPK pathway (Sugden and Clerk, 1998) with direct activation of the classical and novel PKC isoforms by phorbol esters TPA and phorbol 12,13-dibutyrate (PDBu) which stimulated the ERKs in cardiac myocytes. Hence, the ability of diterpene ester EBC-46 to stimulate the MAPK pathway was examined in comparison to TPA.

Controls included in the assay were cells grown in untreated culture media and cells treated with the vehicle EtOH. Tumor cells treated with TPA or EBC-46 for 6 hr or 24 hr were included in the assay as positive controls. Western blot analysis was performed on protein samples extracted from B16-F0 and Sk-Mel-28 cells which were treated with a final concentration of 5 µM BIS-1, a pan-PKC inhibitor 1 hr prior to treatment with PKC activators TPA or EBC-46.

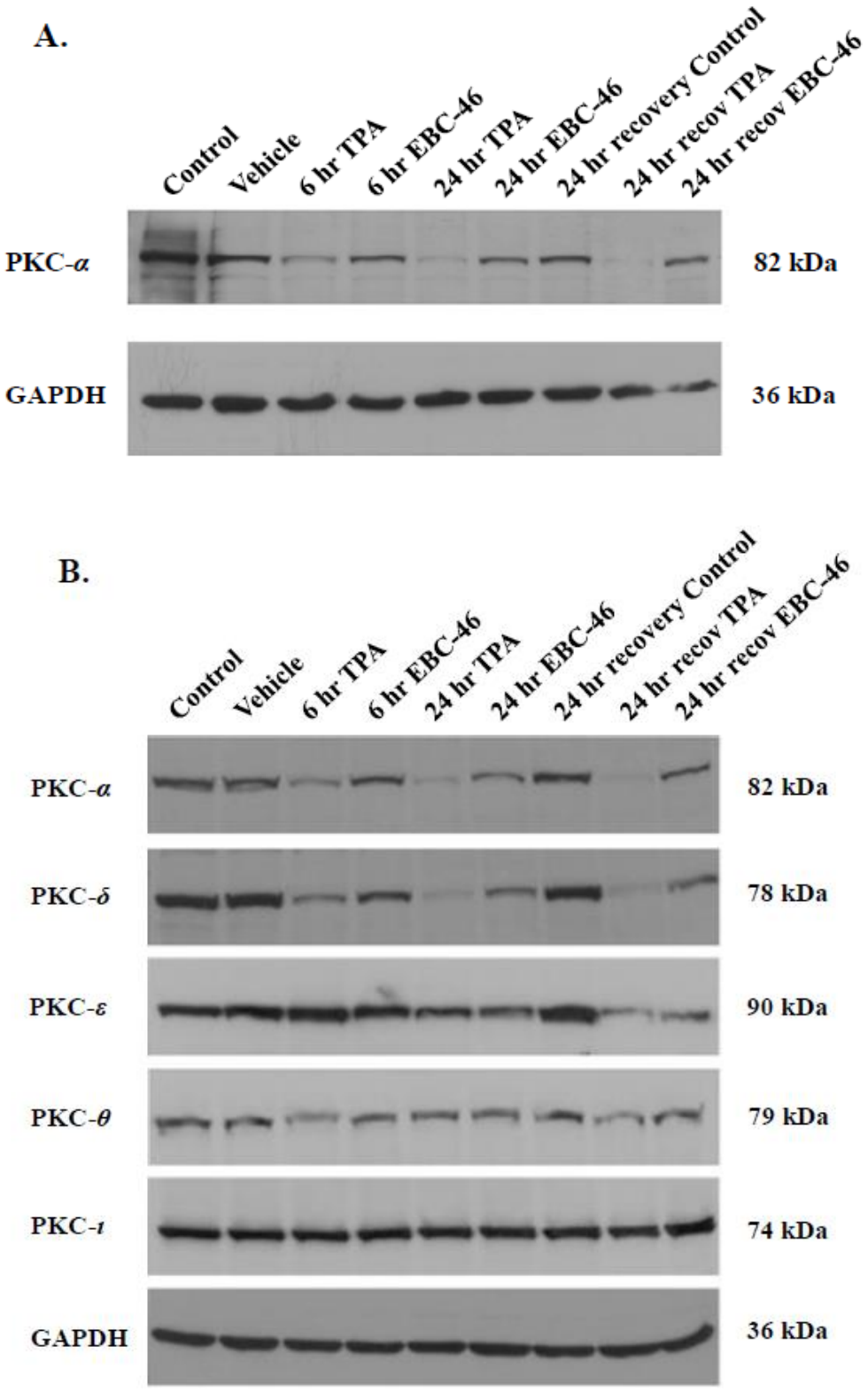
A.
Control
Vehicle
6 hr TPA
6 hr EBC-46
24 hr TPA
24 hr EBC-46
24 hr recovery Control
24 hr recov TPA
24 hr recov EBC-46
PKC-α
82 kDa
GAPDH
36 kDa
B.
Control
Vehicle
6 hr TPA
6 hr EBC-46
24 hr TPA
24 hr EBC-46
24 hr recovery Control
24 hr recov TPA
24 hr recov EBC-46
PKC-α
82 kDa
PKC-δ
78 kDa
PKC-ε
90 kDa
PKC-θ
79 kDa
PKC-ι
74 kDa
GAPDH
36 kDa

Figure 3.4: PKC isoform activation by TPA or EBC-46 in melanoma cells *in vitro*

Panel A: PKC isoforms expressed in B16-F0 cells upon treatment with TPA or EBC-46

Panel B: PKC isoforms expressed in Sk-Mel-28 cells upon treatment with TPA or EBC-46

Melanoma cells B16-F0 and Sk-Mel-28 of mouse and human origin respectively were treated with 1 µg/ml of TPA or EBC-46 for 6 hr, 24 hr and 24 hr recovery in fresh media following 24 hr treatment. The diterpene esters were dissolved in EtOH and added to cultures at a final concentration of 1% (v/v) EtOH. Controls used in the assay included untreated cells grown in media, a vehicle control in which cells were exposed to 1% (v/v) EtOH for 24 hr and a vehicle control recovery in which cells treated for 24 hr with 1% (v/v) EtOH were then exposed to 24 hr recovery in fresh media. Samples corresponding to 30 µg of total protein were electrophoretically separated on 10% (w/v) SDS-PAGE gels and transferred to nitrocellulose membrane (Chapter 2; Section 2.9.3 – 5) following which proteins of interest were blotted using the appropriate antibodies.

There was increased expression of phospho-proteins observed when treated with the PKC activators TPA or EBC-46. Pre-treatment of B16-F0 cells with BIS-1 greatly lowered MEK1/2 and ERK1/2 activation (phospho-MEK1/2 and phospho-ERK1/2) by TPA and EBC-46 when compared to the positive controls (Figure 3.5, Panel A), confirming that diterpene ester-induced PKC activation is responsible for activating the MAPK pathway.

However, a similar effect is not reflected in Sk-Mel-28 cells, where BIS-1 treatment resulted in only a minor decrease in levels of activated MEK1/2 and ERK1/2 compared with the phosphorylated protein controls (Figure 3.5, Panel B). A comparison of p-MEK1/2 and p-ERK1/2 between the two cell lines shows a somewhat higher expression in Sk-Mel-28 than B16-F0 by TPA or EBC-46.

In addition, a time-course analysis of the activation of the PKC isoforms (Figure 3.4) demonstrated a time-dependent expression where the expression levels of these MAPK components decreased between 6 hr to 24 hr after treatment with the diterpene esters, although not very significant. A comparison of the effect of TPA and EBC-46 on the activation of MEK1/2 and ERK1/2 (Figure 3.5) demonstrated a similar profile. This is consistent with the concept that activation of PKC isoforms leads to their depletion via the ubiquitin-proteosome pathway (Hofmann, 2001). These results support the hypothesis of EBC-46 as an activator of PKC isoforms, as evidenced by the lowered expression levels of the MAPK components upon treatment with a specific PKC inhibitor, BIS-1.

3.2.3 The Induction of Respiratory Burst in Neutrophils by TPA and EBC-46 via PKC activation

Another characteristic of PKC activation which has been reported in literature is its ability to induce oxidative burst of neutrophils (Hafeman *et al.*, 1982). Neutrophils are dedicated phagocytic cells that constitute the first line of defense against invading micro-organisms. The intracellular killing mechanism is based on two independent but mutually supportive mechanisms; the generation of toxic oxygen metabolites and the release of microbicidal proteins from the storage granules into phagosome (Dale *et al.*, 2008, Segal, 2005).

The aim of this study was to compare the efficacy of EBC-46 with that of TPA in producing reactive oxygen species by neutrophils and determine the requirement of PKC in this process. Human blood was processed by Dr. Viviana Lutzky and neutrophils were isolated. Cells were

stained with 10 µg/ml dihydroethidium bromide (DHE) for 15 min at 37˚C. Cells were pre-treated with 5 µM BIS-1 (pan-PKC inhibitor) for 1 hr following which cells were treated with a range of concentrations of EBC-46 or TPA (*Chapter Two*; Section 2.13) for 15 min at 37˚C. The generation of reactive oxygen species was measured using FACS Canto flow cytometer.

The results showed that both TPA and EBC-46 induced the production of reactive oxygen species (ROS) in a dose-dependent manner. Both compounds were found to be equally potent in the induction of oxidative burst of human neutrophils. To confirm that the activation of PKC by TPA and EBC-46 is essential for the induction of neutrophil oxidative burst, cells were pre-treated with a pan-PKC inhibitor, BIS-1. Pre-treating neutrophils with BIS-1 followed by treatment with TPA or EBC-46 resulted in nearly complete inhibition of the production of ROS (Figure 3.6) thus confirming the role of PKC activation by the diterpene esters, TPA and EBC-46 in this process.

3.2.3 Cytotoxicity Profiles of Diterpene Esters TPA and EBC-46

In vitro cytotoxicity studies were performed to compare the cytotoxicity profile of TPA and EBC-46 on the tumor cell lines B16-F0 (mouse melanoma), Sk-Mel-28 (human melanoma), A549 and HOP-62 (human lung cancers) and K562 (human leukemia). Given the similarities it shares with TPA, it was hypothesized that EBC-46 would affect tumor cells in a similar manner as TPA.

The aim of these experiments was to study the cytotoxic effect of varying concentrations of TPA or EBC-46 on different tumor cell lines. Based on cell growth rates, flat-bottomed 96 well plates were seeded with B16-F0, Sk-Mel-28, A549 or HOP-62 cells at densities ranging between 3000 – 5000 cells in 100 µl culture media, per well.

K562 cells were seeded into a U-bottom plate as it is a suspension cell line. The cells were treated with varying concentrations of TPA or EBC-46 in media alongside control treatments using the vehicle EtOH, across the plate so that each concentration in each treatment group was tested in quadruplicate (*Chapter Two*; Section 2.1.2). Growth inhibition of cells was assayed by the Sulforhodamine B (SRB) assay on the B16-F0, Sk-Mel-28, HOP-62 and A549 cells while an MTS assay was performed on the K562 cell line.

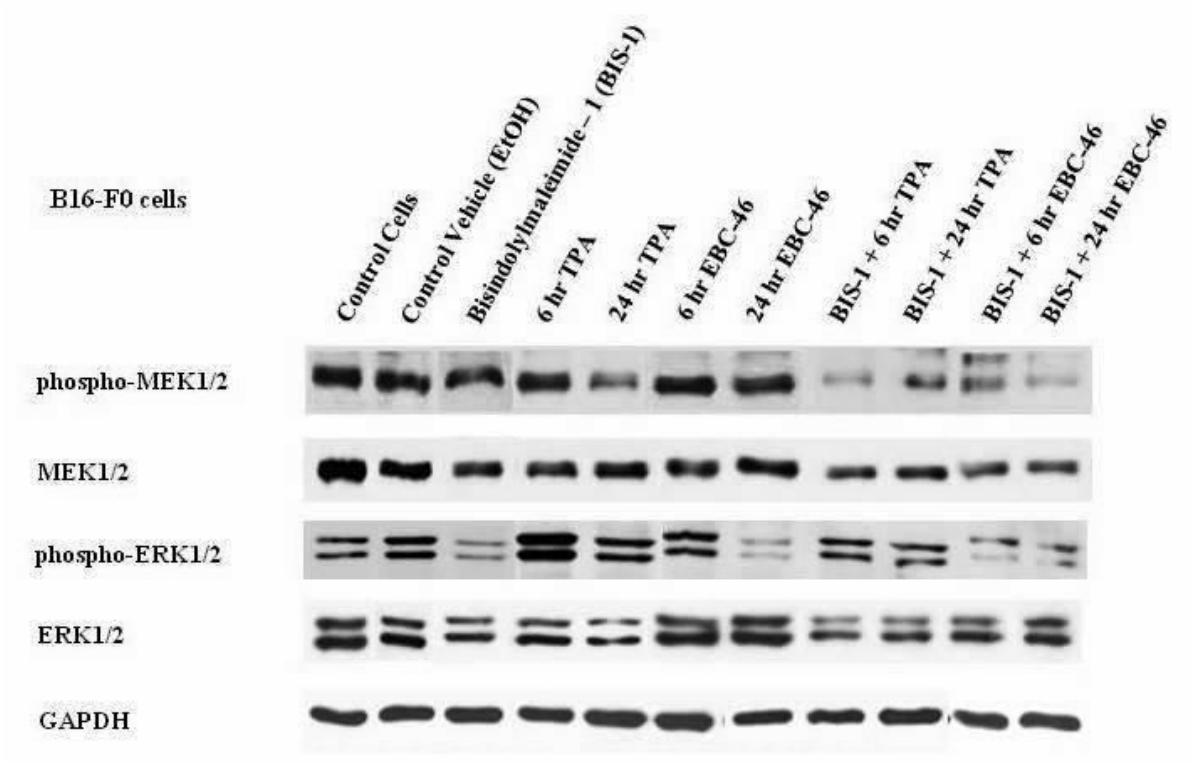
B16-F0 cells
Control Cells
Control Vehicle (EtOH)
Bisindolylmaleimide – 1 (BIS-1)
6 hr TPA
24 hr TPA
6 hr EBC-46
24 hr EBC-46
BIS-1 + 6 hr TPA
BIS-1 + 24 hr TPA
BIS-1 + 6 hr EBC-46
BIS-1 + 24 hr EBC-46
phospho-MEK1/2
MEK1/2
phospho-ERK1/2
ERK1/2
GAPDH

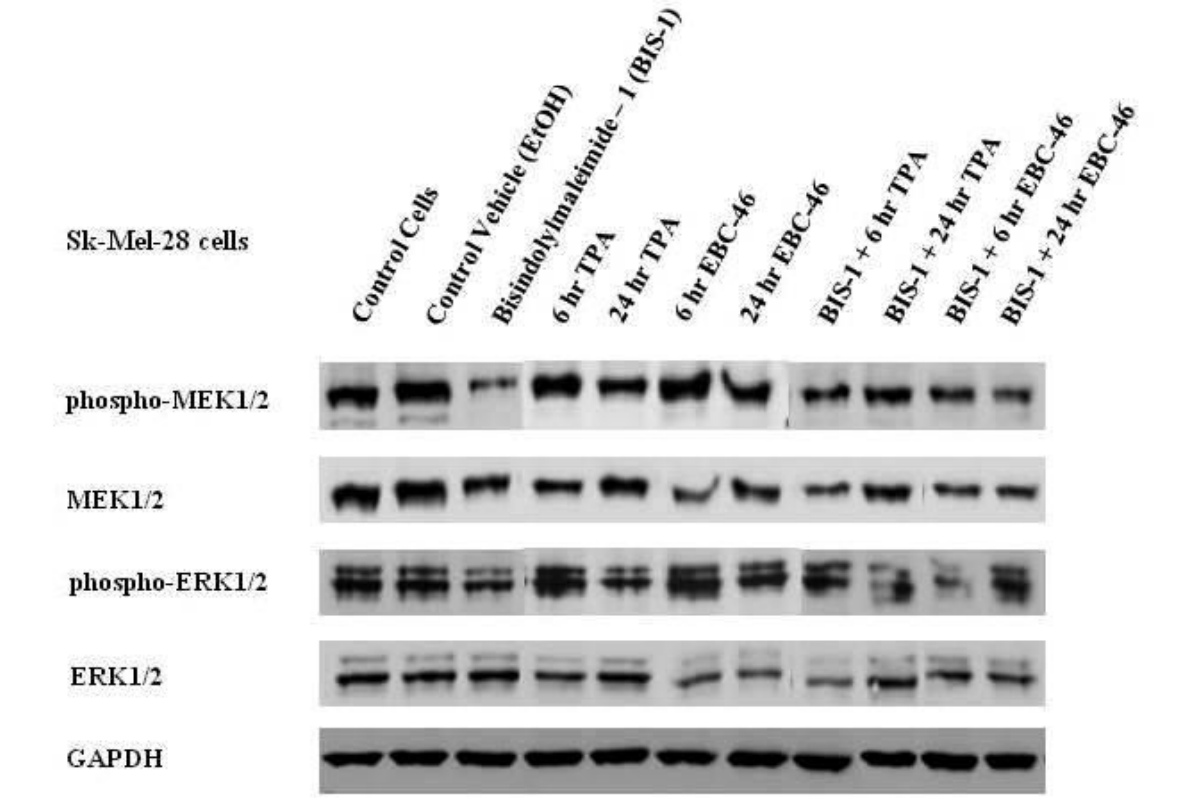
Sk-Mel-28 cells
Control Cells
Control Vehicle (EtOH)
Bisindolylmaleimide – 1 (BIS-1)
6 hr TPA
24 hr TPA
6 hr EBC-46
24 hr EBC-46
BIS-1 + 6 hr TPA
BIS-1 + 24 hr TPA
BIS-1 + 6 hr EBC-46
BIS-1 + 24 hr EBC-46
phospho-MEK1/2
MEK1/2
phospho-ERK1/2
ERK1/2
GAPDH

Figure 3.5: Activation of ERK1/2 and MEK1/2 in melanoma cells treated with Diterpene Esters

Panel A: MAPK activity shown by expression of ERK1/2 and MEK1/2 in B16-F0 mouse melanoma cells treated with 1 µg/ml of TPA or EBC-46.

Panel B: MAPK activity shown by expression of ERK1/2 and MEK1/2 in Sk-Mel-28 human metastatic melanoma cells treated with 1 µg/ml of TPA or EBC-46.

Melanoma cells Sk-Mel-28 and B16-F0 cells of human and mouse origin respectively were pre-treated for 1 hr with 5 µM BIS-1 (pan-PKC inhibitor) following which the cells were treated with 1 µg/ml of either TPA or EBC-46 for 6 hr, 24 hr and 24 hr recovery in fresh media following 24 hr treatement. The diterpene esters were dissolved in EtOH and added to cultures at a final concentration of 1% (v/v) EtOH. Controls used in the assay included untreated cells grown in culture media, cells treated with the vehicle control EtOH for 24 hr and vehicle-treated control recovery where cells were treated for 24 hr with 1% (v/v) EtOH then exposed to 24 hr recovery I fresh culture media., Protein was extracted, ~30 µg of total protein was separated on a 10% SDS-PAGE gel and transferred to nitrocellulose membranes (Chapter 2; Section 2.9.3 – 5) following which the proteins of interest were blotted using appropriate antibodies.

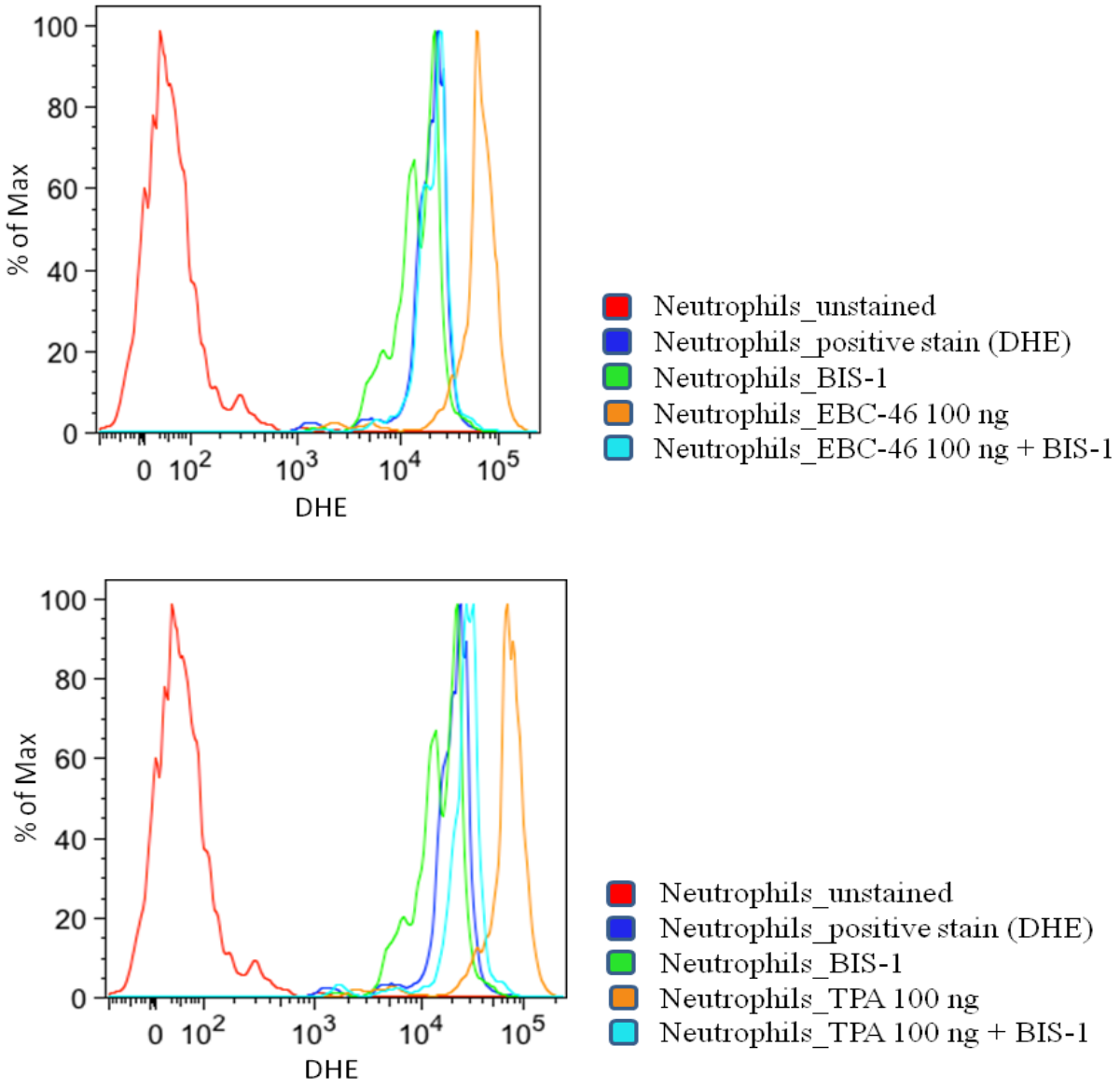

Figure 3.6 Induction of Oxidative Burst in Neutrophils by Diterpene Esters via PKC Activation

Production of reactive oxygen species following treatment of PMN cells. PMN cells were pre-loaded with dihydroethidium bromide and pre-treated where indicated with 1 µM bisindolylmaleimide-l for 15 min, then stimulated with 100 ng/ml of either PMA (top) or EBC-46 (bottom) for 15 min at 37°C. Untreated PMN cells – red, PMN cells pre-loaded – blue, loaded PMN cells treated with either 100 ng/ml PMA or EBC-46 – green, loaded PMN cells treated with either 100 ng/ml PMA or EBC-46 in presence of bisindolylmaleimide-l – yellow.

The results demonstrated that an IC_{50} of 30 µg/ml and greater of EBC-46 was required to induce a cytotoxic effect on some tumor cell lines, namely B16-F0 and Sk-Mel-28 *in vitro*. The same was seen to be true for TPA (Figure 3.7; Panel A). The cytotoxic effect of EBC-46 on some other cell lines was demonstrated at doses as low as 10 ng/ml, and lower again TPA (Figure 3.7; Panels B and C).

Similarly melanoma cells Sk-Mel-28 and B16-F0, were treated *in vitro* at high drug concentrations and for a shorter treatment time. Where the previously described cell survival assays were monitored over a period of 5-6 days incubation time at concentrations **below** 100 µg/ml; in the following assay (Figure 3.8, Panels A, B, C) cells were treated with EBC-46 or TPA at concentrations **above** 100 µg/ml for 30 min. Cells were viewed and imaged using an AMG EvosFL inverted fluorescence microscope to assess cell morphology upon treatment with the diterpene esters. From the images in Figure 3.8, Panels B and C at 30 min after treatment, EBC-46 appears to be more potent than TPA on both Sk-Mel-28 and B16-F0 cells where 100 µg/ml of EBC-46 leads to cell shrinkage which is a characteristic of apoptosis, with a few viable cells. While there are a number of cells which appear shrunken and dead indicating necrosis, on the other hand there are still many viable cells after treatment with 100 µg/ml of TPA. Higher concentration of EBC-46 or TPA (i.e. 200 µg/ml) on Sk-Mel-28 and B16-F0 cells resulted in a necrotic outcome within 30 min after treatment where cells had lost adherence and appeared like debri (Figure 3.8, Panel B and C). Examples of necrotic cells in Sk-Mel-28 and B16-F0 upon treatment with EBC-46 or TPA are indicated with red arrows in Figure 3.8, Panel B and C.

3.2.4 Ectopic expression of PKC isoforms and the effect of EBC-46

To determine if the level of PKC expression influenced the sensitivity of cells to cytotoxic killing by diterpene esters, we engineered cell lines to over-express isoforms by lentiviral transduction. Sk-Mel-28 and D04 melanoma cell lines over-expressing PKC isozymes, specifically, α, δ, and cells expressing *lacZ* as a control, were obtained from Dr. Glen Boyle. Cell lines were treated with TPA or EBC-46 at varying concentrations. Two human melanoma cell lines, one naturally resistant to death/cell cycle arrest induced by PKC activators (Sk-Mel-28) and the other sensitive (D04), were selected. Following the same procedure as the parent lines, cells were seeded into flat-bottom 96-well plate at 4,000 – 5,000 cells in 100 µl culture media per well. The plates were treated with

A.

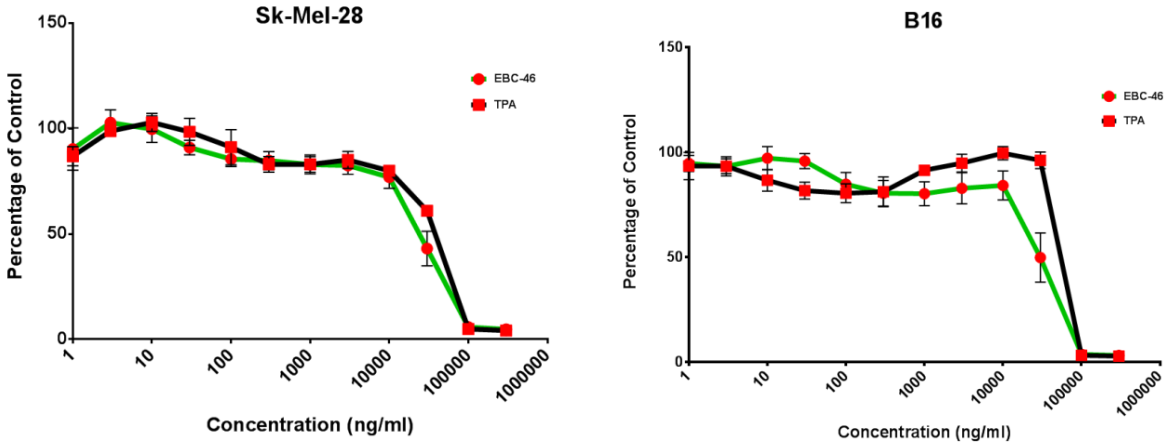
Sk-Mel-28
Percentage of Control
Concentration (ng/ml)
EBC-46
TPA
B16
Percentage of Control
Concentration (ng/ml)
EBC-46
TPA

B.

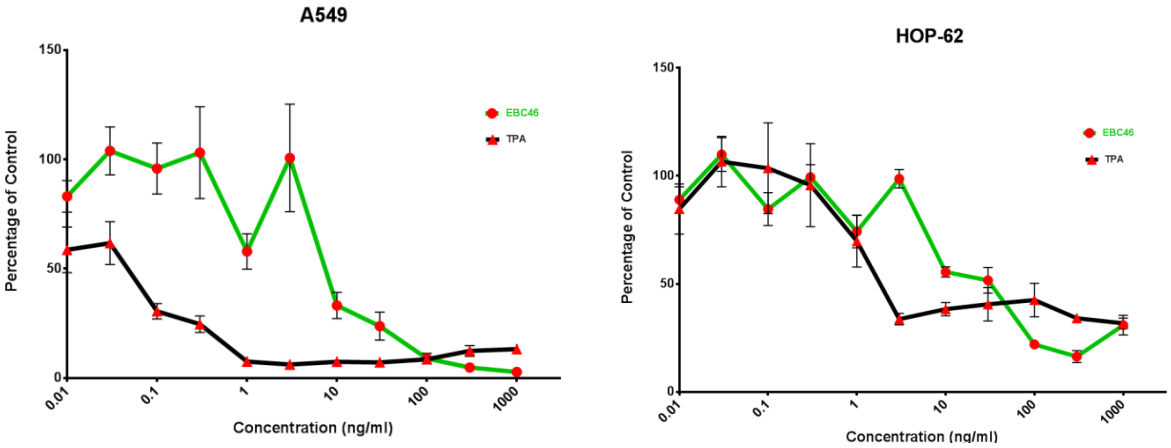
A549
Percentage of Control
Concentration (ng/ml)
EBC46
TPA
HOP-62
Percentage of Control
Concentration (ng/ml)
EBC46
TPA

C.

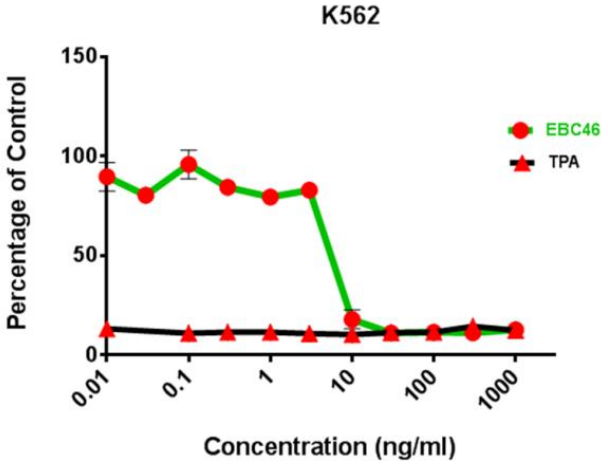
K562
Percentage of Control
Concentration (ng/ml)
EBC46
TPA

Figure 3.7 Dose-Response for Growth Inhibition of Tumor Cell Lines by Diterpene Esters TPA or EBC-46

Panel A: Melanoma cell lines Sk-Mel-28 (human origin) and B16-F0 (mouse origin**)**

Panel B: Lung cancer cell lines A549 and HOP-62 (human origin)

Panel C: Leukemic cell line K562 (human origin)

Cells were plated at varying densities 3000-5000 cells/well in 96-well plates depending on growth rate determined from routine cell culture passaging. Cells were allowed to attach overnight and treated with varying concentrations of the diterpene esters TPA or EBC-46 the following day. Cell survival was monitored daily and growth inhibition was determined by performing an SRB (Sulforhodamine B) or an MTS assay when control cells reached 80% confluency approximately 5-6 days after diterpene ester treatments. Absorbance was read at 564 nm (for SRB assay) and 490 nm (for MTS assay) using ELISA plate reader (VERSA max microplate reader; Molecular Devices). Cell survival was plotted as % control absorbance versus dose.

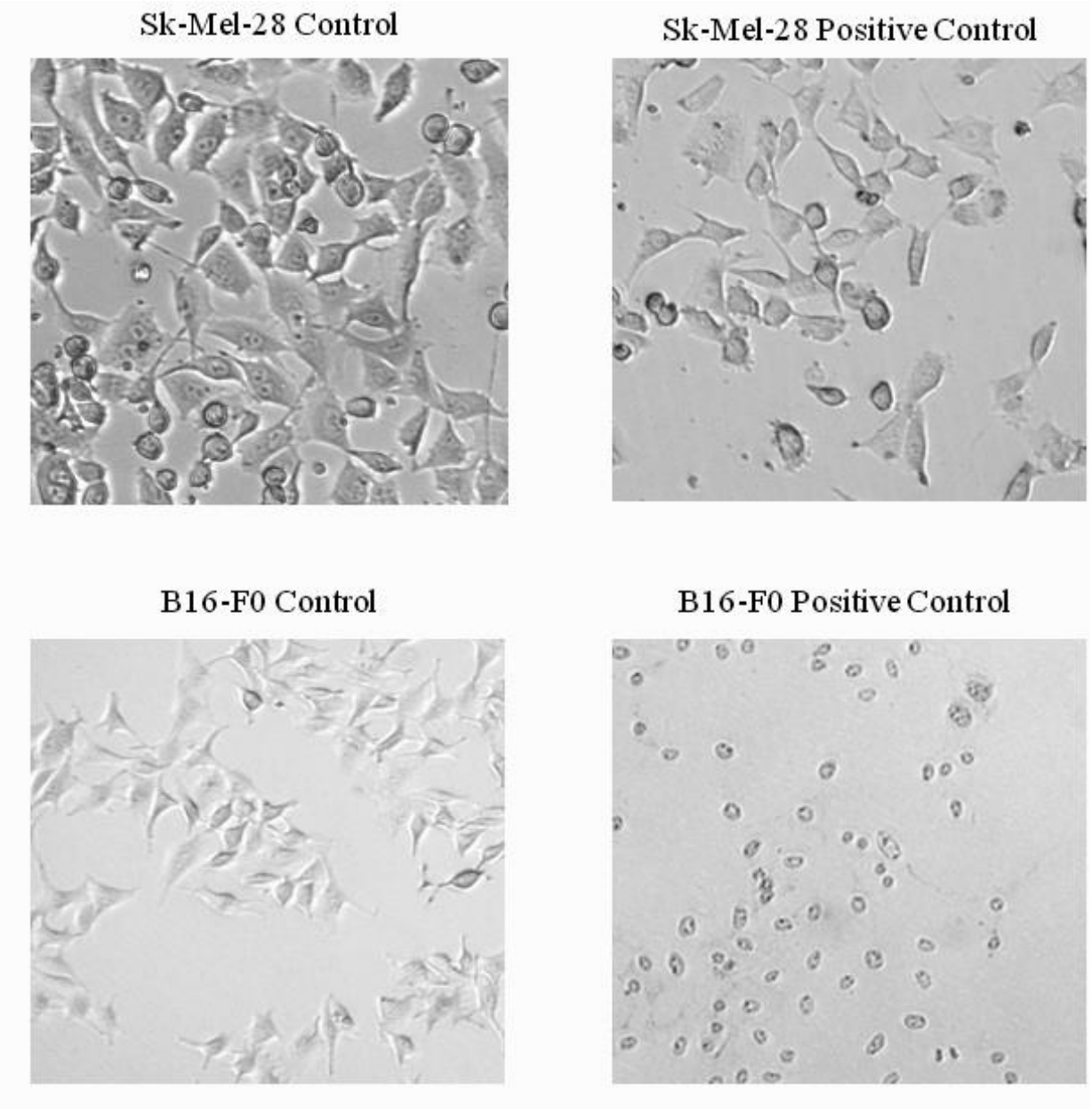

Figure 3.8. Panel A Bright-field images of control melanoma cells of human and mouse origin (Sk-Mel-28 and B16-F0 respectively).

Sk-Mel-28 and B16-F0 cells were used to study the growth inhibitory effect of diterpene esters EBC-46 and TPA. The above bright-field images are of control cells i.e. untreated cells grown in culture media RPMI-1640 and cells treated with 0.1% Triton-X as a positive control.

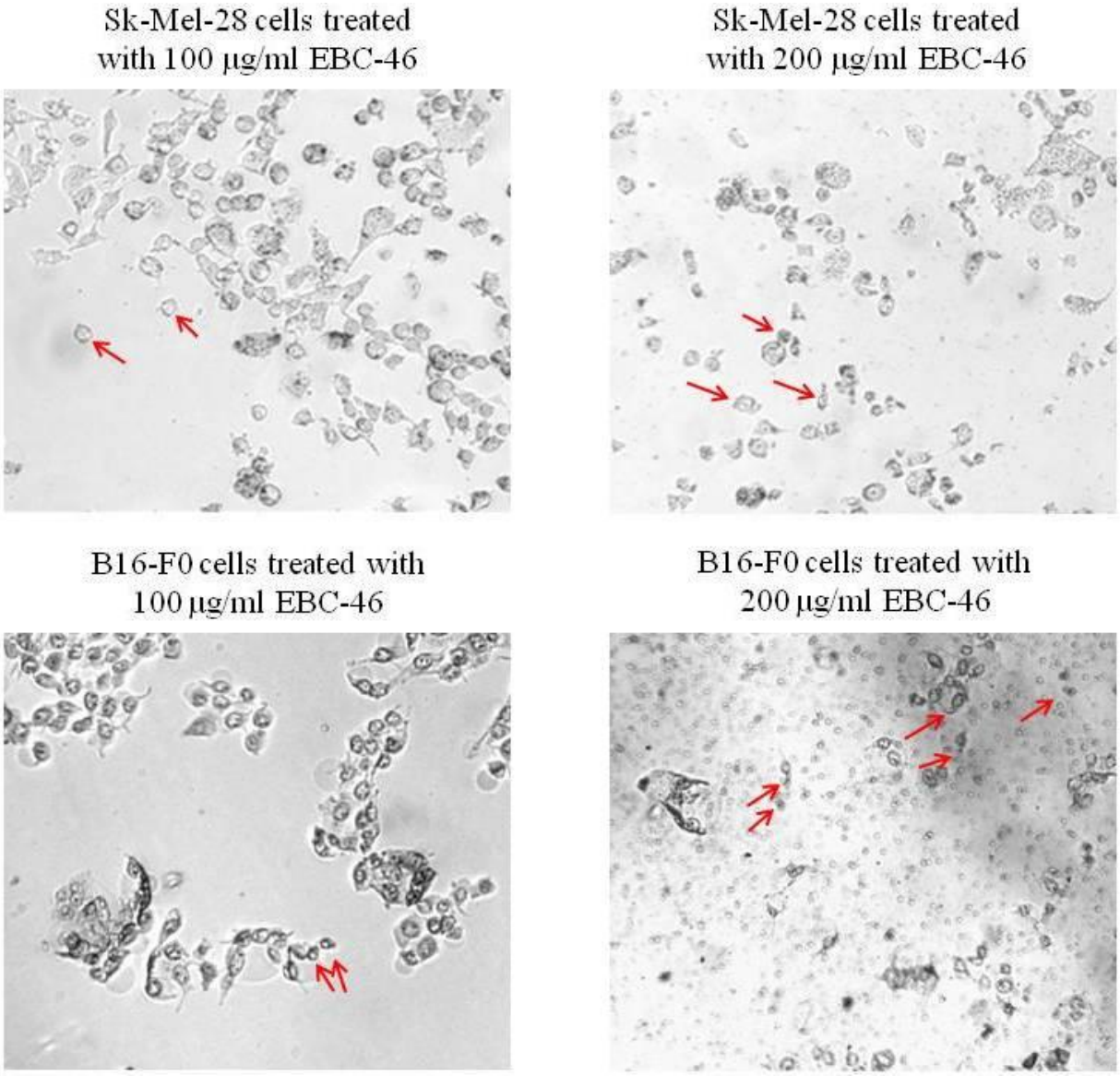

Figure 3.8. Panel B Bright-field images of melanoma cells of human and mouse origin (Sk-Mel-28 and B16-F0 respectively) treated with varying concentrations of EBC-46.

Sk-Mel-28 and B16-F0 cells were used to study the growth inhibitory effect of high concentrations of EBC-46 (100 µg/ml and 200 µg/ml) over 30 min of incubation time. Arrows show examples of necrotic cells.

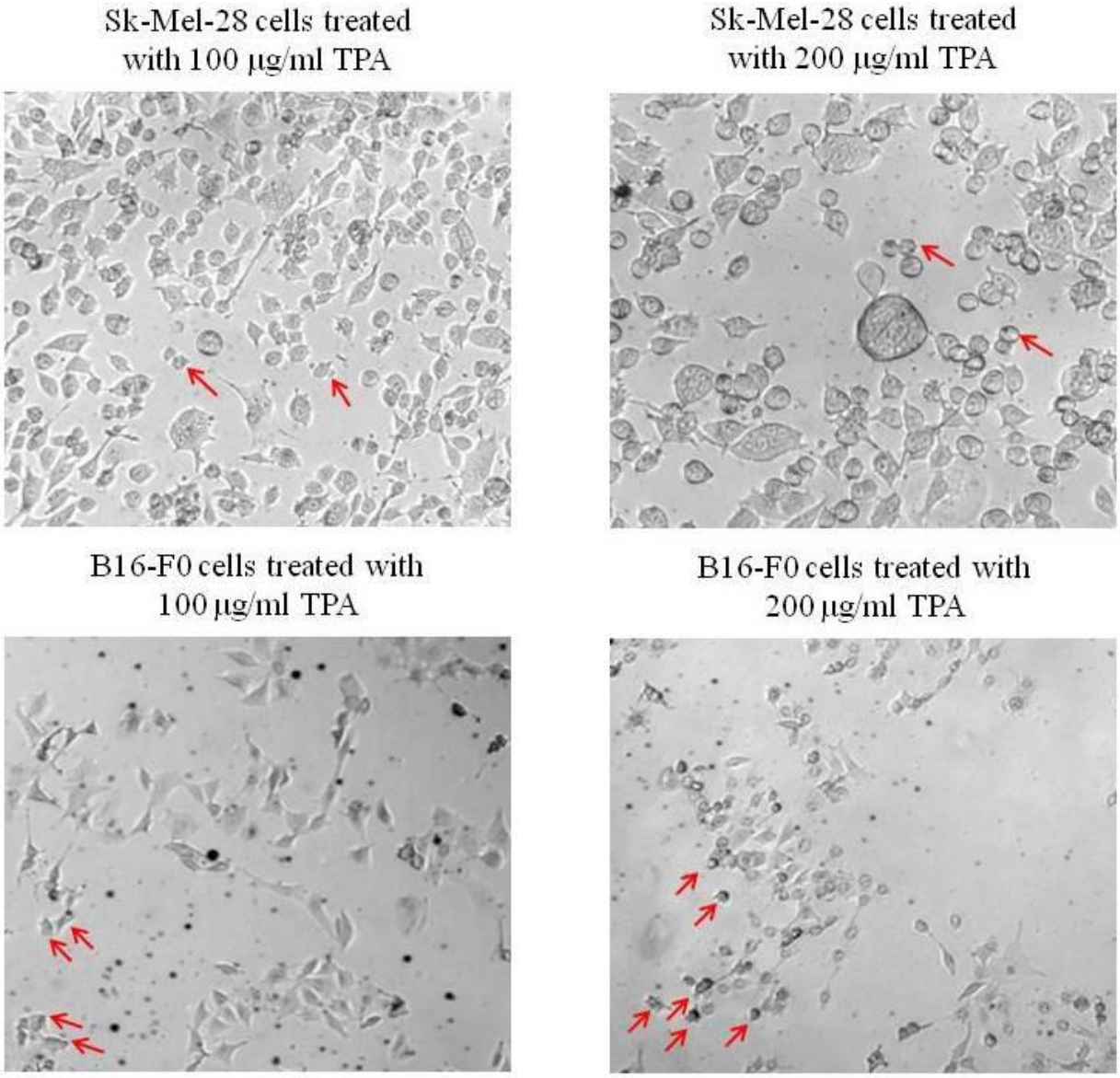

Figure 3.8. Panel C Bright-field images of melanoma cells of human and mouse origin (Sk-Mel-28 and B16-F0 respectively) treated with varying concentrations of TPA.

Sk-Mel-28 and B16-F0 cells were used to study the growth inhibitory effect of high concentrations of TPA (100 µg/ml and 200 µg/ml) over 30 min of incubation time. Arrows show examples of necrotic cells.

different concentrations of TPA or EBC-46 in media, across the plate so that each concentration in each treatment group was tested in quadruplicate. The drug concentrations ranged between 0.01 –10 ng/ml. The cells were allowed to incubate for 4-5 days and were visually examined under a microscope daily for morphological changes. When control cells reached approximately 80% confluency, an SRB cell survival assay was performed. The results in Figure 3.9 on page 90 confirmed that the cell lines over-expressing PKC were highly sensitive to TPA or EBC-46 compared to the wild type cell line, the latter being cells expressing *lacZ* as a control. At doses greater than 0.1 ng/ml both Sk-Mel-28 and D04 were approximately 10-fold more sensitive to treatment, compared to the control cells expressing *lacZ*. At doses below 0.1 ng/ml, growth of D04 cells was arrested, but no cell death was observed.

3.3 Discussion

Protein Kinase C rocketed to the forefront of cancer research, when it was identified as a target for phorbol esters. A widely researched phorbol ester is 12-O-tetradecanoyl-13-acetate (TPA) which has been obtained from latex of *Croton tiglium* L., a leafy shrub of the *Euphorbia* family native to Southeastern Asia (Zong and Thompson, 2006). A prototype PKC activator, TPA is known for its tumor promoting activity albeit in the presence of carcinogens (Blumberg, 1988, Mailloux *et al.*, 2001, Yuspa *et al.*, 1979). *In vitro* studies of the biological effects of TPA on cells demonstrated a range of effects on tumor cells from the induction of bipolar morphology of MM96L melanoma cells to the induction of reactive oxygen species (Fisher and Morgan, 1994, Johnson *et al.*, 2001, Hawkes *et al.*, 2001) which are found to be characteristics of PKC activation. Another diterpene ester identified in this laboratory is the compound ingenol-3-angelate (PEP005), with similar biological properties as TPA and it is also an activator of PKC isozymes (Kedei *et al.*, 2004). Not only has PEP005 been found to be toxic to cells *in vitro* but a high dose of the compound has resulted in ~ 80 % cure of subcutaneous tumors in mice via topical applications (Mailloux, 2001, Ogbourne *et al.*, 2004).

A novel short chain diterpene ester named EBC-46, has recently been extracted and purified from the kernels of the Blushwood plant. Elucidation of the chemical structure of EBC-46 revealed that it

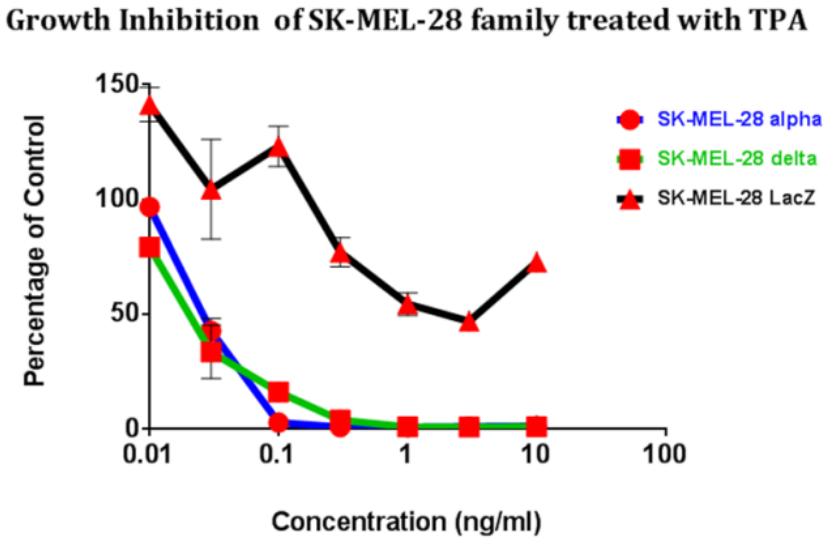
Growth Inhibition of SK-MEL-28 family treated with TPA
Percentage of Control
150
100
50
0
0.01
0.1
1
10
100
Concentration (ng/ml)
SK-MEL-28 alpha
SK-MEL-28 delta
SK-MEL-28 LacZ

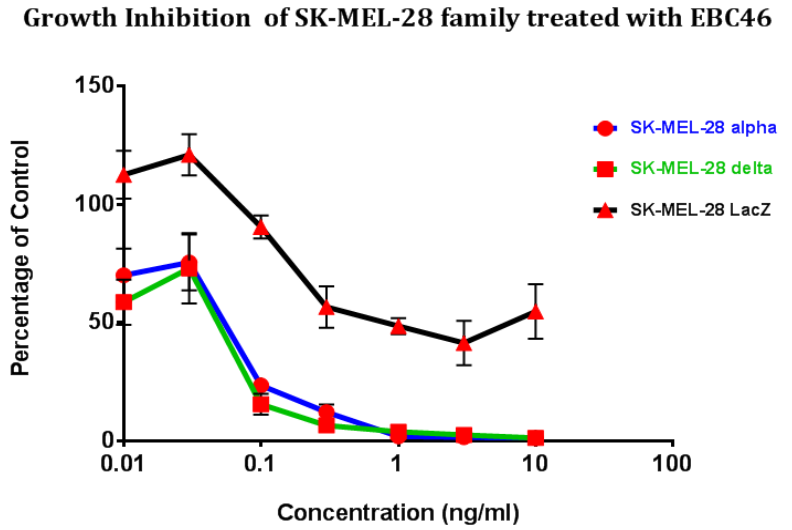
Growth Inhibition of SK-MEL-28 family treated with EBC46
Percentage of Control
150
100
50
0
0.01
0.1
1
10
100
Concentration (ng/ml)
SK-MEL-28 alpha
SK-MEL-28 delta
SK-MEL-28 LacZ

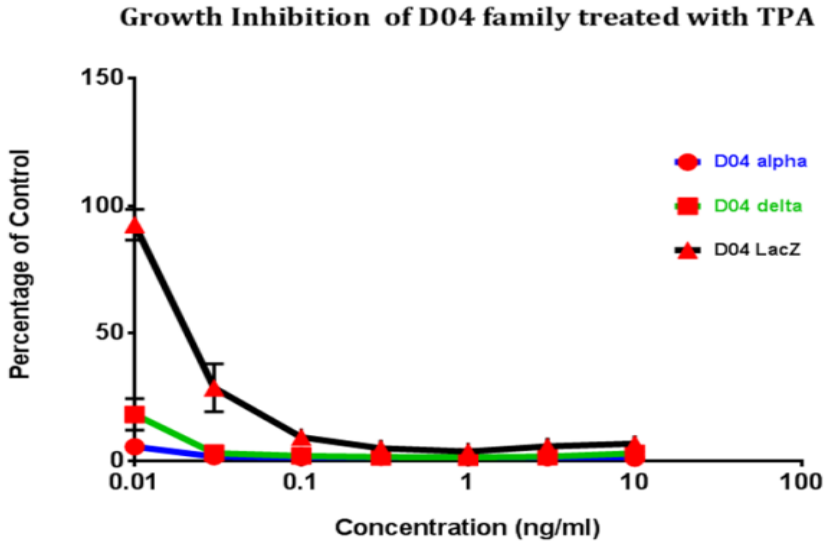
Growth Inhibition of D04 family treated with TPA
Percentage of Control
150
100
50
0
0.01
0.1
1
10
100
Concentration (ng/ml)
D04 alpha
D04 delta
D04 LacZ

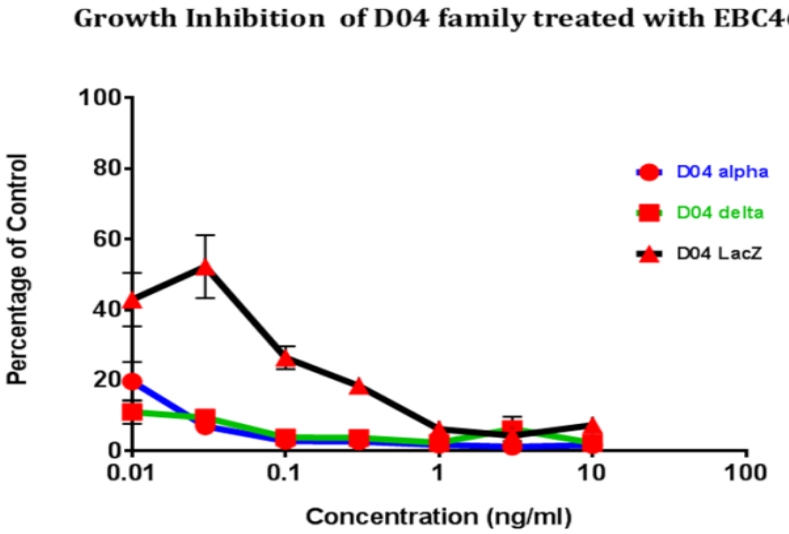
Growth Inhibition of D04 family treated with EBC46
Percentage of Control
100
80
60
40
20
0
0.01
0.1
1
10
100
Concentration (ng/ml)
D04 alpha
D04 delta
D04 LacZ

Figure 3.9 Growth Inhibition Assays of Human Melanoma Cell Lines Over-Expressing PKC isoforms and Treated with Diterpene Esters TPA and EBC-46.

Panel A: Melanoma cell line Sk-Mel-28 (human origin) over-expressing PKC-*α* and -*δ*

Panel B: Melanoma cell lines D04 (human origin) over-expressing PKC-*α* and -*δ*

Cells over-expressing PKC isoforms *α* and *δ* were plated at varying densities 3000-5000 cells/well in 96-well plates depending on growth rate determined from routine cell culture passaging. Cells were allowed to attach overnight and treated with varying concentrations of the diterpene esters TPA or EBC-46 the following day. Cell survival was monitored daily and growth inhibition was determined by performing an SRB (Sulforhodamine B) assay when control cells reached 80% confluency approximately 5-6 days after diterpene ester treatments. Absorbance was read at 564 nm using ELISA plate reader (VERSA max microplate reader; Molecular Devices). Cell survival was plotted as % control absorbance versus dose.

shared a similar backbone as TPA (see Introduction of *Chapter Three*) and hence it was hypothesized to share similar functional properties as TPA.

The initial aim of this project was to determine the activity profile of EBC-46 in comparison to the well-researched PKC activator TPA, by comparing the ability and specificity of the diterpene esters to bind to and activate PKC isozymes and also compare the ability to induce oxidative burst which is a measurable consequence of PKC activation (Hafeman *et al.*, 1982).

3.3.1 Translocation of activated PKC isoforms by EBC-46

PKCs are serine/threonine protein kinases which are present in an inactive state in the cytosol. To date there have been twelve isoforms identified which are categorized into four groups classical (α, β_1, β_2, and γ), novel (δ, ε, η, and θ), atypical (ι/λ, ζ) and distant PKCs (μ, ν), based on their sequence similarities and modes of activation (*Chapter One*: Section 1.2.1). Although the distant PKCs, PKC-μ and $-\nu$, contain some similar certain common structural features that suggest they are members of the PKC family, they remain controversial. Activation of PKCs is brought about by the binding of DAG or phorbol esters in conjunction with Ca^{2+} facilitated by phosphorylations of the serine/threonine or tyrosine residues. These phosphorylations are essential for the priming and stabilization of the PKC isoforms. Once activated, the PKCs translocate to the plasma membrane or other membranous fractions (Newton, 1995, Newton, 1997). Similarly, diterpene esters such as TPA activate the conventional and novel PKC isoforms by forming hydrogen bonds with main-chain groups thereby stabilizing the membrane-inserted state of PKC (Zhang *et al.*, 1995). The conventional and novel PKCs with a C1 domain in their regulatory region are activated by DAG or phorbol esters and are known to subsequently translocate from the cytosol to membranous fractions (Castagna *et al.*, 1982, Cartee *et al.*, 2003). Hence, translocation of PKCs is a good marker of the enzyme activation. To visualize/measure this translocation, GFP-PKC fusion proteins were used which were described by Sakai and colleagues in 1997 (Karasavvas *et al.*, 1996).

The aim of this study was to confirm that EBC-46 is an activator of PKC by analyzing the translocation of the PKC isoforms upon treatment with EBC-46 and TPA. EGFP-tagged PKC isoforms were transiently transfected into HeLa cells and were subsequently treated with EBC-46 or TPA for 01 hr with doses ranging between 10 ng/ml – 100 ng/ml. The translocation of the PKC isoforms was determined by visual examination using the AMG EvosFL inverted fluorescence.

microscope. A hallmark of PKC activation is the translocation to membranous fractions (Oancea and Meyer, 1998, Karasavvas *et al.*, 1996). The results in (Figure 3.3) demonstrated that EBC-46 induced translocation of the conventional PKC isoforms that were tested, but not of novel PKC-θ. On the other hand, TPA induced translocation of both classical and novel PKC isoforms tested. As expected, both diterpene esters TPA and EBC-46 failed to induce translocation of the atypical PKC-ζ which lacks the C1 DAG/phorbol ester binding domain. There were also differences noted in terms of potency of translocation and subcellular localization of the PKC isoforms. Classical PKC–α and –γ were translocated from cytoplasm to plasma membrane by TPA, but not EBC-46 which led to translocation to nuclear or perinuclear regions. However, both TPA and EBC-46 resulted in very efficient translocation of classical PKCs -β_1 and-β_2 from the cytoplasm to the plasma membrane thus confirming the role of EBC-46 as a PKC activator and indicating its specificity for the β isoform. The differences in the subcellular localization of PKC isoforms may result in differences in substrate specificity thereby determining the downstream biological responses.

3.3.2 Role of EBC-46 in activation of the MAPK pathway

The hypothesis that EBC-46 is a PKC activator was further strengthened by immunodetection of proteins influenced by the activation of PKC. Once translocated to the membrane, the activated PKC phosphorylates substrates such as members of the mitogen-activated protein kinase family (MAPK) which play a vital role in growth inhibition (Aeschlimann and Hecker, 1967, Mason et al., 2010). Activation of the MAPK pathway by TPA has been reported in several studies (Krumhaar and Hecker, 1967, Joppich et al., 1967). Hence the effects of EBC-46 in modulating the MAPK pathway were examined in comparison to TPA.

As previously described, both classical and novel PKC isoforms share a common ligand for activation at the C1 domain in the form of 1,2-diacylglycerol (DAG). Phorbol esters with their unique configuration as tetracyclic diterpenes have a close structural relationship with DAG which gives them a high affinity for the PKC regulatory site. As seen in Figures 3.4 and 3.5 of the results, EBC-46 is specific for the PKC isoforms with a C1 domain which include the classical and novel PKC isoforms. The results show a vast reduction in the expression of total PKC levels within cancer cells as a direct result of diterpene ester exposure.

There have been several studies indicating the relationship between PKC isoforms and members of the MAPK pathway. PKC-*β* has been shown to activate ERKs in cardiac myocytes (Sugden and Clerk, 1998), PKC-*δ* has been shown to activate Ras in different cell lines (Kim et al., 2003, Krumhaar and Hecker, 1967, Shanmugam et al., 1998) and PKC-*α* and PKC-*ε* have been shown to directly phosphorylate Raf-1 (Cacace *et al.*, 1996, Cai *et al.*, 1997, Kolch *et al.*, 1993). These results indicated that PKC activity is important in regulating the cell signaling through MAPK pathways. The pre-treatment of B16-F0 cells with BIS-1 greatly lowered the activation of MEK1/2 and ERK1/2 by EBC-46 and TPA (Figure 3.5) confirming that diterpene ester-induced PKC activation is responsible for activating the MAPK pathway. However, Sk-Mel-28 human melanoma cells appeared more resistant to the activity of BIS-1 suggesting the involvement of a different signaling pathway. To further explore this hypothesis, regulation of the other MAPK pathways such as JNK/p38 and *PTEN* need to be assessed. Studies with PEP005 have resulted in the activation of a variety of signaling pathways demonstrated by increased phosphorylation of PKC-*δ*, Raf1, MAPK molecules ERK1/2 and p38, c-Jun (NH)-2 terminal kinase and PTEN (Serova *et al 2008*).

The western blot analysis identified that PKC isoforms also MEK1/2 and ERK1/2 were activated by 6 hr of treatment with TPA or EBC-46. A time-course analysis of B16-F0 and Sk-Mel-28 cells revealed that the activation of ERK1/2 was short-lived with expression levels reducing steadily with time between 6 hr – 24 hr leading eventually loss of intracellular PKC.

3.3.3 Induction of oxidative burst of neutrophils by EBC-46

Neutrophils and macrophages are professional phagocytic cells that play an important role in defending the host against microorganisms by producing *reactive oxygen species* (ROS) via the NADPH oxidase enzyme complex. This process known as *respiratory* or *oxidative burst* involves generation of superoxide anion (O_2^-) and hydrogen peroxide (H_2O_2) (Dahlgren and Karlsson, 1999, Dahlgren *et al.*, 2007). The NADPH oxidase enzyme which is the primary catalyst for this process is a multicomponent enzyme comprising of four oxidase-specific proteins (p22 ^{phox}, p47 ^{phox}, p67 ^{phox}, gp91^{phox}) and GTPase (Rac1/2). Respiratory burst is a highly regulated process involving phosphorylation, translocation and multiple conformational changes (Quinn and Gauss, 2004). A number of soluble and particulate factors such as opsonized bacteria, platelet activating factor (PAF), complement component 5a, diacylglycerol (DAG) and PKC activators such as TPA can stimulate NADPH oxidase in phagocytes. Protein phosphorylation and subsequent translocation of

cytosolic components to the plasma membrane are required to facilitate the phosphorylation of key components of the NADPH oxidase complex (Walker *et al.*, 1991).

The NADPH oxidase system has been mainly studied in neutrophils (el Benna *et al.*, 1994, Uhlinger *et al.*, 1993). The results in Figure 3.6 showed that both TPA and EBC-46 induced the production of reactive oxygen species in neutrophils in a dose-dependent manner. Both compounds were found to be equally potent in the induction of oxidative burst of human neutrophils. Pre-treating neutrophils with the PKC inhibitor BIS-1 followed by co-treatment with TPA or EBC-46 resulted in a complete reduction in the diterpene ester-induced production of ROS by neutrophils (Figure 3.6) thereby confirming the role of PKC activation in the process. The results are in accordance with several studies on the effect of PKC isoforms in inducing respiratory burst that have demonstrated the PKC isoforms to play a vital role in the phosphorylation of p47 ^{phox} (Dang *et al.*, 2001, Fontayne *et al.*, 2002, Zoellner *et al.*, 1996, Reeves *et al.*, 1999). Conversely, compounds that inhibit PKC were shown to prevent the respiratory burst (Dekker *et al.*, 2000, Kramer *et al.*, 1989).

3.3.4 EBC-46 Inhibits Growth in Melanoma cells in a manner similar to TPA

EBC-46 shares not only structural similarities with this prototypic PKC activator, it has also been found to induce respiratory burst in neutrophils via a PKC-dependent process with equal potency as TPA. On the other hand, translocation of individual isoforms in response to treatment with TPA or EBC-46 resulted in differences with respect to isoform-specific potency as well as compartmentalization of the activated isoforms. As a result, it was thought that this unique PKC activity in response to diterpene ester stimulation could account for differences in potency in a biological setting.

TPA has the ability to induce permanent senescence in a subset of melanoma cell lines (Cozzi *et al.*, 2006). *In vitro* cytotoxicity studies were performed to compare the cytotoxicity profile of TPA and EBC-46 on different tumor cell lines. With the similarities it shares with TPA, it was hypothesized that EBC-46 would affect tumor cells in a similar manner as TPA. The cells were treated with either diterpene ester, TPA or EBC-46 at varying concentrations alongside control untreated cells. An initial visual examination followed by protein estimation assay revealed that the different cell lines responded differently to treatment with TPA or EBC-46. This could be due to the differences in cell

type i.e. origin of tumor cells, growth rates of the different lines and sensitivity or resistance of the cells to the drug.

As seen in the results of the growth inhibition assays an IC_{50} of 30 µg/ml and greater of EBC46 was required to induce a cytotoxic effect on tumor cells B16-F0 and Sk-Mel-28 *in vitro*. The cytotoxic effect of EBC-46 on the sensitive cell lines was demonstrated at doses as low as 10 ng/ml which was about 10-fold lower than TPA (Figure 3.7). The different cell lines responded differently to treatment with TPA or EBC-46. This could be due to the differences in cell type i.e. origin of tumor cells, growth rates of the different lines and sensitivity or resistance of the cells to the drug. For instance, A549 is a lung cancer cell line while K562 is a leukemic cell line, both of human origin. Compared to K562 which are a non-adherent, suspension cell line and hence grown in U-bottom well plates, A549 though sensitive to diterpene ester treatments (as seen in preliminary experiments; data not shown), are a more resistant cell line than K562. Also TPA *in vitro* is seen to be more toxic than EBC-46.

Differences were also observed between the two compounds EBC-46 and TPA with respect to concentration and time of treatment. Growth inhibition potential of EBC-46 and TPA was assessed using SRB or MTS stains for cell survival or proliferation where the drug concentrations were maintained lower than 100 µg/ml and cells at densities ranging between 3,000 – 5,000 cells/well were treated for 5-6 days. In contrast, images in Figure 3.8 show melanoma cell lines Sk-Mel-28 and TPA plated at higher cell densities of 10,000 cells/well treated *in vitro* with high concentrations of either EBC-46 or TPA (100 µg/ml or 200 µg/ml; which were equivalent to doses administered *in vivo*) and were treated for 30 min. Over a short treatment time, lower concentrations of the diterpene esters led to apoptosis identified by blebbing and cell shrinkage while treatment with higher concentrations for the same time resulted in necrotic cells (red arrows in Figure 3.8). Propidium Iodide assays have been performed on these treated cells and images shown in Figure 4.12 of *Chapter Four*. These results are in parallel with that observed *in vitro* on cells treated with the diterpene esters long-term for 5-6 days. However, where a long-term assay renders TPA more potent than EBC-46, treatment of tumor cells with the diterpene esters for 30 min shows EBC-46 to work faster to achieve cell death than TPA. The differences in the effects of EBC-46 and TPA on the different cell lines can be attributed to a number of factors including toxicity of the compounds, the cellular pathways they recruit and time of exposure to cancer cells. In addition, apart from the

potency of the compound *in vivo*, there is also a host response that supports the total ablation of tumors by EBC-46 (explained in *Chapters Four* and *Five*).

3.3.5 Over-expression of PKC Isoforms increases sensitivity to diterpene ester treatment

This Chapter has also examined the effects of over-expression of two PKC isoforms, PKC-*α* and PKC-*δ*, on the sensitivity of melanoma cells to growth inhibition by phorbol ester treatment in comparison to the control *lacZ*. These two isoforms were selected as they are widely recognized as key targets of this class of drug although future work will investigate other isoforms of PKC as well. In addition to the PKC-α and –δ over-expressed isoforms, the control *lacZ* in Figure 3.9 also demonstrated increased sensitivity compared to parent cell lines in Figure 3.7. This could probably be due to increased cell fragility as a result of the lentiviral transfection process. However, a comparison of over-expressed PKC-*α* and PKC-*δ* to the control *lacZ* were shown to increase sensitivity of two resistant melanoma cell lines SK-Mel-28 and D04 to growth inhibition by TPA and EBC-46.

While this work provides additional evidence that EBC-46 activates the classical and novel classes of PKC isoforms, the effect of pan-PKC inhibitor BIS-1 on cells over-expressing PKC isoforms needs to be investigated to substantiate the role of PKC on sensitivity of the diterpene esters. The involvement of PKC isoforms in the mechanism of action of EBC-46 could be studied by reducing the expression of individual isoforms to show decreased killing. However, the absence of critical isoforms such as PKC-*α* and *–β* in tumor cells implies that a knock down would not be useful to probe mechanism which is likely a result of the host response to the compound as shown in *Chapters Four* and *Five*.

To reiterate other significant evidences of PKC activation by EBC-46 which have been presented in the course of this Chapter, the diterpene ester EBC-46 has been shown to translocate PKC isoforms to the plasma membrane with specificity for classical and novel isoforms of PKC when compared to the prototype PKC activator, TPA (shown in Figures 3.2 and 3.3). Activated PKC is known to participate in downstream signaling pathways such as the MAPK pathways including ERK1/2, p38, JNK signaling pathways which play a role in cellular growth, differentiation and apoptosis (Serova *et al.*, 2008). Pre-treatment of melanoma cells B16-F0 and Sk-Mel-28 with the pan-PKC inhibitor BIS-1 resulted in lowered activation to almost complete inhibition of MAPK molecules MEK1/2

and ERK1/2 as shown in Figure 3.5. Another characteristic of PKC activation is the induction of oxidative stress as a result of increased production of reactive oxygen species (ROS) which was observed upon treatment of neutrophils with EBC-46 in comparison with TPA in Figure 3.6. TPA has been shown to stimulate neutrophils to produce ROS and consequently lead to accelerated apoptosis (Lundqvist-Gustafsson and Bengtsson, 1999). Over-expression of PKC isoforms α and δ in tumor cells resulted in increased sensitivity to growth inhibition with EBC-46 although less significantly as expected (Figure 3.9).

The results presented in this Chapter support EBC-46 as being an activator of PKC isoforms and resulting in the phosphorylation of ERK1/2 in the MAPK pathway. Although structurally similar to TPA and sharing the same biological functions there were differences observed between EBC-46 and TPA. Both EBC-46 and TPA have a cytotoxic effect on tumor cell growth *in vitro*, however, EBC-46 is not as potent as TPA. Differences were observed between the two diterpene esters on different cell lines in cell survival assays, specificity to and translocation of PKC isoforms and protein analysis via western blots. As mentioned earlier in the discussion, the reason for these differences in the effects of EBC-46 and TPA could be due to a number of factors including toxicity of the compounds, the cellular pathways they recruit and time of exposure to cancer cells. To further investigate the co-dependence of EBC-46 on host specific aspects, the following Chapter will address the potential anti-tumor activity and efficacy of EBC-46 in pre-clinical models of cancer.

Chapter Four

In Vivo Efficacy of EBC-46

4.1 Introduction

From the previous Chapter it has been established that the novel diterpene ester EBC-46, is a potent PKC activator. Similar to the prototypic PKC activator, TPA, it was shown to induce translocation of PKC to the plasma membrane and other subcellular organelles facilitating its participation in downstream cellular signaling pathways. TPA, although labeled as a tumor-promoter in carcinogenic experiments performed on normal mouse skin and xenografts of human foreskins with carcinogens such as urethane (Yuspa *et al.*, 1979), it has also been established to induce cytostatic and cytotoxic effects on cancer cells (Hofmann, 2001).

Previous studies of PKC-activating compounds utilized as localized therapeutics *in vivo* have been limited primarily to topical application of PEP005 in gels to subcutaneous tumors in mice (Li *et al.*, 2010, Ogbourne *et al.*, 2004). The anticancer activity of PEP005 *in vivo* has been demonstrated on B16-F0 melanoma, LK2 UV-induced SCC, Lewis lung carcinoma and D04 human melanoma grown subcutaneously in C57BL/6J or BALB/c *Foxn1*^{nu} mice and treated with three daily topical applications (Gillespie *et al.*, 2004, Ogbourne *et al.*, 2004). In one study (Le *et al.*, 2009), PEP005 was reported to induce a systemic immunostimulatory response and regress metastasis.

Surgery and radiation are the mainstays of local treatment of tumors but are limited with respect to efficiency, inaccessibility and intolerance for repeated courses of treatment. There is need for new and improved forms of local therapy. The concept of intralesional or intratumoral therapy is to let the drug pass the barrier zone and establish a sub-epidermal depot, thus, allowing a higher concentration of the drug to act on the tumor. This mode of treatment eliminates the need for long-term topical medications, coupled with the fact that it works deep into the tissue where topical applications may not penetrate.

Pilot experiments at QIMR Berghofer had shown that intratumoral injection of EBC-46, a novel diterpene ester dissolved in 90% PEG400, ablated B16-F0 tumors in C57BL/6 mice. However, with the realization that aqueous propylene glycol (PG) was a more suitable excipient for eventual clinical use it was desirable to confirm the initial findings from PEG400 and extend the scope of EBC-46 efficacy to other mouse tumor models. Optimization of drug delivery was important to be achieved not only for future use but also to improve reproducibility in studying the mechanism of action *in vivo*.

In this Chapter, the biological response and efficiency of EBC-46 *in vivo* on different tumor models was be investigated. From these studies we aimed to (i) optimize the intratumoral delivery and dose response of EBC-46 in 20% PG, (ii) compare the efficacy of EBC-46 with that of the prototype PKC activator, TPA, (iii) determine whether ectopic expression of PKC isoforms in tumor cells improved efficacy of EBC-46 and (iv) determine the efficacy of EBC-46 on different tumor models, melanomas and non-skin cancers.

4.2 Results

4.2.1 Comparison of the efficacies of EBC-46 and TPA for treatment of tumors in mice

All mouse experiments were conducted with the approval of the QIMR Berghofer Animal Ethics Committee, in Project P345. TPA was compared to EBC-46 *in vivo* to test its efficacy in curing C57BL/6 mice of B16-F0 tumors. Preliminary work in this laboratory had determined a range of doses of EBC-46 that induced a positive response in ablation of tumors in mice which ranged from 30 µg to 135 µg (personal communication Prof. Peter Parsons). Hence, an initial dose of 30 µg of TPA or EBC-46 was used in this study to compare the efficacies of the two compounds. A total of thirty mice were included in this study, which were divided into three groups of ten mice each group. B16-F0 tumor cells at 5 x 10^5 cells in a volume of 50 µl were injected in the bilateral flanks of all C57BL/6J mice. Upon growth of tumors to approximately 100 mm^3, two tumors on each mouse were treated with either 50 µl of the vehicle control 20% PG, 50 µl of 600 µg/ml of TPA or EBC-46 for a final dose of 30 µg per tumor. The day of treatment of tumors was recorded as day 0. Mice were regularly monitored, tumor sizes measured and animals euthanized when the total tumor burden reached 1000 mm^3. The mouse tumors were measured using digital calipers and following the calculation chart in Appendix Table 1 titled "Monitoring of Tumor Bearing Mice". Data obtained from this experiment were used to compare the efficacies of EBC-46 with that of TPA at 30 µg per tumor.

The control mice treated with 20% PG were euthanized by day 4 due to the volume of the tumors (Figure. 4.1). Among the treatment groups, all of the tumors initially treated with 30 µg of TPA per tumor gradually relapsed after treatment as a result of which all the mice in the TPA treatment

group were culled by day 20 due to excessive tumor burden. Whereas tumors that received a dose of 30 µg of EBC-46 per tumor resulted in a cure of 75 % of the tumors with 15 cures among the 20 tumors which were treated (Figure. 4.1). Recurrences were observed at 5 of the treated sites while there were no recurrences recorded among the 15 cures over the remainder of a 62-day monitoring period. Some of the failures in the EBC-46 treatment group may have been due to deeper tumors below the skin, growing in the muscle. This may have resulted at the time of inoculation when the B16-F0 tumor cells were inadvertently injected deeper under the skin instead of intradermally, hence would have required a deeper penetration of the drug.

Plots of individual tumor volume (Figure. 4.2) showed considerable variation, becoming more pronounced as some treated tumors recurred. This meant that having 2 tumors per mouse to minimize the number of animals required, led to some mice being euthanized with 1 recurrence and one potentially cured site, thus underestimating the Kaplan-Meier-based survival.

4.2.2 Dose response for efficacy of EBC-46 on mouse tumors

All mouse experiments were conducted with the approval of the QIMR Berghofer Animal Ethics Committee, in Project P345. Using preliminary *in vivo* results as reference, the previous study (Section 4.2.1) on the comparison of the efficacies of TPA and EBC-46 used 30 µg of either compounds to treat B16-F0 tumors in C57BL/6J mice.

The dose response for efficacy of EBC-46 on B16-F0 tumors in C57BL/6J mice was further investigated to determine a baseline concentration for *in vivo* activity of EBC-46 in killing tumor cells. Thirty C57BL/6J mice were divided into groups of ten mice each and subcutaneously injected with B16-F0 tumor cells at 5×10^5 cells in a volume of 50 µl at 2 sites on the hind quarter of each mouse. Upon growth of tumors to approximately 100 mm^3, two tumors on each mouse were treated with either 50 µl of the vehicle control 20% PG, 50 µl of 200 µg/ml of EBC-46 for a final dose of 10 µg per tumor or 50 µl of 600 µg/ml of EBC-46 for 30 µg final doses per tumor. Mice were monitored regularly and tumor sizes measured. Mice were euthanized when the total tumor size per mouse reached 1000 mm^3. Data recorded from the above treatments were organized to investigate the optimal dose response for the efficacy of EBC-46 in mice.

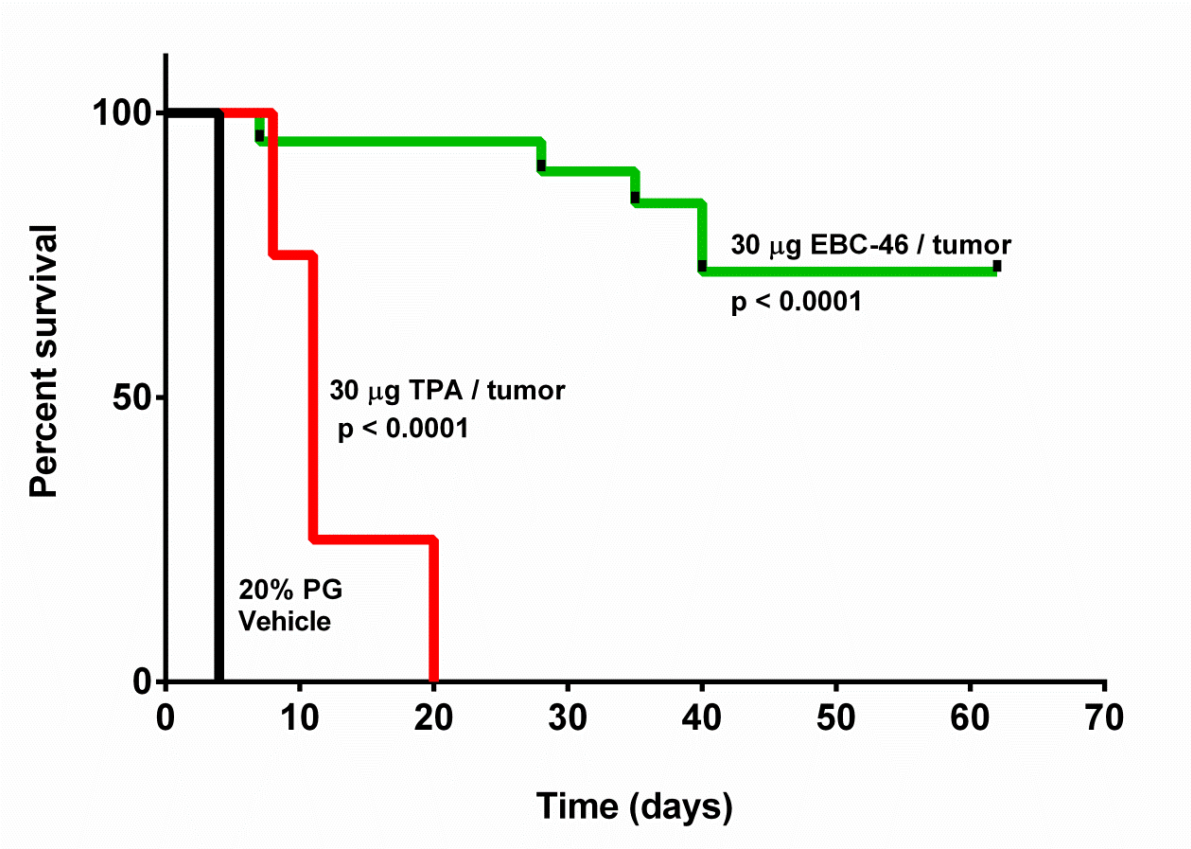

Figure 4.1 Kaplan-Meier plot comparing the differences in efficacy between TPA and EBC-46 on the survival of male C57BL/6J mice treated for B16-F0 tumors.

B16-F0 mouse melanoma cells (5 x 10^5 cells/site) were inoculated subcutaneously into C57BL/6J mice in a volume of 50 µl per site with 10 mice per group and 2 sites per mouse. Upon growth to 100 mm^3, the tumors were treated with a single intratumoral injection of 50 µl of 600 µg/ml EBC-46 in 20% PG for a final concentration of 30 µg/tumor (green line) and 50 µl of 600 µg/ml of TPA in 20% PG for a final of 30 µg/tumor (red line). These treatment groups were compared to mice treated with the vehicle control 20% PG (black line). Data was plotted in GraphPad Prism 6 and the *p* value was calculated to be less than 0.0001 for the two treatment groups (EBC-46 and TPA) compared to vehicle alone treatment (Log-rank (Mantel-Cox) test). TPA versus EBC-46 curves p=0.0004.

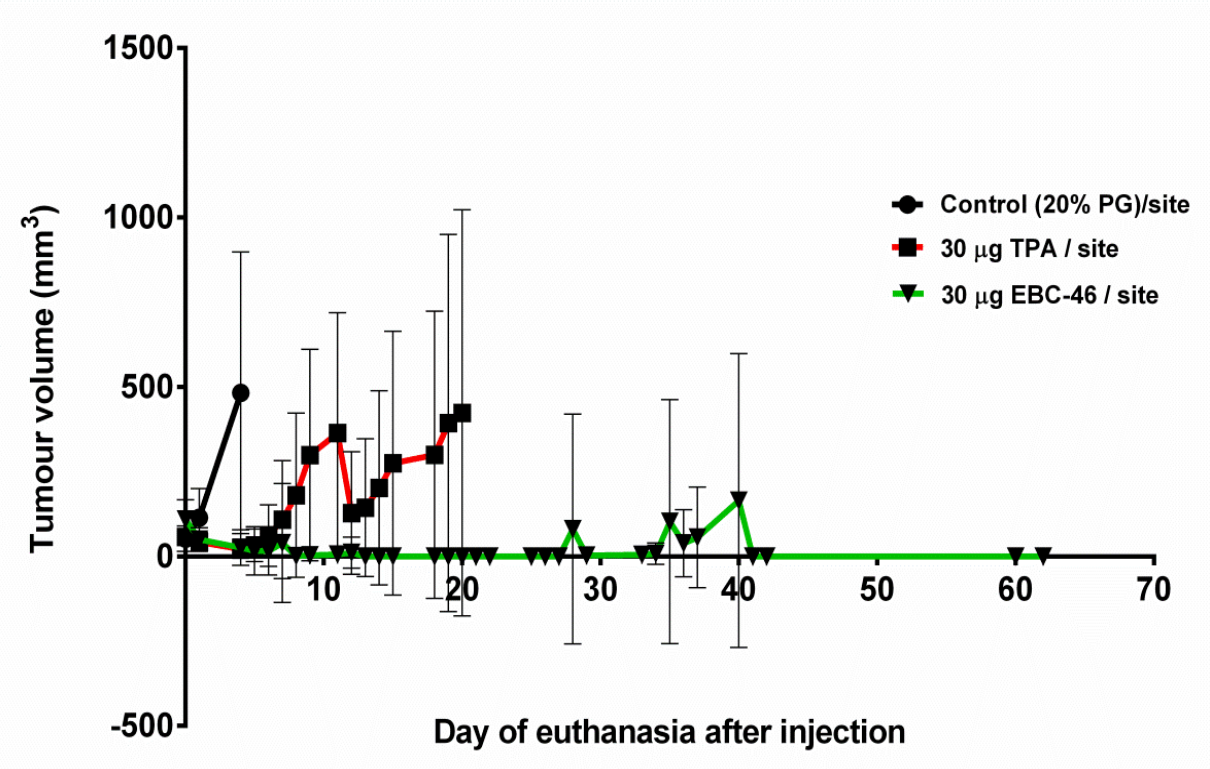

Figure 4.2 Tumor volume of B16-F0 tumors in C57BL/6J mice treated with diterpene esters TPA (■; red line) or EBC-46 (▼; green line) and compared to treatment with 20% PG (●; black line) vehicle control.

B16-F0 cells were inoculated subcutaneously at two sites on the flanks of C57BL/6J mice at 5 x 10^5 cells per site. Tumors were treated with 50 µl of 600 µg/ml of TPA or EBC-46 for a final dose of 30 µg per tumor. The controls included mice that had received an intratumoral injection of 50 µl of the vehicle control 20% PG. Tumor growth was measured in mm^3 and plotted against time as day of euthanasia. Day 0 denotes the day of intratumoral delivery of the respective treatment and the subsequent numbers indicate the days post treatment.

The Kaplan-Meier plot for survival (number of days after treatment to euthanasia) in Figure 4.3 shows that all of the 10 control mice (2 tumors per mouse), which had received injections of 50 µl of 20% propylene glycol (PG), were culled by day 4 due to tumor burden. Among the EBC-46 dose treatments, the 10 µg dose did not result in any cure as all mice had developed recurrences and were culled by day 25 due to tumor burden. In contrast, the 30 µg dosed mice fared much better, with cure of 75 – 80 % of tumors. Henceforth, treatments were carried out with 50 µl of 600 µg/ml EBC-46 in 20% PG; a 30 µg dose per tumor.

The initial major reaction of the mouse to intratumoral injection of EBC-46 or TPA was inflammation at the site, seen as an almost immediate reddening of the overlying skin, followed within 4-8 hr by flattening of the raised tumor and development of a bruised appearance. The inflamed region developed into a scab with the onset of necrosis at the site of inflammation. The PG vehicle alone on the other hand had little effect, except for a slight swelling of the tumor which subsided within 4 hr. Photographs of C57BL/6J mice with B16-F0 tumors (treated when about 100 mm^3 in size) taken over a 2-month observation period (Figure 4.4) showed indurations covering the area of inflammation by 5 days after treatment with EBC-46. This resolved over the next 14 days resulting in long-term healing with minimum scarring. No adverse clinical effects were observed in the treated mice and normal weight and activity were maintained.

4.2.3 Effect of tumor cell inoculation volume on efficacy of EBC-46

The success of local, intratumoral therapy may depend on a number of factors, the area of viable tumor in relation to the injection volume, being one. Varying volumes containing the same number of B16-F0 mouse melanoma cells were therefore injected subcutaneously into the hind quarter of C57BL/6 immunocompetent mice. This was done to assess the volume/concentration of the drug required to ablate tumors of varying inoculation densities. Three different tumor cell inoculation volumes were prepared; 25 µl, 50 µl and 100 µl, each containing a total of 5×10^5 B16-F0 tumor cells per site, injected subcutaneously into mice with 20 mice per group and 2 tumors per mouse. These 20 mice were further divided into 10 in the control group and the other 10 in the treatment group with EBC-46.

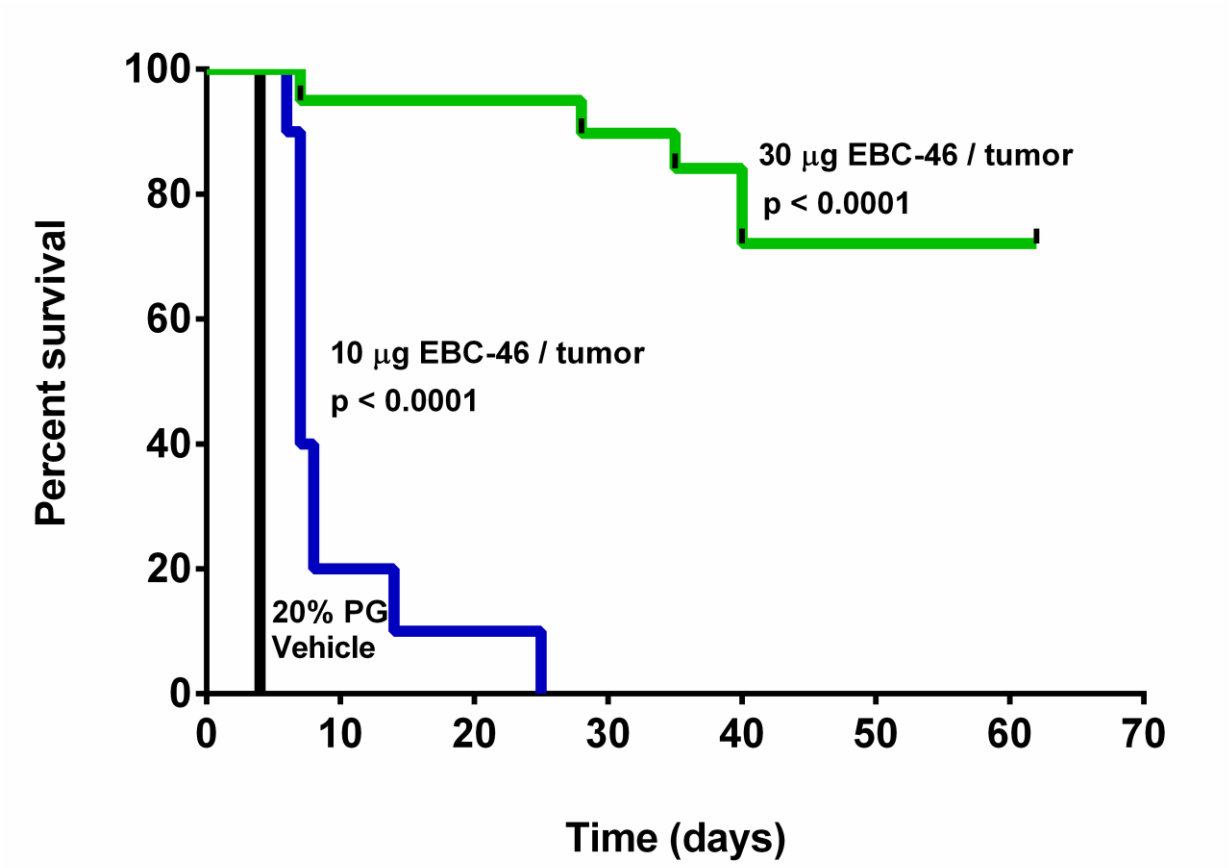

Figure 4.3 Kaplan-Meier plot for dose response of EBC-46 on survival of male C57BL/6J mice with B16-F0 tumors. *P* values <0.0001 showed significance compared with vehicle.

B16-F0 mouse melanoma cells (5 x 10^5 cells/site) were inoculated subcutaneously into C57BL/6J mice in a volume of 50 µl per site with 10 mice per group and 2 sites per mouse. Upon growth of tumors to 100 mm^3, were treated with single intratumoral injection of 50 µl of 200 µg/ml EBC-46 in 20% PG for a final concentration of 10 µg/tumor (blue line) and 50 µl of 600 µg/ml of EBC-46 in 20% PG for a final of 30 µg/tumor (red line). These treatment groups were compared to mice treated with the vehicle control 20% PG (black line). Data was plotted in GraphPad Prism 6 and *p* value was calculated to be less than 0.0001 for the two treatment groups (10 µg and 30 µg of EBC-46; Log-rank (Mantel-Cox) test).

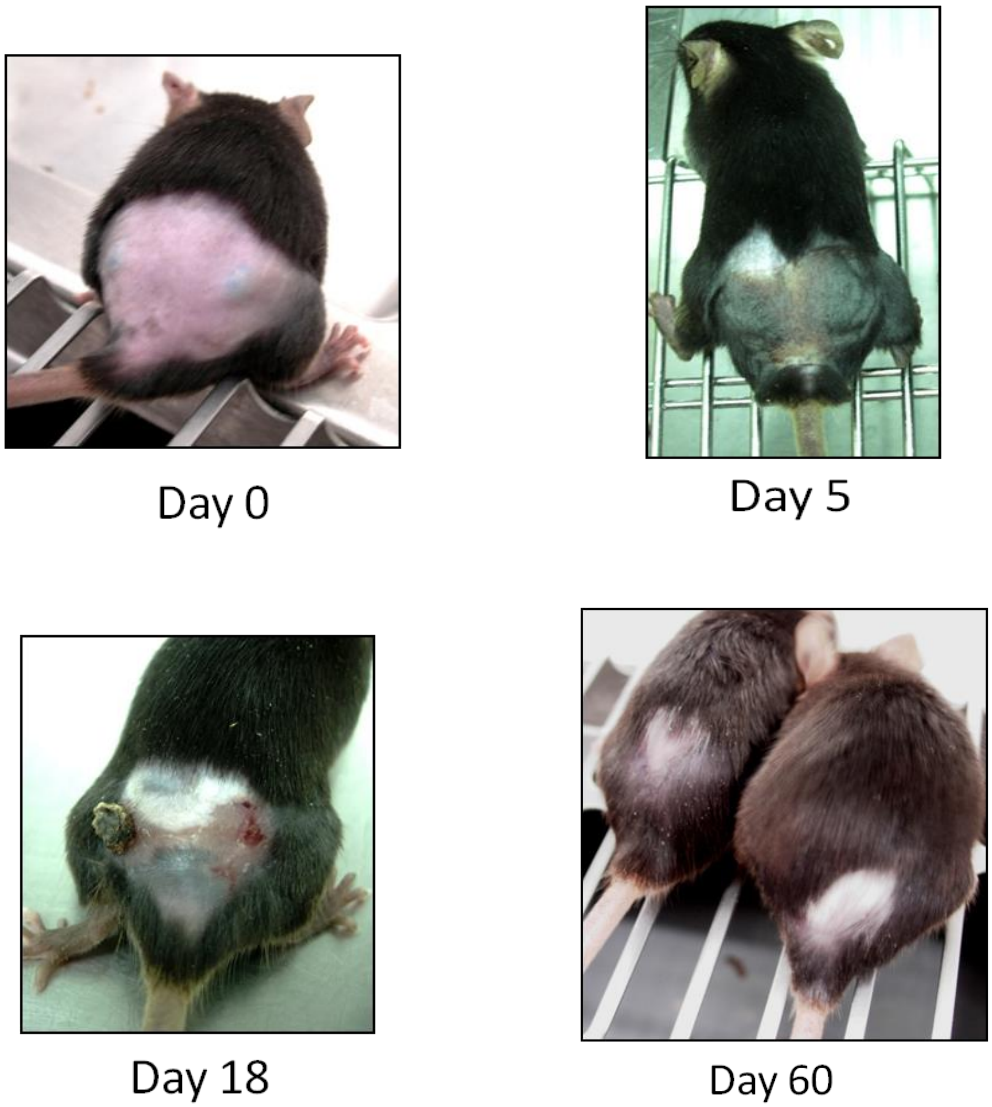

Figure 4.4 Serial photographs of male C57BL/6J mice with B16-F0 mouse melanomas prior to and following treatment with a final of 30 µg/tumor of EBC-46.

C57BL/6J immunocompetent mice were inoculated with B16-F0 mouse melanoma cells subcutaneously at 5 x 10^5 cells per site. Tumors were grown to approximately 100 mm^3, then treated with a single intratumoral injection of 50 µl of 600 µg/ml of EBC-46 in 20% PG for a final concentration per tumor of 30 µg. Mice were monitored daily for the first week following treatment, thereafter periodically three times a week. Mice were weighed and tumor sizes measured regularly.

In the first group (Figure 4.5.A), all the 10 control mice treated with 20% PG per tumor, were culled by day 7 due to tumor burden whereas the treatment with 30 µg of EBC-46 resulted in a 30% cure among the 20 tumors treated with 3 mice surviving tumor-free. The second group included mice inoculated with 5 x 10^5 tumor cells inoculated in 50 µl volume (Figure 4.5.B). In this group, the 10 mice treated with the vehicle (50 µl of 20% PG per tumor) were euthanized by day 4 as a result of tumor sizes. While treatment with 600 µg/ml of EBC-46 (50 µl for a final dose of 30 µg per tumor) fared much better with complete ablation of tumors in 5 mice of the 10 treated and no recurrence up to day 60 post-treatment. From the results, it was apparent that a 100 µl cell inoculation was too dilute to respond favorably to the optimal dose and volume of injection of EBC-46 as achieved in the first part of this experiment (see Section 4.2.2.) While the control mice were all culled by day 11 post-treatment, mice that received an EBC-46 treatment had developed recurrences with all of the mice being culled by day 46 due to tumor burden (Figure 4.5.C).

4.2.4 Efficacy of EBC-46 against B16-F0 tumors over-expressing PKC isoforms α and δ versus *lacZ* control

Since over-expression of PKC isoforms made melanoma cells Sk-Mel-28 and D04 sensitive to killing by EBC-46 in culture compared to the parent cell lines (*Chapter Three*; Section 3.2.4), the efficacy of EBC-46 on tumors over-expressing these PKC isoforms (*α* and *δ)* was compared in B16-F0 cells containing empty plasmid (*lacZ*). B16-F0 cells at 5 x 10^5 cells/site over-expressing PKC-*α* or PKC-*δ* or the control *lacZ* were inoculated into mice subcutaneously in 25 µl (Figure 4.6) or 100 µl inoculation (Figure 4.7) in culture medium using 20 mice per cell type. Mice were further sub-grouped into control and treated, with 10 mice in each group treated with 50 µl of either 20% PG or 30 µg of EBC-46 at 2 tumor sites per mouse.

In both experiments, all of the vehicle-treated mice (20% PG) were culled between days 4 – 7. In the EBC-46 treatment group from the 25 µl inoculum (Figure 4.6), mice carrying B16-F0 with *lacZ* control tumors gradually recurred and were all culled by day 25, while there was a 60% and 40% survival among the mice with B16-F0 tumors over-expressing PKC-*α* and -*δ* respectively. The *p* value was calculated at <0.01 for both the PKC isoforms in Prism. (Log-rank (Mantel-Cox) test).

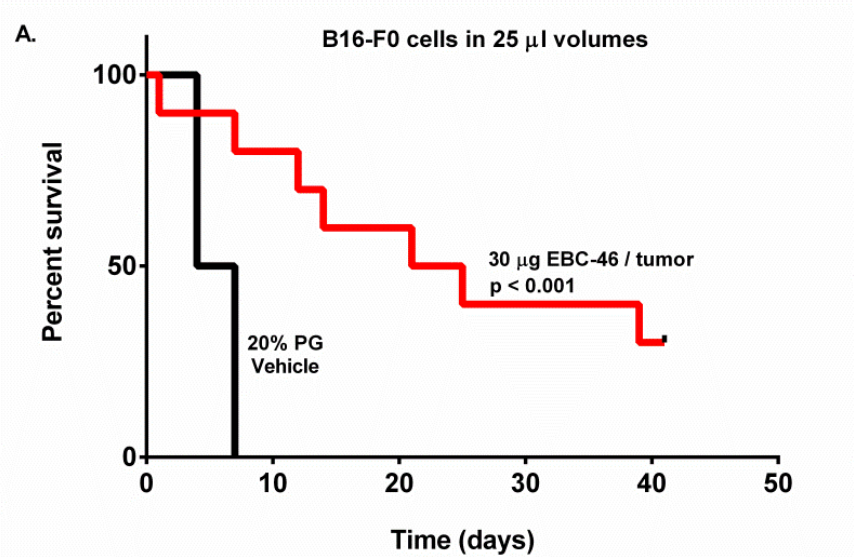
A.
B16-F0 cells in 25 µl volumes
Percent survival
100
50
0
0
10
20
30
40
50
Time (days)
30 µg EBC-46 / tumor
p < 0.001
20% PG
Vehicle

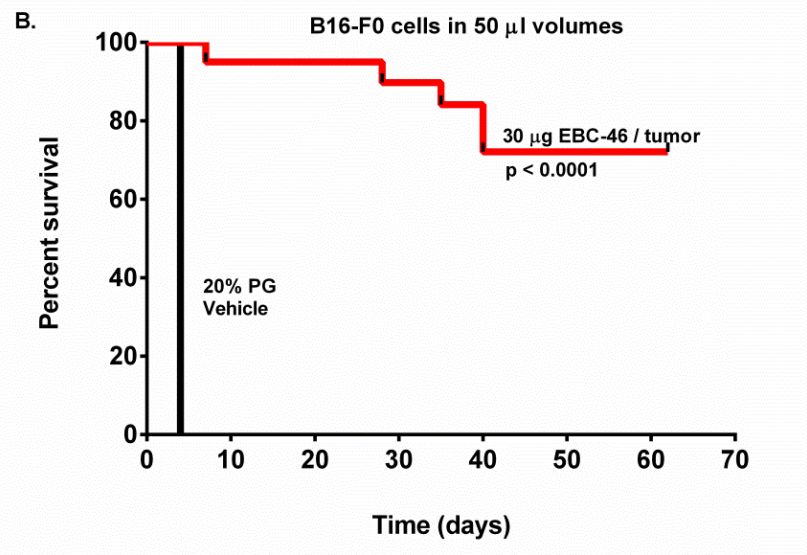
B.
B16-F0 cells in 50 µl volumes
Percent survival
100
80
60
40
20
0
0
10
20
30
40
50
60
70
Time (days)
30 µg EBC-46 / tumor
p < 0.0001
20% PG
Vehicle

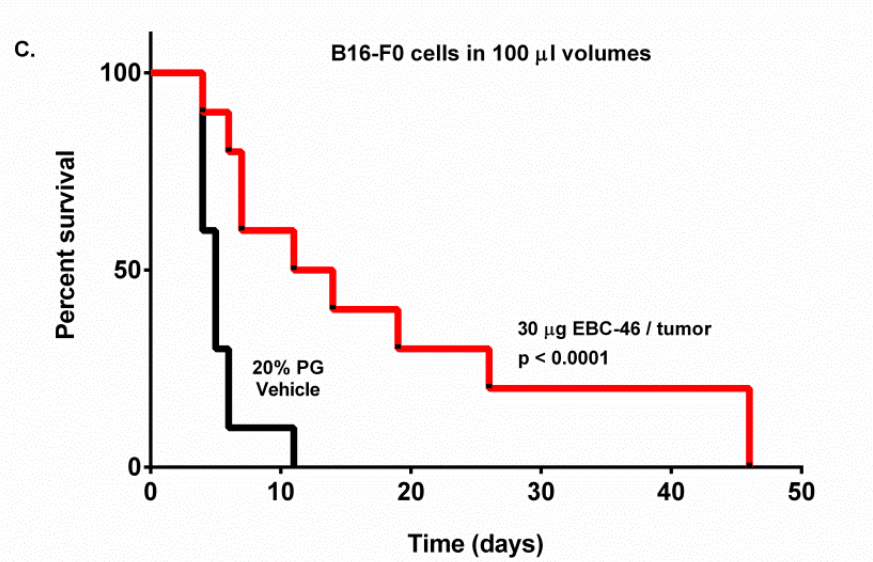
C.
B16-F0 cells in 100 µl volumes
Percent survival
100
50
0
0
10
20
30
40
50
Time (days)
30 µg EBC-46 / tumor
p < 0.0001
20% PG
Vehicle

Figure 4.5 Kaplan-Meier survival plots of male C57BL/6J mice with varying volumes of B16-F0 tumor cell inoculums treated with 50 µl of 600 µg/ml EBC-46 per tumor. Each experimental group consisted of 20 mice; 10 as controls and 10 as treatments.

A. 5 x 10^5 B16-F0 tumor cells in a total of 25 µl volumes were inoculated into bilateral flanks of twenty C57BL/6J mice and treated with 50 µl of 600 µg/ml of EBC-46 or 50 µl of 20% PG vehicle control.

B. 5 x 10^5 B16-F0 tumor cells in a total of 50 µl volumes were inoculated into bilateral flanks of twenty C57BL/6J mice and treated with 50 µl of 600 µg/ml of EBC-46 or 50 µl of 20% PG vehicle control.

C. 5 x 10^5 B16-F0 tumor cells in a total of 100 µl volumes were inoculated into bilateral flanks of twenty C57BL/6J mice and treated with 50 µl of 600 µg/ml of EBC-46 or 50 µl of 20% PG vehicle control.

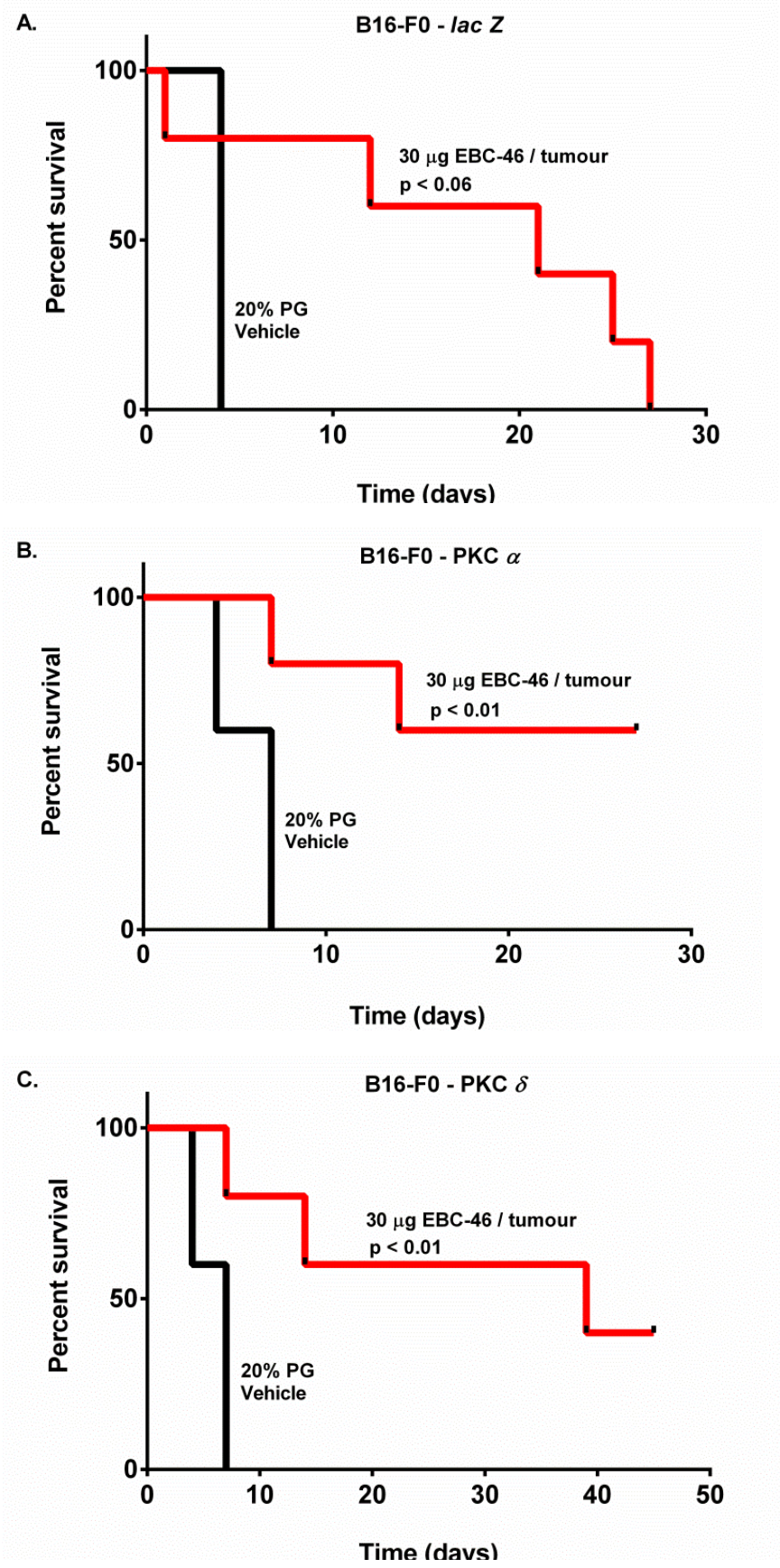
A.
B16-F0 - lac Z
Percent survival
100
50
0
0
10
20
30
Time (days)
30 μg EBC-46 / tumour
p < 0.06
20% PG
Vehicle
B.
B16-F0 - PKC α
Percent survival
100
50
0
0
10
20
30
Time (days)
30 μg EBC-46 / tumour
p < 0.01
20% PG
Vehicle
C.
B16-F0 - PKC δ
Percent survival
100
50
0
0
10
20
30
40
50
Time (days)
30 μg EBC-46 / tumour
p < 0.01
20% PG
Vehicle

Figure 4.6 Efficacy of EBC-46 in B16-F0 tumors over-expressing a PKC isoform compared with an empty vector control cell line (cells inoculated in 25 µl volumes)

A: 5 x 10^5 B16-F0 tumor cells expressing *lacZ* vector control in a total of 25 µl volume were inoculated into bilateral flanks of twenty C57BL/6J mice and treated with 50 µl of 600 µg/ml of EBC-46 or 50 µl of 20% PG vehicle control.

B: 5 x 10^5 B16-F0 tumor cells expressing PKC α in a total of 25 µl volume were inoculated into bilateral flanks of twenty C57BL/6J mice and treated with 50 µl of 600 µg/ml of EBC-46 or 50 µl of 20% PG vehicle control.

C: 5 x 10^5 B16-F0 tumor cells expressing PKC δ in a total of 25 µl volume, were inoculated into bilateral flanks of twenty C57BL/6J mice and treated with 50 µl of 600 µg/ml of EBC-46 or 50 µl of 20% PG vehicle control.

B16-F0 tumors over-expressing PKC isoforms α or δ or the empty vector control *lacZ* were inoculated into the bilateral flanks of male C57BL/6J mice at 5 x 10^5 cells per 25 µl of cell suspension. 10 mice were used per experimental group. When tumors had grown to approximately 100 mm^3 in volume, treatment with 50 µl of 600 µg/ml of EBC-46 (red line) or 50 µl of 20% PG vehicle control (black line) was carried out. Tumors were regularly monitored and tumor volumes measured and recorded. When total tumor burden reached 1000 mm^3, mice were euthanized. P values determined using a Log-rank (Mantel-Cox) test.

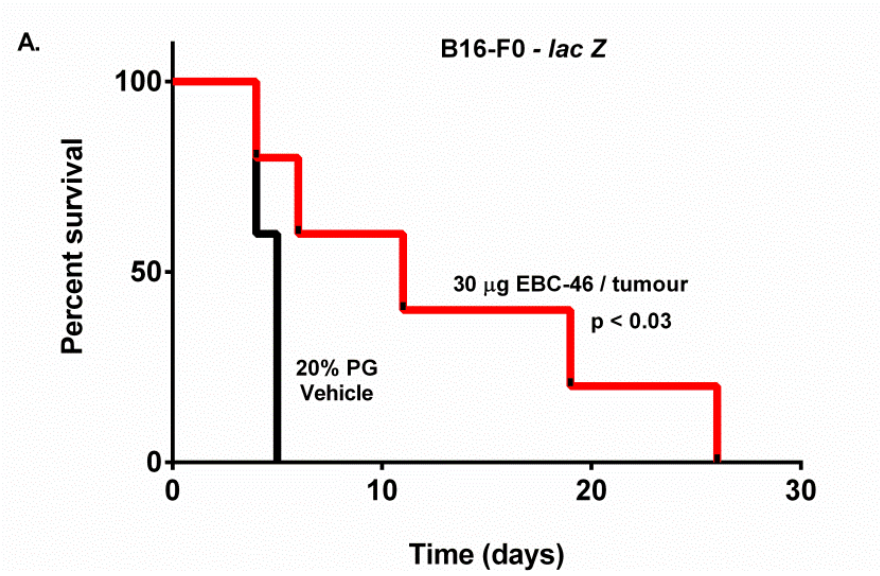
A.
B16-F0 - lac Z
Percent survival
100
50
0
0
10
20
30
Time (days)
30 μg EBC-46 / tumour
p < 0.03
20% PG
Vehicle

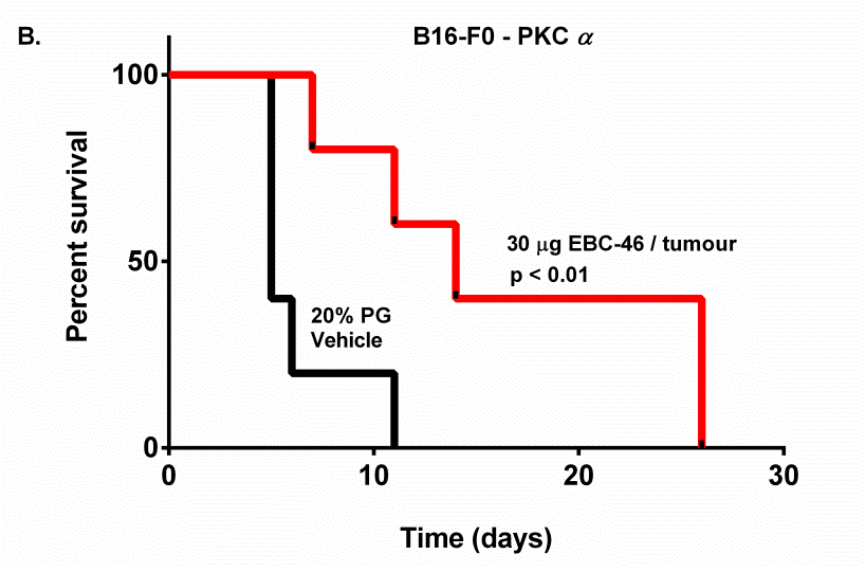
B.
B16-F0 - PKC α
Percent survival
100
50
0
0
10
20
30
Time (days)
30 μg EBC-46 / tumour
p < 0.01
20% PG
Vehicle

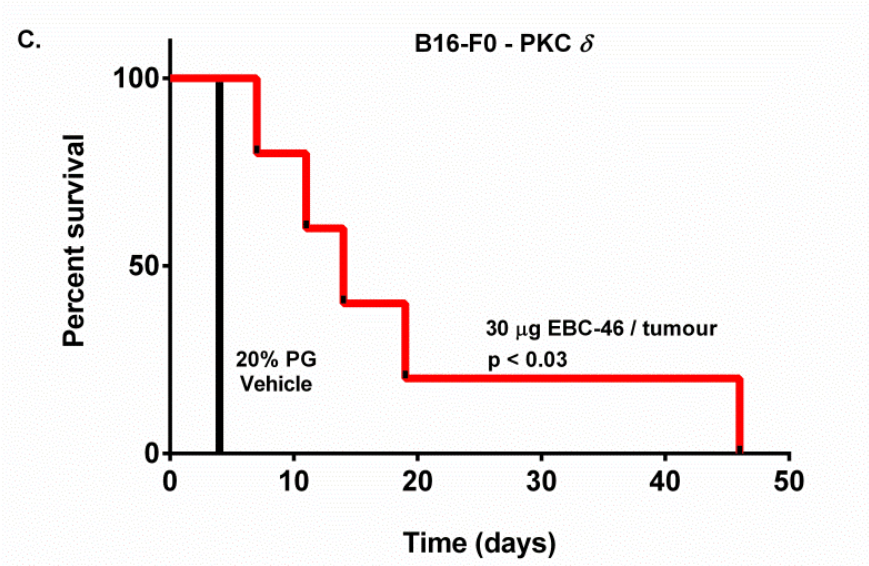
C.
B16-F0 - PKC δ
Percent survival
100
50
0
0
10
20
30
40
50
Time (days)
30 μg EBC-46 / tumour
p < 0.03
20% PG
Vehicle

Figure 4.7 Efficacy of EBC-46 on B16-F0 tumors over-expressing a PKC isoform compared with an empty vector control cell line (cells inoculated in a volume of 100 µl)

A: 5 x 10^5 B16-F0 tumor cells expressing ***lacZ*** vector control in a total of 100 µl volume were inoculated into bilateral flanks of twenty C57BL/6J mice and treated with 50 µl of 600 µg/ml of EBC-46 or 50 µl of 20% PG vehicle control.

B: 5 x 10^5 B16-F0 tumor cells expressing **PKC-*α*** in a total of 100 µl volume were inoculated into bilateral flanks of twenty C57BL/6J mice and treated with 50 µl of 600 µg/ml of EBC-46 or 50 µl of 20% PG vehicle control.

C: 5 x 10^5 B16-F0 tumor cells expressing **PKC-*δ*** in a total of 100 µl volume were inoculated into bilateral flanks of twenty C57BL/6J mice and treated with 50 µl of 600 µg/ml of EBC-46 or 50 µl of 20% PG vehicle control.

B16-F0 tumors over-expressing PKC isoforms -α or -δ or the empty vector control *lacZ* were inoculated into the bilateral flanks of C57BL/6J mice at 5 x 10^5 cells per 100 µl of cell suspension. 10 mice were used per experimental group. When tumors had grown to approximately 100 mm^3 in volume, treatment with 50 µl of 600 µg/ml of EBC-46 (red line) or 50 µl of 20% PG vehicle control (black line) was carried out. Tumors were regularly monitored and tumor volumes measured and recorded. When total tumor burden reached 1000 mm^3, mice were euthanized. P values determined using a Log-rank (Mantel-Cox) test.

As seen in Figure 4.7, tumors grown from a larger inoculation volume of all three B16-F0 sub-lines responded positively to EBC-46 treatment but resulted in recurrences and no cures were obtained.

These recurrences at previously treated tumor sites were most likely residual disease left untreated due to the larger volume of the inoculum. Similarly B16-F0 cells over-expressing PKC isoforms –α and -δ, injected in a volume of 100 µl of 5 x 10^5 tumor cells/ml did not respond well to treatment with 600 µg/ml of EBC-46. There were relapses recorded among the tumors over-expressing PKC-α and -δ with mice culled by days 26 and 46 respectively.

4.2.5 Efficacy of EBC-46 on Sk-Mel-28 human melanoma xenografts

A human melanoma model Sk-Mel-28 was used to test the efficacy of EBC-46 in xenografts in BALB/c *Foxn1*^{nu} mice. These are athymic mice which according to the name lack the thymus that produces T cells and thus test the efficacy of EBC-46 in immunocompromised animals.

Sk-Mel-28 xenografts inoculated subcutaneously at 2 x 10^6 cells/site in the flanks of BALB/c *Foxn1*^{nu} mice (6 mice in control group with 7 tumors total and 7 mice in the treatment group with 17 tumors in total). In the control group, mice treated with 20% PG were all culled by day 25 as a result of tumor burden (Figure 4.8). The discrepancy in the number of tumors per mouse may be a result of the nature of the cell type. Sk-Mel-28 cells are not as proliferative as the B16-F0 cells and are slower growing. Of the 17 tumors in the group treated with 30 µg of EBC-46 per tumor there were 15 cures (Figure 4.8.A). These results were reflected in measurements of tumor size (Figure 4.8.A). The total loss of tumor volume 24 hr after treatment can be seen in the plot for treated cells. The early effects at the injected tumor site were seen more clearly in this nude mouse model than in the C57BL/6 mice: immediate inflammation and a notable bruised appearance at 4 hr (Figure 4.9). By day 13 the inflammatory region encompassing the tumor site and the skin around the perimeter developed into an eschar that detached by day 20. The mice were monitored for a period of 40 days post treatment over which there were no recurrences recorded.

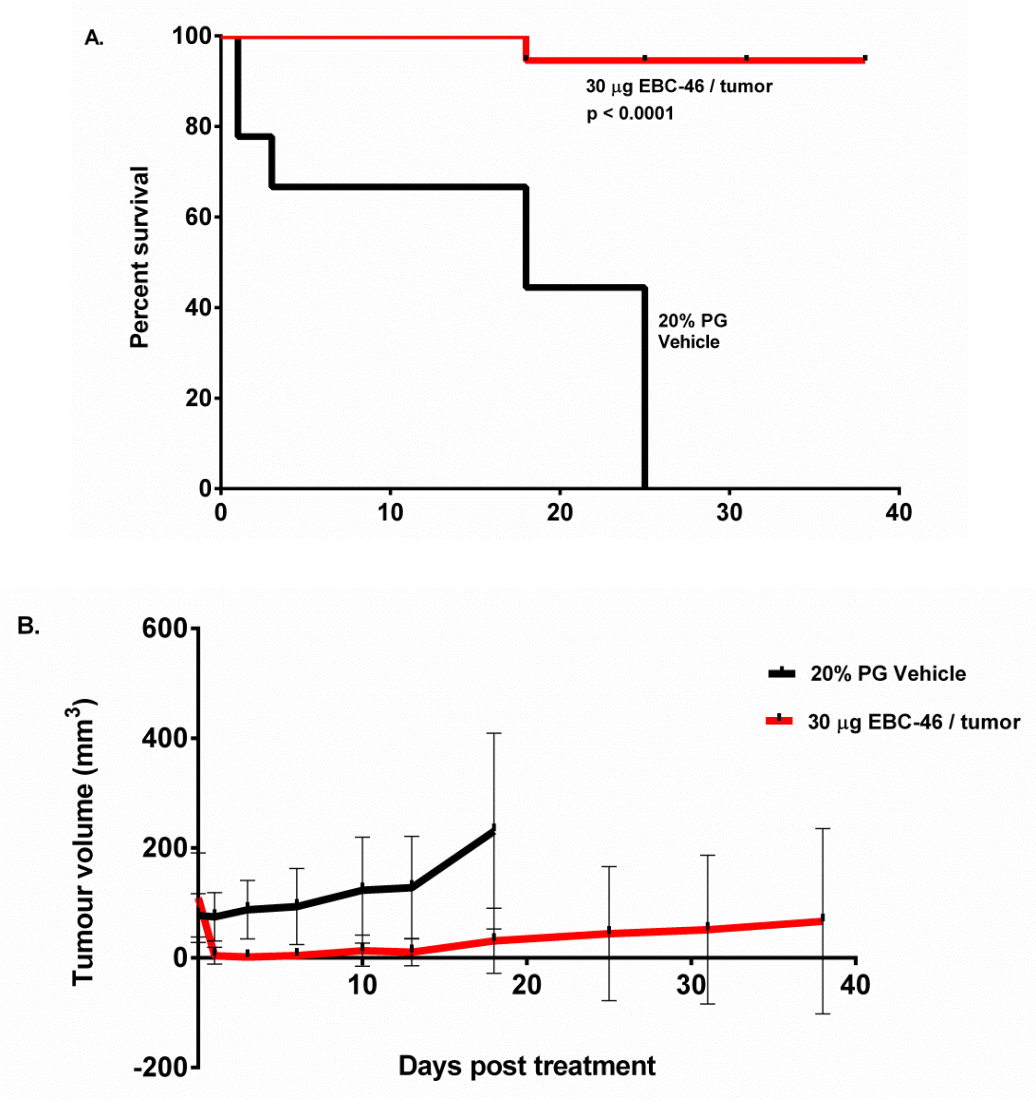

Figure 4.8 Efficacy of EBC-46 in treating Sk-Mel-28 human metastatic melanomas in male BALB/c *Foxn1^{nu}* (nude) mice.

A. Kaplan-Meier plot of survival of BALB/c *Foxn1^{nu}* (nude) mice treated with 30 µg of EBC-46 (red line) for subcutaneous Sk-Mel-28 tumor growth (2 x 10^6 cells/site) and compared to the vehicle control 20% PG (black line). (Log-rank (Mantel-Cox) test).

B. Tumor volumes of SK-Mel-28 human metastatic melanomas in BALB/c *Foxn1^{nu}* (nude) mice following treatment with EBC-46 at a final dose of 30 µg per tumor (red line) in comparison to treatment with the vehicle control 20% PG (black line).

A total of 6 mice with 7 tumors were included in the control group while there were 7 mice with 17 tumors in the treated in this experiment. The discrepancy in the number of tumors per mouse may be a result of the nature of the cell type.

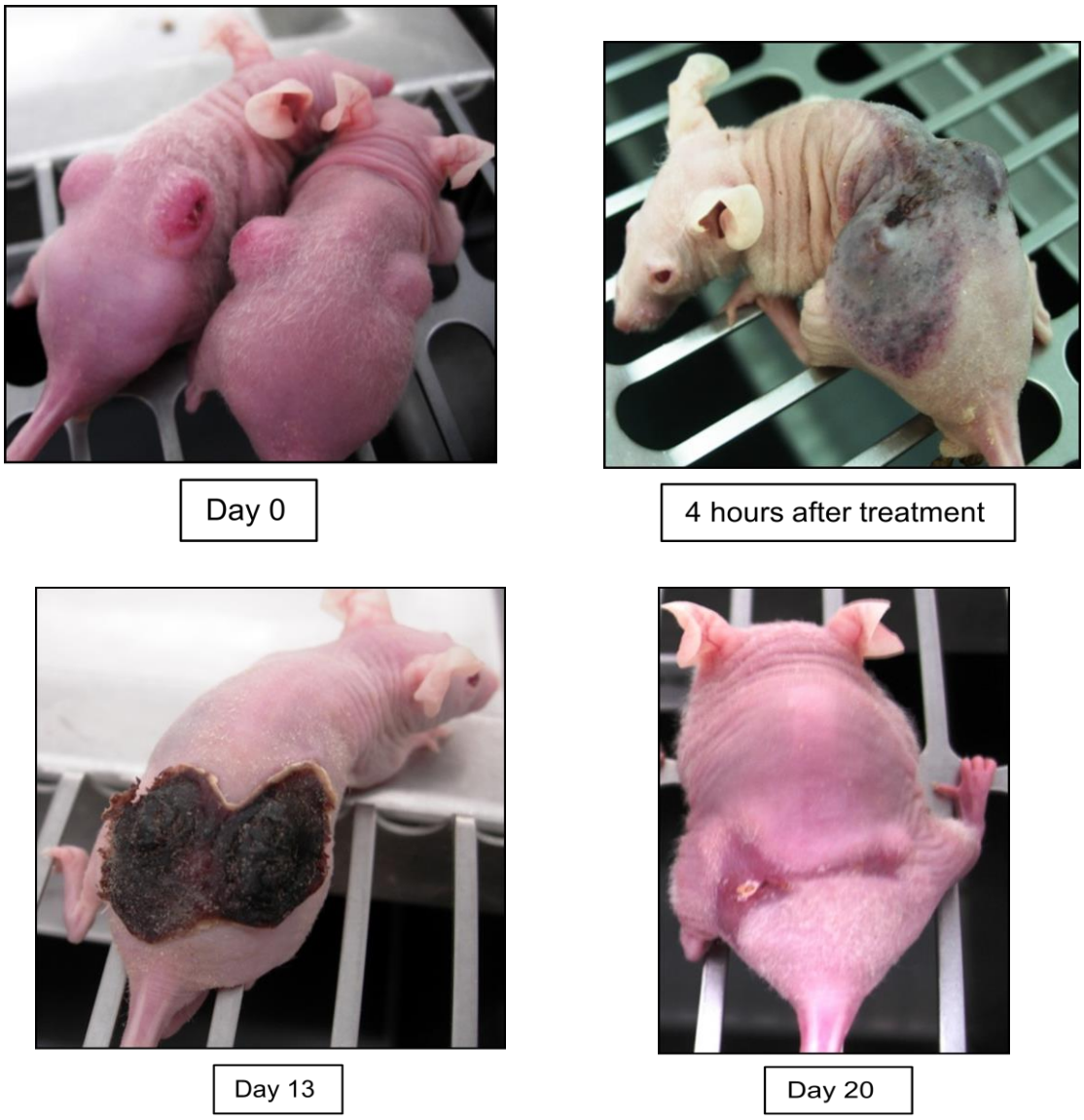

Figure 4.9 Photographs of male BALB/c *Foxn1*^{nu} (nude) mice with Sk-Mel-28 tumors treated with EBC-46.

BALB/c *Foxn1*^{nu} (nude) mice were transplanted with Sk-Mel-28 tumor cells subcutaneously in their bilateral flanks. Tumors were treated with EBC-46 at a final concentration of 30 µg per tumor and compared to control mice treated with the vehicle control 20% PG. Digital photographs were taken starting on the day of intratumoral delivery of EBC-46 or vehicle control.

4.2.6 Effect of EBC-46 on non-melanoma tumors *in vivo*:

The *in vitro* efficacy of EBC-46 had been tested beyond melanomas including lung cancers and leukemia cell lines (*Chapter Three*; Section 3.2.3) resulting in killing tumor cells. The results were extended to non-melanoma tumors *in vivo* where the efficacy of EBC-46 in ablating MC38 tumors in mice was tested.

MC38 mouse colon tumors were grown in C57BL/6J mice by subcutaneous injection of MC38 cells (5×10^5 cells per site) and treated with a single intralesional injection of EBC-46. Treatment with 30 µg of EBC-46 led a rapid ablation of tumors, compared to the control tumors treated with vehicle only (20% propylene glycol). The survival curve in Figure 4.10.A shows that all control mice (black line) treated with 20% PG had to be culled by day 12 due to overall tumor burden. In contrast, MC38 tumors treated with 30 µg per tumor EBC-46 resulted in total ablation of 8 out of 10 tumors. Among the tumors treated with EBC-46 there were only 2 recurrences rising individually on 2 mice which had to eventually be euthanized by day 20 due to tumor burden. In the 49 day observation period following treatment there were no recurrences at the 8 cured sites (Figure 4.10).

4.2.7 *Ex Vivo* clonogenic survival of tumor cells following treatment with EBC-46

The rapid and dramatic changes in visual appearance of the tumor sites following injection of EBC-46 prompted an investigation of how quickly viable, clonogenic tumor cells were being destroyed. This was conducted by removing tumors at early times after treatment, dispersal into culture and determination of clonogenic survival.

Microscopic inspection of cultures from tumors harvested from mice and dispersed in culture showed many granular, non-adherent and presumably dead cells within 1 hr after the *in vivo* treatment. This was confirmed by a clonogenic-type survival assay, in which *ex vivo* cultures were allowed to grow for 5-6 days to assess growth of the surviving cells. All tumor cells were destroyed by 4 hr after treatment with EBC-46 (Figure 4.11). Cells began to lose their viability as early as 1 hr after treatment, indicated by long term growth of 40% compared to cells from control tumors treated with 20% PG. Vehicle injected *in vivo* had very little effect on *ex vivo* clonogenicity compared with tumors not treated at all (results not shown).

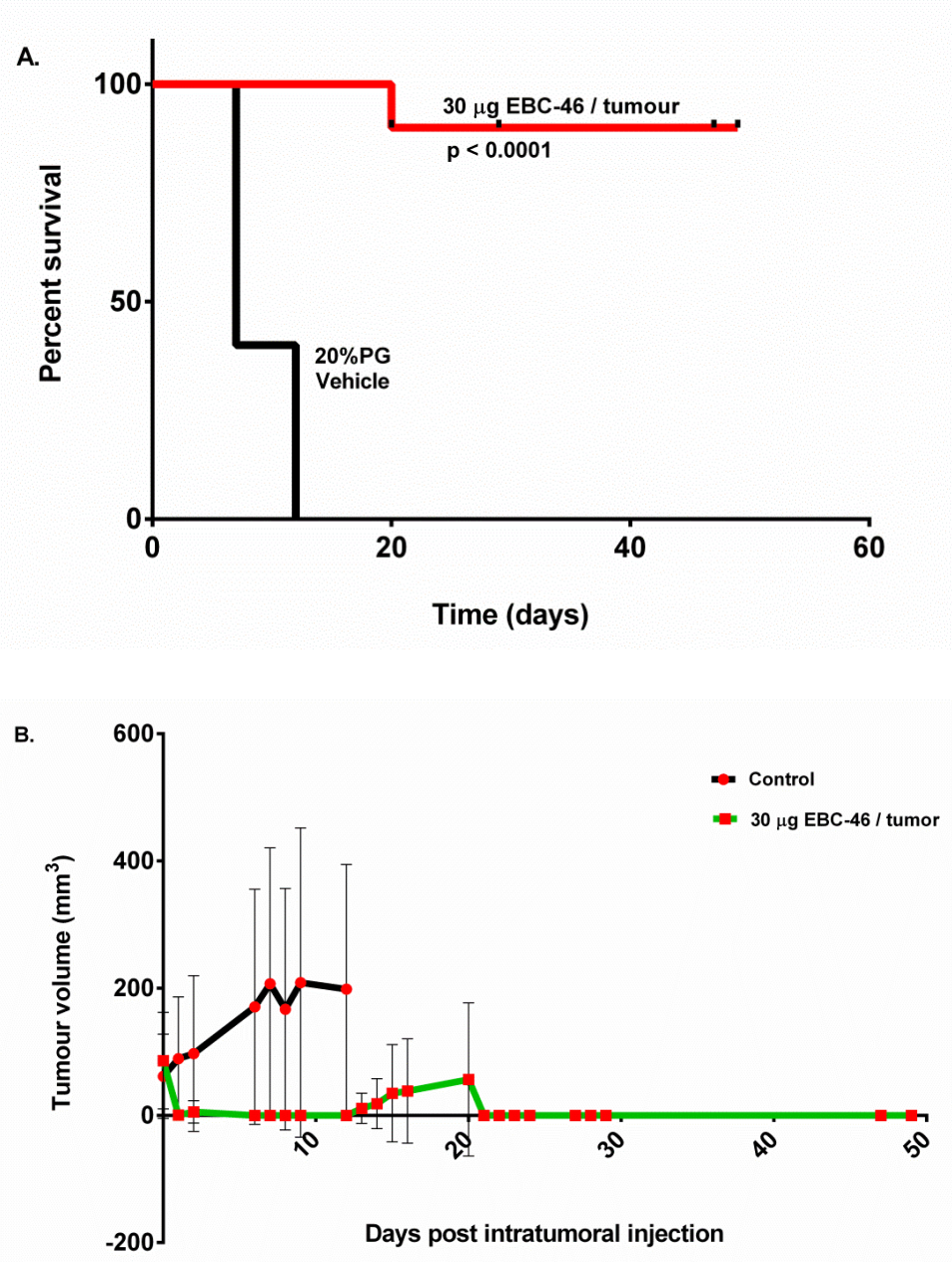

Figure 4.10 Efficacy of EBC-46 on MC38, mouse colon cancer

MC38 mouse colon tumors were grown subcutaneously in C57BL/6J mice on their bilateral flanks. When tumors had grown to approximately 100 mm3, tumors were treated with 50 µl of 30 µg of EBC-46 per tumor or 50 µl of 20% PG vehicle control. Tumors were regularly monitored and volumes measured and recorded. P values determined using a Log-rank (Mantel-Cox) test.

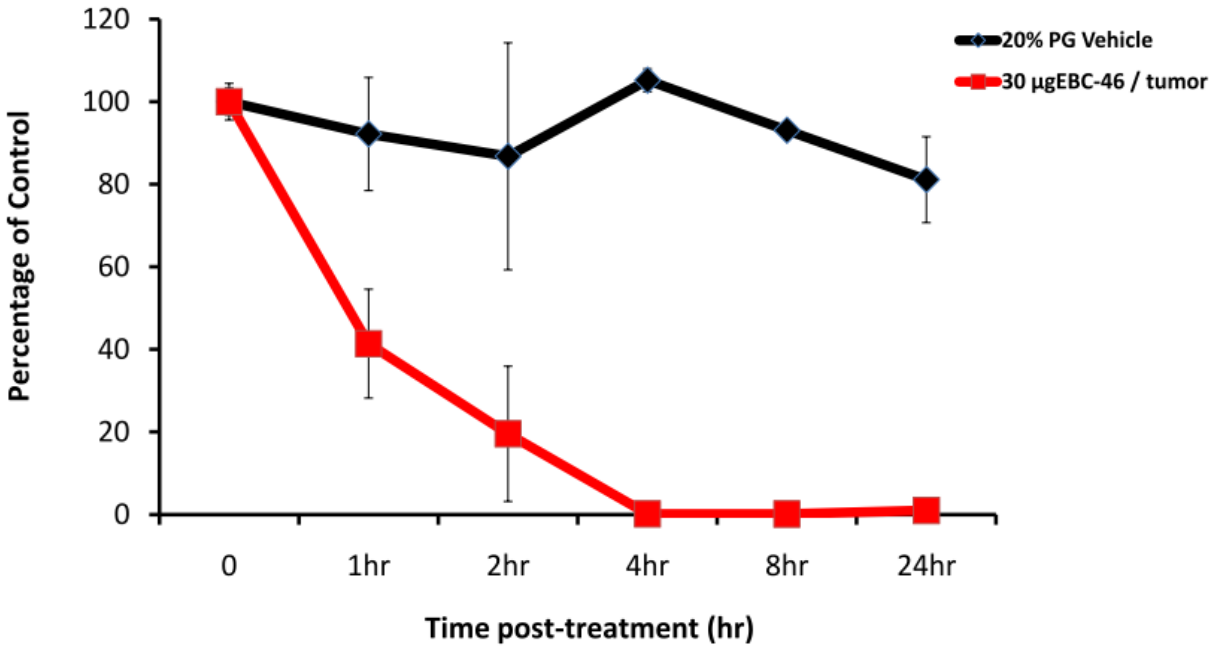

Figure 4.11 Clonogenic survival of Sk-Mel-28 tumor cells destroyed by 4 hr after treatment with EBC-46

Sk-Mel-28 tumors were treated *in vivo* in BALB/c *Foxn1*^{nu} (nude) mice with either 50 µl of 600 µg/ml of EBC-46 in 20% PG or 50 µl of 20% PG vehicle control. Tumors were excised at different times following treatment and the cells recovered back into culture media *in vitro* in serial dilutions. Plates were incubated at 37˚C and reviewed daily. After 4-5 days, when control cells reached a confluency of ~70%, a cell survival assay was performed using the SRB dye to stain and the plate was read at 564 nm using an ELISA plate reader.

4.2.8 Rapid killing of tumor cells in culture with high dose EBC-46: detection of necrosis by uptake of propidium iodide

To determine whether the rapid, high-dose killing of tumor cells inferred from the above *ex vivo* scenario could be reproduced away from the host context *in vitro*, a growth inhibition assay using propidium iodide was carried out *in vitro* using a high EBC-46 concentration range, similar to the 600 µg/ml injected concentration. Propidium iodide (PI) intercalates with DNA and causes nuclei and fragmented nuclei to become strongly fluorescent. PI is membrane impermeant and is excluded from viable cells. It can therefore be used to detect cell death associated with disruption of the plasma membrane, allowing ingress of charged molecules. This includes primary or secondary necrosis of cells, as well as apoptosis where fragmented nuclei will be seen. In this assay, cells were plated at a high density to mimic the *in vivo* scenario where tumor cells are present at high density within the tumor capsule. It was not possible to reproduce exactly the drug delivery method used *in vivo* because 20% PG alone was toxic in culture. Instead, a stock solution of 20 mg/ml EBC-46 in ethanol was diluted directly into the cultures. The final 2% level of ethanol was not toxic to cells, and the presence of 10% FCS enabled the EBC-46 to remain in solution, albeit bound reversibly to protein. Pilot studies had previously shown that EBC-46, a water-insoluble molecule, could be solubilized in 4% albumin and still retain its potency against cultured cells.

Cells were treated with TPA or EBC-46 at varying doses (300 µg/ml, 100 µg/ml and 50 µg/ml) for different times (5, 10 and 30 min). The controls were untreated cells and EtOH-only (vehicle). 0.1% Triton-X100 was used as a positive control, to instantly lyse cells for propidium iodide uptake and allow the total cell number to be determined. Cells were photographed with the AMG EvosFL inverted fluorescence microscope at 4X, under bright-field or red fluorescence illumination. Micrographs of at least 3 different fields per well were captured.

Bright field images showed numerous blebs forming on the plasma membranes of the Sk-Mel-28 cells within several minutes of treatment. By 30 min the blebs had disappeared, and many cells could be seen with the faint outline of grossly swollen cytoplasm and shrunken nuclei. No nuclear fragments typical of apoptotic bodies were seen. Fluorescence examination of the cells (Figure 4.12 on p.126-127) and counting of PI-stained cells showed 80 – 90% killing of cells treated with EBC-46 at the highest dose (300 µg/ml) within 30 min of treatment. However, the cytotoxic effect of TPA detected by PI uptake was delayed, with maximum cell death reached 24 hr after treatment.

4.3 Discussion

In order to establish a strong correlation between the outcomes of experimentation and the indications of EBC-46 in future treatment of patients with cancers, it is vital to investigate the action of EBC-46 within the host biological system. Bearing in mind the dose ranges tested in the cell based assays in *Chapter Three* and the optimal dose of TPA and EBC-46 at which an IC_{50} was obtained, a range of doses was tested on tumors *in vivo*, that would have a clinically relevant outcome in ablating the tumors in mice. The results in this Chapter showed that a single intratumoral injection of 600 µg/ml of EBC-46 rapidly ablates subcutaneous tumors in a range of mouse models, accompanied by an inflammatory response resulting in long term cures.

Judging by the enhanced potency of TPA *in vitro*, compared with EBC-46 (refer Figure 3.7) it was hypothesized that TPA would be just as potent as EBC-46, if not more so, on tumor cells *in vivo* upon intratumoral injection. Hence, its efficacy was tested in parallel to EBC-46 on different tumor models. Surprisingly, TPA failed to demonstrate the expected outcome in curing tumors in mice given its cytotoxic action *in vitro*. Previous studies using a PKC activator to treat tumors *in vivo* involved the use of PEP005 (ingenol 3-angelate; Ing3A) via topical application. It was shown to be able to penetrate deeper into the dermis compared to TPA following application, as PEP005 is a substrate for P-glycoprotein 1 (also known as MDR1, ABCB1) which is an ABC transporter (Li *et al.*, 2010). Studies have shown that TPA was restricted to the epidermis of the skin hence leading to a lack of anti-cancer activity. Our studies showed that intratumoral injection of TPA, bypassing the epidermis, failed to cure mice of the subcutaneously transplanted B16-F0 tumors. On the other. hand, a single intratumoral injection of EBC-46 led to a distinct anti-tumor effect over the long term. B16-F0 mouse melanoma is a well-established solid-tumor model and is regarded as highly invasive and metastatic in nature (Corbett *et al.*, 2002). Hence, it is a difficult model to treat and positive results have more credibility than with some other models. B16-F0 first arose spontaneously in C57BL/6 mice in 1954 (Alvarez, 2002) which makes the mouse strain immuno-competent for growth of transplanted syngeneic tumors. This compatibility therefore provides a more complete test system than growth of human tumor cells implanted into immuno-compromised mice. SK-Mel-28 is a human metastatic melanoma obtained from ATCC for research work in nude BALB/c *Foxn1*^{nu} mice to complement the immune-competent locally aggressive murine counterpart B16-F0.

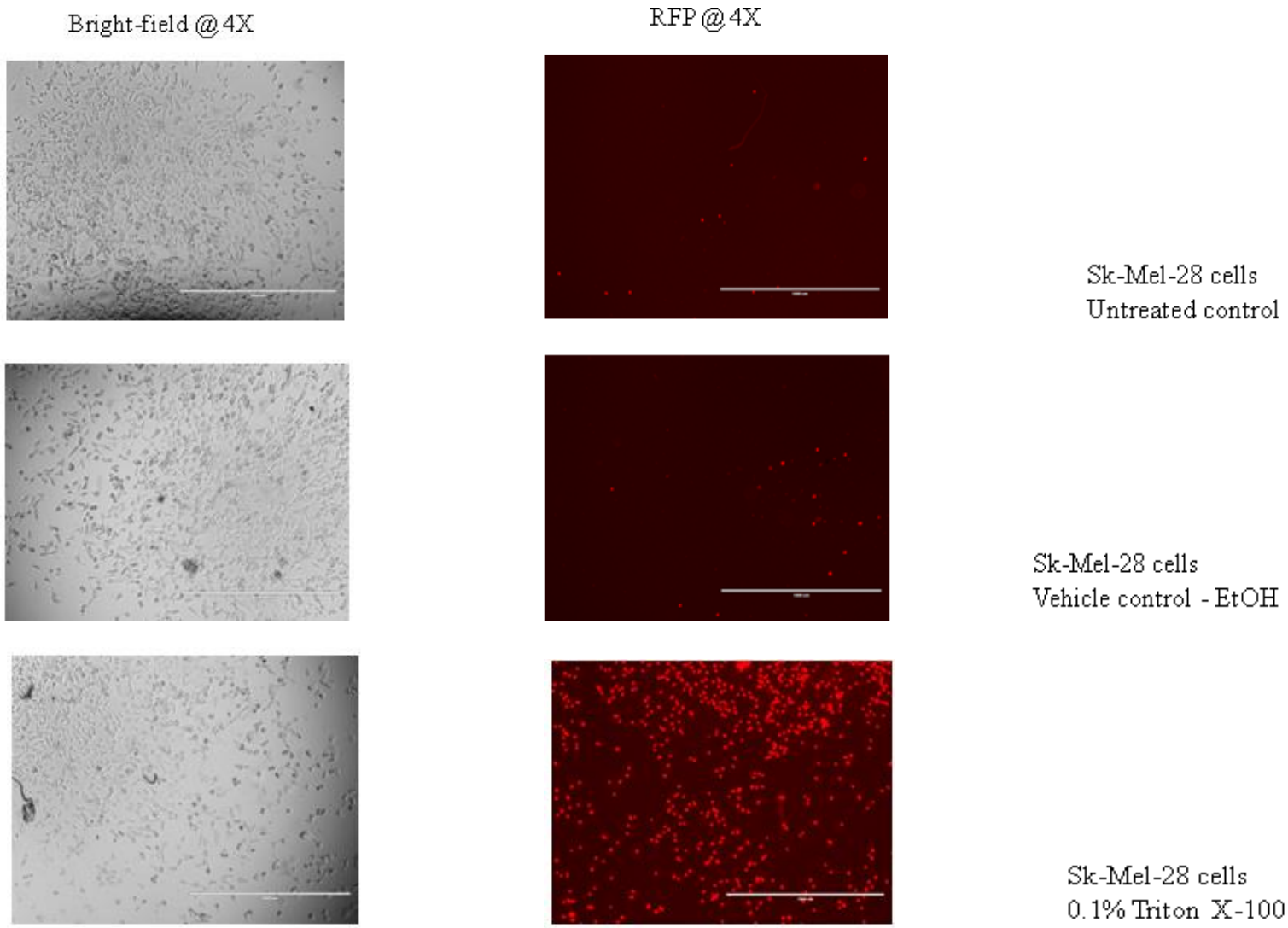
Bright-field @ 4X
RFP @ 4X
Sk-Mel-28 cells
Untreated control
Sk-Mel-28 cells
Vehicle control - EtOH
Sk-Mel-28 cells
0.1% Triton X-100

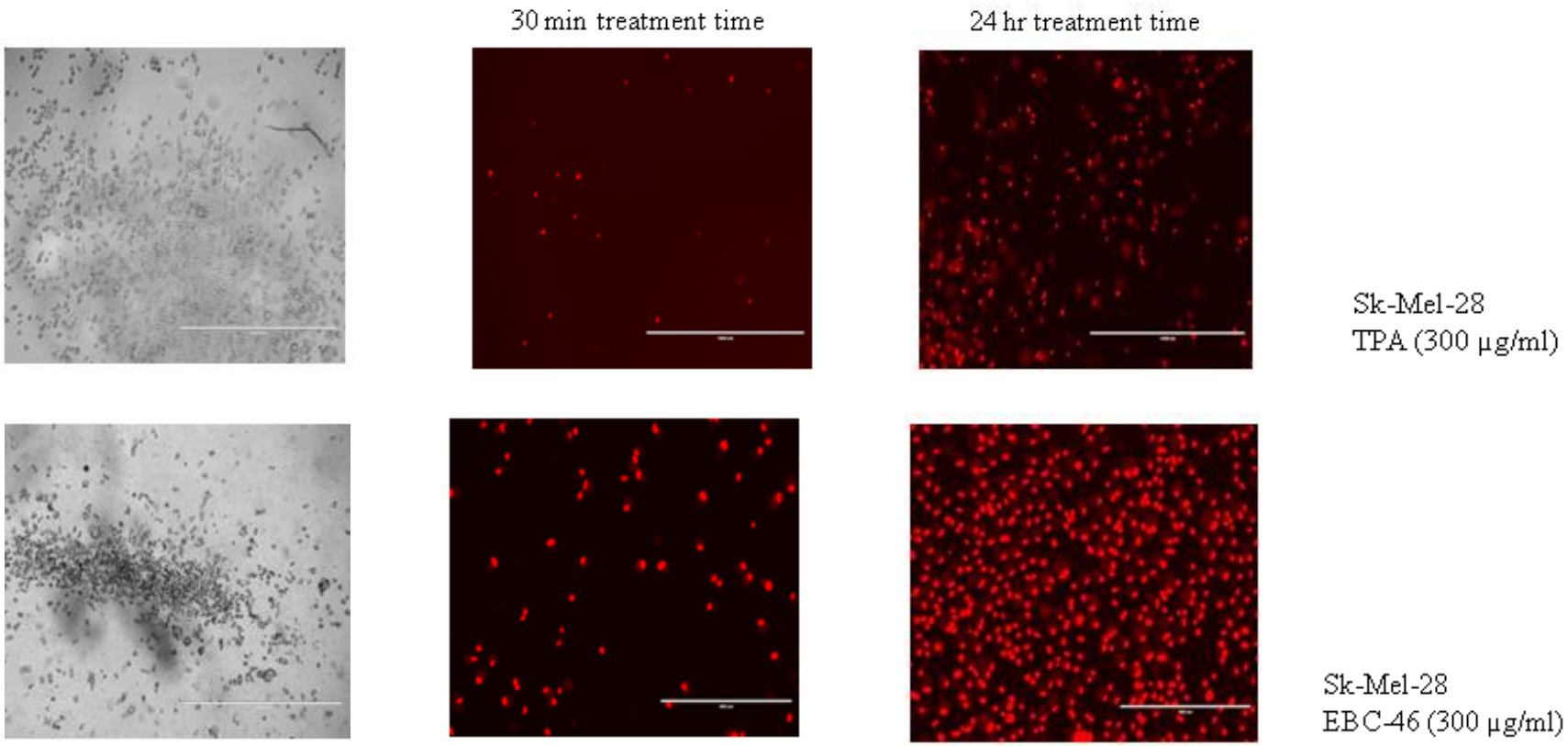

Figure 4.12. Photomicrographs of Sk-Mel-28 tumor cells treated with TPA or EBC-46 *in vitro* and stained with propidium iodide.

Sk-Mel-28 melanoma cells were treated with either 300 µg/ml EBC-46 or 300 µg/ml TPA for 30 min and 24 hr prior to staining with 5 µg/ml (w/v) propidium iodide for 5 min. Cells were imaged using the AMG EvosFL inverted fluorescence microscope at 4x, under bright-field or red fluorescence illumination.

Nude BALB/c *Foxn1*^{nu} mice have been utilized in this project to treat human xenografts of Sk-Mel-28 metastatic melanomas. This is a well utilized athymic strain of laboratory mice with a spontaneous deletion in the *FOXN1* gene lacking thymus thus, resulting in an inhibited adaptive immune system. The BALB/c *Foxn1*^{nu} (Nude) mice allow for a more accurate inoculation of tumor cells subcutaneously due to their hairless skin and docile nature. In addition, the hairless phenotype makes it easier to monitor tissue reaction to the treatment with EBC-46, inflammation at the treated site and ulceration. The deficiency of a cell-mediated immune response in these mice helped to determine the role of an immune response in the mechanism of action of intratumoral EBC-46. The depletion of T-cells did not prevent the high cure rates obtained from this model which implies that either the innate immune system is activated or other direct pathways are responsible for the mechanism of action of intratumoral EBC-46, rather than the adaptive immune response mediated by T-cells.

As a PKC activator, the effect of EBC-46 on PKC over-expression in the target tumor cells *in vivo* was investigated. In *Chapter Three*, Sk-Mel-28 cells over-expressing PKC isoforms were tested in the presence of diterpene esters to determine their sensitivity to killing. It was found that EBC-46 had greatly enhanced potency in killing cell lines with over-expressed PKC isoforms, at doses as low as 0.1 ng/ml compared to the more resistant response of Sk-Mel-28 cells with *lacZ* controls. However from a comparison of the survival curves of these over-expressed PKC cell lines to the parent cell lines it can be extrapolated that the sensitivity of EBC-46 on cells over-expressing PKC isoforms is not as heightened as expected. A level of enhanced sensitivity was found *in vivo* when B16-F0 tumors over-expressing PKC isoforms -*α* or -*δ* were treated with 30 µg EBC-46 per tumor, where more cures were recorded compared to the *lacZ* controls. However, similar to the cell survival assay in *Chapter Three*, the increased sensitivity of B16-F0 tumors over-expressing PKC-α or –δ cannot be justified as mice carrying tumors over-expressing PKC-α were monitored for less than a month with 60% cure, while those mice with tumors over-expressing PKC-δ were monitored for about 45 days with 40% cure. The most important observation from this experiment was that the volume of EBC-46 injected was a crucial factor in treatment of tumors. Here the volume of the tumor inoculum in relation to the volume of the diterpene ester injected was investigated as a possible determinant of anti-tumor efficacy. Between the two experimental groups (Figure 4.5) tumors which arose from an initial inoculum of 25 µl responded positively to treatment with 30 µg per tumor of EBC-46 which has been established as an optimal dose for intratumoral treatment

(Figure 4.2). There were re-growths of tumors among the mice of the second experimental group which received an inoculum of 100 µl of B16-F0 cells with over-expressing PKC isoforms, which was most likely due to a more spread-out target area, allowing residual tumor to escape treatment from the single injection of 50 µl of the diterpene ester. In addition, pilot experiments using co-injection with BIS-1 has shown some loss of efficacy (data not shown) but optimization of the BIS-1 dose is needed. Overall, the results suggest that PKC levels in the tumor are not closely associated with efficacy *in vivo*.

The *in* vivo efficacy studies have shown that EBC-46 caused a marked inhibition in growth of all tumor types tested, with similar clinical outcome of initial inflammation, followed by eschar development and eventual healing. Despite the differences in origin, growth rate and morphology of the tumor subtypes, there was a similar significant regression of tumor growth following treatment via a single intralesional injection of EBC-46. There was rapid enduring response to treatment with EBC-46 that began with a visible inflammatory reaction as soon as 2 hr post treatment, through to development of an eschar and clearance of tumors by 20 days.

The early effects including development of a bruised appearance prompted the use of an *ex vivo* functional assay to determine how quickly and total tumor cell death occurred. An *ex vivo* clonogenic survival assay of treated Sk-Mel-28 cells was performed by harvesting tumors from the euthanized mouse and assessing the clonogenic potential of teased-out tumor cells in culture. It became evident that EBC-46 destroyed tumor cells by 4 hr post treatment, leaving no viable tumor cells. A parallel *in vitro* assay in which cultured cells were treated with comparable doses of EBC-46 showed total ablation of viability within 30 min, considerably faster than *in vivo*, thus leaving open the question of whether direct lysis of tumor cells by EBC-46 could fully explain its potency *in vivo*. Though the propidium iodide assays did not show definitive nuclear fragmentation, bright field images of the treated cells showed irregular cell morphologies and shrinkage indicative of necrotic cells which have been identified by red arrows in Figure 3.8, Panel B and C of *Chapter Three*.

Similar to previous studies of PEP005 and TPA on tumors *in vivo*, EBC-46 also resulted in a cutaneous inflammation and hemorrhaging. The inflammatory reaction observed upon treatment of tumors with EBC-46 suggested potential involvement of the innate immune system. Surgical examination of control and treated tumors at different times following treatment with EBC-46 or

TPA indicated a loss of blood supply to the tumor by possibly damaging the blood vessels in the tumor periphery, as early as 4 hr following treatment with the diterpene esters. The resulting vascular disruption caused by treatment with EBC-46 led to the subsequent development of tumor necrosis. This observation has been validated by histological and immunohistochemical analysis in *Chapter Five* of this thesis. To investigate this further, the following Chapter (*Chapter Five*) studied the effect of EBC-46 on the immune and other host cells and the involvement of pro-inflammatory cytokines.

In conclusion, single intratumoral injection of EBC-46 ablates tumors in a range of mouse and human tumor xenografts models where the ration of tumor volume and spread to the volume of injected EBC-46 may affect efficacy. As demonstrated in *Chapter Three*, TPA was more potent as a PKC activator *in vitro* than EBC-46 where TPA can attain increased growth inhibition of tumor cells at doses about 10-fold more than EBC-46. However, EBC-46 has a strong negative effect on the tumor cell growth and survival *in vivo* compared to TPA which failed to cure tumors in mice with eventual recurrences. This increased efficiency of EBC-46 in ablating tumor cells *in vivo* may be due to a PKC-dependent intracellular pathway in addition to a host response triggered by the presence of the diterpene ester in the tumor microenvironment. Sustained PKC activation in cultured melanoma cells leads to hyper-activation of the MAPK pathway and can induce cell death (Arita *et al.*, 1994, Deng *et al.*, 2004). On the other hand, prolonged activation of PKC leads to its subsequent degradation making it difficult to ascertain if the growth inhibition is due to PKC activation or a result of its absence. Previous work in this laboratory with PKC activators indicated that overstimulation of the Ras/Raf/MEK/ERK pathway is associated with induction of senescence in human melanoma cells (Cozzi *et al.*, 2006). Western blot analysis in *Chapter Three* has shown that loss of protein levels was a prolonged effect, where after 24 hr of recovery following 24 hr treatment with TPA or EBC-46, PKC isoform levels did not return to original levels. Over-expression of the two PKC isoforms $-\alpha$ and $-\delta$ in the target tumor in mice did not greatly enhance the efficacy of EBC-46 unlike the sensitivity obtained *in vitro*. This may be due to the ratio of tumor volume to the volume of EBC-46 injected into the tumor (Figures 4.9 and 4.10). The rapid changes in visual appearance of the tumor sites following injection of EBC-46 prompted the use of an *ex vivo* assay to assess the cellular response which established a rapid disappearance of viable clonogenic tumor cells within 4 hr following treatment. Further, the inflammatory reaction and associated hemorrhage is hypothesized to lead to tumor disruption. To better understand the

mechanism of action, it would be useful to analyze the histology and immunohistochemistry of the tumors and surrounding skin, conduct multiplex bead arrays for cytokine/chemokine analysis and visual analysis of the mouse skin and tumor vasculature.

Chapter Five

Host Immune Response to Activity of EBC-46

5.1 Introduction

TPA is a skin irritant and induces an inflammatory response on contact with the skin. EBC-46 has a strong negative effect on tumor growth and survival as demonstrated in *Chapter Four* in C57BL/6J and BALB/c *Foxn1*^{nu} mice. Previous work with PKC activators such as TPA and PEP005 suggested there was a host-mediated inflammatory response to treatment with these compounds, and in the case of PEP005 efficacy of the topical application was abrogated in neutrophil deficient mice (Challacombe *et al.*, 2006).

A similar inflammatory response was observed upon injection of EBC-46 into tumors in mice. A dose of 30 µg of EBC-46 delivered into each tumor via intratumoral injection resulted in a visible inflammatory reaction within 2 hr of treatment with a purplish bruising coloration on the skin of BALB/c *Foxn1*^{nu} mice around the area of treatment. However *in vitro* TPA appeared to be more potent in killing tumor cells than EBC-46, which raised the possibility that the increased efficacy of EBC-46 witnessed in mice relies on a PKC-dependent pathway as well as a host immune response triggered by the presence of the diterpene ester within the tumor microenvironment.

In addition, EBC-46 activates neutrophils to produce reactive oxygen species (*Chapter Three*; Section 3.2.3) which are known to have antitumor activity (Zivkovic *et al.*, 2005, Zivkovic *et al.*, 2007). While the production of ROS has been shown to be PKC-dependent (Marks and Hecker, 1967) as supported by results shown in Figure 3.6 (*Chapter Three*), it was hypothesized that EBC-46 activated PKC which in turn led to the recruitment of neutrophils to the site of infection.

It was therefore desirable to ascertain the pro-inflammatory profile of EBC-46 in the mouse and determine whether such effects formed part of the anticancer efficacy of the compound. Immunohistochemical analysis of the cellular response to the activity of EBC-46 was conducted wherein tissue sections of control and treated tumors in mice were stained for immune cells such as neutrophils and macrophages. To further develop this profile flow cytometry was used to investigate the expression of immune modulators such as inflammatory and chemotactic interleukins and interferons.

5.2 Results

5.2.1 Histology and immunohistochemistry of SK-Mel-28 tumors treated with EBC-46 *in vivo*

As shown in *Chapter Four* there was an inflammatory reaction within 2-4 hr of treatment with 30 µg of EBC-46 at each tumor site. Hence, the histology of the cellular response was important information for piecing together the mode of action of EBC-46. The aim was to study the inflammatory response in the skin and tumor during the early stages following intratumoral injection with EBC-46. SK-Mel-28 metastatic melanoma cells were grown subcutaneously in BALB/c *Foxn1*^{nu} nude mice and were treated with single intratumoral injections of 20% propylene glycol (PG) as control and 30 µg of EBC-46 which was determined to be the optimal dose to successfully cure tumors in mice (*Chapter Four*; Section 4.2.4). The tumors along with the skin within the inflammatory area were excised at different times (30 min, 1 hr, 2 hr, 4 hr, 8 hr, 24 hr, 48 hr and 7 days). Tissue samples were processed and stained by Clay Winterford at QIMR Berghofer Histology Facility after which the slides were scanned using the Aperio Scanscope XT and analyzed in the lab.

Myeloperoxidase (MPO) is a peroxidase enzyme expressed in neutrophil granulocytes, hence histological sections of the tumors were stained with anti-myeloperoxidase antibody to detect neutrophils infiltrating the tissue. This stain gets localized to the cytoplasm and lysosomes. Microscopic analysis of the stained tumor sections showed no neutrophils at 1 hr after treatment however they began to appear in small numbers along the periphery of the tumor in the early stages of treatment, between 2 – 4 hr. The neutrophils were identified by their multilobed nuclei and reddish-brown cytoplasm. Within the next 4 hr, neutrophils had penetrated into the tumor mass (Figure 5.1; A). Cell count of the neutrophils detected upon treatment with the control vehicle 20% PG or 30 µg EBC-46 at different times showed a gradual increase in the number migrating into the tumor by 8 hr (Figure 5.1; B). Figure 5.1; C shows presence of neutrophils within the tumor at 48 hr after treatment. An inflammatory reaction is known to result in hemorrhaging and tumor disruption. The onset of necrosis is at 48 hr is indicated with a green arrow in Figure 5.1; C. The immunohistochemical changes observed in tumors with respect to presence and activity of neutrophils are shown collectively in the Appendix (p.250-258) as photomicrographs, comparing

the treatment of EBC-46 to that of the control vehicle 20% PG. A similar outcome has been observed upon treatment of normal skin comparing EBC-46 with the vehicle (Appendix, Figure 2).

Macrophages also called macrophagocytes, are phagocytes and are produced by the differentiation of monocytes in tissues. Their role is to phagocytose or engulf and then digest cellular debris and pathogens. They also stimulate lymphocytes and other immune cells to respond to pathogens. Macrophages are identified by the expression of a number of proteins such as CD14, CD40, CD64, F4/80 (mice)/ERM1 (human), and CD68 (Khazen *et al.*, 2005).

The F4/80 protein expression in mice was targeted to detect the presence of macrophages in the host upon treatment of tumors with EBC-46. Following treatment with a single intratumoral injection of 30 µg of EBC-46, tumors were excised and processed for immunohistochemical analysis. The F4/80 antibody localizes to the cellular membrane staining cells with a brown colour. From the images of the stained tumor sections, tumors treated with the control vehicle 20% PG as well as those treated with 30 µg of EBC-46 showed the presence of macrophages along the periphery of the tumor as blood vessels surround the tumor (Figure 5.2; A). With increase in time of exposure of the tumor cells to EBC-46, there was a migration of macrophages into the tumor (Figure 5.2; B**)** followed by a gradual decline in macrophage numbers after 48 hr of treatment with EBC-46 (Figure 5.2; C). A detailed time-course graphic representation of the activity of macrophages is included in the Appendix (p.255-258) showing the comparison between treatment with EBC-46 and the control vehicle 20% PG.

Examination of the H&E tissue sections revealed the loss of sheet-like arrangement of cells treated with 30 µg of EBC-46 compared to 20% PG vehicle control (Figure 5.3). The progression towards necrosis among tumors treated with 30 µg of EBC-46 each tumor was clearly evident from the first day of treatment to day 7. H&E staining showed lightly-stained pockets of cells within the tumor from as early as 4 hr after treatment (Figure 5.3). These pockets were of necrotic cells which lacked nuclei hence the light stain with hematoxylin. The decrease in vascular pockets was observed by 24 hr post- treatment with EBC-46 (Figure 5.4). CD-31 was used to evaluate the degree of tumor angiogenesis upon treatment with EBC-46. From the images of the treated and control cells it was demonstrated that EBC-46 has an anti effect on the vascular structure within and around the tumor. The gradual decrease in the number of endothelial cells (indicated by brown pigmentation) was

A.

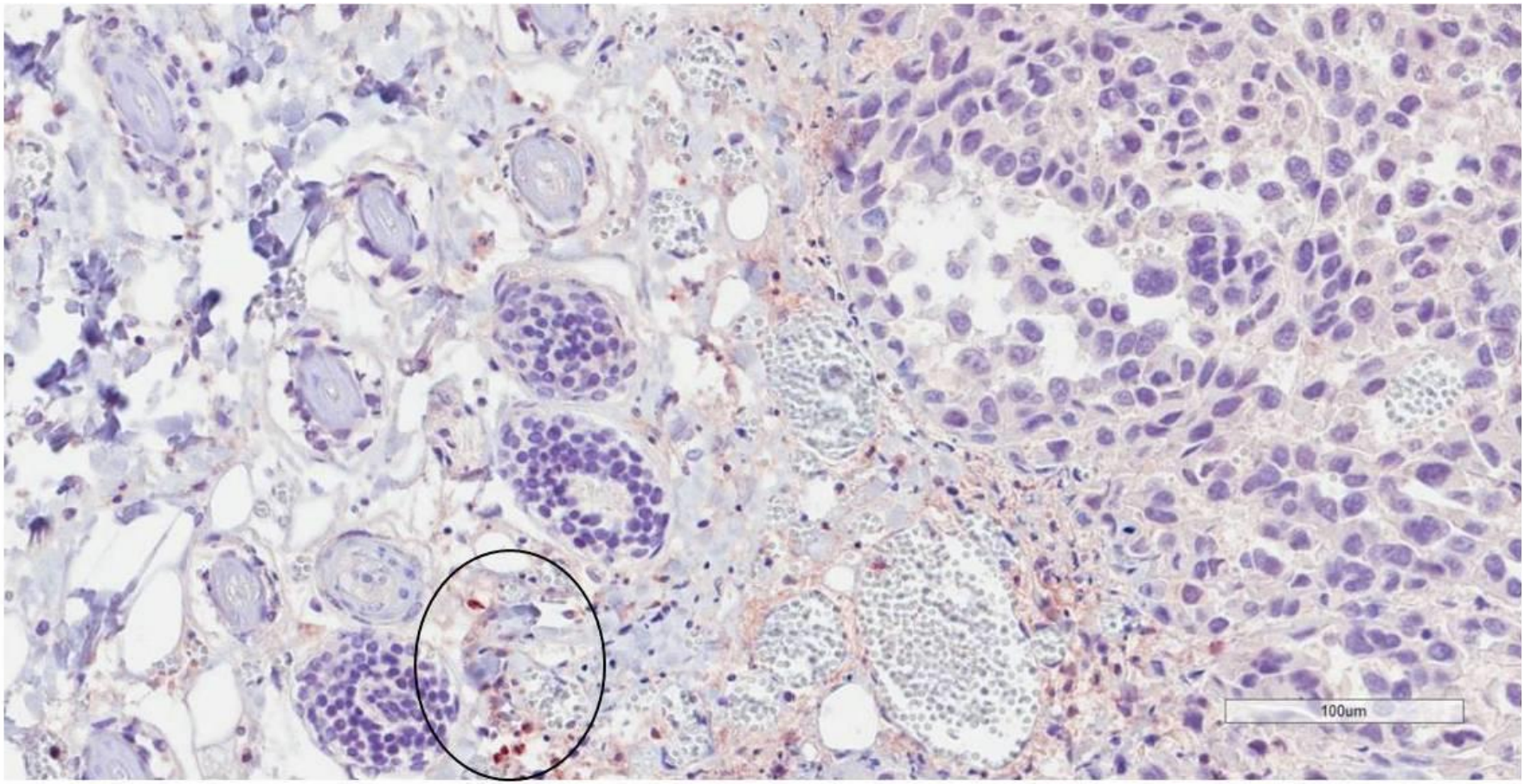

Neutrophils at 4 hr after treatment of Sk-Mel-28 tumor

Figure 5.1.A. Photomicrographs of Sk-Mel-28 tumors stained for neutrophils (MPO) after single intratumoral injection of 30 µg EBC-46 per tumor

Sk-Mel-28 tumor section stained with MPO, show neutrophils present along the periphery of the tumor at 4 hr after treatment with 30 µg of EBC-46, although in small numbers. The circle highlights neutrophils identified by the reddish-brown cytoplasmic stain and their multilobed nuclei.

Sk-Mel-28 tumors were treated with 30 µg EBC-46 or 20% PG vehicle control for various times. Tumors were processed for immunohistological analysis and stained with MPO for detection of neutrophils. Stained tissue sections were scanned and imaged using the Aperio ScanScope XT at 20X magnification. Photographs of tumor sections treated with the control vehicle 20% PG are included in the Appendix (page.252-254).

B.

Tumor section stained with MPO at 4 hr

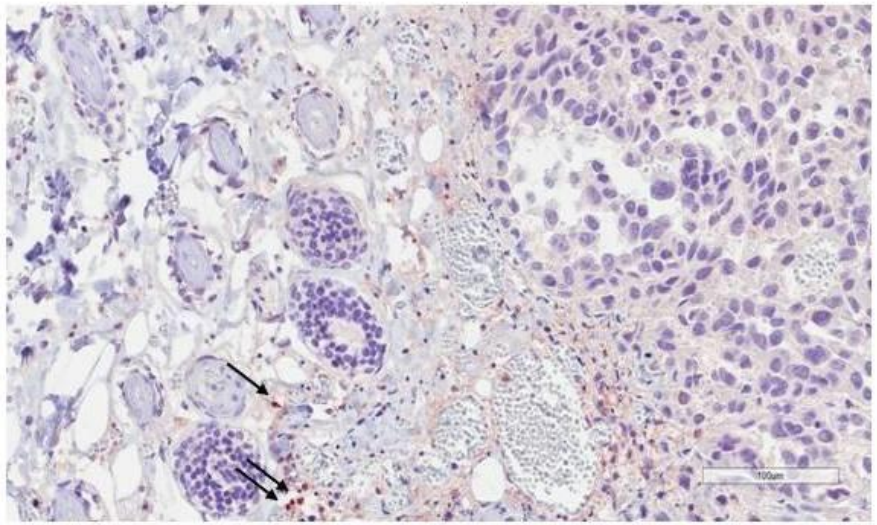

Tumor section stained with MPO at 8 hr

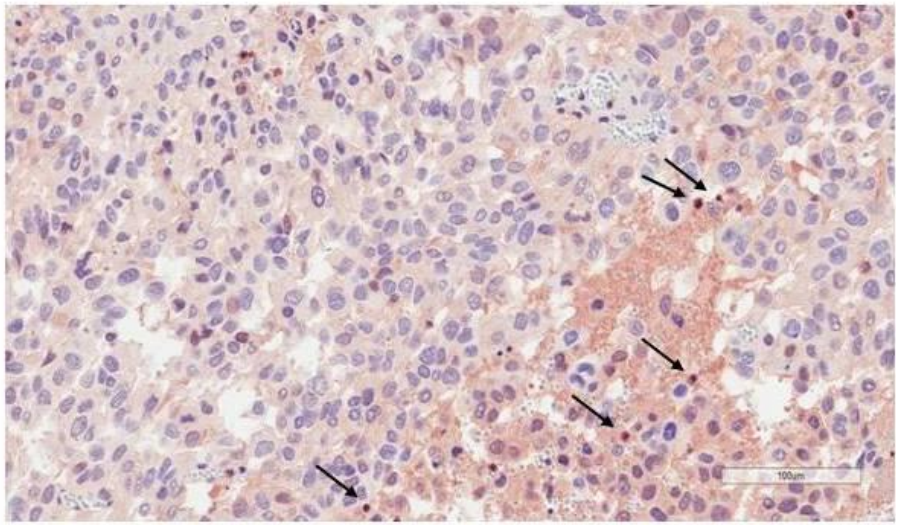

A gradual increase in number and migration of neutrophils into the tumor site from 4 – 8 hr after treatment

Figure 5.1.B. Photomicrographs of Sk-Mel-28 tumors stained for neutrophils (MPO) after single intratumoral injection of 30 µg EBC-46 per tumor

A gradual increase in the number of neutrophils recruited to the tumor site and their migration into the tumor is seen. Tumor section at 4 hr (same as Figure 5.1;A) shows neutrophils along the periphery of the tumor wile tumor section at 8 hr shows neutrophils within the tumor identified by the black arrows.

Sk-Mel-28 tumors were treated with 30 µg EBC-46 or 20% PG vehicle control for various times. Tumors were processed for immunohistological analysis and stained with MPO for detection of neutrophils. Stained tissue sections were scanned and imaged using the Aperio ScanScope XT at 20X magnification. Photographs of tumor sections treated with the control vehicle 20% PG are included in the Appendix (page.252-254).

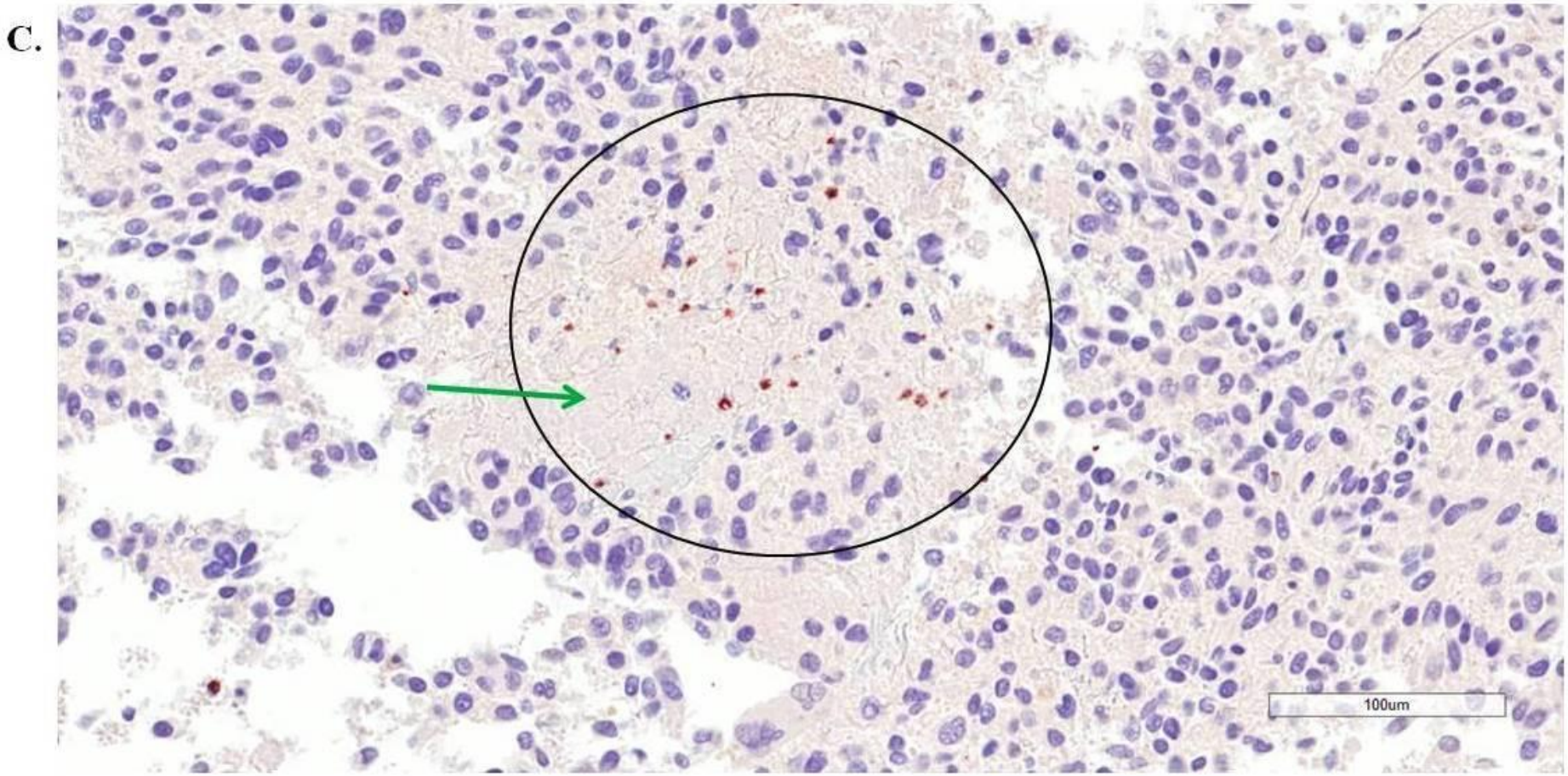

Neutrophils within the tumor by 48 hr after treatment with EBC-46
Green arrow indicates area of necrotic cells

Figure 5.1.C. Photomicrographs of Sk-Mel-28 tumors stained for neutrophils (MPO) after single intratumoral injection of 30 µg EBC-46 per tumor

Scan of the tumor section shows neutrophils well within the tumor mass by 48 hr after treatment with 30 µg of EBC-46.

Sk-Mel-28 tumors were treated with 30 µg EBC-46 or 20% PG vehicle control for various times. The black circled area shows neutrophils within the tumor at 8 hr and the green arrow indicates an area of necrotic cells. Photographs of tumor sections treated with the control vehicle 20% PG are included in the Appendix (page.252-254).

Sk-Mel-28 tumors were treated with 30 µg EBC-46 or 20% PG vehicle control for various times. Tumors were processed for immunohistological analysis and stained with MPO for detection of neutrophils. Stained tissue sections were scanned and imaged using the Aperio ScanScope XT at 20X magnification.

A.

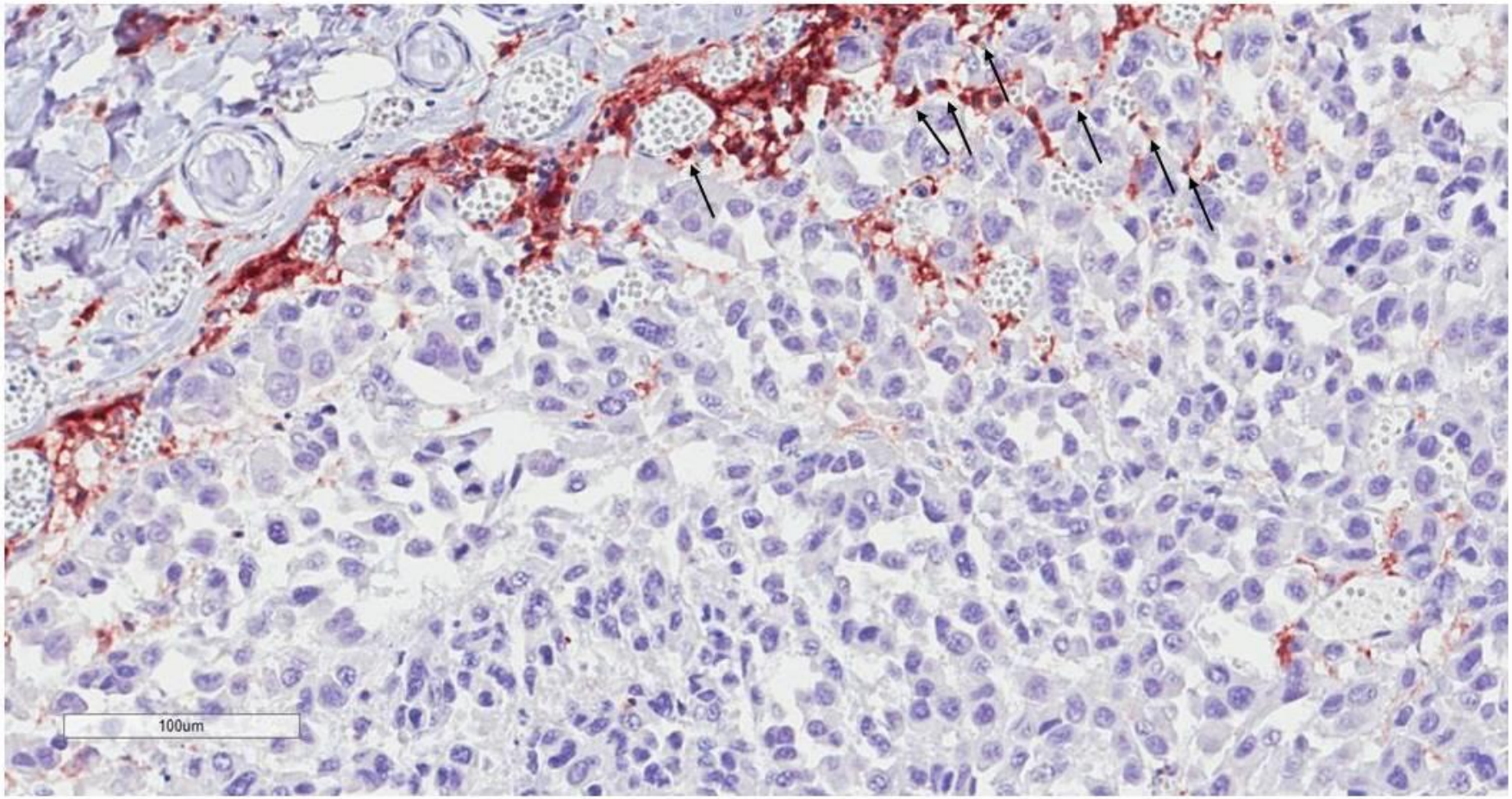

Macrophages along the periphery of the tumor at 4 hr after treatment with EBC-46

Figure 5.2.A. Photomicrographs of Sk-Mel-28 tumors stained for macrophages (F4/80) after single intratumoral injection of 30 µg EBC-46 per tumor

Sk-Mel-28 tumor section stained with F4/80, show macrophages present along the periphery of the tumor at 4 hr after treatment with 30 µg of EBC-46, although in small numbers. The black arrows indicate towards macrophages which are identified by the reddish-brown cytoplasmic stain and a blue nucleus.

Sk-Mel-28 tumors were treated with 30 µg EBC-46 or 20% PG vehicle control for various times. Tumors were processed for immunohistochemical analysis and probed with F4/80 which is specific for macrophages. Stained tissue sections were scanned and imaged using the Aperio ScanScope XT at 20X magnification.Photographs of tumor sections treated with the control vehicle 20% PG are included in the Appendix (page.255-256).

B.

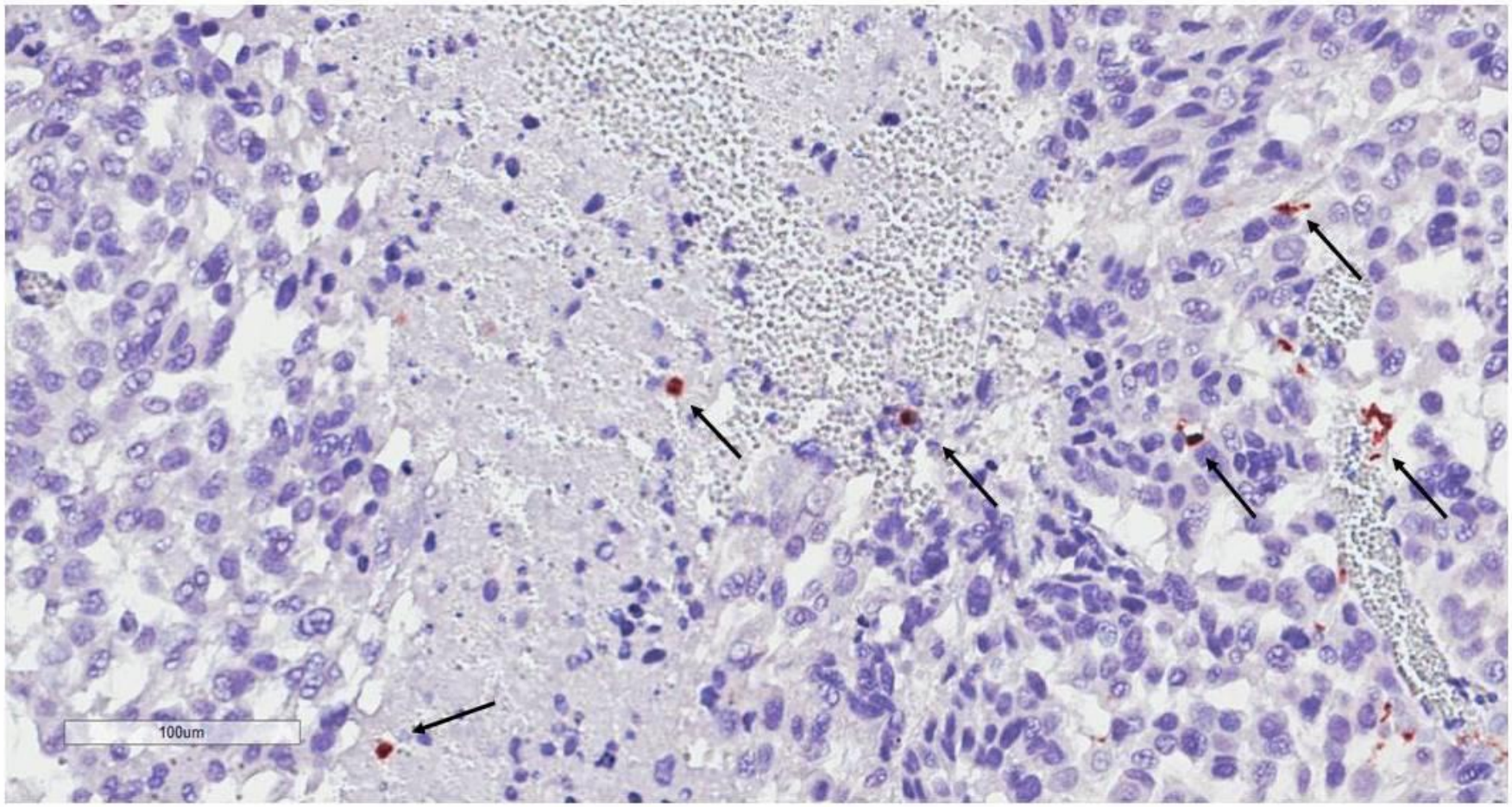

Macrophages within tumor at 8 hr after treatment with EBC-46

Figure 5.2.B. Photomicrographs of Sk-Mel-28 tumors stained for <u>macrophages</u> (F4/80) after single intratumoral injection of 30 µg EBC-46 per tumor

Scan shows macrophages within the tumor following 8 hr of exposure to 30 µg of EBC-46.

Sk-Mel-28 tumors were treated with 30 µg EBC-46 or 20% PG vehicle control for various times. Tumors were processed for immunohistochemical analysis and probed with F4/80 which is specific for macrophages. Stained tissue sections were scanned and imaged using the Aperio ScanScope XT at 20X magnification.Photographs of tumor sections treated with the control vehicle 20% PG are included in the Appendix (page. 255-256).

C. **Tumor section at 48 hr after treatment** **Tumor section on day 7 after treatment**

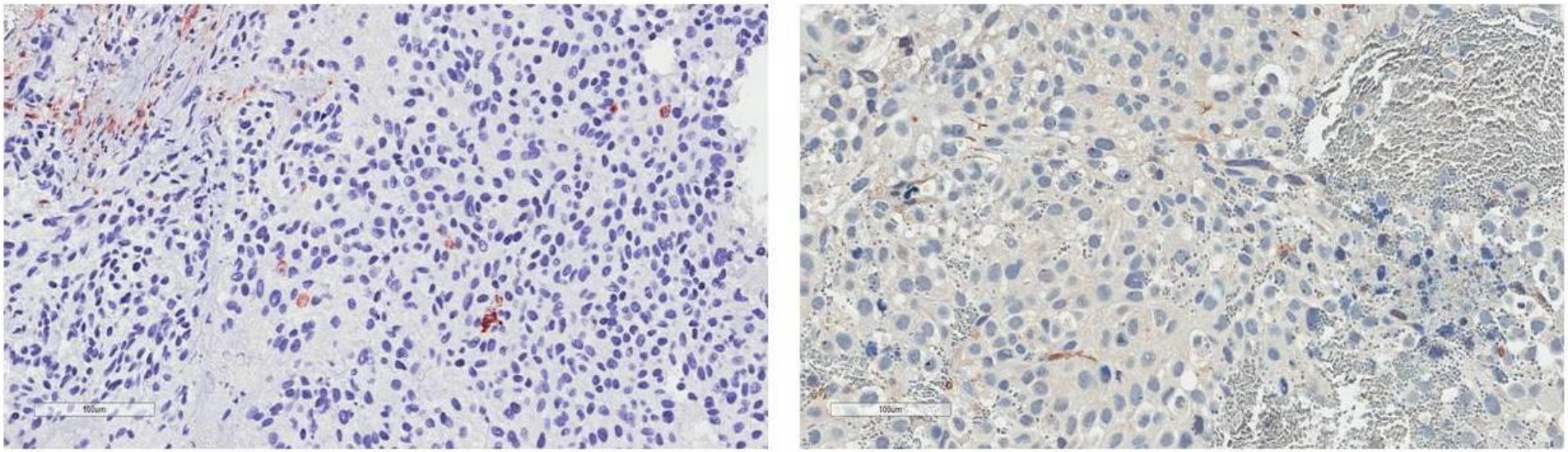

Macrophage numbers begin to decline by 48 hr after treatment with EBC-46

Figure 5.2.C. Photomicrographs of Sk-Mel-28 tumors stained for macrophages (F4/80) after single intratumoral injection of 30 µg EBC-46 per tumor

Macrophage numbers gradually begin to decline 48 hr after treatment. Tumor section at 48 hr shows macrophages within the tumor mass which decreased in number by day 7.

Sk-Mel-28 tumors were treated with 30 µg EBC-46 or 20% PG vehicle control for various times. Tumors were processed for immunohistochemical analysis and probed with F4/80 which is specific for macrophages. Stained tissue sections were scanned and imaged using the Aperio ScanScope XT at 20X magnification.Photographs of tumor sections treated with the control vehicle 20% PG are included in the Appendix (page. 255-256).

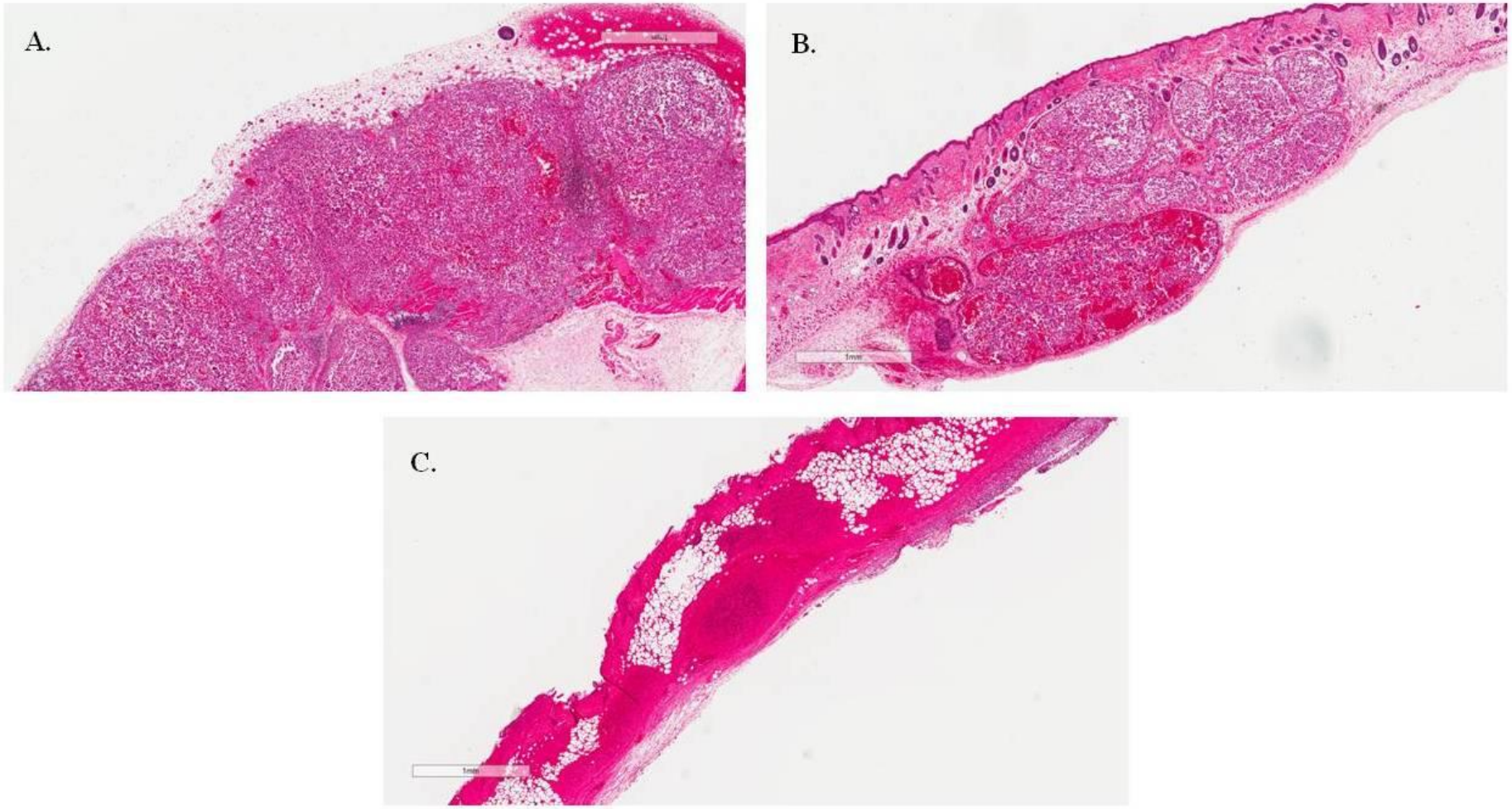
A.
B.
C.

Figure 5.3 Photomicrographs of Sk-Mel-28 tumors stained with H&E for histopathological analysis after single intratumoral injection of 30 µg EBC-46 per tumor showing disintegration of tumor.

A. H&E staining of Sk-Mel-28 tumor treated with 30 µg of EBC-46 for 2 hr
B. H&E staining of Sk-Mel-28 tumor treated with 30 µg of EBC-46 for 4 hr
C. H&E staining of Sk-Mel-28 tumor treated with 30 µg of EBC-46 for 7 days

Sk-Mel-28 tumors were treated with 30 µg EBC-46 or 20% PG vehicle control for various times. Tumors were processed for histological analysis. Stained tissue sections were scanned and imaged using the Aperio ScanScope XT at 20X magnification. Photographs of tumor sections treated with the control vehicle 20% PG are included in the Appendix (page.250-251).

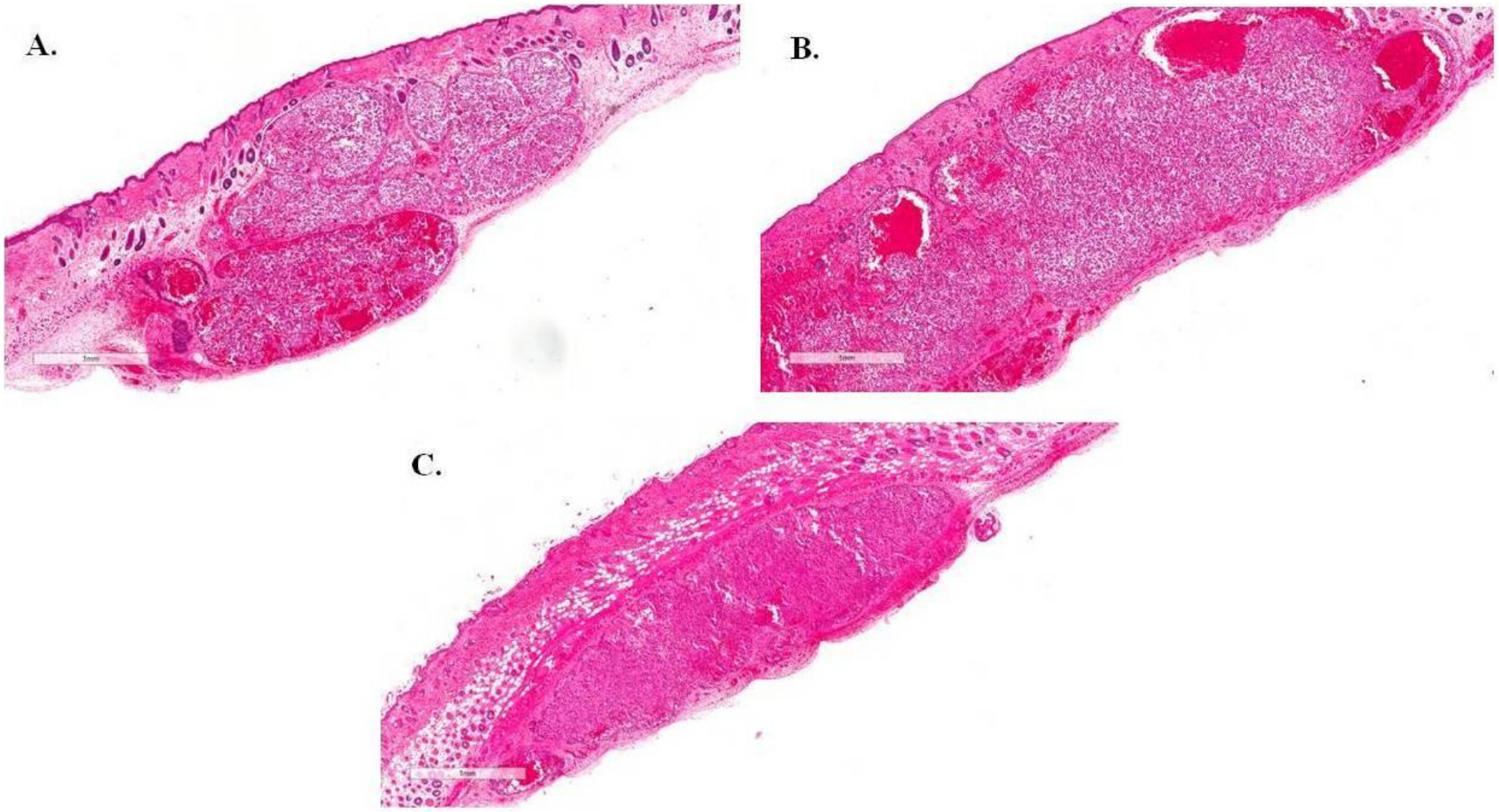
A.
B.
C.

Figure 5.4 Photomicrographs of Sk-Mel-28 tumors stained with H&E for histopathological analysis after treatment with 30 µg EBC-46 per tumor showing decrease in blood supply.

A. H&E staining of Sk-Mel-28 tumor treated with 30 µg of EBC-46 for 4 hr
B. H&E staining of Sk-Mel-28 tumor treated with 30 µg of EBC-46 for 8 hr.
C. H&E staining of Sk-Mel-28 tumor treated with 30 µg of EBC-46 for 24 hr

Sk-Mel-28 tumors were treated with 30 µg EBC-46 or 20% PG vehicle control for various times. Tumors were processed for histological analysis and stained with H&E. Stained tissue sections were scanned and imaged using the Aperio ScanScope XT at 20X magnification. Photographs of tumor sections treated with the control vehicle 20% PG are included in the Appendix (page. 250-251). There was loss of blood supply within the tumor between 4 hr – 8 hr – 24 hr. This figure also indicated areas of haemmorhage around the periphery and within the tumor between 4 – 8 hr after treatment with EBC-46.

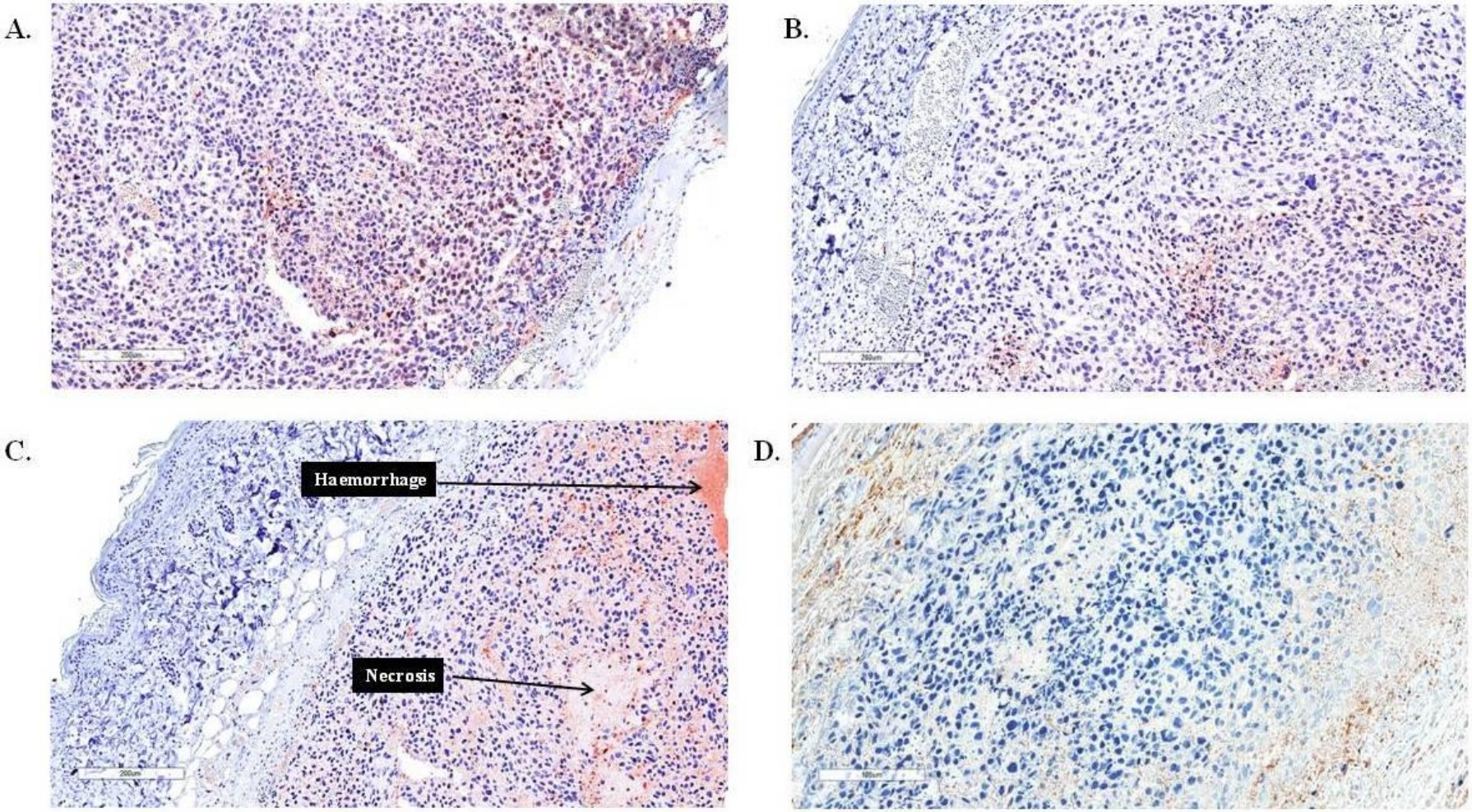
A.
B.
C.
Haemorrhage
Necrosis
D.

Figure 5.5 Photographs of Sk-Mel-28 tumors stained with CD-31 for detection of endothelial cells after treatment with 30 µg EBC-46 per tumor

A. Sk-Mel-28 tumor sections stained with CD-31 show presence of endothelial cells at 4 hr following treatment with EBC-46.
B. Sk-Mel-28 tumor sections show a gradual decline in presences of endothelial cells by 8 hr after treatment with EBC-46 as seen by a reduction in the dark brown pigmented cells characteristic of CD-31/PECAM1 Ab staining indicating a loss of blood supply to the tumor.
C. Sk-Mel-28 tumor sections staining with CD-31 demonstrated haemorrhaging and the development of necrosis within the tumor at 48 hr following treatment with EBC-46.
D. By day 7 after treatment with EBC-46, no endothelial cells were found present within the tumor with the resultant onset of necrosis.

Sk-Mel-28 tumors were treated with 30 µg EBC-46 or 20% PG vehicle control for various times. Tumors were processed for immunohistological analysis and stained with CD-31/PECAM1 for identification for endothelial cells which stain with a **brown colouration**. Stained tissue sections were scanned and imaged using the Aperio ScanScope XT at 20X magnification. Photographs of tumor sections treated with the control vehicle 20% PG are included in the Appendix (page.257-258). There is apparent decrease in the number of endothelial cells seen by the reduction of brown pigmentation with time.

observed from 4 hr post-treatment and beyond (Figure 5.5). Image C (Figure 5.5) also indicated areas of hemorrhage and necrosis within the tumor at 48 hr following treatment with 30 µg of EBC-46.

5.2.2 Neutrophil Requirement for the Efficacy of EBC-46

From immunohistochemical analysis it was apparent that the main leukocyte involved in the inflammatory response was the neutrophil. However, it was not clear whether EBC-46 required neutrophils or another immune response for its cytotoxic effect on cancer cells, or whether it caused a direct cytotoxic effect on the cells and neutrophils were a secondary response to the tissue necrosis.

The aim of this study was to deplete the peripheral neutrophils in mice with a neutralizing antibody to determine if the efficacy of subsequent intralesional treatments of EBC-46 would be affected. Mice were administered the neutrophil-neutralizing monoclonal antibody anti-Ly-6G or the control IgG_2 via intraperitoneal (IP) injection. Two days after the initial antibody treatment, re-administered the anti-Ly-6G antibody or control IgG_2 via IP injection. Sk-mel-28 tumors in BALB/c *Foxn1*^{nu} mice were treated with 20% PG or 30 µg EBC-46. Two days after treatment with EBC-46, the mice received a third treatment with the anti-Ly-6G antibody or the control IgG_2 via IP injection. The mice were monitored regularly at intervals of 2 days during the first week of treatment, expanding the time interval to 4 days in the consecutive weeks until tumors were ablated or mice were culled as a result of tumor burden. From the start of the treatment with the antibodies up to day 10, blood smears were prepared to establish a leukocyte count.

There was an obvious clinical difference between the EBC-46 and EBC-46 + Ly-6G groups at the site of EBC-46 injection. The Ly-6G + EBC-46 mice did not show any visible signs of inflammation, however there was tumor regression in 2 mice out of the 5 mice in the group. By day 27, 3 mice in this group had relapsed at a total of 4 sites (Figure 5.6; A.).

In contrast, the mice treated with EBC-46 or EBC-46 + IgG_2 resulted in cure as expected, except for 1 mouse in the EBC-46 + IgG_2 group that had a recurrence at one site which was due to an intramuscular growth of the tumor (Figure 5.6; A.). In other words, the group depleted of

A.

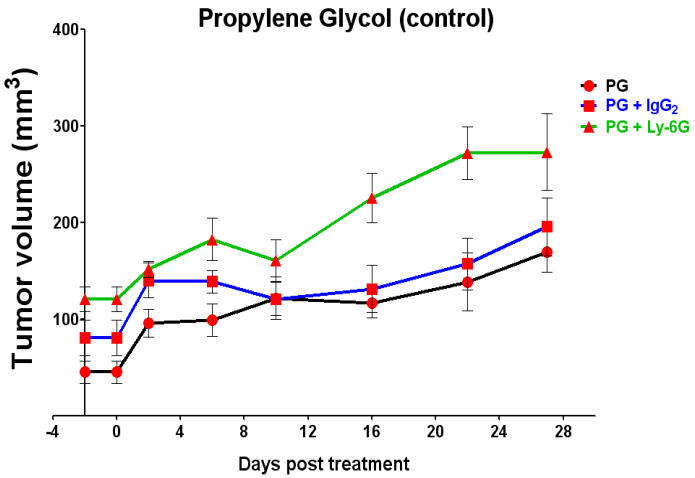
Propylene Glycol (control)
Tumor volume (mm3)
400
300
200
100
-4
0
4
8
12
16
20
24
28
Days post treatment
PG
PG + IgG2
PG + Ly-6G

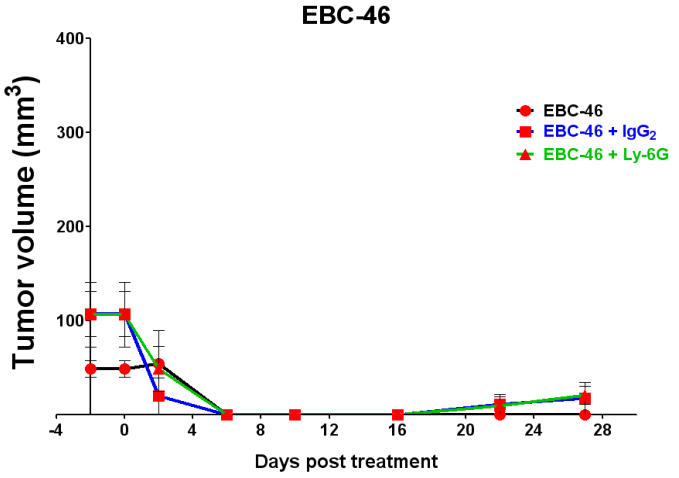
EBC-46
Tumor volume (mm3)
400
300
200
100
-4
0
4
8
12
16
20
24
28
Days post treatment
EBC-46
EBC-46 + IgG2
EBC-46 + Ly-6G

B.

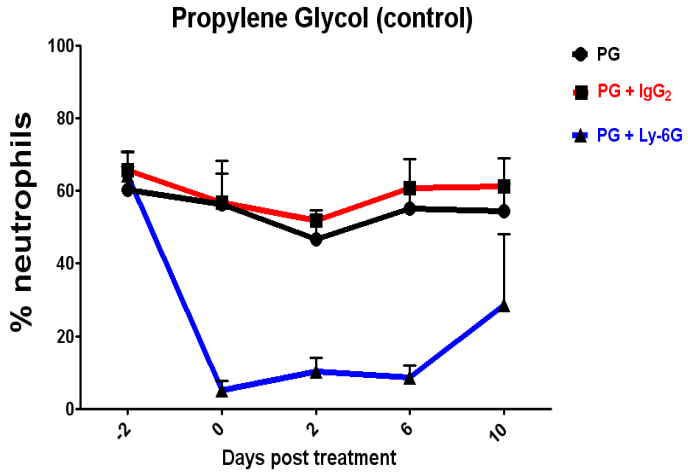
Propylene Glycol (control)
% neutrophils
100
80
60
40
20
0
-2
0
2
6
10
Days post treatment
PG
PG + IgG2
PG + Ly-6G

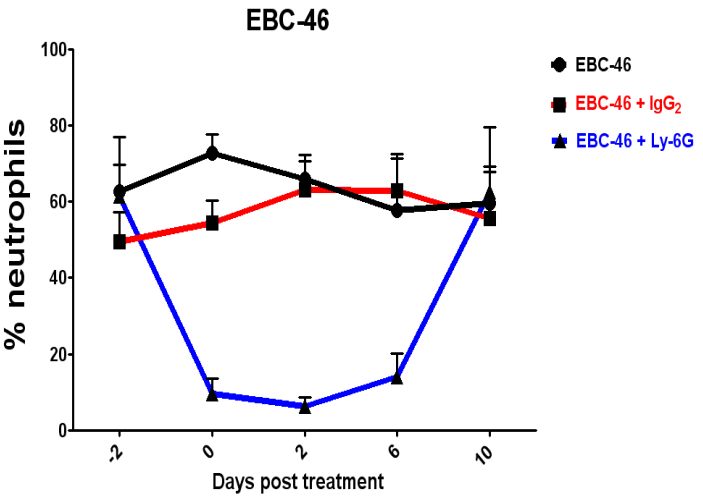
EBC-46
% neutrophils
100
80
60
40
20
0
-2
0
2
6
10
Days post treatment
EBC-46
EBC-46 + IgG2
EBC-46 + Ly-6G

Figure 5.6; A **Effect of neutrophil depletion in BALB/c *Foxn1*^{nu} mice on EBC-46 treatment of Sk-Mel-28 tumors.**

Figure 5.6; B **Neutrophil counts in mice given anti-Ly-6G and control (IgG_2) antibodies**

Tumor growth in mice given anti-Ly-6G antibody, isotype control antibody or no antibody. Sk-Mel-28 cells were injected subcutaneously (10 tumors/group, 2 tumors/mouse, 5 mice/group). When tumors were grown to approximately 100 mm^3, mice were injected with the anti-Ly-6G antibody (clone 1A8; 100 µg i.p, on days -2, 0 and 2) with isotype control antibody (IgG2a, clone 2A3; 100 µg i.p, on days -2, 0 and 2) or with nothing. The tumor volumes represent the mean volume of individual tumors.

neutrophils had a greater number of persisting tumors or a faster recurrence rate. The lack of a visible inflammatory reaction at the site of treatment among the EBC-46 + Ly-6G mice was less obvious by day 10, most likely as the neutrophil levels had begun to return to normal levels (Figure 5.6; B.) The neutrophil counts were determined for each group. In mice treated with the vehicle, EBC-46 or with the control Ab (PG / EBC- 46 + IgG_2), the neutrophil count as a percentage of total white cells was unchanged (Figure 5.6, B) throughout the experiment. In contrast, the percentage of neutrophils dropped dramatically from ~60% to ~10% following treatment with the neutrophil neutralizing Ab Ly-6G in both the vehicle-treated and EBC-46 – treated groups.

5.2.3 Induction of cytokines following EBC-46 treatment in vivo

Production of cytokines was also assessed *in vivo* using blood from mice where tumors were treated with EBC-46, to obtain the systemic host response, and from supernatants of the treated tumors to ascertain the local response. A series of three cytokine bead assays each on mouse serum and tumor supernatants was performed demonstrating similar results: minimal expression levels, below an accepted detection cut off (< 10 pg/ml),except for MCP-1 and IL-6 in mouse blood and IL-1β and IL-8 in the tumor supernatants. The results have been summarized in Figure 5.7

Overall, the level of cytokines induced by EBC-46 that could be detected in mice were low and varied, possibly because the process of hemorrhagic necrosis cut off circulating lymphocytes from exposure to significant concentrations of the drug. The question of cytokine induction in lymphocytes was therefore addressed with the use of human PBMCs in culture.

5.2.4 Induction of cytokines by EBC-46 in human peripheral blood lymphocytes (PBMCs) in vitro

Cultured human lymphocytes were used as a substitute for mouse lymphocytes *in vivo*, to determine whether the rapid inflammation induced by EBC-46 could have been associated with the production of proinflammatory cytokines. A cytokine bead array was used to assess the expression of cytokines IL-12p70, TNF α, IL-10, IL-6, IL-1β and IL-8 by PBMCs treated with EBC-46 *in vitro*. In an additional arm of the experiment, PBMCs were co-cultured with tumor cells or human endothelial cells (HUVEC) in an attempt to simulate at least part of the *in vivo* context. These cytokines are mainly produced by macrophages, dendritic cells and other immune cells.

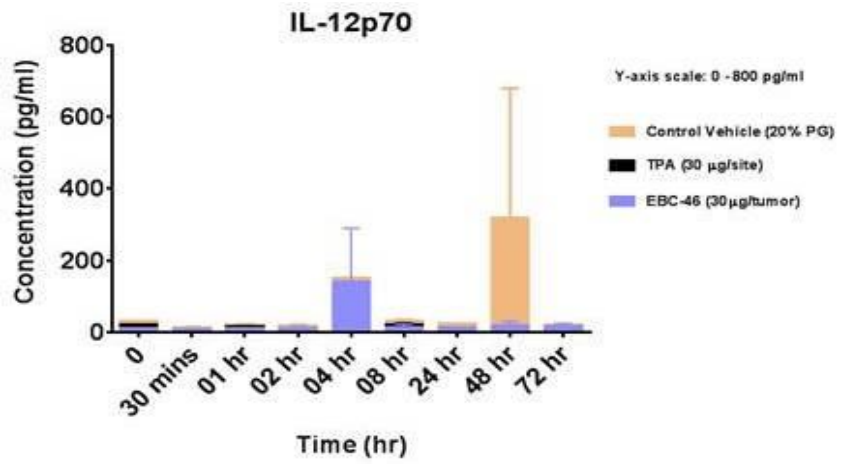
IL-12p70
Concentration (pg/ml)
800
600
400
200
0
0
30 mins
01 hr
02 hr
04 hr
08 hr
24 hr
48 hr
72 hr
Time (hr)
Y-axis scale: 0 - 800 pg/ml
Control Vehicle (20% PG)
TPA (30 µg/site)
EBC-46 (30µg/tumor)

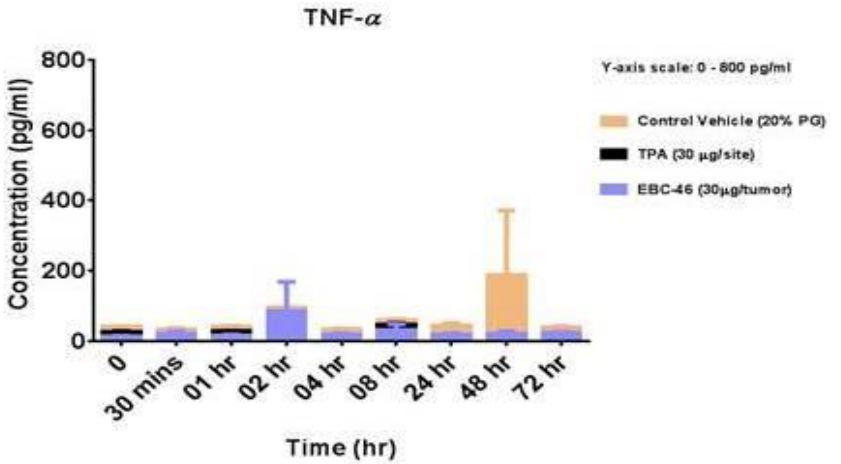
TNF-α
Concentration (pg/ml)
800
600
400
200
0
0
30 mins
01 hr
02 hr
04 hr
08 hr
24 hr
48 hr
72 hr
Time (hr)
Y-axis scale: 0 - 800 pg/ml
Control Vehicle (20% PG)
TPA (30 µg/site)
EBC-46 (30µg/tumor)

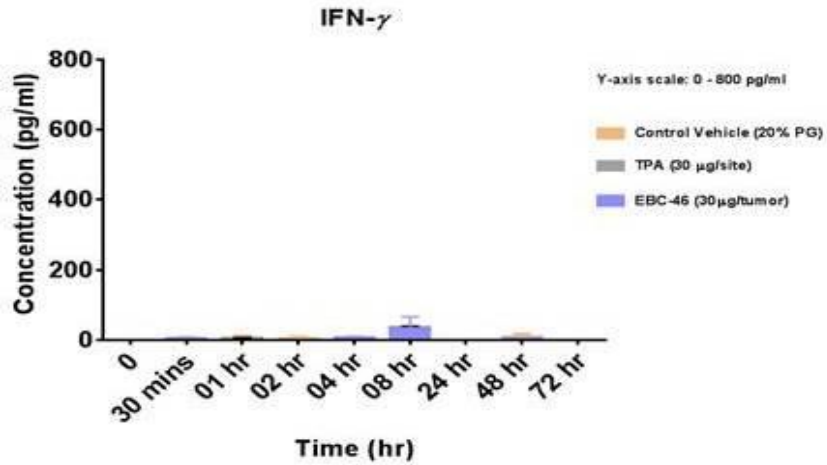
IFN-γ
Concentration (pg/ml)
800
600
400
200
0
0
30 mins
01 hr
02 hr
04 hr
08 hr
24 hr
48 hr
72 hr
Time (hr)
Y-axis scale: 0 - 800 pg/ml
Control Vehicle (20% PG)
TPA (30 µg/site)
EBC-46 (30µg/tumor)

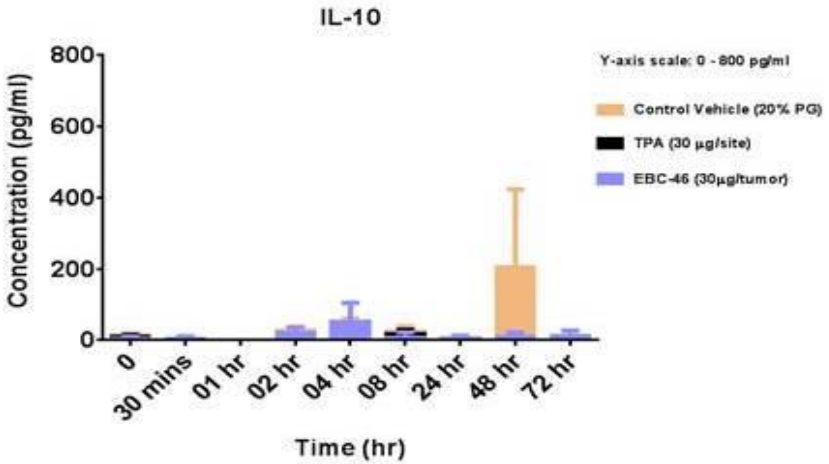
IL-10
Concentration (pg/ml)
800
600
400
200
0
0
30 mins
01 hr
02 hr
04 hr
08 hr
24 hr
48 hr
72 hr
Time (hr)
Y-axis scale: 0 - 800 pg/ml
Control Vehicle (20% PG)
TPA (30 µg/site)
EBC-46 (30µg/tumor)

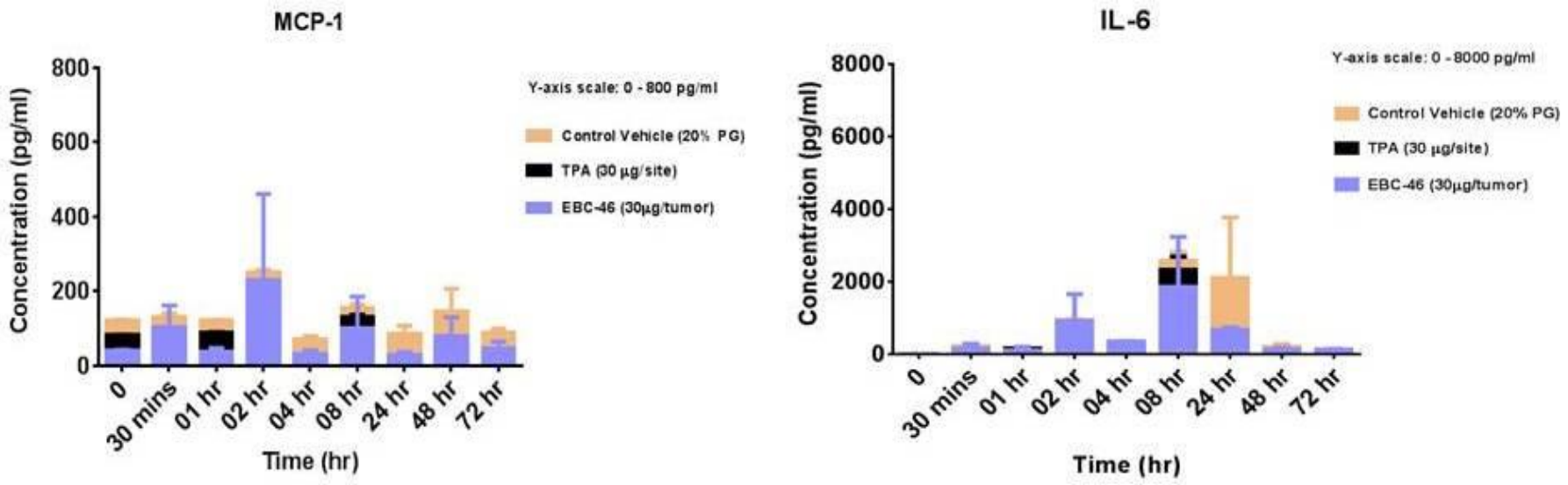

Figure 5.7; A Cytokine expression levels in <u>serum of BALB/c *Foxn1*^{nu} mice.</u>

BALB/c *Foxn1*^{nu} mice growing Sk-Mel-28 tumors were treated with 30 µg of EC-46 via intralesional injection. Whole blood was collected at different times from the mice (2 mice per treatment per time-point) and serum was separated to be analysed for the production of cytokines. A BD Biosciences Cytokine Bead Assay Mouse Inflammation kit was used to perform the assay testing a panel of six cytokines, namely IL-12p70, TNF-α, IFN-γ, MCP-1, IL-10 and IL-6. The assay was performed following instructions as per the manual provided testing each sample in duplicate. A BD FACS Array was used to measure the absorbance and results were analysed using the FCAP Array software. The assay was repeated twice and the results of both were averaged and plotted using the GraphPad Prism software.

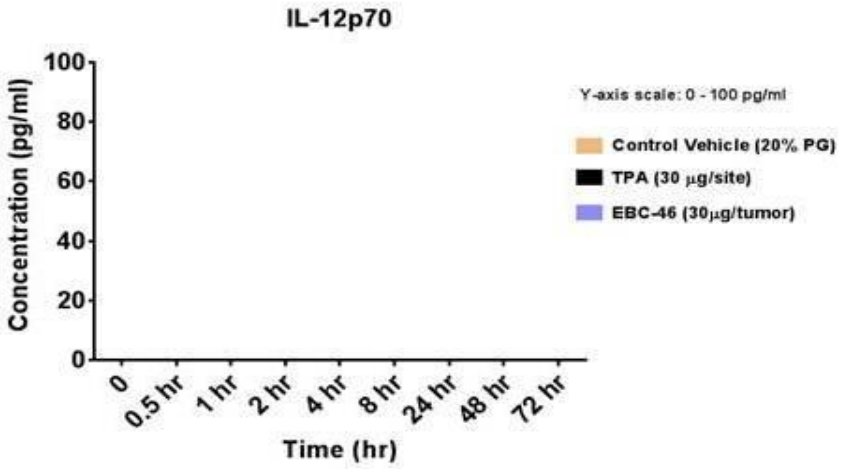
IL-12p70
Concentration (pg/ml)
100
80
60
40
20
0
0
0.5 hr
1 hr
2 hr
4 hr
8 hr
24 hr
48 hr
72 hr
Time (hr)
Y-axis scale: 0 - 100 pg/ml
Control Vehicle (20% PG)
TPA (30 μg/site)
EBC-46 (30μg/tumor)

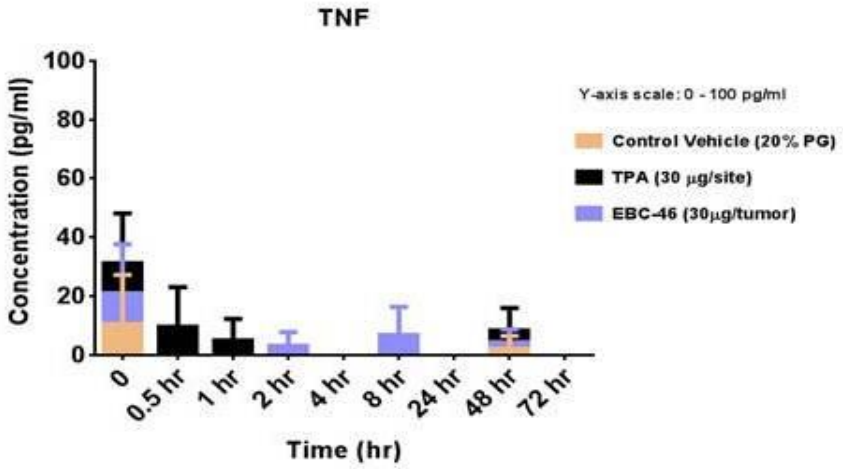
TNF
Concentration (pg/ml)
100
80
60
40
20
0
0
0.5 hr
1 hr
2 hr
4 hr
8 hr
24 hr
48 hr
72 hr
Time (hr)
Y-axis scale: 0 - 100 pg/ml
Control Vehicle (20% PG)
TPA (30 μg/site)
EBC-46 (30μg/tumor)

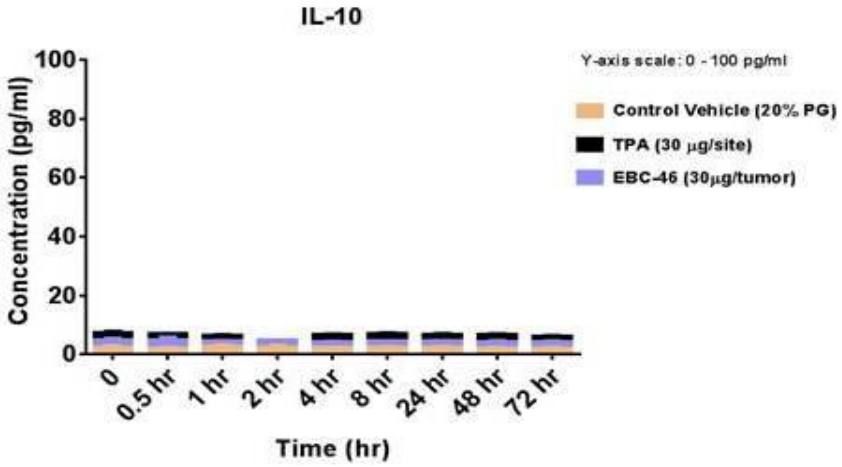
IL-10
Concentration (pg/ml)
100
80
60
40
20
0
0
0.5 hr
1 hr
2 hr
4 hr
8 hr
24 hr
48 hr
72 hr
Time (hr)
Y-axis scale: 0 - 100 pg/ml
Control Vehicle (20% PG)
TPA (30 μg/site)
EBC-46 (30μg/tumor)

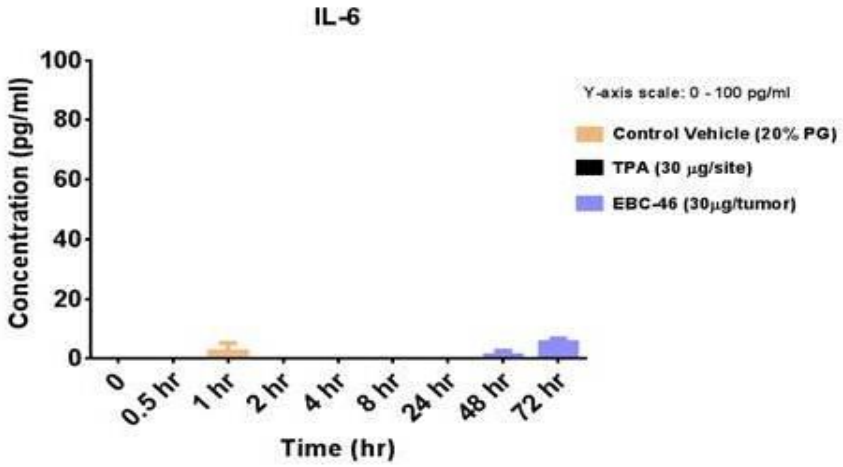
IL-6
Concentration (pg/ml)
100
80
60
40
20
0
0
0.5 hr
1 hr
2 hr
4 hr
8 hr
24 hr
48 hr
72 hr
Time (hr)
Y-axis scale: 0 - 100 pg/ml
Control Vehicle (20% PG)
TPA (30 μg/site)
EBC-46 (30μg/tumor)

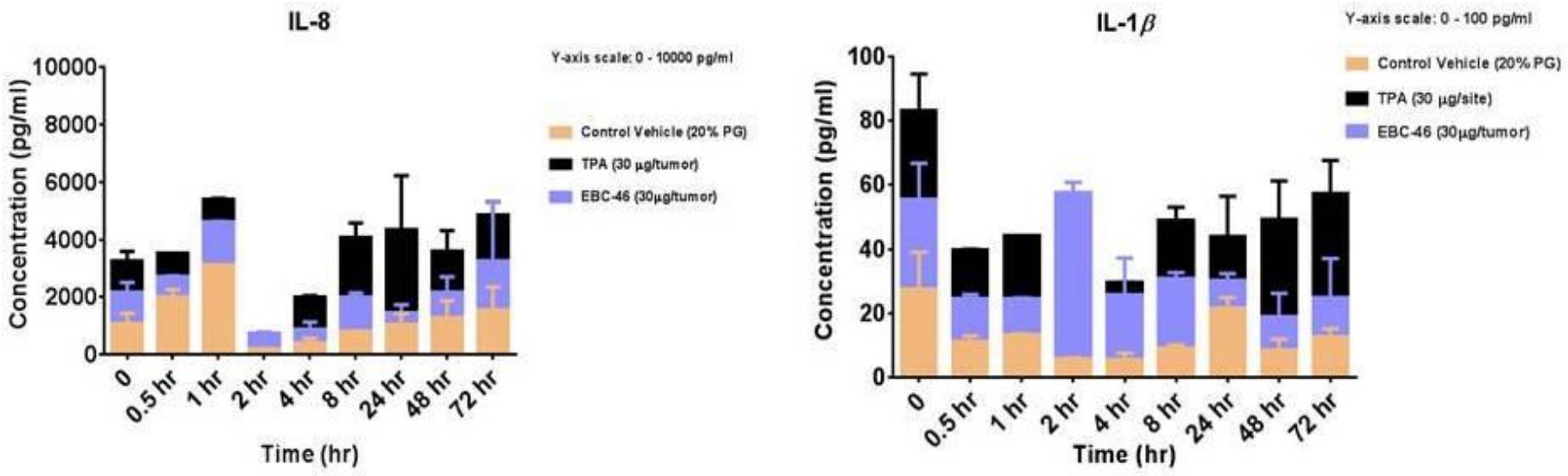

Figure 5.7; B Cytokine expression levels from xenografts of <u>human SK-Mel-28 tumor supernatants</u>

BALB/c *Foxn1*^{nu} mice growing Sk-Mel-28 tumors were treated with 30 µg of EC-46 via intralesional injection. Tumors were harvested at different times after treatment (2 tumors per treatment per time-point). Cells from the tumors were scrapped out and used in *ex vivo* studies while the supernatant was utilized to assess the expression levels of cytokines as a result of EBC-46 activity. A BD Biosciences Cytokine Bead Assay Mouse Inflammation kit was used to perform the assay testing a panel of six cytokines, namely IL-12p70, TNF-α, IFN-γ, MCP-1, IL-10 and IL-6. The assay was performed following instructions as per the manual provided testing each sample in duplicate. A BD FACS Array was used to measure the absorbance and results were analysed using the FCAP Array software. This assay was repeated twice and the results of both were averaged and plotted using the GraphPad Prism software.

Tumor cells were co-cultured with PBMC's and treated with 100 ng/ml of EBC-46 for 24 hr before harvesting cells and assaying for cytokine production. In Table.5.3, it is clear that there is high expression of TNF, IL-6 and IL-8. LPS was used as a pro-inflammatory positive control. Lipopolysaccharides (LPS) are large molecules consisting of a lipid ad a polysaccharide joined by a covalent bond. They act as endotoxins and elicit strong immune responses and for this reason were used in this assay as an alternative immunostimulant to tumor cells. The results show that LPS significantly increased the expression of cytokines by PBMCs, not only of the human TNFs, but also IL-10, IL-6, IL-1β and IL-8. A further increase was noted upon the addition of EBC-46. Co-culture of the tumor cells Sk-Mel-28 and MCF7 with PBMCs induced a weaker response compared to LPS, but all the same result in a high expression of IL-6 and IL-8. Relative to the expression of cytokines in the presence of tumor cells, high levels of human TNF, IL-6, IL-1β and IL-8 were noted upon treatment of the co-cultures with EBC-46.

Treatment of NFF's in a PBMC environment resulted in higher expression of TNF α, IL-6 and IL-8. EBC-46 appeared to have an agonistic effect on cytokine production. Cytokine assays were also performed on B16 and HUVEC's *in vitro,* giving a similar cytokine expression profile as the tumor cells. Production of cytokines were also assessed *in vivo* using blood from mice treated with EBC-46 for tumors to obtain a host response and from tumor supernatants of the treated tumors to obtain a tumor response. However, the expression levels were minimal below an accepted detection cut off (< 10 pg/ml), except for MCP-1 and IL-6 in the mouse blood and IL-1β and IL-8 in the tumor supernatants.

Table 5.1 Induction of cytokines upon treatment of tumor cells co-cultured with PBMC cells with EBC-46 *in vitro*.

	IL-12p70	Human TNF	IL-10	IL-6	IL-1β	IL-8
PBMC	3.01 ± 0.25	11.96 ± 3.92	2.97 ± 0.38	15.80 ± 5.63	5.58 ± 0.94	911.14 ± 246.95
PBMC + LPS	5.23 ± 2.81	10704.55 ± 80.97	1176.12 ± 22.33	28726.45 ± 259.68	5446.69 ± 99.03	8267.26 ± 268.56
PBMC + EBC-46	2.45 ± 0.26	4532.06 ± 110.51	3.43 ± 0.42	52.36 ± 3.79	141.96 ± 11.28	20059.96 ± 363.94
PBMC + LPS +EBC- 46	3.02 ± 0.55	34731.41 ± 1223.1	18.79 ± 1.77	9502.47 ± 162.60	12319.31 ± 158.10	13258.83 ± 1325.43
SK-MEL-8	2.66 ± 0.30	0.00	2.04 ± 0.22	0.00	6.97 ± 0.99	5400.96 ± 154.27
SK-MEL-28 + PBMC	2.89 ± 0.24	0.00	1.97 ± 0.66	34.28 ± 4.61	12.00 ± 1.78	4540.29 ± 377.61
SK-MEL-28 + EBC-46	2.22 ± 0.54	0.00	2.04 ± 0.22	0.00	9.41 ± 2.21	9465.25 ± 609.79
SK-MEL-28 + PBMC + EBC-46	2.55 ± 0.58	5339.38 ± 2642.25	8.15 ± 0.69	1189.09 ± 989.02	1179.90 ± 877.05	12976.93 ± 2351.48
MCF7	2.62 ± 0.83	0.00	1.76 ± 0.47	11.94 ± 0.91	3.97 ± 1.19	4.94 ± 0.45
MCF7 + PBMC	2.75 ± 0.63	17.80 ± 35.60	29.06 ± 7.83	165.95 ± 48.94	8.07 ± 1.43	1019.10 ± 309.13
MCF7 + EBC-46	2.65 ± 0.38	0.00	1.56 ± 0.66	279.79 ± 40.04	3.59 ± 0.95	384.28 ± 28.99
MCF7 + PBMC + 46	3.24 ± 1.90	1342.96 ± 156.71	20.23 ± 1.74	2985.46 ± 270.99	141.09 ± 19.77	13858.07 ± 514.39
NFF	3.76 ± 0.96	95.64 ± 92.46	3.25 ± 0.66	3965.72 ± 375.37	5.49 ± 1.81	445.30 ± 64.50
NFF + PBMC	4.01 ± 0.91	128.71 ± 98.99	8.12 ± 1.76	15685.93 ± 5251.62	7.08 ± 2.10	5588.36 ± 2600.88
NFF + PBMC + EBC-46	3.56 ± 2.61	2190.87 ± 241.47	4.37 ± 2.08	23611.91 ± 3957.21	61.34 ± 7.47	18725.17 ± 72.31

Tumor cells (~$3x10^5$ cells/well) and NFF's (~$5x10^4$ cells/well) were separately co-cultured with PBMC's (~$3x10^5$ cells/well) and treated with 100 ng/ml of EBC-46 for 24hr. The supernatants were analysed in quadruplicate. (mean ± standard deviation).

5.3 Discussion:

To understand the mechanism of action of EBC-46 injected directly into tumors and to further investigate the inflammatory response observed in *Chapter Four*, immunohistochemical analysis and subsequent cytokine assays were performed. Using histopathology it was possible to visually assess not only the effect of EBC-46 on tumor cellular architecture but also confirm the increased presence of neutrophils and macrophages within the tumor following treatment with 30 µg of EBC-46. The requirement of neutrophils for efficacy of EBC-46 was tested by ablating neutrophils in mice prior to treatment of tumors with EBC-46 using an anti-neutrophil neutralizing antibody. A modest depletion of efficacy was found, but considerably less than for topical efficacy of PEP005.

Following intratumoral delivery of EBC-46 there was an increase in endothelial permeability leading to the extravasation of macrophages and neutrophils and a disruption of the tumor vasculature which together were associated with necrosis of cancer cells. Moreover, the timeline of these cellular changes within the tumor microenvironment coincided with results observed in the previous Chapter: development of an inflammatory reaction to EBC-46; the loss of clonogenic survival by 4 hr following treatment, determined by *ex vivo* assay.

The infiltration of neutrophils and macrophages into the tumor by 4 hr after treatment, the disintegration of the tumor mass beginning at the early time-points between 2-4 hr following treatment with EBC-46, the vascular damage and obstruction of blood supply to the tumor between 4-8 hr would explain the extensive necrosis seen by day 7 following treatment. The overall action of EBC-46 thus leads to destruction of the tumor microenvironment through hemorrhagic necrosis.

The immunological profile of tumors and the host upon treatment with EBC-46 was further investigated with cytokine assays. Cytokine expression levels from tumors treated *in vivo* and from mouse serum were minimal except for IL-1β, IL-8, IL-6 and MCP-1. This was possibly due to the vascular damage and loss of blood supply. As an alternative approach, PBMC cells were co-cultured with tumor cells and treated *in vitro*, although at a much lower concentration of EBC-46 than the 600 µg/ml injected dose. In part support of the *in vivo* results obtained in mice from the cytokine bead assays, *in vitro* treatment of human PBMCs revealed an increase in the numbers of

pro-inflammatory cytokines and chemokines that regulate expression of immune cells such as neutrophils and macrophages.

The elevated expression of IL-6, IL-8, IL-1β, TNF-α correlated with the immunohistochemical observations of the increased presence of neutrophils and macrophages. These are important cytokines involved in the immune activity triggered by EBC-46. IL-8 is a chemokine also known as neutrophil chemotactic factor where it induces chemotaxis in target cells, primarily neutrophils, causing them to migrate toward the site of infection. Similarly, IL-6 and IL-1β are also important mediators of inflammatory responses. TNF α is involved in systemic inflammation and is produced chiefly by activated macrophages (M1). Its primary role is the regulation of immune cells and is able to induce apoptotic cell death, inflammation and inhibit tumorigenesis in addition to other functions. IL-10 on the other hand, is an anti-inflammatory cytokine and is involved in the regulation of the JAK-STAT signaling pathway. Also known as a cytokine synthesis inhibitory factor, is it capable of inhibiting synthesis of pro-inflammatory cytokines such as IFN γ, IL-2, TNF α produced by cells such as macrophages and regulatory T cells. IL-12 is an interleukin produced by dendritic cells and macrophages in response to antigenic stimulation. It is stimulates the growth and function of T cells by stimulating the production of IFN γ and TNF α.

The importance of neutrophils for the anticancer activity of EBC-46 was investigated by using Anti-Ly-6G antibody, a neutrophil neutralizing agent. An overall of 4 recurrences were observed in mice receiving the anti-Ly-6G antibody compared to a single recurrence in the mice treated with the isotype control IgG_2 antibody. However, this study was not statistically significant, in part due to the larger volume of the recurring tumors in mice treated with the isotype antibody control and with the normalization of the depleted neutrophil count. One study reported that following the anti-Ly-6G antibody administration, the peripheral neutrophil counts return to pretreatment level by day 5 (Tateda *et al.*, 2001). Hence, while it does appear that neutrophils are responsible at least in part for the anti-cancer efficacy of EBC-46, further studies using serial injections of the anti-Ly-6G antibody every 2 days to maintain the depletion of neutrophils could be carried out. Another factor to consider may be a larger experimental size with an increased number of mice.

Chapter Six

Molecular Responses to the Action of EBC-46

6.1 Introduction

In the earlier Chapters it was established that EBC-46 is a PKC activator that translocates PKC isoforms containing a C1 domain and subsequently activates ERK1/2 of the MAPK signaling pathway. Compared to the prototype PKC activator TPA, EBC-46 was found to be less cytotoxic on tumor cells *in vitro.* However, treatment of xenografts with EBC-46 resulted in cure of tumors in mice while tumors treated with TPA relapsed at all of the respective treatment sites. Either as an initial response or a secondary phenomenon to treatment with EBC-46, an inflammatory reaction developed within 4 hr of exposure to the drug which indicated the involvement of the host immune system in the efficacy of EBC-46 action on tumors *in vivo*. This was confirmed through immunohistochemical analysis of tumor tissue staining for neutrophils and macrophages, which showed infiltration of immune cells into the tumor site within 4 hr of EBC-46 treatment, declining in numbers by 24 hr. In addition, histological staining of tumors with CD-31 showed reduction in the number of endothelial cells from 8 hr after treatment with EBC-46 leading to the gradual onset of necrosis. Cytokine expression was shown to be greatly increased from 4 - 24 hr following treatment of tumor cells with EBC-46 *in vitro* when co-cultured with PBMCs. Hence, this indicated that 4-8 hr of treatment with EBC-46 was a significant time-frame where the effects of the compound reached its peak.

To determine the molecular pathways involved, human and murine-specific microarray analysis was performed of gene expressions of tumor and host respectively in response to treatment with EBC-46 and TPA. It was possible that the differences in gene expression following treatment with EBC-46 compared with TPA would help explain why TPA was less effective than EBC-46 *in vivo*.

6.2 Results

cRNA microarray analysis was performed to determine the likely molecular pathways involved in the activity of EBC-46 and TPA on tumors and the host. To determine the changes resulting from activity of the diterpene esters, the treated RNA samples were compared to samples treated with the control vehicle 20% propylene glycol (PG).

BALB/c *Foxn1*^{nu} mice with two Sk-Mel-28 tumors per mouse were treated with EBC-46 or TPA at 30 µg per tumor site following which tumors were harvested at 1 hr, 2 hr, 4 hr, 8 hr, 24 hr or 48 hr. Total RNA was extracted from these tumors by homogenization in RLT buffer containing β-mercaptoethanol, followed by extraction and purification using the Qiagen Plus RNeasy Kit (see *Chapter Two*; Materials and Methods; Section 2.8.1). The amount of total RNA extracted and purified was measured using the NanoDrop instrument followed by an assessment of the integrity of the RNA extracted. Samples were loaded and run through a denaturing agarose gel and stained with ethidium bromide (EtBr) alongside a 1kb DNA marker.

Ideally total intact RNA run on a denaturing agarose gel will have sharp clear bands of 28S and 18S, where the 28S rRNA band should be approximately twice as intense as the 18S rRNA band. The ratio of absorbance at 260 nm and 280 nm was used to assess the purity of RNA where a ratio between 1.8 -2.0 is accepted as "pure" RNA. Ratios outside of this range may indicate presence of protein, genomic DNA or other contaminants (NanoDrop Protocols).

Among the RNA samples extracted from treated Sk-Mel-28 tumors and run on a 1% denaturing agarose gel, intact total RNA resulted in two clear bands 28S and 18S in samples from tumors treated with EBC-46 and TPA from 1 hr to 8 hr. However, by 24 hr after treatment, partial degradation of total RNA was observed. Extracted RNA was found to be completely degraded by 48 hr following treatment. In contrast, intact total RNA was successfully extracted from tumors treated with vehicle alone (20% PG). Note the ratios highlighted in red which are relevant to RNA after 24 and 48 hr of exposure to EBC-46 (Table 6.1 and Figure 6.1). Repetitions of treatments and extractions to obtain intact total RNA post 8 hr of treatment with the diterpene esters resulted in the same observation of partial degradation by 24 hr- (Table 6.2).

Table 6.1 Concentration of RNA extracted from Sk-Mel-28 tumors after treatment with 30 µg EBC-46 per tumor or the vehicle control 20% PG.

Sample ID	ng/ul	$A_{260\ nm}$	$A_{280\ nm}$	260/280	Constant
Sk-Mel-28 - untreated	315.84	7.896	3.906	2.02	40
Sk-Mel-28 - 1 hr 20%PG	857.02	21.425	10.436	2.05	40
Sk-Mel-28 - 1 hr EBC-46	627.29	15.682	7.574	2.07	40
Sk-Mel-28 - 2 hr 20%PG	665	16.625	8.088	2.06	40
Sk-Mel-28 - 2 hr EBC-46	904.4	22.61	10.919	2.07	40
Sk-Mel-28 - 4 hr 20%PG	646.33	16.158	7.8	2.07	40
Sk-Mel-28 - 4 hr EBC-46	897.44	22.436	10.933	2.05	40
Sk-Mel-28 - 8 hr 20%PG	947.16	23.679	11.423	2.07	40
Sk-Mel-28 - 8 hr EBC-46	607.9	15.197	7.36	2.06	40
Sk-Mel-28 - 24 hr 20%PG	230.28	5.757	2.843	2.03	40
Sk-Mel-28 - 24 hr EBC-46	193.36	4.834	2.029	**2.38**	40
Sk-Mel-28 - 48 hr 20%PG	1112.23	27.806	13.565	2.05	40
Sk-Mel-28 - 48 hr EBC-46	117.4	2.935	1.748	**1.68**	40

Abbreviations: $A_{260\ nm}$ – absorbance at 260 nm; $A_{280\ nm}$ – absorbance at 280 nm.

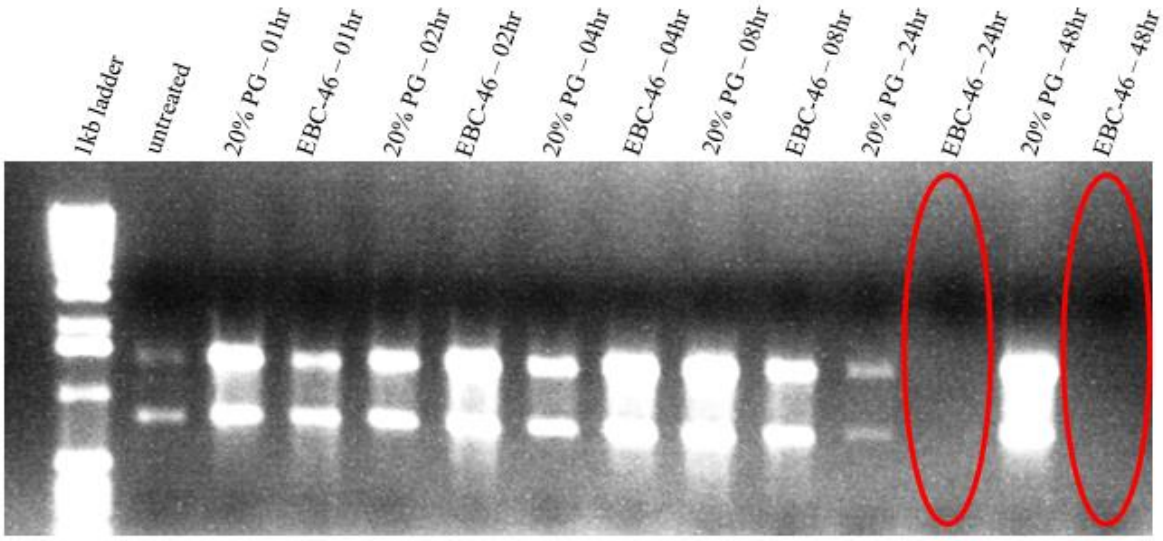

Figure 6.1 RNA extracted from Sk-Mel-8 tumors treated with EBC-46 at 30µg per tumor and compared to 20% PG at different times following treatment.

Integrity of RNA from Sk-Mel-28 tumors was assessed by agarose gel electrophoresis where ~ 2 µl of RNA sample with formamide loading buffer was loaded into wells of agarose gel alongside 1 kb marker and run at 80 V for 45 min to separate the bands for visualization on UV gel doc. RNA was partially degraded in lanes 12 and 14 where Sk-Mel-28 tumors were treated with EBC-46 for 24 hr and 48 hr respectively.

Table 6.2 Concentration of RNA extracted from Sk-Mel-28 tumors after treatment with 30 µg EBC-46 per tumor for 24 hr and 48 hr.

Sample ID	ng/ul	$A_{260\ nm}$	$A_{280\ nm}$	260/280	Constant
Sk-Mel-28 24hr EBC-46	398.68	9.967	4.912	2.03	40
Sk-Mel-28 48hr EBC-46	394.59	9.865	4.029	2.45	40

Abbreviations: $A_{260\ nm}$ – absorbance at 260 nm; $A_{280\ nm}$ – absorbance at 280 nm.

A time-course analysis was performed to investigate the changes in gene expression after treatment of Sk-Mel-28 tumors on the host and tumor with TPA or EBC-46, using microarrays. The tumors were treated with a final dose of 30 µg of TPA or EBC-46 per tumor for 0.5 hr, 1 hr, 2 hr, 4 hr, and 8 hr prior to extraction of total RNA. To determine the changes brought about by the diterpene esters, the samples were compared to treatments with the vehicle control 20% PG at the same times as mentioned above. Total RNA was extracted from tumors (Sk-Mel-28, human metastatic melanoma grown in BALB/c *Foxn1*^{nu} mice) and profiled using Illumina Human HT-12 v4 chips to assess the effects on the tumor, or Mouse Ref8 v2.0 BeadChips to assess the effects on the host. The chips carry 50-mer oligonucleotides representing cDNA of the whole of the expressed mouse or human genome, with 30- or 15-fold redundancy respectively. Total RNA was reverse transcribed to cDNA, which was then transcribed in turn to produce biotin-labelled cRNA.

cRNA microarray analysis was performed using the Illumina Whole-Genome Gene Expression Direct Hybridization Assay. The expression data read by the iScan System were decoded using GenomeStudio software (Illumina) before being exported to Agilent Technologies' GeneSpring GX v12.5 where they were normalized across the genome by quantile normalization across all probes on the Bead Array and filtered to ensure that the gene lists were robust. The fold change was calculated as an average expression across replicates treated with the drug and divided by the expression of the vehicle only at different treatment times; e.g. expression at 4 hr of treatment with EBC-46 was divided by the expression resulting from treatment with the vehicle 20% PG alone to calculate the fold change. The statistical differences were then calculated as pair-wise analysis where expression of treated samples at each time-point was compared to the control; e.g. expression at 4 hr of treatment with EBC-46 was compared to vehicle control 20% PG. Hence, t-test was appropriate. Further, human PBMC cells were treated *in vitro* with 30 ng/ml of TPA or EBC-46 for 4 hr, 24 hr and 96 hr, to additionally assess the effects of the compounds on cells of the immune system.

6.2.1 Tumor response to activity of diterpene esters EBC-46 and TPA in vivo

Microarrays were performed for three individual experimental groups of RNA extracted from Sk-Mel-28 tumors treated in BALB/c *Foxn1*^{nu} mice with 30 µg of EBC-46 or TPA in parallel with the vehicle control 20% PG. The resulting raw data generated were combined in GeneSpring GX v12.5

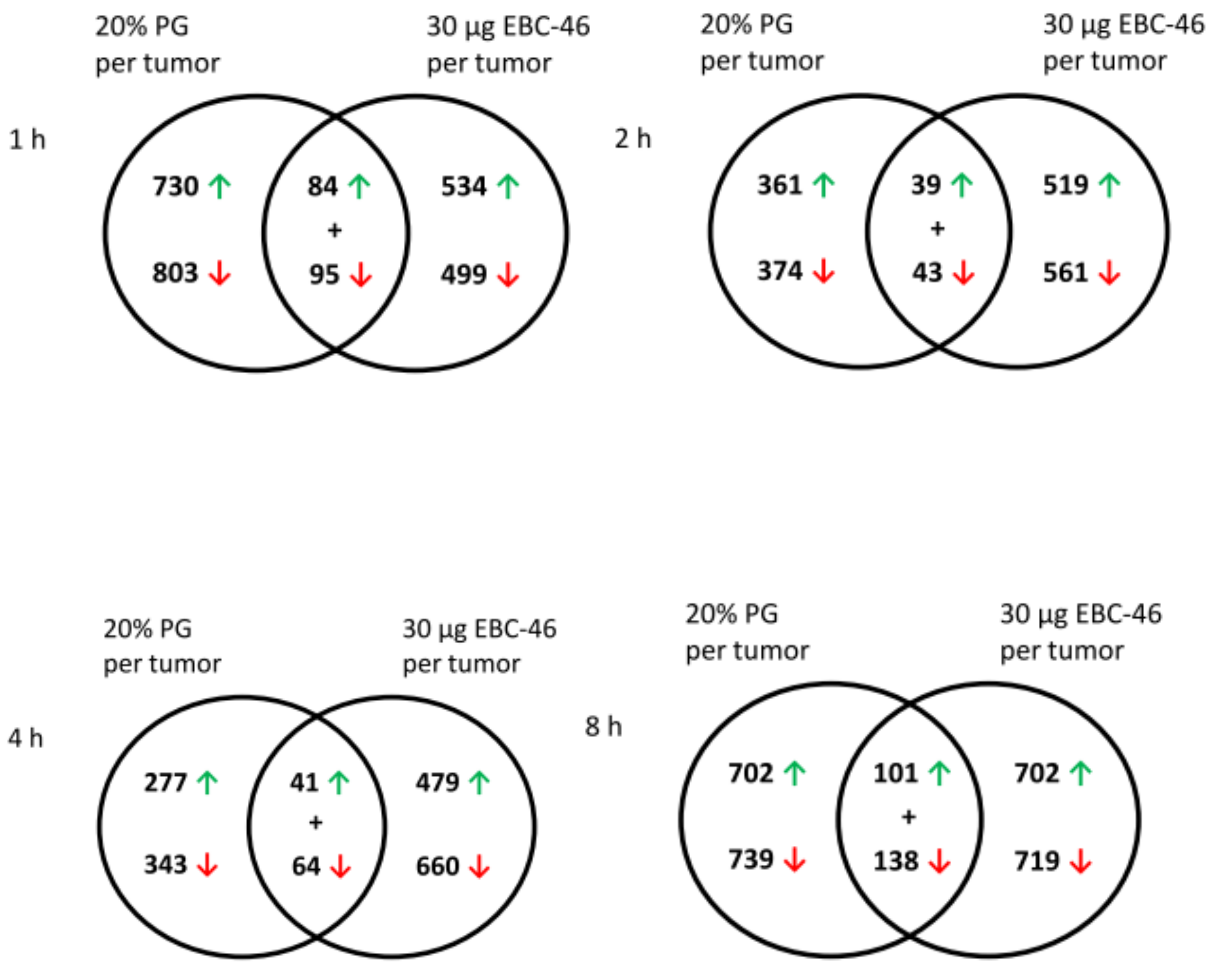

Figure 6.2 Venn diagrams comparing the changes in gene expression effected by diterpene ester EBC-46 at a final dose of 30 µg per tumor and vehicle control 20% PG, showing genes (↑) up- or (↓) down-regulated with $p \leq 0.05$

RNA extracted from Sk-Mel-28 tumors treated with 30 µg EBC-46 per tumor or vehicle control 20% PG were analysed on Illumina HumanHT-12 v4 BeadChips to assess the response of the tumor to treatment with the diterpene ester EBC-46 at 1 hr, 2 hr, 4 hr and 8 hr after treatment. The gene lists were compared using Venn diagrams in GeneSpring GX v12.5 to understand the changes induced by EBC-46.

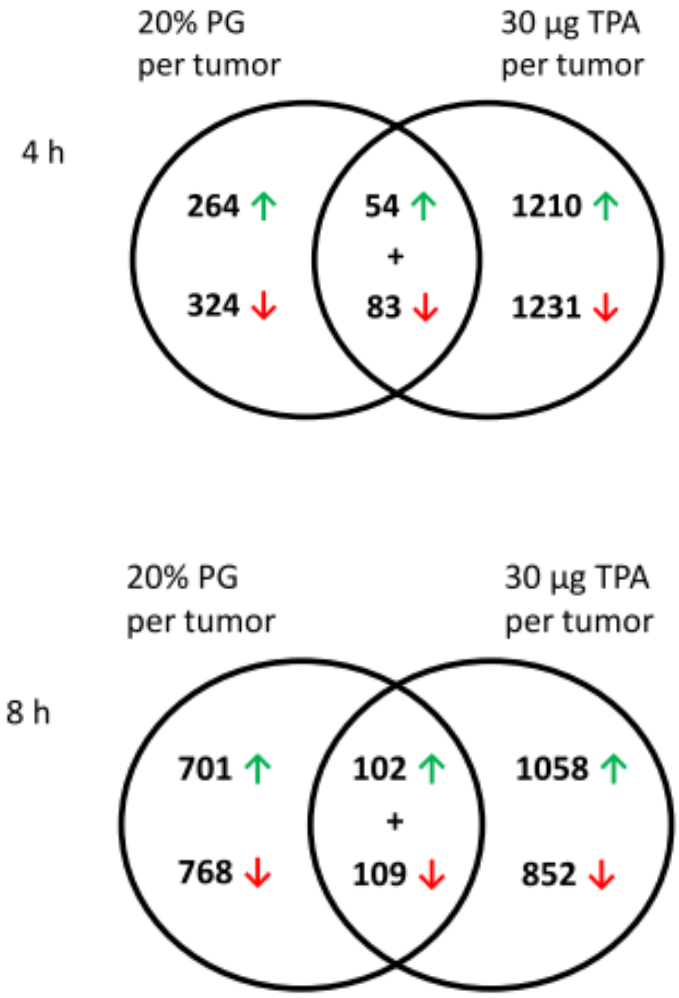

Figure 6.3 Venn diagrams comparing of the changes in gene expression effected by diterpene ester TPA at a final dose of 30 µg per tumor and vehicle control PG, showing genes that are (↑) up- or (↓) down-regulated with $p \leq 0.05$

RNA extracted from Sk-Mel-28 tumors treated with 30 µg TPA per tumor or vehicle control 20% PG were analysed on Illumina HumanHT-12 v4 BeadChips to assess the response of the tumor to treatment with the diterpene ester TPA at 4 hr and 8 hr after treatment. The gene lists were compared using Venn diagrams in GeneSpring GX v12.5 to understand the changes induced by TPA.

Table 6.3 Top twenty genes significantly UP-regulated following 4 hr treatment by 30 µg EBC-46 (compared to vehicle control 20% PG) in Sk-Mel-28 tumors as detected on Illumina HumanHT-12 v4 BeadChips.

ProbeID	p Value	Regulation	FC (abs)	Symbol	Definition
580161	0.001	up	13.249	SNORD3C	Homo sapiens small nucleolar RNA, C/D box 3C (SNORD3C), small nucleolar RNA.
2510164	0.003	up	12.796	SNORD3A	Homo sapiens small nucleolar RNA, C/D box 3A (SNORD3A), small nucleolar RNA.
380685	0.003	up	12.718	SNORD3D	Homo sapiens small nucleolar RNA, C/D box 3D (SNORD3D), small nucleolar RNA.
2570220	0.001	up	3.907	RN5S9	Homo sapiens RNA, 5S ribosomal 9 (RN5S9), ribosomal RNA.
2450020	0.009	up	2.878	SNORD56	Homo sapiens small nucleolar RNA, C/D box 56 (SNORD56), small nuclear RNA.
3850189	0.021	up	1.968	RNU4-2	Homo sapiens RNA, U4 small nuclear 2 (RNU4-2), small nuclear RNA.
4200379	0.029	up	1.934	RNU11	Homo sapiens RNA, U11 small nuclear (RNU11), small nuclear RNA.
240594	0.043	up	1.870	ANXA3	Homo sapiens annexin A3 (ANXA3), mRNA.
3990463	0.008	up	1.770	RNU4-1	Homo sapiens RNA, U4 small nuclear 1 (RNU4-1), small nuclear RNA.
7560041	0.035	up	1.705	AXUD1	Homo sapiens AXIN1 up-regulated 1 (AXUD1), mRNA.
2600747	0.043	up	1.681	IFIT2	Homo sapiens interferon-induced protein with tetratricopeptide repeats 2 (IFIT2), mRNA.
2190184	0.041	up	1.665	PRSS23	Homo sapiens protease, serine, 23 (PRSS23), mRNA.
4220255	0.017	up	1.649	VTRNA1-1	Homo sapiens vault RNA 1-1 (VTRNA1-1), non-coding RNA.
5700725	0.048	up	1.644	EPSTI1	Homo sapiens epithelial stromal interaction 1 (breast) (EPSTI1), transcript variant 2, mRNA.
2340072	0.021	up	1.613	PARP12	Homo sapiens poly (ADP-ribose) polymerase family, member 12 (PARP12), mRNA.
1240142	0.003	up	1.609	SAMD9	Homo sapiens sterile alpha motif domain containing 9 (SAMD9), mRNA.
990176	0.048	up	1.597	RN7SK	Homo sapiens RNA, 7SK small nuclear (RN7SK), non-coding RNA.
7400743	0.012	up	1.588	KIAA1618	Homo sapiens KIAA1618 (KIAA1618), mRNA.
2120079	0.002	up	1.570	EIF2AK2	Homo sapiens eukaryotic translation initiation factor 2-alpha kinase 2 (EIF2AK2), mRNA.
5720040	0.008	up	1.550	EYA1	Homo sapiens eyes absent homolog 1 (Drosophila) (EYA1), transcript variant 1, mRNA.

FC; fold change in expression compared with controls

Table 6.4 Top twenty genes significantly DOWN-regulated following 4 hr treatment by 30 µg EBC-46 (compared to vehicle control 20% PG) in Sk-Mel-28 tumors as detected on Illumina HumanHT-12 v4 BeadChips.

ProbeID	p Value	Regulation	FC (abs)	Symbol	Definition
7150296	0.044	down	2.232	LOC100130562	PREDICTED: Homo sapiens hypothetical protein LOC100130562, transcript variant 1 (LOC100130562), mRNA.
5900564	0.002	down	2.112	SLC16A6	Homo sapiens solute carrier family 16, member 6 (monocarboxylic acid transporter 7) (SLC16A6), mRNA.
6330730	0.007	down	1.774	SNAI2	Homo sapiens snail homolog 2 (Drosophila) (SNAI2), mRNA.
50255	0.018	down	1.682	SNAI2	Homo sapiens snail homolog 2 (Drosophila) (SNAI2), mRNA.
780762	0.035	down	1.591	CSNK1D	Homo sapiens casein kinase 1, delta (CSNK1D), transcript variant 1, mRNA.
770743	0.029	down	1.565	MIR1978	Homo sapiens microRNA 1978 (MIR1978), microRNA.
5270520	0.001	down	1.560	FAIM3	Homo sapiens Fas apoptotic inhibitory molecule 3 (FAIM3), mRNA.
4590020	0.020	down	1.520	YOD1	Homo sapiens YOD1 OTU deubiquinating enzyme 1 homolog (S. cerevisiae) (YOD1), mRNA.
520468	0.041	down	1.517	LOC402175	PREDICTED: Homo sapiens misc_RNA (LOC402175), miscRNA.
1430138	0.016	down	1.504	MAFF	Homo sapiens v-maf musculoaponeurotic fibrosarcoma oncogene homolog F (avian) (MAFF), transcript variant 1, mRNA.
4390300	0.025	down	1.491	TOB1	Homo sapiens transducer of ERBB2, 1 (TOB1), mRNA.
4150278	0.002	down	1.477	DUSP14	Homo sapiens dual specificity phosphatase 14 (DUSP14), mRNA.
2750280	0.044	down	1.471	CDK5R1	Homo sapiens cyclin-dependent kinase 5, regulatory subunit 1 (p35) (CDK5R1), mRNA.
1240228	0.026	down	1.467	PAG1	Homo sapiens phosphoprotein associated with glycosphingolipid microdomains 1 (PAG1), mRNA.
360242	0.020	down	1.455	LOC440459	PREDICTED: Homo sapiens similar to solute carrier family 16, member 6 (LOC440459), miscRNA.
1430598	0.000	down	1.444	FBXO32	Homo sapiens F-box protein 32 (FBXO32), transcript variant 1, mRNA.
6860162	0.036	down	1.432	LOC441019	PREDICTED: Homo sapiens hypothetical LOC441019 (LOC441019), mRNA.
4890358	0.049	down	1.426	LOC100131866	PREDICTED: Homo sapiens misc_RNA (LOC100131866), miscRNA.
460193	0.001	down	1.420	MAD2L1BP	Homo sapiens MAD2L1 binding protein (MAD2L1BP), transcript variant 2, mRNA.
6290598	0.007	down	1.418	TMEM138	Homo sapiens transmembrane protein 138 (TMEM138), mRNA.

FC; fold change in expression compared with controls

Table 6.5 Top twenty genes significantly UP-regulated following 8 hr treatment by 30 µg EBC-46 (compared to vehicle control 20% PG) in Sk-Mel-28 tumors as detected on Illumina HumanHT-12 v4 BeadChips.

ProbeID	p Value	Regulation	FC (abs)	Symbol	Definition
2510164	0.031	up	25.916	SNORD3A	Homo sapiens small nucleolar RNA, C/D box 3A (SNORD3A), small nucleolar RNA.
380685	0.032	up	23.662	SNORD3D	Homo sapiens small nucleolar RNA, C/D box 3D (SNORD3D), small nucleolar RNA.
580161	0.036	up	21.770	SNORD3C	Homo sapiens small nucleolar RNA, C/D box 3C (SNORD3C), small nucleolar RNA.
2360091	0.040	up	3.913	RNU1G2	Homo sapiens RNA, U1G2 small nuclear (RNU1G2), small nuclear RNA.
5670152	0.047	up	3.697	RNU1-3	Homo sapiens RNA, U1 small nuclear 3 (RNU1-3), small nuclear RNA.
2570220	0.012	up	3.441	RN5S9	Homo sapiens RNA, 5S ribosomal 9 (RN5S9), ribosomal RNA.
3780767	0.000	up	2.907	LOC100132564	PREDICTED: Homo sapiens hypothetical protein LOC100132564 (LOC100132564), mRNA.
6860377	0.008	up	2.382	DUSP1	Homo sapiens dual specificity phosphatase 1 (DUSP1), mRNA.
4220255	0.022	up	1.959	VTRNA1-1	Homo sapiens vault RNA 1-1 (VTRNA1-1), non-coding RNA.
990176	0.027	up	1.921	RN7SK	Homo sapiens RNA, 7SK small nuclear (RN7SK), non-coding RNA.
4280017	0.033	up	1.913	FOS	Homo sapiens v-fos FBJ murine osteosarcoma viral oncogene homolog (FOS), mRNA.
3990463	0.036	up	1.723	RNU4-1	Homo sapiens RNA, U4 small nuclear 1 (RNU4-1), small nuclear RNA.
6400364	0.031	up	1.711	NR4A2	Homo sapiens nuclear receptor subfamily 4, group A, member 2 (NR4A2), transcript variant 1, mRNA.
2260309	0.031	up	1.659	RPPH1	Homo sapiens ribonuclease P RNA component H1 (RPPH1), RNase P RNA.
4210044	0.039	up	1.519	SNORD46	Homo sapiens small nucleolar RNA, C/D box 46 (SNORD46), small nucleolar RNA.
6520129	0.027	up	1.514	ZNF148	Homo sapiens zinc finger protein 148 (ZNF148), mRNA.
50608	0.019	up	1.470	MTP18	Homo sapiens mitochondrial protein 18 kDa (MTP18), nuclear gene encoding mitochondrial protein, transcript variant 2, mRNA.
1510228	0.042	up	1.462	SNORD12C	Homo sapiens small nucleolar RNA, C/D box 12C (SNORD12C), small nucleolar RNA.
650639	0.013	up	1.424	NR4A2	Homo sapiens nuclear receptor subfamily 4, group A, member 2 (NR4A2), transcript variant 1, mRNA.
6450424	0.006	up	1.422	NME3	Homo sapiens non-metastatic cells 3, protein expressed in (NME3), mRNA.

FC; fold change in expression compared with controls

Table 6.6 Top twenty genes significantly DOWN-regulated following 8 hr treatment by 30 µg EBC-46 (compared to vehicle control 20% PG) in Sk-Mel-28 tumors as detected on Illumina HumanHT-12 v4 BeadChips.

ProbeID	p Value	Regulation	FC (abs)	Symbol	Definition
630128	0.040	down	2.442	LOC286444	PREDICTED: Homo sapiens misc_RNA (LOC286444), miscRNA.
7040008	0.039	down	1.961	CD74	Homo sapiens CD74 molecule, major histocompatibility complex, class II invariant chain (CD74), transcript variant 2, mRNA.
4590576	0.029	down	1.955	LOC286444	PREDICTED: Homo sapiens misc_RNA (LOC286444), miscRNA.
4560047	0.018	down	1.955	CD74	Homo sapiens CD74 molecule, major histocompatibility complex, class II invariant chain (CD74), transcript variant 1, mRNA.
770743	0.026	down	1.862	MIR1978	Homo sapiens microRNA 1978 (MIR1978), microRNA.
2000673	0.036	down	1.846	GAGE12C	Homo sapiens G antigen 12C (GAGE12C), mRNA.
7560047	0.040	down	1.827	CIRBP	Homo sapiens cold inducible RNA binding protein (CIRBP), mRNA.
990672	0.029	down	1.803	VPS18	Homo sapiens vacuolar protein sorting 18 homolog (S. cerevisiae) (VPS18), mRNA.
6660601	0.032	down	1.798	HMOX1	Homo sapiens heme oxygenase (decycling) 1 (HMOX1), mRNA.
3610544	0.039	down	1.727	GAGE2B	Homo sapiens G antigen 2B (GAGE2B), mRNA.
2350553	0.018	down	1.654	LOC645037	Homo sapiens similar to GAGE-2 protein (G antigen 2) (LOC645037), mRNA.
2470161	0.019	down	1.654	PLEKHF1	Homo sapiens pleckstrin homology domain containing, family F (with FYVE domain) member 1 (PLEKHF1), mRNA.
780762	0.029	down	1.627	CSNK1D	Homo sapiens casein kinase 1, delta (CSNK1D), transcript variant 1, mRNA.
2450725	0.028	down	1.618	SLC3A2	Homo sapiens solute carrier family 3 (activators of dibasic and neutral amino acid transport), member 2 (SLC3A2), transcript variant 6, mRNA.
3520044	0.004	down	1.591	LOC100133866	PREDICTED: Homo sapiens similar to phosphodiesterase 4D interacting protein (myomegalin) (LOC100133866), mRNA.
50220	0.024	down	1.574	GAGE4	Homo sapiens G antigen 4 (GAGE4), mRNA.
4590670	0.021	down	1.562	LOC646294	PREDICTED: Homo sapiens misc_RNA (LOC646294), miscRNA.
1240440	0.003	down	1.522	TXNIP	Homo sapiens thioredoxin interacting protein (TXNIP), mRNA.
1990079	0.031	down	1.520	FBXO32	Homo sapiens F-box protein 32 (FBXO32), transcript variant 2, mRNA.
2120703	0.032	down	1.520	LOC645173	PREDICTED: Homo sapiens misc_RNA (LOC645173), miscRNA.

FC; fold change in expression compared with controls

and the statistical significance in gene expression was determined using *P* values calculated from the unpaired Student's *T* test where $p \leq 0.05$ was considered significant. Once the gene lists were generated, Venn diagrams were utilized to compare differential gene expression effected by TPA or EBC-46 specifically.

The treatments with EBC-46 (at 1 hr, 2 hr, 4 hr and 8 hr) or TPA (at 4 hr and 8 hr) were independently compared to the vehicle control 20% PG at each of the mentioned time-points (Figures. 6.2 and 6.3 respectively) to find differentially expressed genes only regulated by the compound of interest and not altered by the vehicle control (20% PG) treatment. The top 20 genes from these lists are shown for treatment time 4 hr and 8 hr in Tables 6.3 – 6.6 showing differential gene expression (up- and down-regulated genes) following treatment with EBC-46 only, after comparison with the vehicle control 20% PG. Gene expression lists were generated after analysis of expression upon treatment with EBC-46 at 1 hr and 2 hr after comparison with 20% PG at the different treatment times. These lists showing top 20 differentialy regulated genes have been included in the Appendix (p.259-262) Genes that were consistently up-regulated by EBC-46 at 1 hr, 2 hr, 4 hr and 8 hr following intratumoral treatment were *SNORD3A*, *SNORD3C* and *SNORD3D* (Tables 6.3 and 6.5) SNORD3A is also known as RNU3, U3; SNORD3C as U3-3 and SNORD3D as U3-4. The top 20 genes differentially expressed by TPA only, after comparison with the vehicle control 20% PG at 4 hr and 8 hr after treatment are included in the Appendix (p.263-266).

In *Chapter Four*, treatments of tumors with EBC-46 or TPA resulted in a significant difference between the efficacies of the two compounds. While TPA was the more potent cytotoxic agent in culture, it failed to cure tumors in mice compared to the positive response obtained with EBC-46. Bearing this in mind, the subsequent microarray **analysis investigated the genes differentially expressed by EBC-46 in comparison to TPA**. As observed in previous time-course experiments, the most significant time-frame for optimal activity of EBC-46 was between 4 hr – 8 hr after treatment. Hence the gene expression changes effected by EBC-46 (after comparison with the vehicle control 20% PG) and TPA (after comparison with the vehicle control 20% PG) were further compared against each other at 4 hr and 8 hr using Venn diagrams (Figure 6.4), to determine the changes in gene expression in SK-Mel-28 tumors due to treatment with 30 µg of EBC-46 or TPA. The gene

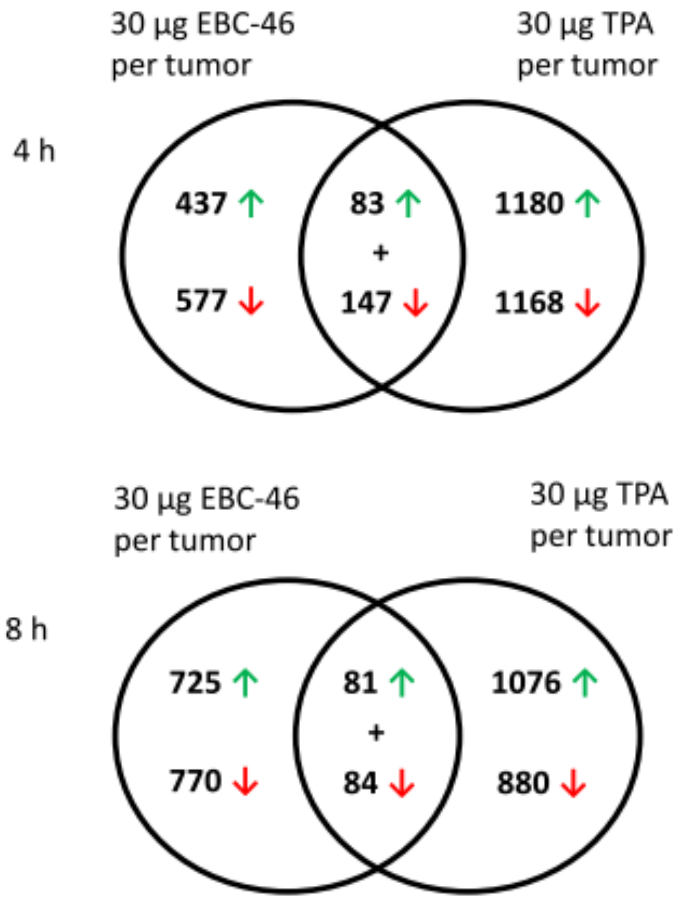

Figure 6.4 Comparison using Venn diagrams of differential gene expression upon treatment with diterpene esters EBC-46 or TPA after removal of 20% PG effects at a final dose of 30 µg per tumor at 4 h and 8 h where p value was calculated ≤ 0.05 showing genes that were (↑) up- or (↓) down-regulated.

RNA extracted from Sk-Mel-28 tumors treated with 30 µg EBC-46 or TPA per tumor were analysed on Illumina HumanHT-12 v4 BeadChips to evaluate the response of the tumor to treatment with the diterpene ester EBC-46 in comparison to TPA after removal of 20% PG effects at 4 hr and 8 hr after treatment and determine the difference in gene expression between the two compounds.

Table 6.7 Top twenty genes significantly UP-regulated following 4 hr treatment by 30 µg EBC-46 (after comparison with TPA) in Sk-Mel-28 tumors as detected on Illumina HumanHT-12 v4 BeadChips.

ProbeID	p Value	Regulation	FC (abs)	Symbol	Definition
380685	0.003	up	101.003	SNORD3D	Homo sapiens small nucleolar RNA, C/D box 3D (SNORD3D), small nucleolar RNA.
2510164	0.003	up	93.659	SNORD3A	Homo sapiens small nucleolar RNA, C/D box 3A (SNORD3A), small nucleolar RNA.
580161	0.004	up	55.830	SNORD3C	Homo sapiens small nucleolar RNA, C/D box 3C (SNORD3C), small nucleolar RNA.
2570220	0.005	up	5.518	RN5S9	Homo sapiens RNA, 5S ribosomal 9 (RN5S9), ribosomal RNA.
6620170	0.044	up	3.765	HBA2	Homo sapiens hemoglobin, alpha 2 (HBA2), mRNA.
2260349	0.014	up	2.994	MIR1974	Homo sapiens microRNA 1974 (MIR1974), microRNA.
3780767	0.003	up	2.364	LOC100132564	PREDICTED: Homo sapiens hypothetical protein LOC100132564 (LOC100132564), mRNA.
5670753	0.045	up	2.075	RNU1F1	Homo sapiens RNA, U1F1 small nuclear (RNU1F1), small nuclear RNA.
4640689	0.021	up	1.978	EIF4A2	Homo sapiens eukaryotic translation initiation factor 4A, isoform 2 (EIF4A2), mRNA.
4150519	0.003	up	1.960	FAM108C1	Homo sapiens family with sequence similarity 108, member C1 (FAM108C1), mRNA.
6580368	0.035	up	1.804	LOC387753	PREDICTED: Homo sapiens similar to 60S ribosomal protein L21, transcript variant 1 (LOC387753), mRNA.
610019	0.026	up	1.729	POLR3F	Homo sapiens polymerase (RNA) III (DNA directed) polypeptide F, 39 kDa (POLR3F), mRNA.
1240142	0.017	up	1.716	SAMD9	Homo sapiens sterile alpha motif domain containing 9 (SAMD9), mRNA.
5960181	0.019	up	1.715	ASNS	Homo sapiens asparagine synthetase (ASNS), transcript variant 1, mRNA.
4220437	0.024	up	1.671	UCN2	Homo sapiens urocortin 2 (UCN2), mRNA.
1090500	0.022	up	1.664	LOC645166	PREDICTED: Homo sapiens similar to lymphocyte-specific protein 1 (LOC645166), mRNA.
6220600	0.028	up	1.664	LOC113386	Homo sapiens similar to envelope protein (LOC113386), mRNA.

FC; fold change in expression compared with TPA

Table 6.8 Top twenty genes significantly DOWN-regulated following 4 hr treatment by 30 µg EBC-46 (after comparison with TPA) in Sk-Mel-28 tumors as detected on Illumina HumanHT-12 v4 BeadChips.

ProbeID	p Value	Regulation	FC (abs)	Symbol	Definition
630128	0.046	down	3.544	LOC286444	PREDICTED: Homo sapiens misc_RNA (LOC286444), miscRNA.
3390463	0.049	down	2.165	KU-MEL-3	Homo sapiens KU-MEL-3 protein (KU-MEL-3), mRNA.
510731	0.047	down	2.104	RRM2	Homo sapiens ribonucleotide reductase M2 polypeptide (RRM2), mRNA.
150544	0.031	down	2.016	PSMC4	Homo sapiens proteasome (prosome, macropain) 26S subunit, ATPase, 4 (PSMC4), transcript variant 1, mRNA.
5360646	0.034	down	1.997	PSMC4	Homo sapiens proteasome (prosome, macropain) 26S subunit, ATPase, 4 (PSMC4), transcript variant 1, mRNA.
6180440	0.036	down	1.984	PSMC4	Homo sapiens proteasome (prosome, macropain) 26S subunit, ATPase, 4 (PSMC4), transcript variant 1, mRNA.
1740543	0.046	down	1.926	JAK1	Homo sapiens Janus kinase 1 (JAK1), mRNA.
6650482	0.014	down	1.919	EPHA4	Homo sapiens EPH receptor A4 (EPHA4), mRNA.
2570553	0.041	down	1.788	LOC652615	PREDICTED: Homo sapiens similar to Anaphase promoting complex subunit 1 (APC1) (Cyclosome subunit 1) (Protein Tsg24) (Mitotic checkpoint regulator) (LOC652615), mRNA.
5560561	0.031	down	1.786	TNS3	Homo sapiens tensin 3 (TNS3), mRNA.
6550754	0.030	down	1.755	EVL	Homo sapiens Enah/Vasp-like (EVL), mRNA.
1410408	0.023	down	1.750	ARID5B	Homo sapiens AT rich interactive domain 5B (MRF1-like) (ARID5B), mRNA.
1410333	0.024	down	1.740	LOC643668	PREDICTED: Homo sapiens similar to peptidase (prosome, macropain) 26S subunit, ATPase 1 (LOC643668), mRNA.
780762	0.042	down	1.725	CSNK1D	Homo sapiens casein kinase 1, delta (CSNK1D), transcript variant 1, mRNA.
2750719	0.027	down	1.709	DDX21	Homo sapiens DEAD (Asp-Glu-Ala-Asp) box polypeptide 21 (DDX21), mRNA.
6580605	0.034	down	1.683	LOC646294	PREDICTED: Homo sapiens misc_RNA (LOC646294), miscRNA.
4590670	0.034	down	1.666	LOC646294	PREDICTED: Homo sapiens misc_RNA (LOC646294), miscRNA.
6660768	0.029	down	1.662	IRF2BP2	Homo sapiens interferon regulatory factor 2 binding protein 2 (IRF2BP2), transcript variant 1, mRNA.
2480468	0.048	down	1.636	RANBP10	Homo sapiens RAN binding protein 10 (RANBP10), mRNA.
6110736	0.045	down	1.629	IRS2	Homo sapiens insulin receptor substrate 2 (IRS2), mRNA.

FC; fold change in expression compared with TPA

Table 6.9 Top twenty genes significantly UP-regulated following 8 hr treatment by 30 µg EBC-46 (after comparison with TPA) in Sk-Mel-28 tumors as detected on Illumina HumanHT-12 v4 BeadChips.

ProbeID	p Value	Regulation	FC (abs)	Symbol	Definition
580161	0.010	up	56.909	SNORD3C	Homo sapiens small nucleolar RNA, C/D box 3C (SNORD3C), small nucleolar RNA.
2970482	0.028	up	5.344	RNU1-5	Homo sapiens RNA, U1 small nuclear 5 (RNU1-5), small nuclear RNA.
5670152	0.025	up	5.256	RNU1-3	Homo sapiens RNA, U1 small nuclear 3 (RNU1-3), small nuclear RNA.
2360091	0.024	up	4.835	RNU1G2	Homo sapiens RNA, U1G2 small nuclear (RNU1G2), small nuclear RNA.
2570220	0.006	up	4.332	RN5S9	Homo sapiens RNA, 5S ribosomal 9 (RN5S9), ribosomal RNA.
2260349	0.016	up	3.777	MIR1974	Homo sapiens microRNA 1974 (MIR1974), microRNA.
7330681	0.045	up	3.452	RNU1A3	Homo sapiens RNA, U1A3 small nuclear (RNU1A3), small nuclear RNA.
70167	0.045	up	3.348	LY96	Homo sapiens lymphocyte antigen 96 (LY96), mRNA.
4780504	0.025	up	3.011	RNU6-15	Homo sapiens RNA, U6 small nuclear 15 (RNU6-15), small nuclear RNA.
7560041	0.047	up	2.919	AXUD1	Homo sapiens AXIN1 up-regulated 1 (AXUD1), mRNA.
3610279	0.037	up	2.874	RNU6-1	Homo sapiens RNA, U6 small nuclear 1 (RNU6-1), small nuclear RNA.
6040731	0.034	up	2.487	TYRP1	Homo sapiens tyrosinase-related protein 1 (TYRP1), mRNA.
3780767	0.001	up	2.432	LOC100132564	PREDICTED: Homo sapiens hypothetical protein LOC100132564 (LOC100132564), mRNA.
4010452	0.048	up	2.184	SLC38A6	Homo sapiens solute carrier family 38, member 6 (SLC38A6), mRNA.
4640689	0.040	up	2.138	EIF4A2	Homo sapiens eukaryotic translation initiation factor 4A, isoform 2 (EIF4A2), mRNA.
7050451	0.035	up	2.080	LOC100134504	PREDICTED: Homo sapiens hypothetical protein LOC100134504 (LOC100134504), mRNA.
460386	0.018	up	2.021	PTMA	Homo sapiens prothymosin, alpha (PTMA), transcript variant 1, mRNA.
2510338	0.044	up	1.985	GGH	Homo sapiens gamma-glutamyl hydrolase (conjugase, folylpolygammaglutamyl hydrolase) (GGH), mRNA.
6370091	0.032	up	1.982	ATP6V1G1	Homo sapiens ATPase, H+ transporting, lysosomal 13kDa, V1 subunit G1 (ATP6V1G1), mRNA.
4640743	0.032	up	1.971	CNN3	Homo sapiens calponin 3, acidic (CNN3), mRNA.

FC; fold change in expression compared with TPA

Table 6.10 Top twenty genes significantly DOWN-regulated following 8 hr treatment by 30 µg EBC-46 (after comparison with TPA) in Sk-Mel-28 tumors as detected on Illumina HumanHT-12 v4 BeadChips.

ProbeID	p Value	Regulation	FC (abs)	Symbol	Definition
630128	0.014	down	3.646	LOC286444	PREDICTED: Homo sapiens misc_RNA (LOC286444), miscRNA.
1740673	0.045	down	3.594	LOC399942	PREDICTED: Homo sapiens similar to Tubulin alpha-2 chain (Alpha-tubulin 2), transcript variant 5 (LOC399942), mRNA.
5310634	0.031	down	3.213	FASN	Homo sapiens fatty acid synthase (FASN), mRNA.
7150296	0.040	down	2.821	LOC100130562	PREDICTED: Homo sapiens hypothetical protein LOC100130562, transcript variant 1 (LOC100130562), mRNA.
4590576	0.011	down	2.760	LOC286444	PREDICTED: Homo sapiens misc_RNA (LOC286444), miscRNA.
2000025	0.030	down	2.607	LOC648024	PREDICTED: Homo sapiens similar to eukaryotic translation initiation factor 4A, isoform 1 (LOC648024), mRNA.
6980376	0.001	down	2.510	LOC388681	PREDICTED: Homo sapiens similar to phosphodiesterase 4D interacting protein isoform 1 (LOC388681), mRNA.
7560047	0.034	down	2.328	CIRBP	Homo sapiens cold inducible RNA binding protein (CIRBP), mRNA.
6180440	0.015	down	2.321	PSMC4	Homo sapiens proteasome (prosome, macropain) 26S subunit, ATPase, 4 (PSMC4), transcript variant 1, mRNA.
1740543	0.021	down	2.234	JAK1	Homo sapiens Janus kinase 1 (JAK1), mRNA.
1410408	0.020	down	2.160	ARID5B	Homo sapiens AT rich interactive domain 5B (MRF1-like) (ARID5B), mRNA.
5550220	0.034	down	2.129	NOP56	Homo sapiens NOP56 ribonucleoprotein homolog (yeast) (NOP56), transcript variant 1, mRNA.
630167	0.026	down	2.123	SDCBP	Homo sapiens syndecan binding protein (syntenin) (SDCBP), transcript variant 2, mRNA.
2640088	0.041	down	2.115	ALDOA	Homo sapiens aldolase A, fructose-bisphosphate (ALDOA), transcript variant 2, mRNA.
2360414	0.040	down	2.097	PI4KAP1	Homo sapiens phosphatidylinositol 4-kinase, catalytic, alpha pseudogene 1 (PI4KAP1), non-coding RNA.
770079	0.035	down	2.095	ATP2A2	Homo sapiens ATPase, Ca++ transporting, cardiac muscle, slow twitch 2 (ATP2A2), transcript variant 1, mRNA.
150544	0.039	down	2.077	PSMC4	Homo sapiens proteasome (prosome, macropain) 26S subunit, ATPase, 4 (PSMC4), transcript variant 1, mRNA.
5810189	0.049	down	2.046	ATP2A2	Homo sapiens ATPase, Ca++ transporting, cardiac muscle, slow twitch 2 (ATP2A2), transcript variant 1, mRNA.
6550754	0.025	down	2.031	EVL	Homo sapiens Enah/Vasp-like (EVL), mRNA.
4590670	0.010	down	1.998	LOC646294	PREDICTED: Homo sapiens misc_RNA (LOC646294), miscRNA.

FC; fold change in expression compared with TPA

lists generated from the Venn diagrams were then assessed to determine the differential gene expression brought about by EBC-46 alone (without the effect of the vehicle control or TPA) and the top 20 genes differentially regulated by EBC-46 alone, at 4 hr and 8 hr are listed in Tables 6.7 – 6.10). Once more, the *SNORD3A*, *SNORD3C* and *SNORD3D* genes were found to be up-regulated by more than 2-fold following treatment with EBC-46 alone at 4 hr and 8 hr. snoRNAs are small nucleolar RNAs involved in post-translational modifications.

6.2.2 Host response to activity of diterpene esters EBC-46 and TPA in vivo

RNA extracted from SK-Mel-28 treated and control tumors were analyzed using HumanHT-12 v4 BeadChips to determine the tumor response in Section 6.2.1. The same amplified RNA samples were hybridized to Illumina MouseRef-8 v2.0 BeadChips to investigate the response of the host and infiltrating cells to the activity of EBC-46 in comparison to TPA at 0.5 hr, 1 hr, 2 hr, 4 hr and 8 hr. The MouseRef-8 v2.0 BeadChip targets at least 25,600 well-annotated RefSeq transcripts and over 19,100 unique genes. The data generated were combined in GeneSpring and were subjected to quality control by filtering probe sets based on the detection score calculated by GenomeStudio where $p \leq 0.05$ was considered significant. The next filtering step involved identifying those genes that were at least 2-fold differentially regulated. Treatments with the diterpene esters EBC-46 or TPA were independently compared to treatments with the vehicle control 20% PG. The lists of genes differentially regulated by EBC-46 (versus 20% PG) and TPA (versus 20% PG) were then compared against each other using Venn diagram to identify the differences between the two treatments, namely TPA and EBC-46 at the various time-points (Figure 6.5) on the host BALB/c *Foxn1*^{nu} mice.

There was a vast difference in the number of genes differentially regulated by EBC-46 or TPA specifically, in the host. The subsequent gene lists obtained were analyzed where the top 20 genes differentially regulated more than 2-fold by EBC-46 or TPA were selected and are included in the Appendix (p.267-285). The majority of the genes of interest included those associated with an immune response. The purpose of analyzing treated tumor RNA on mouse array chips was to understand the effect of the diterpene ester EBC-46 on the host at a molecular level and correlate the findings with the previous observations. Genes expressed by the activity of EBC-46 did not

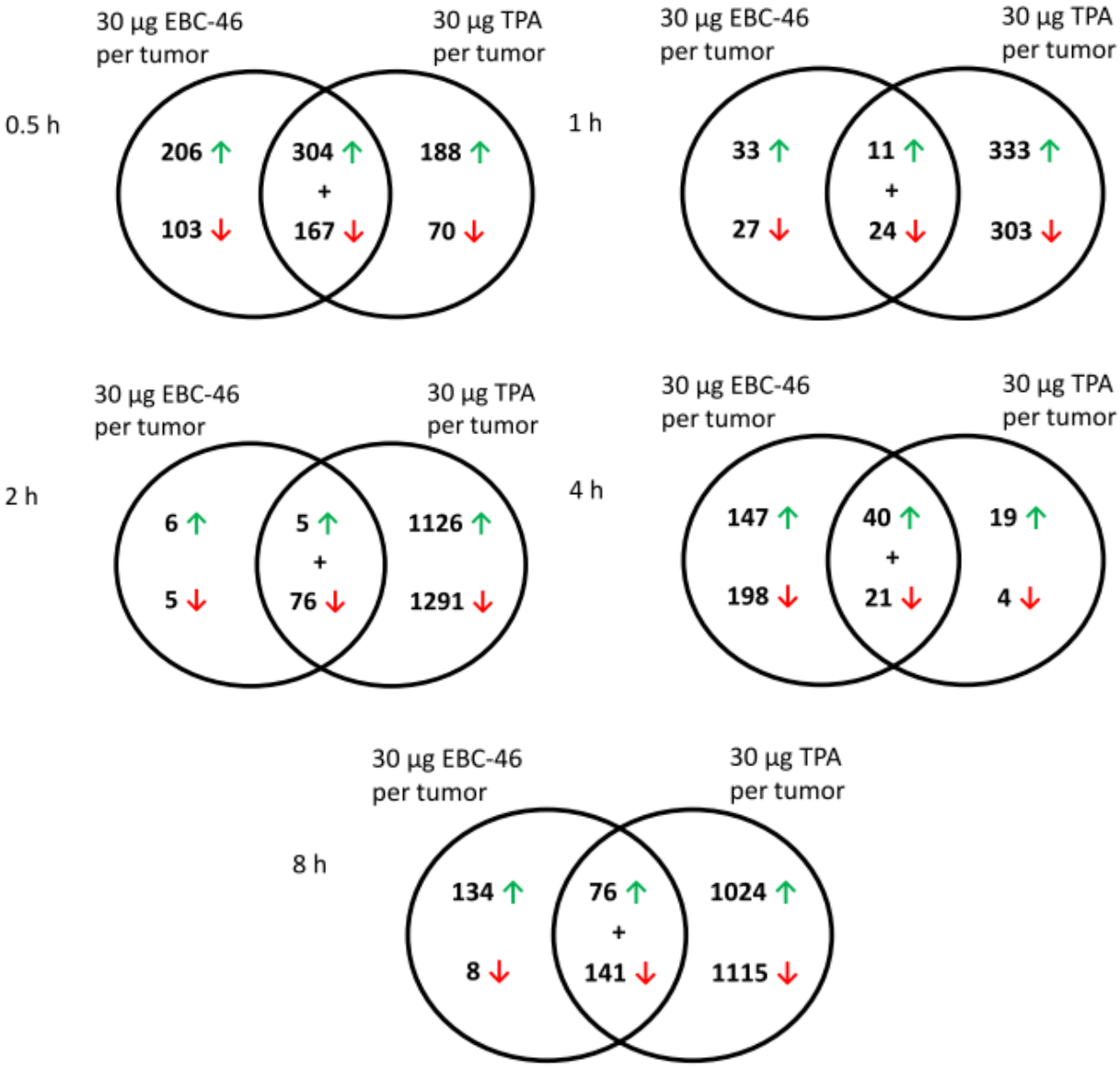

Figure 6.5 Differences in the host responses to treatment with EBC-46 and TPA where genes at least 2-fold (↑) up- or (↓) down-regulated were compared using Venn diagrams.

RNA extracted from Sk-Mel-28 tumors treated with 30 µg EBC-46 or TPA per tumor were analysed on MouseRef-8 v2.0 Illumina BeadChips to evaluate the response of the host to treatment with the diterpene ester EBC-46 in comparison to TPA at 30 min, 1 hr, 2 hr, 4 hr and 8 hr after treatment and determine the difference in gene expression between the two compounds.

show any significant changes in gene expression in the early time-points of 30 min to 2 hr following treatment. However, between 4-8 hr following treatment there was increased expression of genes regulating chemokines and inflammatory molecules where genes were significantly up-regulated ≥ 2-fold. The top 20 genes differentially regulated by the host upon treatment with EBC-46 alone at 4 hr and 8 hr are included in Tables catalogued in the Appendix (p.272-275). The genes of interest which were significantly up-or down- regulated included *Cxcl1, Defb6, Ly6g6c Gja1, Ccl4* and *Ifi27*. These results confirm the observations made in the previous Chapters with regards to the inflammatory reaction and the time- frame during which activity of EBC-46 is at its peak. In contrast, TPA does not induce expression of any of the genes involved in regulation of immune responses except for Jun-B at 30 min after treatment and *Infγ* at 2 hr after treatment. However, the expression of these genes was not constant. A significantly up-regulated gene after 8 hr of treatment with TPA was *Ncf1*, encoding the cytosolic neutrophil factor-1 protein. The top 20 genes differentially regulated by the host in response to treatment with TPA alone at 4 hr and 8 hr are included in the Appendix (p.282-285).

6.2.3 Transcriptional response of PBMCs to EBC-46 and TPA in vitro

The concentration of EBC-46 and TPA injected into tumors (600 µg/ml) was clearly toxic to tumor and murine cells, and little information about gene expression changes could therefore be expected from lymphocytes at non-toxic concentrations at the limits of drug diffusion areas where lymphocyte activation might play a role in efficacy. Microarray experiments were therefore conducted on human PBMCs readily available from human blood. Cultures were treated with TPA or EBC-46 at 30 ng/ml each for 4 hr, 24 hr and 96 hr. As a control, untreated PBMCs were used. Total RNA was extracted and amplified to produce biotinylated cRNAs that were used in the microarray assay. Data was normalized across the human genome using Human BeadChips from Illumino, in GeneSpring GX v12.5 by quantile normalization and put through filtering steps to ensure a strong data set and decrease the number of uninformative entities. Genes at least 2 – fold up- and down-regulated were determined by dividing the average expression of the treatments with the expression of the vehicle control. Diterpene ester-treated PBMCs were independently compared to the untreated PBMCs and gene lists were generated following which Venn diagrams

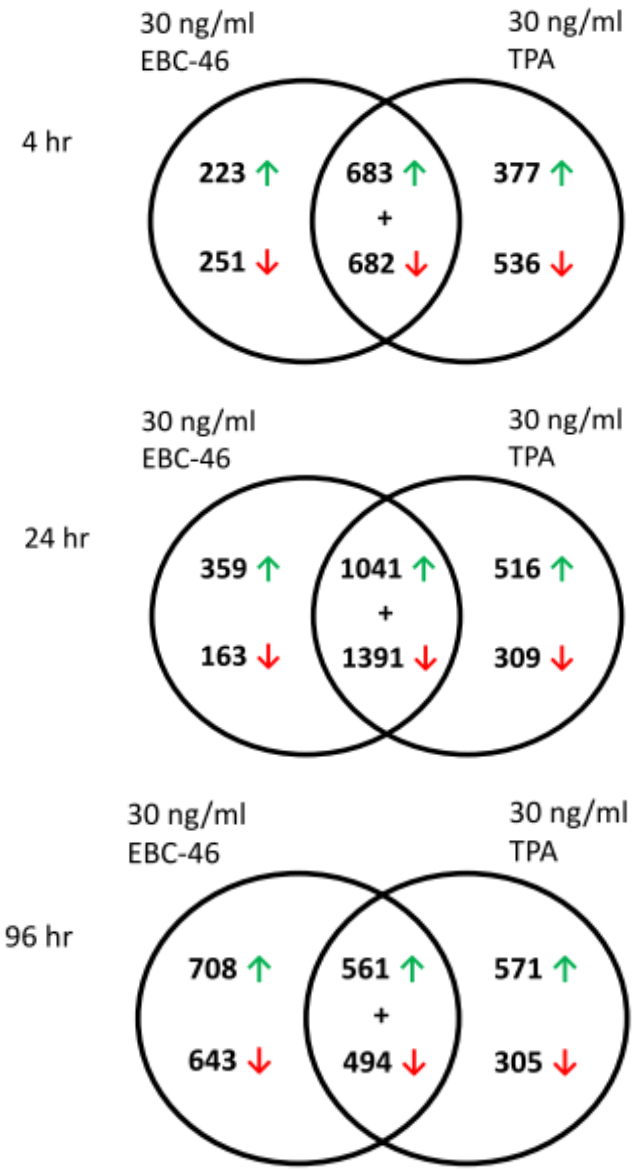

Figure 6.6 Comparison of the cellular response of human PBMCs treated with EBC-46 or TPA at 30 ng/ml each where genes at least 2 – fold (↑) up- or (↓) down-regulated were determined.

RNA extracted from human PBMCs and treated *in vitro* with 30 ng/ml of EBC-46 or TPA were analysed on HumanHT-12 v4 Illumina BeadChips to investigate the immune response to activity of the diterpene ester EBC-46 in comparison to TPA at 4 hr, 24 hr and 96 hr after treatment and determine the difference in gene expression between the two compounds.

were used to determine the changes in gene expression between treatments with TPA and EBC-46 at the different time-points (Figure 6.6).

More gene changes common to both treatments, namely EBC-46 and TPA occurred than those specific to either diterpene ester activity (Figure 6.6). The gene lists of the top 20 differentially regulated genes in response to treatment with EBC-46 or TPA alone are included in the Appendix (p.286-297). .

Treatment with EBC-46 on PBMCs *in vitro* resulted in an increased expression of pro-inflammatory mediators. Genes of interest included *IL28RA, IL1F5, CSF1*, *IL12RB1*, *MMP19* and *TNFRSF12A*. Among the genes differentially regulated by TPA were heat shock proteins and TNF receptors CD40, *IFiT3* (see Appendix).

6.2.4 Functional pathway and upstream regulator analysis of gene expression data

The data obtained in GeneSpring GX v12.5 following stringent methods of filtering for significant data, were subsequently uploaded to Ingenuity Pathway Analysis software (IPA Ingenuity Systems, Redwood City, CA, USA; www.ingenuity.com). To identify biological functions/diseases that were significant to the data sets, functional analyses were performed.

As seen in Tables 6.11 – 6.14, there is no overlap of pathways involved upon treatment of the two compounds. The effects of TPA and EBC-46 individually on tumors were very different from each other. EBC-46 has proved to be efficacious on tumors *in vivo* compared to TPA. Hence, studying the pathways activated by EBC-46 at 4 h and 8 h after treatment showed significant up-regulation of pathways involved in inflammation: interferon pathways, IL-1, JAK/STAT pathways all of which clearly indicate the involvement of the immune system in the activity of EBC-46 on tumors. The top 20 canonical pathways identified following treatment for 4 hr and 8 hr with 30 µg of EBC-46 (Tables 6.11 and 6.12) and TPA (Tables 6.13 and 6.14) are listed.

The IPA Upstream Regulator Analysis was used to predict which upstream regulators were activated or inhibited to explain the pattern of significantly up- or down-regulated gene expression. A Z-activation score was statistically calculated at ≥ 2.0 to evaluate the known targets of upstream regulators and the predicted direction of change in gene expression by comparing the target's actual

Table 6.11 List of top twenty Canonical Pathways identified following Ingenuity Pathway Analysis of the Sk-Mel-28 tumors in response to 30 µg of EBC-46 after 4 hr of treatment.

Ingenuity Canonical Pathways	-log(p-value)	Ratio
LPS/IL-1 Mediated Inhibition of RXR Function	2.72E+00	7.76E-02
TNFR2 Signaling	2.20E+00	1.47E-01
Lactose Degradation III	1.98E+00	2.86E-01
Interferon Signaling	1.95E+00	1.39E-01
Induction of Apoptosis by HIV1	1.88E+00	1.04E-01
Activation of IRF by Cytosolic Pattern Recognition Receptors	1.84E+00	9.46E-02
TNFR1 Signaling	1.82E+00	1.11E-01
Role of JAK1, JAK2 and TYK2 in Interferon Signaling	1.74E+00	1.43E-01
Dermatan Sulfate Biosynthesis (Late Stages)	1.51E+00	1.04E-01
Retinoic acid Mediated Apoptosis Signaling	1.42E+00	8.22E-02
Chondroitin Sulfate Biosynthesis (Late Stages)	1.40E+00	9.09E-02
Thiamin Salvage III	1.37E+00	2.00E-01
4-hydroxybenzoate Biosynthesis	1.37E+00	5.00E-02
4-hydroxyphenylpyruvate Biosynthesis	1.37E+00	2.00E-01
D-myo-inositol (1,3,4)-trisphosphate Biosynthesis	1.33E+00	1.20E-01
TWEAK Signaling	1.28E+00	1.03E-01
Heparan Sulfate Biosynthesis (Late Stages)	1.26E+00	8.06E-02
Agrin Interactions at Neuromuscular Junction	1.16E+00	8.57E-02
Chondroitin Sulfate Biosynthesis	1.14E+00	6.94E-02
Neuregulin Signaling	1.13E+00	6.73E-02

Table 6.12 List of top twenty Canonical Pathways identified following Ingenuity Pathway Analysis of the Sk-Mel-28 tumors in response to 30 µg of EBC-46 after 8 hr of treatment.

Ingenuity Canonical Pathways	-log(p-value)	Ratio
Polyamine Regulation in Colon Cancer	3.05E+00	1.67E-01
Fatty Acid β-oxidation III (Unsaturated, Odd Number)	2.43E+00	4.00E-01
Antigen Presentation Pathway	2.07E+00	1.19E-01
Factors Promoting Cardiogenesis in Vertebrates	1.92E+00	8.16E-02
Pyrimidine Deoxyribonucleotides De Novo Biosynthesis I	1.92E+00	8.82E-02
Mechanisms of Viral Exit from Host Cells	1.88E+00	1.11E-01
UDP-N-acetyl-D-galactosamine Biosynthesis I	1.45E+00	3.33E-01
Histidine Degradation VI	1.41E+00	1.00E-01
Role of CHK Proteins in Cell Cycle Checkpoint Control	1.34E+00	8.47E-02
Thyroid Cancer Signaling	1.28E+00	9.09E-02
Sulfate Activation for Sulfonation	1.16E+00	1.25E-01
CTLA4 Signaling in Cytotoxic T Lymphocytes	1.15E+00	6.25E-02
Acute Phase Response Signaling	1.13E+00	5.52E-02
TGF-β Signaling	1.13E+00	6.67E-02
Intrinsic Prothrombin Activation Pathway	1.12E+00	8.11E-02
Choline Biosynthesis III	1.12E+00	9.09E-02
GABA Receptor Signaling	1.10E+00	7.14E-02
Fatty Acid β-oxidation I	1.08E+00	6.67E-02
Ethanol Degradation II	1.05E+00	6.98E-02
Telomere Extension by Telomerase	1.01E+00	1.11E-01

Table 6.13 List of top twenty Canonical Pathways identified following Ingenuity Pathway Analysis of the Sk-Mel-28 tumors in response to 30 µg of TPA after 4 hr of treatment.

Ingenuity Canonical Pathways	-log(p-value)	Ratio
LXR/RXR Activation	2.06E+00	3.60E-02
Role of CHK Proteins in Cell Cycle Checkpoint Control	1.71E+00	5.08E-02
Flavin Biosynthesis IV (Mammalian)	1.68E+00	1.25E-01
Glycerol-3-phosphate Shuttle	1.68E+00	1.11E-01
Mitotic Roles of Polo-Like Kinase	1.57E+00	4.05E-02
Thyroid Hormone Metabolism II (via Conjugation and/or Degradation)	1.53E+00	3.77E-02
Acute Phase Response Signaling	1.52E+00	2.76E-02
Thyronamine and Iodothyronamine Metabolism	1.51E+00	7.69E-02
Methionine Salvage II (Mammalian)	1.51E+00	1.11E-01
Thyroid Hormone Metabolism I (via Deiodination)	1.51E+00	7.69E-02
Triacylglycerol Biosynthesis	1.34E+00	4.35E-02
AMPK Signaling	1.33E+00	2.22E-02
Cardiac β-adrenergic Signaling	1.31E+00	2.53E-02
Glycerol Degradation I	1.29E+00	8.33E-02
Citrulline-Nitric Oxide Cycle	1.29E+00	6.25E-02
Cell Cycle Regulation by BTG Family Proteins	1.29E+00	5.13E-02
tRNA Splicing	1.29E+00	4.35E-02
Antigen Presentation Pathway	1.27E+00	4.76E-02
MIF Regulation of Innate Immunity	1.19E+00	3.85E-02
Tryptophan Degradation to 2-amino-3-carboxymuconate Semialdehyde	1.15E+00	5.56E-02

Table 6.14 List of top twenty Canonical Pathways identified following Ingenuity Pathway Analysis of the Sk-Mel-28 tumors in response to 30 µg of TPA after 8 h of treatment.

Ingenuity Canonical Pathways	-log(p-value)	Ratio
Signaling by Rho Family GTPases	2.53E+00	8.78E-02
IL-8 Signaling	2.32E+00	8.44E-02
RhoGDI Signaling	2.26E+00	8.96E-02
Ephrin A Signaling	1.86E+00	1.30E-01
2-ketoglutarate Dehydrogenase Complex	1.79E+00	2.22E-01
Ephrin B Signaling	1.78E+00	1.10E-01
GADD45 Signaling	1.77E+00	1.67E-01
DNA damage-induced 14-3-3σ Signaling	1.77E+00	1.82E-01
Germ Cell-Sertoli Cell Junction Signaling	1.71E+00	8.88E-02
G Beta Gamma Signaling	1.70E+00	8.26E-02
IL-1 Signaling	1.61E+00	9.17E-02
Lymphotoxin β Receptor Signaling	1.60E+00	1.13E-01
Cell Cycle: G2/M DNA Damage Checkpoint Regulation	1.57E+00	1.22E-01
Agrin Interactions at Neuromuscular Junction	1.56E+00	1.14E-01
Regulation of Actin-based Motility by Rho	1.49E+00	9.89E-02
TCA Cycle II (Eukaryotic)	1.48E+00	9.76E-02
Actin Cytoskeleton Signaling	1.45E+00	7.44E-02
Ceramide Degradation	1.42E+00	1.43E-01
IL-17A Signaling in Fibroblasts	1.41E+00	1.25E-01
Paxillin Signaling	1.41E+00	8.55E-02

direction of change in the dataset to expectations derived from the literature (Chen *et al.*, 2013).

Similarly, functional analysis of the top 20 pathways involved and the upstream regulator analysis of gene expression relative to the host response to EBC-46 or TPA, as well as the specific cellular response of human PBMCs to the effect of either diterpene esters have been included in the Appendix (298-301). Analysis of the canonical pathways regulated by EBC-46 or TPA did not result in any significant correlation between the differentially expressed genes to the canonical pathways at any of the time points which may indicate a rapidly changing gene expression.

6.3 Discussion

The results in the previous Chapters established that treatment of tumors *in vivo* with 30 µg of EBC-46 delivered as 50 µl of 600 µg/ml led to tumor ablation with the induction of a host innate immune response. In this Chapter the molecular pathways involved for the phenotypic changes induced by treatment with EBC-46 were investigated in comparison to TPA using changes in gene expression specific for either mouse or human sequences. As expected for the rapid tumor ablation described in earlier Chapters, RNA yield dropped rapidly after treatment and transcriptional responses were likely to be changing rapidly and skewed towards the remaining survivors at the particular time point assayed. Nevertheless some useful pointers emerged from the analysis and could be followed up. In an attempt to model lymphocyte responses to non-toxic levels of drug, transcriptional changes were also followed in human PBMCs treated in culture; this also enabled some of the cytokine responses to be compared with the cytokines released as protein (*Chapter Five*).

Human tumor genes differentially regulated in response to treatment with EBC-46

The one group of genes that was strikingly up-regulated (>10X) at all early time points by EBC-46 but not by TPA: small nucleolar RNAs (snoRNAs). SNORD3A is also known as RNU3, U3; SNORD3C as U3-3 and SNORD3D as U3-4. SnoRNAs are a class of small RNA molecules that primarily guide post-transcriptional modifications of cellular RNAs. Post-transcriptional modification in eukaryotic cells is a process by which precursor messenger RNA (pre-mRNA) is converted to mature messenger RNA (mRNA) by splicing of the introns which are non-coding

sections of the primary transcript RNA. There are two classes of snoRNAs, the C/D box snoRNAs, which are associated with methylation and the H/ACA box snoRNAs which are involved in pseudouridylation. snoRNAs are non-coding RNAs which are transcribed by RNA Pol II, which in turn are required for the maturation of pre-RNAs (Kiss, 2002). There is evidence in the literature that protein kinase C phosphorylates RNA Pol II through a reaction which is calcium and phospholipid dependent. Phosphorylation by PKC was shown to increase the downstream rate of RNA synthesis. This suggested a mechanism by which gene expression can be regulated by PKC (Chuang *et al.*, 1987), in this situation associated with necrosis.

Genes differentially regulated by the host in response to treatment with EBC-46 but not by TPA

The murine host response to EBC-46, *supplemented in part by the human PBMC response in vitro*, demonstrated an increased involvement of the host innate immune system with significant expression of cytokines and other pro-inflammatory molecules. An evaluation of the gene lists obtained from the microarray analysis (Appendix) showed differential gene expression of the following genes of interest:

Cxcl1: Cytokine belonging to the chemokine family and was previously called GRO1 oncogene, Neutrophil-activating protein 3 (NAP-3). This gene is expressed in macrophages, neutrophils and epithelial cells (Becker *et al.*, 1994, Iida and Grotendorst, 1990) and has neutrophil chemoattractant activity (Moser *et al.*, 1990, Schumacher *et al.*, 1992).

Gja1: encodes the Gap junction alpha-1 protein. The encoded protein interacts with MAPK7/ERK5 of the MAPK pathway family which is essential for endothelial cell function (Roberts *et al.*, 2009, Roberts *et al.*, 2010). It is interesting to note that the immunohistochemical results from *Chapter Four* show that endothelial cells are reduced in number following EBC-46 treatment, as indicated by CD-31 staining.

Defb6: Beta defensins are mammalian defensins which are antimicrobial peptides involved in the resistance of epithelial surfaces to microbial migration. Beta defensin genes are responsible for the production of antimicrobial peptides found in leukocytes such as neutrophils, macrophages and NK-cells and are also found in epithelial cells (Ganz, 2003).

Ly6g6c: The *Ly6g6c* gene belongs to a cluster of leukocyte antigen-6 (LY6) gene located in major histocompatibility complex (MHC) class III region on chromosome 6. It is also known as G6c, C6orf24, NG24. Most of the LY6 proteins are attached to the cell surface by a glycosylphosphatidylinositol (GPI) anchor which is directly involved in signaling transduction (Mallya *et al.*, 2002).

Ccl4: also known as Macrophage inflammatory protein-1*β* (MIP-1*β*) is a chemoattractant for NK-cells, monocytes and other immune cells (Bystry *et al.*, 2001). It interacts with CCL3/MIP-1*α* which is involved in the recruitment and activation of granulocytes (Wolpe *et al.*, 1988).

Ncf1: The Neutrophil cytosolic factor 1 protein encoded by *Ncf1* is a 47 kDa cytosolic subunit of neutrophil NADPH oxidase and is also called p47. The phosphorylated form of p47 plays a role in the respiratory burst of neutrophils (el Benna *et al.*, 1994, El Benna *et al.*, 1996).

Ifi27: Interferon, alpha-inducible protein 27 is involved in epithelial proliferation and is a marker for cancer (Suomela *et al.*, 2004).

Genes differentially regulated in human PBMCs in vitro by treatment with EBC-46 but not by TPA

Treatment of human PBMCs *in vitro* with 30 ng/ml of EBC-46 resulted in up-regulation within 4 hr of cytokines and other molecules involved in immune regulation such as *IL28RA*, *IL1F5*, *MMP19*, *MAPKAP1* and *CSF1* increased by 24 hr though none of these genes were consistently expressed at all time-points. Among genes encoding cytokines, some of the other genes of interest from those catalogued in the Appendix.

MMP19: Matrix metalloproteinase-19 is a matrix metalloproteinase gene which is involved in the breakdown of the extracellular matrix. MMPs are known to be involved in the release of apoptotic ligands, cleavage of cell surface receptors and cytokine/chemokine activation/inhibition. Apart from cell proliferation, migration and apoptosis, they are also considered to play a role in immune defense mechanisms.

MAPKAP1: is a mitogen-activated protein kinase which encodes a protein similar to the yeast *SIN1* protein which is a stress-activated protein kinase.

CSF1: Macrophage colony stimulating factor-1 is a cytokine which influences the proliferation, differentiation and survival of monocytes and macrophages (Stanley *et al.*, 1997).

The expression of some potentially relevant cytokines is shown in Table 6.15, a stronger and/or more prolonged response being found for several cytokines induced by EBC-46 compared with TPA.

Table 6.15 Expression levels of Cytokines in PBMC microarray data upon treatment with 30 ng/ml TPA or EBC-46 at varying times, relative to controls

	Treatment (hr)		
	4	24	96
IL-1alpha			
46	1+	15	1
TPA	1	6	1
IL-1beta			
46	1	26	1
TPA	2.6	15	0.25
IL6			
46	1	33	1
TPA	1	29	1
IL-8			
46	1	18	1
TPA	2.4	19	0.4
IL-9			
46	1	1	3.7
TPA	1	1	1

+ Ratios >0.5 and <2.0 were assigned the control value of 1.

Conclusion

From the experimental data in *Chapter Four*, it was clear that EBC-46 was efficacious in treating tumors in mice compared to TPA. This may be due to the strong host inflammatory response upon intratumoral delivery of the drug as shown in *Chapter Five*. The results from the expression profiling of the tumor and the host response after treatment of human tumor Sk-Mel-28 xenografts in BALB/c *Foxn1*^{nu} mice with EBC-46 in this chapter, may further support the results of the previous chapters. These results indicate that EBC-46 may induce recruitment of the host immune response in curing tumors in mice. Analysis of the expression profiles following treatment revealed an up-regulation of pro-inflammatory markers, as predicted by the structure of EBC-46, and also showed an up-regulation of some cytokines which were validated by protein assays as shown in *Chapter Five* (Sections 5.2.3 and 5.2.4 on p.155 & 158-163). The profiles were then further examined by pathway analysis. However, functional analysis of gene expression patterns using IPA did not give any clear indication of any strongly regulated canonical pathway following EBC-46 treatment; nor was there much of an overlap between the time points. The same was also demonstrated by the Venn diagram analysis, where differential gene expression in PBMCs treated with EBC-46 or TPA did not result in significant pathways regulated by EBC-46 treatment.

Interestingly, EBC-46 treatment resulted in constant up-regulation of snoRNAs (small nucleolar RNAs) in Sk-Mel-28 tumors throughout the treatment period. snoRNAs are non-protein-coding RNAs whose main function is to guide site-specific rRNA modifications. Several functions have been tentatively attributed to transcripts of snoRNAs such as being regulators of stress responses including oxidative and metabolic stress (Cohen *et al.*, 2013, Michel *et al.*, 2011). However, these are mostly uncharacterized genes, hence there was no connection found between the EBC-46 – differentially regulated genes in tumors and the canonical pathways obtained through the Ingenuity Pathway Analysis (IPA) software. The mechanism of action of EBC-46 is hypothesized to involve the expression of *SNORD3* because oxidative and ER stress are known to result in cell death (Aoshiba and Nagai, 2003, Choi *et al.*, 2009, Han *et al.*, 2013). To validate the microarray results in Section 6.2.1, expression levels of *SNORD3* could be examined in control and treated tumors by real-time PCR. To further understand the pathways involved in the antitumor activity of EBC-46 and the correlation with snoRNA regulation, over-expression of *SNORD3* would need to be induced to determine its involvement on tumor growth inhibition in relation to EBC-46.

In summary the results provide a novel insight into the gene expression profile induced by EBC-46 in comparison to TPA, notably in the context of *in vivo* treatment where profiling of the tumor site with mouse and human-specific arrays allowed tumor and host responses to be distinguished from each other.. The gene expression changes brought about in the tumor and the host as well as the specific cellular response of human PBMCs from treatment with the diterpene ester EBC-46 in comparison to TPA were determined. There was consistent up-regulation of snoRNAs in the tumor, which facilitate post-translational modifications occurring with EBC-46 from the earliest time after intratumoral injection up to 8 hr but not with TPA. In addition, the host response to treatment with EBC-46 indicated activation of some components of the host immune system, with potential for enhancing the antitumor activity of EBC-46 in mice. These observations of the host response to EBC-46 (Table 6.15) were consistent with the gene expression profile of human PBMCs (primarily B- and T-cells) suggesting the ability of EBC-46 to up-regulate proinflammatory cytokines that can recruit and activate neutrophils and macrophages to the site of infection. The results therefore provided molecular leads for understanding EBC-46 action in the complex tumour-host situation, as well as for probing the lack of efficacy of the more potent PMA.

Chapter Seven

Conclusions & Future Directions

7.1 Protein kinase C (PKC) as a therapeutic target for cancer.

Protein kinase C has attracted considerable research attention since its discovery. PKC is a serine-threonine protein kinase C family activated by calcium and phospholipids which include twelve isoforms sub-classified into 4 classes; classical, novel, atypical and distant. The protein kinase C isoforms are physiologically activated by 1,2-diacylglycerol (DAG) by binding to the C1 domain of the enzyme. Activated PKCs are involved in a number of cellular functions such as cell proliferation, cell cycle progression, differentiation, cytoskeletal remodelling and apoptosis (Dekker *et al.*, 1995, Olson *et al.*, 1993).

Previously, PKC inhibitors have been used to treat cancers. Some common PKC inhibitors used in cancer therapy are PKC412, Go6976, LY317615, UCN-01/02 (Masur et al., 2001, Seynaeve et al., 1993a). These compounds have been shown to either decrease invasion of tumor cells or inhibit angiogenesis. PKC inhibitors PKC412 and UCN-01 have been tested in Phase I-III studies in human clinical trials. However, as they bind strongly to plasma proteins, there was limited bioavailability thus resulting in poor clinical effects. As a result, and with the knowledge that PKCs have many and different functions within the cell, research interest has widened to include PKC activators such as phorbol ester TPA, Bryostatin-1 and PEP005 (ingenol-3-angelate).

The affinity of PKCs to bind with phorbol esters and be subsequently activated proved to be of significance in understanding the intracellular signal transduction systems (Blumberg, 1988). Phorbol esters initially became the object of research interest as a result of their potency as skin tumor promoters (Fisher and Morgan, 1994, Boutwell, 1974). Phorbol esters are PKC activators which compete with DAG for the C1 binding domain of PKC isoforms. Recently PKC activators have received attention as more favourable anti-cancer agents to PKC inhibitors. The prototypic PKC activator TPA (12-O-tetradecanoylphorbol-13-acetate) has been established to induce cytotoxic effects on cancer cells (Hofmann, 2001). TPA has also been trialed systemically on humans for the treatment of myeloid leukaemia with positive results showing complete or partial remission of cancer cells and also resulted in an increase of depressed count of white blood cells and neutrophils in chemotherapeutic patients (Han *et al.*, 1998 (ii), Han *et al.*, 1998 (i)). Previously in this laboratory another PKC

activator had been studied. PEP005 (ingenol 3-angelate; Ing3A), derived from *Euphorbia peplus* sap, was shown to cure mice of subcutaneous tumors with the induction of a host inflammatory reaction following topical application of this drug (Challacombe *et al.*, 2006). PEP005 had also shown efficacy for melanoma models in pre-clinical studies with the disruption of the mitochondria and plasma membrane leading to primary necrosis (Ogbourne *et al.*, 2004). A 2010 Phase III trial of PEP005 in gel formulation successfully reached a primary clinical endpoint of complete clearance of actinic keratosis in non-head locations (Pharma, 2010). Depending on the tumor type, PKC may be a good target for inhibition or activation.

7.2 The cytotoxic profile of EBC-46 on tumor cell lines *in vitro*

QBiotics, a sister concern of EcoBiotics Pty Ltd, located in North Queensland, Australia recently discovered another compound of the same class as TPA and PEP005, named EBC-46 (12-tigloyl/angeloyl-13-(2-methylbutanoyl)-6,7-epoxy-4,5,9,12,13,20-hexahydroxy-1-tigliaen-3-one). Upon discovery it has been clinically tested on larger animals such as dogs, cats and horses resulting in more than 80% successful treatment of the various solid tumors. Elucidation of the structure of EBC-46, revealed similarities to the prototype PKC activator TPA, where both compounds shared a similar polycyclic backbone (Figure 3.1). We initially aimed to establish the bioactivity profile of the compound EBC-46 and determine its PKC activating ability. Preliminary studies on the effect of EBC-46 on melanoma cells *in vitro* demonstrated the bipolar transformation of MM96L melanoma cells upon treatment with the compound. This morphological change is an indication of PKC activity.

The evidence provided in *Chapter Three* confirmed PKC as a target for EBC-46 as it demonstrated that EBC-46 translocated PKC isoforms with a C1 domain, namely the classical and novel PKCs, as effectively as TPA. Translocation of PKC isoforms, particularly –β, was detected from the cytosol to the plasma membrane or other subcellular organelles such as the Golgi apparatus or mitochondria. An important difference between TPA and EBC-46 was the selective translocation of PKC isozymes. While TPA led to efficient

translocation of -α, -β_1, -β_2, -γ and –θ isoforms expressed in HeLa cells; EBC-46 demonstrated more specificity for PKC-β, while PKC-α and –γ were less efficiently translocated possibly to nuclear/perinuclear regions. The differences in the subcellular localization of PKC isoforms may result in differences in substrate specificity thereby determining the downstream biological responses.

Activation of PKC isoforms and their subsequent involvement in the MAPK pathway was confirmed by western blot analysis on B16-F0 mouse melanoma and Sk-Mel-28 human metastatic melanoma when treated with 1 µg/ml of TPA or EBC-46 following pre-treatment with 5 µM BIS-1 (pan PKC inhibitor) for 1 hr. B16-F0 cells once again established the strong expression of PKC-α as seen previously (Oka and Kikkawa, 2005, Rosenbaum and Niles, 1992) while human metastatic melanoma Sk-Mel-28 established the activation of PKC isoforms -α, -δ, -ε, -θ and -ι (Figure 3.4) where there was high expression of α and δ in intact cells that lowered in expression levels upon treatment with the diterpene esters. Results of *Chapter Three* indicated the involvement of PKC activity in cell signaling where pre-treatment with the pan PKC inhibitor BIS-1 greatly lowered the activation of the MAPK pathway.

As shown in *Chapter Three*, activation of neutrophils by EBC-46 provided a molecular basis for PKC-dependent activation of the innate immune system by very low doses of TPA or EBC-46. In intact cells phorbol esters lead to activation of NADPH oxidase enzyme, the prime catalyst for this process which is brought about by the protein phosphorylation and its translocation to the plasma membrane (Cox *et al.*, 1985). EBC-46 was found to be equally potent in inducing the production of ROS as TPA, at an optimal dose of 100 ng/ml (Figure 3.6) which was inhibited upon pre-treatment with BIS-1 thus confirming the role of PKC activation.

The preliminary studies looking at the effect of EBC-46 on MM96L melanoma cells *in vitro* also indicated a cytotoxic effect of the compound on cancer cells. To further analyze this effect, tumor cells of human and mouse origin were subjected to treatment with EBC-46 and TPA where growth inhibition of melanoma cell lines was obtained at an IC_{50} of $\leq$ 30 µg/ml of both diterpene esters. Other cancer cell lines assayed were derived from lung and blood, were

more sensitive to treatment with either diterpene ester where the cytotoxic effect of EBC-46 was achieved at ~ 10 ng/ml. Comparison of the diterpene esters showed that TPA was more potent than EBC-46 *in vitro* resulting in approximately 10-fold difference in cytotoxicity which may be attributed to the differences in cell type, growth rates, sensitivity to the drug and metastatic nature of the cells. Diterpene ester sensitivity appeared to be increased with over-expression of PKC isoforms in melanoma cell lines. However this observation is arguable as the control *lacZ* showed increased sensitivity to EBC-46. Despite the increased sensitivity of the *lacZ* controls to growth inhibition by EBC-46 or TPA, the additional increase in sensitivity in the two cell lines (Sk-Mel-28 and D04) shown in Figure 3.9 of *Chapter Three* where PKC isoforms α and δ were over-expressed, indicate that the compounds activate PKC.

7.3 The efficacy of EBC-46 in mouse tumor models

Preliminary work with this compound *in vivo* suggested the possibility of the involvement of the innate immune response upon activation of PKC. *Chapter Three* provided evidence for the same, demonstrating the ability of EBC-46 to activate neutrophils to produce reactive oxygen species (ROS) via a PKC-dependent process. The potential anti-tumor activity and efficacy of EBC-46 on pre-clinical tumor models *in vivo* including melanoma and non-melanomas was determined.

Mice were subcutaneously inoculated with tumor cells injected at two sites per mouse. A comparison between a single intralesional injection of 30 µg of EBC-46 and 30 µg of TPA resulted in EBC-46 being more potent *in vivo* with 75% cures of B16-F0 tumors in C57BL/6J mice while TPA failed to cure tumors in mice resulting in relapses at all treated sites (Figure 4.1). Topical application of TPA compared to PEP005 in previous studies demonstrated a more efficient penetration of PEP005 through the dermis than TPA since PEP005 is a substrate for the epidermal multidrug transporter (ABCB1) (Li *et al.*, 2010).An optimal dose for treatment of tumors approximately 100 mm^3 in volume was determined by comparing two treatment groups 10 µg versus 30 µg of EBC-46 against the control vehicle 20% PG

treatment where 30 µg of BEC-46 effectively cured 75% of the tumors. The cure rate was calculated based on cure at each tumor site where the remaining 25% signifies the 5 relapsed tumor sites out of the 20 treated (Figure 4.3).

Similarly, EBC-46 on human melanoma xenografts Sk-Mel-28 in BALB/c *Foxn1*^{nu} mice resulted in approximately 88% cure with total loss of tumor cells after 24 hr of treatment. There was an inflammatory reaction observed immediately after injection, which was more prominent on the hairless nude mice (BALB/c *Foxn1*^{nu}). This reaction lead to the development of an eschar by day 13 which detached by day 20 after treatment. Phorbol ester TPA is known to be a skin irritant and inflammatory agent that induces prompt remodelling of the vasculature, resulting in edema formation (Janoff *et al.*, 1970). A similar outcome was noted upon topical application of PEP005 for treatment of a range of tumors where neutrophils were identified as the major infiltrate playing a central role in preventing relapse through a mechanism known as antibody-dependent cell-mediated cytotoxicity (ADCC) (Challacombe *et al.*, 2006, Ogbourne *et al.*, 2004).

As demonstrated in *Chapter Three*, over-expression of PKC isoforms in B16-F0 tumor cells did not significantly increase their sensitivity to treatment with EBC-46 *in vitro* reflecting a similar result *in vivo* when 30 µg of EBC-46 was used to treat B16-F0 tumors over-expressing PKC isoforms -α and –δ. The volume of tumor inoculum in relation to volume of diterpene ester injected into the tumor was also investigated as a possible determinant of anti-tumor efficacy which demonstrated that the smaller inoculums of tumor cells (Figures 4.5; A & B and Figure 4.9) responded positively to treatment with a single intratumoral injection 50 µl of 600 µg/ml of EBC-46, suggesting that a larger tumor volume may require a larger volume of the drug to cover the wider target area.

Apart from melanoma tumor models the efficacy of EBC-46 was tested on non-melanoma tumors, namely MC38 which is a mouse colon cancer. Similar to results obtained with treatment of 30 µg of EBC-46 on B16-F0 and Sk-Mel-28 tumors, MC38 tumor cell responded positively to the activity of EBC-46 resulting in 80% of total ablation of tumor cells with only 2 recurrences. This was most likely due to the growth of tumor cells deep below the skin in the muscle which may have occurred at the time of inoculation. Hence,

EBC-46 showed efficacy in ablating different types of tumors based on species of origin and type of tumor.

7.4 Is the efficacy of EBC-46 dependent on its pro-inflammatory properties?

The first indication of the link between inflammation and cancer was observed by Rudolf Virchow in the 19th century. The *in vivo* efficacy studies in *Chapter Four* resulted in a marked inhibition of growth of tumor cells with a clinical outcome of initial inflammation, followed by eschar development and eventual healing. Despite the differences in tumor types and growth rates and morphology, there was similar significant regression of tumor growth following treatment with a single intralesional injection of 30 µg of EBC-46. The rapid inflammatory reaction was visible as early as 2 hr after injection and either as a primary response or through a secondary mechanism resulted in clearance of tumors by day 20.

From the histological results in *Chapter Five* it became clear that the predominant infiltrating cells into the EBC-46 – treated tumor were the peripheral blood mononuclear cells (PBMCs) or neutrophils and macrophages. Apart from these cells there was sparse presence of other immune cells such as mast cells (data not shown). Generally neutrophils exist to defend the host from invading pathogens and also assist in wound healing. Neutrophils are the most abundant leukocytes in the blood stream though they have very short life, which lasts for a few hours but survive longer under inflammatory conditions. Their release of soluble chemotactic factors changes the tumor microenvironment thus guiding the recruitment of immune effector cells (Di Carlo *et al.*, 2001). However, other studies have indicated that the presence of granulocytes can result in tumor promotion with the release of cytokines and other inflammatory mediators (Coussens and Werb, 2001).

There was no substantial expression of cytokines in mouse serum or the supernatants of treated tumor because the vascular damage leading to hemorrhagic necrosis cut off the circulating lymphocytes from exposure to significant concentrations of the drug. The only cytokines expressed above the accepted detection limit of < 10 pg/ml were MCP-1 and IL-6. However an *in vitro* co-culture of tumor cells in the presence of PBMCs and treated with 100

ng/ml EBC-46 resulted in high expression of cytokines that increased with time. Cytokine expression was shown to be greatly increased from 4-24 hr following treatment of tumor cells with EBC-46 *in vitro* when co-cultured with PBMCs resulting in high expression of IL-1β, IL-8, IL-6 and TNF-α which correlated with the histological observation of increased neutrophils and macrophages.

These results indicated the importance of neutrophils in the activity of EBC-46. However, it was not clear whether EBC-46 required neutrophils or another immune response for its cytotoxic response on cancer cells, or whether it resulted in the direct cytotoxic effect on the cells and neutrophils were a secondary response to the tissue necrosis. To understand the requirement of neutrophils in the efficacy of EBC-46, peripheral neutrophils were depleted with a neutralizing antibody. There was an obvious clinical difference among the control EBC-46 treated group and the EBC-46 – treatment group which received the antibody Ly-6G. The group depleted of neutrophils had a greater number of persisting tumors or a faster recurrence rate while those that received only EBC-46 were totally ablated of tumors by days 5-6.

7.5 Mechanism of action of EBC-46 *in vitro*

The mechanism of action of EBC-46 raises the question whether the compound has a direct cytotoxic effect on the cells with a secondary immune response or induces an immune response which results in its cytotoxic effect on tumor cells. There is support for the first theory of a direct cytotoxic effect of EBC-46 on tumor cells in culture. Tumor cell lines treated *in vitro* with high doses of either TPA or EBC-46 resulted in rapid killing of cells from as quickly as 30 min after treatment. More so, this effect is most likely a PKC-dependent process which was established with the use of BIS-1 (a pan-PKC inhibitor). Histological analysis of the EBC-46 – treated tumors showed a decrease in the presence of endothelial cells with prolonged exposure to the compound supporting the observation of lack of blood pockets with the tumor by 4 hr after treatment leading to hemorrhagic necrosis and eventual tumor destruction. The *in vitro* results from high dose killing of HUVEC cells (data

not shown) further supported the hypothesis of endothelial and tumor destruction resulting in rapid killing of tumor cells *in vivo* in the dose range of 600 µg/ml administered intratumoraly.

It was hypothesized that the cytotoxic activity of EBC-46 caused the rupture of the plasma membrane with subsequent organelle destruction. High concentrations of EBC-46 or TPA both resulted in necrosis at early treatment times in culture. Necrotic death results from the disruption of plasma and nuclear membrane and was identified by the loss of cellular structure and shrinkage appearing as black debris in culture plates (Figure 3.8, Panel B and C of *Chapter Three*). This loss of plasma membrane integrity was seen by the uptake of propidium iodide which provided evidence of necrosis *in vitro* when tumor cell lines were treated with high doses of EBC-46 (100 µg/ml, 200 µg/ml and 300 µg/ml) and stained with propidium iodide (Figure 4.12 of *Chapter Four*).

7.6 Mechanism of action of EBC-46 *in vivo* and significance of the host response

In contrast, there is evidence to support the second theory of the mechanism of action of EBC-46 with the stimulation of the innate immune system resulting in a cytotoxic effect on tumor cells. Infiltration of neutrophils and macrophages into the tumor microenvironment can carry out a destructive effect. The recruited PBMCs produce several cytotoxic mediators, including reactive oxygen species (ROS), proteases and soluble mediators of cell killing such as IL-1β, TNF-α, IL-8, interferon (IFN), IL-6 and MCP-1(Di Carlo *et al.*, 2001) (*Chapter Five*). Neutrophils can either directly kill tumor cells by recruiting defensins or their release of cytokines/chemokines can recruit other mediators. Defensins are reported to be the most abundant component of the primary granule present in PBMCs and are highly toxic against several types of tumors (Di Carlo *et al.*, 2001). Neutrophils can also exert their effect on tumor cells via an antibody-dependent cell mediated cytotoxicity (ADCC) (Di Carlo *et al.*, 2001, Kindzelskii and Petty, 1999) and hemorrhagic necrosis (Westlin and Gimbrone, 1993).

Neutrophils migrate out of the vascular system to the site of infection in response to inflammatory stimuli; phagocytose foreign material with the release of superoxide, and other oxygen radicals produced by the NADPH oxidase and release inflammatory cytokines ad

chemokines into the tissue. Migration and stimulation of neutrophils to the site of infection is mediated by PKC isoforms. Neutrophils are reported to express PKC-*α, -β* and *–δ* (Balasubramanian *et al.*, 1998, Bertram and Ley, 2011, Devalia *et al.*, 1992, Smallwood and Malawista, 1992). This further strengthens our findings in *Chapters Three* and *Five* which show the expression of PKCs-α, -δ and –β by EBC-46 and the host innate immune response to its activity, respectively.

Under inflammatory conditions, neutrophils and macrophages roll along the endothelium aided by mediators such as L-selectins and bind to proteins such as PSGL-1, LFA-1, Mac-1 and ICAM-1 present on endothelial cells leading to the adhesion and extravasation of the immune cells to the site of infection with the help of pro-inflammatory mediators such as TNF-α and IL-8 (reviewed by Bertram *et al.* 2011). Cytokine expression levels following exposure to EBC-46 in mouse serum and tumor supernatants were found to be enhanced for IL-6 and MCP-1 in serum and IL-1β and IL-8 in the tumor microenvironment. However, gene expression data did not reveal any significant changes in expression levels for these specific molecules except for an up-regulation of TNF receptor 12A in PBMCs treated *in vitro* by EBC-46. The most significant differentially expressed genes were small nucleolar RNAs (*SNORD3A, SNORD3C* and *SNORD3D*) which were consistently up-regulated by EBC-46. These genes are said to be involved in post-transcriptional modifications. However, they are largely uncharacterized; hence further functional pathway analysis did not reveal any involvement of significant pathways relative to these genes.

7.7 Concluding remarks and Future directions

The results presented in this thesis have demonstrated that the *in vitro* activity of EBC-46 and TPA are similar with TPA being more potent resulting in cytotoxicity of tumor cells at doses 10-fold lower than EBC-46 on certain tumor cell types. However, the same was not true for its efficacy in ablating tumors *in vivo* where EBC-46 resulted in more than 80% cure in mice. Further analysis of other MAPK pathways such as p38MAPK, JNK, PTEN, should be carried

out upon treatment with EBC-46 as phorbol esters such as TPA and PEP005 have shown to activate these molecules too in addition to the ERK1/2.

As hypothesized, it was found that EBC-46 stimulated the innate immune system of the host through PKC isoform activation. Depending on the PKC isoform activated, diterpene esters can cause either tumor cell death or differentiation (Chang and Lee, 2006). Activation of PKC-α and –δ in neutrophils and the expression of cytotoxic leukocytes results in neutrophil and macrophage recruitment. In addition the endothelial cell marker was found to gradually decrease 8 hr after treatment with EBC-46, consistent with H&E histological analysis indicating a reduction in blood supply to the tumor site. It could therefore be concluded that EBC-46 ruptures the surrounding blood capillaries leading to devascularization of the tumor microenvironment. However the exact molecular mechanism is not clear yet and requires further investigation. The inflammatory responses including the evident hemorrhaging are both significant outcomes to the treatment with EBC-46. Such pathways should be studied by testing EBC-46 in 3D cultures with or without the presences of hemorrhage pathway inhibitors. Electron microscopy of treated HUVECs, fibroblasts, skin and tumor cells should be performed to provide a better understanding of the morphological effects of EBC-46 on the tumor microenvironment and vasculature alongside the molecular analysis.

The requirement for neutrophils by EBC-46 in localized antitumor activity has been validated in Figure 5.6 of *Chapter Five* where tumor-bearing mice ablated of neutrophils were treated with EBC-46 and resulted in tumor recurrences in all mice by day 27. On the negative side, activation of neutrophils by EBC-46 that is released into the circulation could make the drug cytotoxic to the animal and thus could preclude treatment of metastasis.

Previously interaction of P-gp (P-glycoprotein 1, also known as MDR1 or ABCB1), with phorbol esters has been shown to result in disruption of the tumor vasculature. PEP005 compared to TPA was shown to be a substrate for P-gp. Hence PEP005 was better transported past the skin barrier to the tumor unlike TPA and similarly in contrast to the activity of TPA, it inhibited the function of P-gp as demonstrated by Li *et al.* in 2010. A similar inflammatory response and haemorrhaging has been observed upon intratumoral

injections with EBC-46. To further understand the mechanism of action of EBC-46 it would be worth investigating the interaction of EBC-46 with P-gp.

Bright field images of tumor cells treated with EBC-46 in comparison to TPA, showed a necrotic effect of EBC-46. Though definitive nuclear fragmentation was indistinguishable, the disruption of the cell membrane and shrinkage was clearly evident in Figure 3.8, Panel B and C of *Chapter Three*. Comparable evidence of cell death is seen in the histological sections of treated tumors stained with hematoxylin & eosin in Figure 5.3, *Chapter Five*. Immunohistological analysis as well as *in vitro* cell death indicated by the uptake of propidium iodide determines the disruption of the plasma membrane. Though the photomicrographs of propidium iodide staining did not show definitive nuclear fragmentation (Figure 4.12, *Chapter Four*), the increased uptake of PI stain with increase in concentration was evidence of plasma and nuclear membrane disruption. Electron microscopy of cells treated with the diterpene ester EBC-46 would provide further insight into the morphological effect of the compound on tumor cells which can be further analyzed at a molecular level to determine the pathways leading up to cell death. Also the cytotoxic effect of EBC-46 on intracellular organelles such as mitochondria will be further studied through EM analysis of tumor samples.

Altogether, EBC-46 was found to be an activator of PKC isoforms with a C1 binding domain, and is also efficacious in ablating tumors in mouse models of cancer. It displays a direct cytotoxic effect on tumor cells and stimulates the innate immune system resulting in tumor cell death by inflammation and hemorrhagic necrosis (Figure 7.1).

Exploration of structure/activity relationships is usually desirable for fine tuning prototype drugs. *Fontainea picrosperma,* the plant from which EBC-46 is purified, produces a wide variety of related structures that have more or less hydrophobic C-12 and C-13 esters. These could be tested for efficacy *in vivo* because of potentially improved solubility, efficacy or long term stability. The complex phorbol skeleton has yet to be synthesized *in toto*. The ingenol ester PEP005 has recently been synthesized from a simple natural starting material, but required many steps and overall yield was very poor. Collaborating chemists have been able to vary the EBC-46 ester groups by partial synthesis, providing opportunities for more

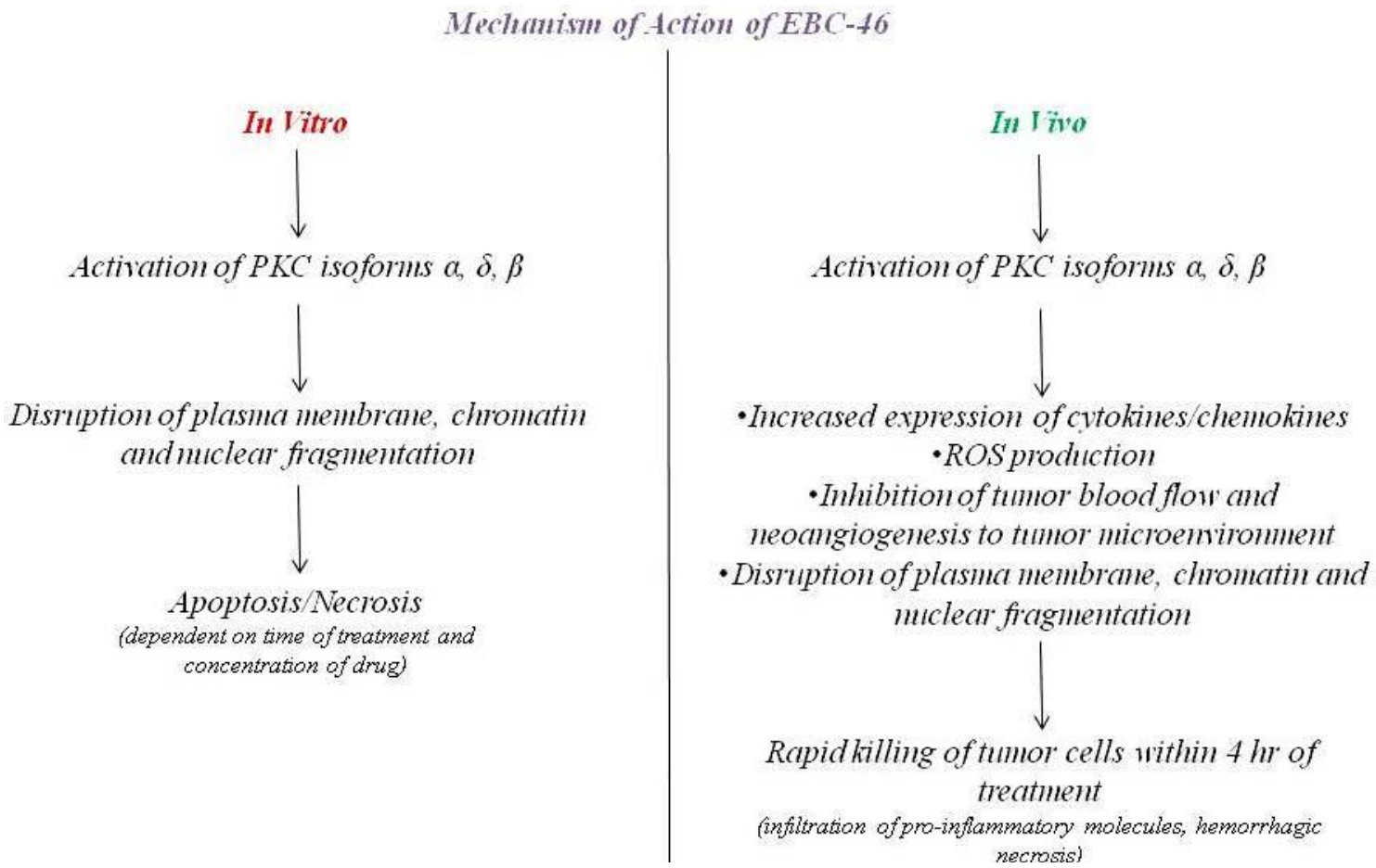

Figure 7.1 Proposed Mechanism of Action of EBC-46

Treatment with EBC-46, a PKC activator, results in rapid killing of tumor cells co-dependent on a host inflammatory response.

discoveries, but have found modification of the southern part of the molecule to be problematic. This is due to the 6-7 epoxy groups. The possibility of the epoxide reacting covalently with a highly reactive protein thiol should also be explored.

A single formulation based on propylene glycol was used in this study because the excipient dissolved EBC-46 to the required level and because it is an accepted excipient for parenteral administration. The vehicle alone had little effect on mouse tumors but the high osmolarity of propylene glycol may contribute synergistically to local vascular damage. A range of alternative solubilizing agents are available for testing such as the cyclodextrins and even human albumen.

Much was learnt during this project about the mechanism of action of EBC-46 but many questions remain unanswered, as well as for PEP005 discovered for topical treatment of tumor nearly 10 years ago. Such questions include why TPA is more effective than EBC-46 *in vitro* but less effective *in vivo*, the relative contributions of host *versus* tumor responses to efficacy, whether the proximal molecular target is a PKC isoform or some other C1 peptide bearing protein, and which of the various signaling pathways involving such molecules lead to the rapid destruction of tumors *in vivo*.

With the realization that TPA activates non-kinase proteins, the effects of TPA treatment cannot be solely attributed to PKC regulation. To address this, EBC-46 was assessed in cytotoxicity experiments against cancer cells *in vitro* in the presence of a pan-PKC inhibitor, BIS-1 where cells pre-treated with BIS-1 failed to show the cytotoxic effect of EBC-46. Another study on the roles of activation and depletion of PKC isoforms in cell lines treated for 24 hr with TPA or PEP005 at 1 µg/ml in the presence of BIS-1 showed similar results indicating the affinity of PEP005 for PKC isoforms (Cozzi et al., 2006). However, PEP005 was later shown to activate RasGRPs, which are Ras activators (Song et al., 2013). Hence, this would warrant further investigation into the downstream targets of EBC-46, other than PKC isoforms.

Bibliography

AESCHLIMANN, A. & HECKER, H. 1967. [Preliminary studies on the ulstrastructure of the ovocyte in development in Ornithodorus moubata, Murray]. *Acta Trop,* 24**,** 225-43.

AGARWALA, S. S. 2010. Novel immunotherapies as potential therapeutic partners for traditional or targeted agents: cytotoxic T-lymphocyte antigen-4 blockade in advanced melanoma. *Melanoma Research,* 20**,** 1-10.

AHN, N. G., SEGER, R., BRATLIEN, R. L., DILTZ, C. D., TONKS, N. K. & KREBS, E. G. 1991. Multiple components in an epidermal growth factor-stimulated protein kinase cascade. In vitro activation of a myelin basic protein/microtubule-associated protein 2 kinase. *J Biol Chem,* 266**,** 4220-7.

AIBA, Y., OH-HORA, M., KIYONAKA, S., KIMURA, Y., HIJIKATA, A., MORI, Y. & KUROSAKI, T. 2004. Activation of RasGRP3 by phosphorylation of Thr-133 is required for B cell receptor-mediated Ras activation. *Proceedings of the National Academy of Sciences of the United States of America,* 101**,** 16612-7.

AIHW. 2012. *Cancer in Australia: an overview, 2012* [Online]. [Accessed].

ALAM, M. & RATNER, D. 2001. Cutaneous Squamous - Cell Carcinoma. *N Engl J Med,* 344**,** 975-83.

ALVAREZ, E. 2002. B16 Murine Melanoma. *Tumor Models in Cancer Research***,** 73-89.

AOSHIBA, K. & NAGAI, A. 2003. Oxidative stress, cell death, and other damage to alveolar epithelial cells induced by cigarette smoke. *Tob Induc Dis,* 1**,** 219-26.

ARITA, Y., O'DRISCOLL, K. R. & WEINSTEIN, I. B. 1994. Growth inhibition of human melanoma-derived cells by 12-O-tetradecanoyl phorbol 13-acetate. *International journal of cancer. Journal international du cancer,* 56**,** 229-35.

ASAOKA, Y., NAKAMURA, S., YOSHIDA, K. & NISHIZUKA, Y. 1992. Protein kinase C, Calcium and Phospholipid degradation. *Trends Biochem Sci,* 17**,** 414-7.

BALASUBRAMANIAN, N., ADVANI, S. H. & ZINGDE, S. M. 1998. Protein kinase C isoforms in normal and chronic myeloid leukemic neutrophils. Distinct signal for PKC alpha by immunodetection on PVDF membrane, decreased expression of PKC alpha and increased expression of PKC delta in leukemic neutrophils. *Leukemia research,* 22**,** 597-604.

BARR, L. F., MABRY, M., NELKIN, B. D., TYLER, G., MAY, W. S. & BAYLIN, S. B. 1991. c-myc gene-induced alterations in protein kinase C expression: a possible mechanism facilitating myc-ras gene complementation. *Cancer Res,* 51**,** 5514-9.

BARSYTE-LOVEJOY, D., GALANIS, A. & SHARROCKS, A. D. 2002. Specificity determinants in MAPK signaling to transcription factors. *J Biol Chem,* 277**,** 9896-903.

BECKER, S., QUAY, J., KOREN, H. S. & HASKILL, J. S. 1994. Constitutive and stimulated MCP-1, GRO alpha, beta, and gamma expression in human airway epithelium and bronchoalveolar macrophages. *The American journal of physiology,* 266**,** L278-86.

BERRIDGE, M. J. & IRVINE, R. F. 1984. Inositol trisphosphate, a novel second messenger in cellular signal transduction. *Nature,* 312**,** 315-21.

BERTRAM, A. & LEY, K. 2011. Protein kinase C isoforms in neutrophil adhesion and activation. *Archivum immunologiae et therapiae experimentalis,* 59**,** 79-87.

BHONDE, M. R., HANSKI, M. L., MAGRINI, R., MOORTHY, D., MULLER, A., SAUSVILLE, E. A., KOHNO, K., WIEGAND, P., DANIEL, P. T., ZEITZ, M. & HANSKI, C. 2005. The broad-range cyclin-dependent kinase inhibitor UCN-01 induces apoptosis in colon carcinoma cells through transcriptional suppression of the Bcl-x(L) protein. *Oncogene,* 24**,** 148-56.

BISWAS, D. K., DAI, S. C., CRUZ, A., WEISER, B., GRANER, E. & PARDEE, A. B. 2001. The nuclear factor kappa B (NF-kappa B): a potential therapeutic target for estrogen receptor negative breast cancers. *Proc Natl Acad Sci U S A,* 98**,** 10386-91.

BISWAS, D. K., MARTIN, K. J., MCALISTER, C., CRUZ, A. P., GRANER, E., DAI, S. C. & PARDEE, A. B. 2003. Apoptosis caused by chemotherapeutic inhibition of nuclear factor-kappaB activation. *Cancer Res,* 63**,** 290-5.

BLACK, J. D. 2000. Protein kinase C-mediated regulation of the cell cycle. *Front Biosci,* 5**,** D406-23.

BLANK, J. L., GERWINS, P., ELLIOTT, E. M., SATHER, S. & JOHNSON, G. L. 1996. Molecular cloning of mitogen-activated protein/ERK kinase kinases (MEKK) 2 and 3. Regulation of sequential phosphorylation pathways involving mitogen-activated protein kinase and c-Jun kinase. *J Biol Chem,* 271**,** 5361-8.

BLUMBERG, P. M. 1988. Protein Kinase C as the receptor for the phorbol ester tumour promoters: Sixth Rhoads Memorial Award lecture. *Cancer Research,* 48**,** 1-8.

BODE, A. M. & DONG, Z. 2007. The functional contrariety of JNK. *Mol Carcinog,* 46**,** 591-8.

BOGOYEVITCH, M. A., NGOEI, K. R., ZHAO, T. T., YEAP, Y. Y. & NG, D. C. 2010. c-Jun N-terminal kinase (JNK) signaling: recent advances and challenges. *Biochim Biophys Acta,* 1804**,** 463-75.

BOULTON, T. G., NYE, S. H., ROBBINS, D. J., IP, N. Y., RADZIEJEWSKA, E., MORGENBESSER, S. D., DEPINHO, R. A., PANAYOTATOS, N., COBB, M. H. & YANCOPOULOS, G. D. 1991. ERKs: a family of protein-serine/threonine kinases that are activated and tyrosine phosphorylated in response to insulin and NGF. *Cell,* 65**,** 663-75.

BOULTON, T. G., YANCOPOULOS, G. D., GREGORY, J. S., SLAUGHTER, C., MOOMAW, C., HSU, J. & COBB, M. H. 1990. An insulin-stimulated protein kinase similar to yeast kinases involved in cell cycle control. *Science,* 249**,** 64-7.

BOUTWELL, R. K. 1974. The function and mechanism of promoters of carcinogenesis. *CRC critical reviews in toxicology,* 2**,** 419-43.

BRASH, D. E., RUDOLPH, J. A., SIMON, J. A., LIN, A., MCKENNA, G. J., BADEN, H. P., HALPERIN, A. J. & PONTEN, J. 1991. A role for sunlight in skin cancer: UV-induced p53 mutations in squamous cell carcinoma. *Proc Natl Acad Sci U S A,* 88**,** 10124-8.

BRENNER, W., FARBER, G., HERGET, T., WIESNER, C., HENGSTLER, J. G. & THUROFF, J. W. 2003. Protein kinase C eta is associated with progression of renal cell carcinoma (RCC). *Anticancer Res,* 23**,** 4001-6.

BRODIE, C., STEINHART, R., KAZIMIRSKY, G., RUBINFELD, H., HYMAN, T., AYRES, J. N., HUR, G. M., TOTH, A., YANG, D., GARFIELD, S. H., STONE, J. C. & BLUMBERG, P. M. 2004. PKCdelta associates with and is involved in the phosphorylation of RasGRP3 in response to phorbol esters. *Molecular pharmacology,* 66**,** 76-84.

BUENSUCESO, C. S., WOODSIDE, D., HUFF, J. L., PLOPPER, G. E. & O'TOOLE, T. E. 2001. The WD protein Rack1 mediates protein kinase C and integrin-dependent cell migration. *Journal of Cell Science,* 114**,** 1691-8.

BYSTRY, R. S., ALUVIHARE, V., WELCH, K. A., KALLIKOURDIS, M. & BETZ, A. G. 2001. B cells and professional APCs recruit regulatory T cells via CCL4. *Nature immunology,* 2**,** 1126-32.

CACACE, A. M., UEFFING, M., PHILIPP, A., HAN, E. K., KOLCH, W. & WEINSTEIN, I. B. 1996. PKC epsilon functions as an oncogene by enhancing activation of the Raf kinase. *Oncogene,* 13**,** 2517-26.

CAI, H., SMOLA, U., WIXLER, V., EISENMANN-TAPPE, I., DIAZ-MECO, M. T., MOSCAT, J., RAPP, U. & COOPER, G. M. 1997. Role of diacylglycerol-regulated protein kinase C isotypes in growth factor activation of the Raf-1 protein kinase. *Molecular and Cellular Biology,* 17**,** 732-41.

CAMPHAUSEN, K. A. & LAWRENCE, R. C. 2008. *Principles of Radiation Therapy*.

CANCER COUNCIL NSW 2007. Minimum Dataset for Colorectal Cancer.

CARGNELLO, M. & ROUX, P. P. 2011. Activation and Function of the MAPKs and Their Substrates, the MAPK-Activated Protein Kinases. *Microbiol Mol Biol Rev,* 75**,** 50-83.

CARTEE, L., MAGGIO, S. C., SMITH, R., SANKALA, H. M., DENT, P. & GRANT, S. 2003. Protein kinase C-dependent activation of the tumor necrosis factor receptor-mediated extrinsic cell death pathway underlies enhanced apoptosis in human myeloid leukemia cells exposed to bryostatin 1 and flavopiridol. *Mol Cancer Ther,* 2**,** 83-93.

CASTAGNA, M., TAKAI, Y., KAIBUCHI, K., SANO, K., KIKKAWA, U. & NISHIZUKA, Y. 1982. Direct activation of calcium-activated, phospholipid-dependent protein kinase by tumour-promoting phorbol esters. *The Journal of Biological Chemistry,* 257**,** 7847-7851.

CATLING, A. D., SCHAEFFER, H. J., REUTER, C. W., REDDY, G. R. & WEBER, M. J. 1995. A proline-rich sequence unique to MEK1 and MEK2 is required for raf binding and regulates MEK function. *Mol Cell Biol,* 15**,** 5214-25.

CHALLACOMBE, J. M., SUHRBIER, A., PARSONS, P. G., JONES, B., HAMPSON, P., KAVANAGH, D., RAINGER, G. E., MORRIS, M., LORD, J. M., LE, T. T., HOANG-LE, D. & OGBOURNE, S. M. 2006. Neutrophils are a key component of the antitumor efficacy of topical chemotherapy with ingenol-3-angelate. *J Immunol,* 177**,** 8123-32.

CHANG, Z. F. & LEE, H. H. 2006. RhoA signaling in phorbol ester-induced apoptosis. *Journal of biomedical science,* 13**,** 173-80.

CHELLAPPAN, S. P., GIORDANO, A. & FISHER, P. B. 1998. Role of cyclin-dependent kinases and their inhibitors in cellular differentiation and development. *Curr Top Microbiol Immunol,* 227**,** 57-103.

CHEN, X., WANG, Y., LI, Q., TSAI, S., THOMAS, A., SHIZURU, J. A. & CAO, T. M. 2013. Pathways analysis of differential gene expression induced by engrafting doses of total body irradiation for allogeneic bone marrow transplantation in mice. *Immunogenetics,* 65**,** 597-607.

CHOI, K., KIM, J., KIM, G. W. & CHOI, C. 2009. Oxidative stress-induced necrotic cell death via mitochondira-dependent burst of reactive oxygen species. *Curr Neurovasc Res,* 6**,** 213-22.

CHOU, M. M., HOU, W., JOHNSON, J., GRAHAM, L. K., LEE, M. H., CHEN, C. S., NEWTON, A. C., SCHAFFHAUSEN, B. S. & TOKER, A. 1998. Regulation of protein kinase C zeta by PI 3-kinase and PDK-1. *Curr Biol,* 8**,** 1069-77.

CHUANG, L. F., COOPER, R. H., YAU, P., BRADBURY, E. M. & CHUANG, R. Y. 1987. Protein Kianse C phosphorylates leukamia RNA polymerase II. *Biochem Biophys Res Commun,* 145**,** 1376-1383.

COHEN, E., AVRAHAMI, D., FRID, K., CANELLO, T., LEVY LAHAD, E., ZELIGSON, S., PERLBERG, S., CHAPMAN, J., COHEN, O. S., KAHANA, E., LAVON, I. & GABIZON, R. 2013. Snord 3A: a molecular marker and modulator of prion disease progression. *PLoS One,* 8**,** e54433.

COPPOCK, D. L., BUFFOLINO, P., KOPMAN, C. & NATHANSON, L. 1995. Inhibition of the melanoma cell cycle and regulation at the G1/S transition by 12-O-tetradecanoylphorbol-13-acetate (TPA) by modulation of CDK2 activity. *Exp Cell Res,* 221**,** 92-102.

CORBETT, T. H., POLIN, L., ROBERTS, B. J., LAWSON, A. J., LEOPOLD, W. R., WHITE, K., KUSHNER, J., PALUCH, J., HAZELDINE, S., MOORE, R., RAKE, J. & HORWITZ, J. P. 2002. Transplantable Syngeneic Rodent Tumors. *Tumor Models in Cancer Research***,** 41-71.

COUSSENS, L. M. & WERB, Z. 2001. Inflammatory cells and cancer: think different! *The Journal of experimental medicine,* 193**,** F23-6.

COX, J. A., JENG, A. Y., SHARKEY, N. A., BLUMBERG, P. M. & TAUBER, A. I. 1985. Activation of the human neutrophil nicotinamide adenine dinucleotide phosphate (NADPH)-oxidase by protein kinase C. *The Journal of clinical investigation,* 76**,** 1932-8.

COZZI, S. J., PARSONS, P. G., OGBOURNE, S. M., PEDLEY, J. & BOYLE, G. M. 2006. Induction of senescence in diterpene ester-treated melanoma cells via protein kinase C-dependent hyperactivation of the mitogen-activated protein kinase pathway. *Cancer Res,* 66**,** 10083-91.

CREWS, C. M., ALESSANDRINI, A. & ERIKSON, R. L. 1992. The primary structure of MEK, a protein kinase that phosphorylates the ERK gene product. *Science,* 258**,** 478-80.

DAHLGREN, C. & KARLSSON, A. 1999. Respiratory burst in human neutrophils. *J Immunol Methods,* 232**,** 3-14.

DAHLGREN, C., KARLSSON, A. & BYLUND, J. 2007. Measurement of respiratory burst products generated by professional phagocytes. *Methods Mol Biol,* 412**,** 349-63.

DALE, D. C., BOXER, L. & LILES, W. C. 2008. The phagocytes: neutrophils and monocytes. *Blood,* 112**,** 935-45.

DANG, P. M., FONTAYNE, A., HAKIM, J., EL BENNA, J. & PERIANIN, A. 2001. Protein kinase C zeta phosphorylates a subset of selective sites of the NADPH oxidase component p47^{phox} and participates in formyl peptide-mediated neutrophil respiratory burst. *J Immunol,* 166**,** 1206-13.

DEKKER, L. V., LEITGES, M., ALTSCHULER, G., MISTRY, N., MCDERMOTT, A., ROES, J. & SEGAL, A. W. 2000. Protein kinase C-beta contributes to NADPH oxidase activation in neutrophils. *Biochem J,* 347 Pt 1**,** 285-9.

DEKKER, L. V., PALMER, R. H. & PARKER, P. J. 1995. The protein kinase C and protein kinase C related gene families. *Curr Opin Struct Biol,* 5**,** 396-402.

DENG, Q., LIAO, R., WU, B. L. & SUN, P. 2004. High intensity ras signaling induces premature senescence by activating *p38* pathway in primary human fibroblasts. *J Biol Chem,* 279**,** 1050-9.

DENNING, M. F., DLUGOSZ, A. A., HOWETT, M. K. & YUSPA, S. H. 1993. Expression of an oncogenic rasHa gene in murine keratinocytes induces tyrosine phosphorylation and reduced activity of protein kinase C delta. *J Biol Chem,* 268**,** 26079-81.

DERIJARD, B., HIBI, M., WU, I. H., BARRETT, T., SU, B., DENG, T., KARIN, M. & DAVIS, R. J. 1994. JNK1: a protein kinase stimulated by UV light and Ha-Ras that binds and phosphorylates the c-Jun activation domain. *Cell,* 76**,** 1025-37.

DERIJARD, B., RAINGEAUD, J., BARRETT, T., WU, I. H., HAN, J., ULEVITCH, R. J. & DAVIS, R. J. 1995. Independent human MAP-kinase signal transduction pathways defined by MEK and MKK isoforms. *Science,* 267**,** 682-5.

DEVALIA, V., THOMAS, N. S., ROBERTS, P. J., JONES, H. M. & LINCH, D. C. 1992. Down-regulation of human protein kinase C alpha is associated with terminal neutrophil differentiation. *Blood,* 80**,** 68-76.

DEWAS, C., FAY, M., GOUGEROT-POCIDALO, M. A. & EL-BENNA, J. 2000. The mitogen-activated protein kinase extracellular signal-regulated kinase 1/2 pathway is involved in formyl-methionyl-leucyl-phenylalanine-induced p47^{phox} phosphorylation in human neutrophils. *J Immunol,* 165**,** 5238-44.

DHAVAN, R. & TSAI, L. H. 2001. A decade of CDK5. *Nat Rev Mol Cell Biol,* 2**,** 749-59.

DI CARLO, E., FORNI, G., LOLLINI, P., COLOMBO, M. P., MODESTI, A. & MUSIANI, P. 2001. The intriguing role of polymorphonuclear neutrophils in antitumor reactions. *Blood,* 97**,** 339-45.

DIAZ, B., BARNARD, D., FILSON, A., MACDONALD, S., KING, A. & MARSHALL, M. 1997. Phosphorylation of Raf-1 serine 338-serine 339 is an essential regulatory event for Ras-dependent activation and biological signaling. *Mol Cell Biol,* 17**,** 4509-16.

DOWLATI, A., LAZARUS, H. M., HARTMAN, P., JACOBBERGER, J. W., WHITACRE, C., GERSON, S. L., KSENICH, P., COOPER, B. W., FRISA, P. S., GOTTLIEB, M., MURGO, A. J. & REMICK, S. C. 2003. Phase I and correlative study of combination bryostatin 1 and vincristine in relapsed B-cell malignancies. *Clin Cancer Res,* 9**,** 5929-35.

DUNN, G. P., OLD, L. J. & SCHREIBER, R. D. 2004. The Three Es of Cancer Immunoediting. *Annual Review of Immunology,* 22**,** 329-360.

DUPREZ, L., WIRAWAN, E., VANDEN BERGHE, T. & VANDENABEELE, P. 2009. Major cell death pathways at a glance. *Microbes Infect,* 11**,** 1050-62.

DUTIL, E. M., TOKER, A. & NEWTON, A. C. 1998. Regulation of conventional protein kinase C isozymes by phosphoinositide-dependent kinase 1 (PDK-1). *Curr Biol,* 8**,** 1366-75.

EBINU, J. O., BOTTORFF, D. A., CHAN, E. Y., STANG, S. L., DUNN, R. J. & STONE, J. C. 1998. RasGRP, a Ras guanyl nucleotide- releasing protein with calcium- and diacylglycerol-binding motifs. *Science,* 280**,** 1082-6.

EDWARDS, A. S., FAUX, M. C., SCOTT, J. D. & NEWTON, A. C. 1999. Carboxyl-terminal phosphorylation regulates the function and subcellular localization of protein kinase C betaII. *J Biol Chem,* 274**,** 6461-8.

EDWARDS, A. S. & NEWTON, A. C. 1997. Phosphorylation at conserved carboxyl-terminal hydrophobic motif regulates the catalytic and regulatory domains of protein kinase C. *J Biol Chem,* 272**,** 18382-90.

EL BENNA, J., FAUST, L. P. & BABIOR, B. M. 1994. The phosphorylation of the respiratory burst oxidase component p47^{phox} during neutrophil activation. Phosphorylation of sites recognized by protein kinase C and by proline-directed kinases. *J Biol Chem,* 269**,** 23431-6.

EL BENNA, J., FAUST, R. P., JOHNSON, J. L. & BABIOR, B. M. 1996. Phosphorylation of the respiratory burst oxidase subunit p47^{phox} as determined by two-dimensional phosphopeptide mapping. Phosphorylation by protein kinase C, protein kinase A, and a mitogen-activated protein kinase. *J Biol Chem,* 271**,** 6374-8.

ELDER, D. E. 2006. Pathology of melanoma. *Clin Cancer Res,* 12**,** 2308s-2311s.

EMOTO, Y., MANOME, Y., MEINHARDT, G., KISAKI, H., KHARBANDA, S., ROBERTSON, M., GHAYUR, T., WONG, W. W., KAMEN, R., WEICHSELBAUM, R. & *ET AL*. 1995. Proteolytic activation of protein kinase C delta by an ICE-like protease in apoptotic cells. *EMBO J,* 14**,** 6148-56.

ENGLISH, J. M., VANDERBILT, C. A., XU, S., MARCUS, S. & COBB, M. H. 1995. Isolation of MEK5 and differential expression of alternatively spliced forms. *J Biol Chem,* 270**,** 28897-902.

ERHARDT, P., TROPPMAIR, J., RAPP, U. R. & COOPER, G. M. 1995. Differential regulation of Raf-1 and B-Raf and Ras-dependent activation of mitogen-activated protein kinase by cyclic AMP in PC12 cells. *Mol Cell Biol,* 15**,** 5524-30.

EVANS, F. J. 1986. Naturally occurring phorbol esters. Boca Raton, FL: CRC Press.

EVANS, J. D., CORNFORD, P. A., DODSON, A., NEOPTOLEMOS, J. P. & FOSTER, C. S. 2003. Expression patterns of protein kinase C isoenzymes are characteristically modulated in chronic pancreatitis and pancreatic cancer. *Am J Clin Pathol,* 119**,** 392-402.

FABBRO, D., RUETZ, S., BODIS, S., PRUSCHY, M., CSERMAK, K., MAN, A., CAMPOCHIARO, P., WOOD, J., O'REILLY, T. & MEYER, T. 2000. PKC412--a protein kinase inhibitor with a broad therapeutic potential. *Anticancer Drug Des,* 15**,** 17-28.

FABIAN, J. R., DAAR, I. O. & MORRISON, D. K. 1993. Critical tyrosine residues regulate the enzymatic and biological activity of Raf-1 kinase. *Mol Cell Biol,* 13**,** 7170-9.

FERNANDEZ, M. C., MARUCHA, P. T., ROJAS, I. G. & WALTERS, J. D. 2000. The role of protein kinase C and calcium in induction of human polymorphonuclear leukocyte IL-1 beta gene expression by GM-CSF. *Cytokine,* 12**,** 445-9.

FINCH, A., HOLLAND, P., COOPER, J., SAKLATVALA, J. & KRACHT, M. 1997. Selective activation of JNK/SAPK by interleukin-1 in rabbit liver is mediated by MKK7. *FEBS Lett,* 418**,** 144-8.

FISHER, D. E. 1994. Apoptosis in cancer therapy: crossing the threshold. *Cell,* 78**,** 539-42.

FISHER, R. P. & MORGAN, D. O. 1994. A novel cyclin associates with MO15/CDK7 to form the CDK-activating kinase. *Cell,* 78**,** 713-24.

FLAHERTY, K. T., PUZANOV, I., KIM, K. B., RIBAS, A., MCARTHUR, G. A., SOSMAN, J. A., O'DWYER, P. J., LEE, R. J., GRIPPO, J. F., NOLOP, K. & CHAPMAN, P. B. 2010. Inhibition of mutated, activated BRAF in metastatic melanoma. *The New England journal of medicine,* 363**,** 809-19.

FONTAYNE, A., DANG, P. M., GOUGEROT-POCIDALO, M. A. & EL-BENNA, J. 2002. Phosphorylation of $p47^{phox}$ sites by PKC alpha, beta II, delta, and zeta: effect on binding to p22phox and on NADPH oxidase activation. *Biochemistry,* 41**,** 7743-50.

FOURNIER, D. B., CHISAMORE, M., LURAIN, J. R., RADEMAKER, A. W., JORDAN, V. C. & TONETTI, D. A. 2001. Protein kinase C alpha expression is inversely related to ER status in endometrial carcinoma: possible role in AP-1-mediated proliferation of ER-negative endometrial cancer. *Gynecol Oncol,* 81**,** 366-72.

FUJII, T., GARCIA-BERMEJO, M. L., BERNABO, J. L., CAAMANO, J., OHBA, M., KUROKI, T., LI, L., YUSPA, S. H. & KAZANIETZ, M. G. 2000. Involvement of protein kinase C delta (PKCdelta) in phorbol ester-induced apoptosis in LNCaP prostate cancer cells. Lack of proteolytic cleavage of PKCdelta. *J Biol Chem,* 275**,** 7574-82.

GAILANI, M. R., STAHLE-BACKDAHL, M., LEFFELL, D. J., GLYNN, M., ZAPHIROPOULOS, P. G., PRESSMAN, C., UNDEN, A. B., DEAN, M., BRASH, D. E., BALE, A. E. & TOFTGARD, R. 1996. The role of the human homologue of Drosophila patched in sporadic basal cell carcinomas. *Nat Genet,* 14**,** 78-81.

GANZ, T. 2003. Defensins: antimicrobial peptides of innate immunity. *Nature reviews. Immunology,* 3**,** 710-20.

GAVRIELIDES, M. V., FRIJHOFF, A. F., CONTI, C. J. & KAZANIETZ, M. G. 2004. Protein kinase C and prostate carcinogenesis: targeting the cell cycle and apoptotic mechanisms. *Curr Drug Targets,* 5**,** 431-43.

GERWINS, P., BLANK, J. L. & JOHNSON, G. L. 1997. Cloning of a novel mitogen-activated protein kinase kinase kinase, MEKK4, that selectively regulates the c-Jun amino terminal kinase pathway. *J Biol Chem,* 272**,** 8288-95.

GILLESPIE, S. K., ZHANG, X. D. & HERSEY, P. 2004. Ingenol 3-angelate induces dual modes of cell death and differentially regulates tumor necrosis factor-related apoptosis-inducing ligand-induced apoptosis in melanoma cells. *Molecular cancer therapeutics,* 3**,** 1651-8.

GOEL, G., MAKKAR, H. P., FRANCIS, G. & BECKER, K. 2007. Phorbol esters: structure, biological activity, and toxicity in animals. *Int J Toxicol,* 26**,** 279-88.

GOKMEN-POLAR, Y., MURRAY, N. R., VELASCO, M. A., GATALICA, Z. & FIELDS, A. P. 2001. Elevated protein kinase C betaII is an early promotive event in colon carcinogenesis. *Cancer Res,* 61**,** 1375-81.

GOMPERTS, B. D., KRAMER, I. M. & TATHAM, P. E. R. 2003. *Phosphorylation And Dephosphorylation: Protein Kinase A and C,* Elsevier Academic Press.

GONZALEZ, F. A., RADEN, D. L., RIGBY, M. R. & DAVIS, R. J. 1992. Heterogeneous expression of four MAP kinase isoforms in human tissues. *FEBS Lett,* 304**,** 170-8.

GOPALAKRISHNA, R., CHEN, Z. H. & GUNDIMEDA, U. 1994. Tobacco smoke tumor promoters, catechol and hydroquinone, induce oxidative regulation of protein kinase C and influence invasion and metastasis of lung carcinoma cells. *Proc Natl Acad Sci U S A,* 91**,** 12233-7.

GRANA, X., GARRIGA, J. & MAYOL, X. 1998. Role of the retinoblastoma protein family, pRB, p107 and p130 in the negative control of cell growth. *Oncogene,* 17**,** 3365-83.

GRINER, E. M. & KAZANIETZ, M. G. 2007. Protein kinase C and other Diacylglycerol effectors in cancer. *Nat Rev Cancer,* 7**,** 281-94.

GUPTA, S., CAMPBELL, D., DERIJARD, B. & DAVIS, R. J. 1995. Transcription factor ATF2 regulation by the JNK signal transduction pathway. *Science,* 267**,** 389-93.

HAFEMAN, D. G., MCCONNELL, H. M., GRAY, J. W. & DEAN, P. N. 1982. Neutrophil activation monitored by flow cytometry: stimulation by phorbol diester is an all-or-none event. *Science,* 215**,** 673-5.

HAGEMANN, C. & BLANK, J. L. 2001. The ups and downs of MEK kinase interactions. *Cell Signal,* 13**,** 863-75.

HAGEMANN, C. & RAPP, U. R. 1999. Isotype-specific functions of Raf kinases. *Exp Cell Res,* 253**,** 34-46.

HALPERN, A. C. & ALTMAN, J. F. 1999. Genetic predisposition to skin cancer. *Curr Opin Oncol,* 11**,** 132-8.

HAN, J., BACK, S. H., HUR, J., LIN, Y. H., GILDERSLEEVE, R., SHAN, J., YUAN, C. L., KROKOWSKI, D., WANG, S., HATZOGLOU, M., KILBERG, M. S., SARTOR, M. A. & KAUFMAN, R. J. 2013. ER-stress-induced transcriptional regulation increases protein synthesis leading to cell death. *Nat Cell Biol,* 15**,** 481-90.

HAN, J., JIANG, Y., LI, Z., KRAVCHENKO, V. V. & ULEVITCH, R. J. 1997. Activation of the transcription factor MEF2C by the MAP kinase p38 in inflammation. *Nature,* 386**,** 296-9.

HAN, J., LEE, J. D., JIANG, Y., LI, Z., FENG, L. & ULEVITCH, R. J. 1996. Characterization of the structure and function of a novel MAP kinase kinase (MKK6). *J Biol Chem,* 271**,** 2886-91.

HAN, Z. T., TONG, Y. K., HE, L. M., ZHANG, Y., SUN, J. Z., WANG, T. Y., ZHANG, H., CUI, Y. L., NEWMARK, H. L., CONNEY, A. H. & CHANG, R. L. 1998 (ii). 12-O-Tetradecanoylphorbol-13-acetate (TPA)-induced increase in depressed white blood cell

counts in patients treated with cytotoxic cancer chemotherapeutic drugs. *Proc Natl Acad Sci U S A,* 95**,** 5362-5.

HAN, Z. T., ZHU, X. X., YANG, R. Y., SUN, J. Z., TIAN, G. F., LIU, X. J., CAO, G. S., NEWMARK, H. L., CONNEY, A. H. & CHANG, R. L. 1998 (i). Effect of intravenous infusions of 12-O-tetradecanoylphorbol-13-acetate (TPA) in patients with myelocytic leukemia: preliminary studies on therapeutic efficacy and toxicity. *Proc Natl Acad Sci U S A,* 95**,** 5357-61.

HANNUN, Y. A. & BELL, R. M. 1989. Functions of sphingolipids and sphingolipid breakdown products in cellular regulation. *Science,* 243**,** 500-7.

HAUBEN, D. J., ZIRKIN, H., MAHLER, D. & SACKS, M. 1982. The biologic behavior of basal cell carcinoma: Part I. *Plast Reconstr Surg,* 69**,** 103-9.

HAWKES, N. C., STRATTON, B. C., TALA, T., CHALLIS, C. D., CONWAY, G., DEANGELIS, R., GIROUD, C., HOBIRK, J., JOFFRIN, E., LOMAS, P., LOTTE, P., MAILLOUX, J., MAZON, D., RACHLEW, E., REYES-CORTES, S., SOLANO, E. & ZASTROW, K. D. 2001. Observation of zero current density in the core of jet discharges with lower hybrid heating and current drive. *Phys Rev Lett,* 87**,** 115001.

HAYASHI, A., SEKI, N., HATTORI, A., KOZUMA, S. & SAITO, T. 1999. PKC*ν*, a new member of the Protein Kinase C family, composes a fourth subfamily with PKC*μ*. *Biochim Biophys Acta,* 1450**,** 99-106.

HECKER, E. 1968. Cocarcinogenic principles from the seed oil of Croton tiglium and from other Euphorbiaceae. *Cancer Res,* 28**,** 2338-49.

HERLYN, M. 2009. Driving in the melanoma landscape. *Exp Dermatol,* 18**,** 506-8.

HOCEVAR, B. A. & FIELDS, A. P. 1991. Selective translocation of beta II-protein kinase C to the nucleus of human promyelocytic (HL60) leukemia cells. *J Biol Chem,* 266**,** 28-33.

HOFMANN, J. 2001. Modulation of protein kinase C in antitumor treatment. *Rev Physiol Biochem Pharmacol,* 142**,** 1-96.

HORNUNG, R. L., PEARSON, J. W., BECKWITH, M. & LONGO, D. L. 1992. Preclinical evaluation of bryostatin as an anticancer agent against several murine tumor cell lines: in vitro versus in vivo activity. *Cancer Res,* 52**,** 101-7.

HOWE, L. R., LEEVERS, S. J., GOMEZ, N., NAKIELNY, S., COHEN, P. & MARSHALL, C. J. 1992. Activation of the MAP kinase pathway by the protein kinase raf. *Cell,* 71**,** 335-42.

IIDA, N. & GROTENDORST, G. R. 1990. Cloning and sequencing of a new gro transcript from activated human monocytes: expression in leukocytes and wound tissue. *Molecular and Cellular Biology,* 10**,** 5596-9.

INOUE, M., KISHIMOTO, A., TAKAI, Y. & NISHIZUKA, Y. 1977. Studies on a cyclic nucleotide-independent protein kinase and its proenzyme in mammalian tissues. II. Proenzyme and its activation by calcium-dependent protease from rat brain. *J Biol Chem,* 252**,** 7610-6.

JAKEN, S. 1996. Protein Kinase C isozymes and substrates. *Current Opinion in Cell Biology,* 8**,** 168-173.

JANOFF, A., KLASSEN, A. & TROLL, W. 1970. Local vascular changes induced by the cocarcinogen, phorbol myristate acetate. *Cancer Res,* 30**,** 2568-71.

JIANG, Y., CHEN, C., LI, Z., GUO, W., GEGNER, J. A., LIN, S. & HAN, J. 1996. Characterization of the structure and function of a new mitogen-activated protein kinase (p38beta). *J Biol Chem,* 271**,** 17920-6.

JIANG, Y., GRAM, H., ZHAO, M., NEW, L., GU, J., FENG, L., DI PADOVA, F., ULEVITCH, R. J. & HAN, J. 1997. Characterization of the structure and function of the fourth member of p38 group mitogen-activated protein kinases, p38delta. *J Biol Chem,* 272**,** 30122-8.

JOHANNES, F. J., PRESTLE, J., EIS, S., OBERHAGEMANN, P. & PFIZENMAIER, K. 1994. PKCμ is a novel, atypical member of the Protein Kinase C family. *J Biol Chem,* 269**,** 6140-8.

JOHNSON, G. L. & LAPADAT, R. 2002. Mitogen-activated protein kinase pathways mediated by ERK, JNK, and p38 protein kinases. *Science,* 298**,** 1911-2.

JOHNSON, W. P., ZHANG, P., FULLER, M. E., SCHEIBE, T. D., MAILLOUX, B. J., ONSTOTT, T. C., DEFLAUN, M. F., HUBBARD, S. S., RADTKE, J., KOVACIK, W. P. & HOLBEN, W. 2001. Ferrographic tracking of bacterial transport in the field at the narrow channel focus area, Oyster, VA. *Environ Sci Technol,* 35**,** 182-91.

JONES, R. J., SHARKIS, S. J., MILLER, C. B., ROWINSKY, E. K., BURKE, P. J. & MAY, W. S. 1990. Bryostatin 1, a unique biologic response modifier: anti-leukemic activity in vitro. *Blood,* 75**,** 1319-23.

JOPPICH, I., HECKER, W. C., SCHMID, F. & EPPEL, M. 1967. [Analysis and treatment results in pleural empyemas in infancy and childhood]. *Arch Kinderheilkd,* 176**,** 113-27.

KALDIS, P. 1999. The cdk-activating kinase (CAK): from yeast to mammals. *Cell Mol Life Sci,* 55**,** 284-96.

KAMIMURA, K., HOJO, H. & ABE, M. 2004. Characterization of expression of protein kinase C isozymes in human B-cell lymphoma: Relationship between its expression and prognosis. *Pathol Int,* 54**,** 224-30.

KARASAVVAS, N., ERUKULLA, R. K., BITTMAN, R., LOCKSHIN, R. & ZAKERI, Z. 1996. Stereospecific induction of apoptosis in U937 cells by N-octanoyl-sphingosine

stereoisomers and N-octyl-sphingosine. The ceramide amide group is not required for apoptosis. *Eur J Biochem,* 236**,** 729-37.

KASTEN, M. & GIORDANO, A. 2001. Cdk10, a Cdc2-related kinase, associates with the Ets2 transcription factor and modulates its transactivation activity. *Oncogene,* 20**,** 1832-8.

KATAKAMI, Y., KAIBUCHI, K., SAWAMURA, M., TAKAI, Y. & NISHIZUKA, Y. 1984. Synergistic action of protein kinase C and calcium for histamine release from rat peritoneal mast cells. *Biochem Biophys Res Commun,* 121**,** 573-8.

KATO, Y., KRAVCHENKO, V. V., TAPPING, R. I., HAN, J., ULEVITCH, R. J. & LEE, J. D. 1997. BMK1/ERK5 regulates serum-induced early gene expression through transcription factor MEF2C. *EMBO J,* 16**,** 7054-66.

KAVANAUGH, A. F., LIGHTFOOT, E., LIPSKY, P. E. & OPPENHEIMER-MARKS, N. 1991. Role of CD11/CD18 in adhesion and transendothelial migration of T cells. Analysis utilizing CD18-deficient T cell clones. *J Immunol,* 146**,** 4149-56.

KAZANIETZ, M. G. 2002. Novel "nonkinase" phorbol ester receptors: the C1 domain connection. *Molecular pharmacology,* 61**,** 759-67.

KEDEI, N., LUNDBERG, D. J., TOTH, A., WELBURN, P., GARFIELD, S. H. & BLUMBERG, P. M. 2004. Characterization of the interaction of ingenol 3-angelate with protein kinase C. *Cancer Res,* 64**,** 3243-55.

KERANEN, L. M., DUTIL, E. M. & NEWTON, A. C. 1995. Protein kinase C is regulated in vivo by three functionally distinct phosphorylations. *Curr Biol,* 5**,** 1394-1403.

KERFOOT, C., HUANG, W. & ROTENBERG, S. A. 2004. Immunohistochemical analysis of advanced human breast carcinomas reveals downregulation of protein kinase C alpha. *J Histochem Cytochem,* 52**,** 419-22.

KERR, J. F. 1971. Shrinkage necrosis: a distinct mode of cellular death. *J Pathol,* 105**,** 13-20.

KERR, J. F., WYLLIE, A. H. & CURRIE, A. R. 1972. Apoptosis: a basic biological phenomenon with wide-ranging implications in tissue kinetics. *Br J Cancer,* 26**,** 239-57.

KEYES, K. A., MANN, L., SHERMAN, M., GALBREATH, E., SCHIRTZINGER, L., BALLARD, D., CHEN, Y. F., IVERSEN, P. & TEICHER, B. A. 2004. LY317615 decreases plasma VEGF levels in human tumor xenograft-bearing mice. *Cancer Chemother Pharmacol,* 53**,** 133-40.

KHAZEN, W., M'BIKA J, P., TOMKIEWICZ, C., BENELLI, C., CHANY, C., ACHOUR, A. & FOREST, C. 2005. Expression of macrophage-selective markers in human and rodent adipocytes. *FEBS letters,* 579**,** 5631-4.

KHOKHLATCHEV, A., XU, S., ENGLISH, J., WU, P., SCHAEFER, E. & COBB, M. H. 1997. Reconstitution of mitogen-activated protein kinase phosphorylation cascades in bacteria. Efficient synthesis of active protein kinases. *J Biol Chem,* 272**,** 11057-62.

KIM, I. S., RYANG, Y. S., KIM, Y. S., JANG, S. W., SUNG, H. J., LEE, Y. H., KIM, J., NA, D. S. & KO, J. 2003. Leukotactin-1-induced ERK activation is mediated via Gi/Go protein/PLC/PKC delta/Ras cascades in HOS cells. *Life sciences,* 73**,** 447-59.

KINDZELSKII, A. L. & PETTY, H. R. 1999. Early membrane rupture events during neutrophil-mediated antibody-dependent tumor cell cytolysis. *Journal of immunology,* 162**,** 3188-92.

KINZLER, K. W. & VOGELSTEIN, B. 2002. *Colorectal tumours.,* New York, McGraw-Hill.

KISHIMOTO, A., TAKAI, Y., MORI, T., KIKKAWA, U. & NISHIZUKA, Y. 1980. Activation of calcium and phospholipid-dependent protein kinase by diacylglycerol, its possible relation to phosphatidylinositol turnover. *J Biol Chem,* 255**,** 2273-6.

KISS, T. 2002. Small nucleolra RNAs: an abundant group of noncoding RNAs with diverse cellular functions. *Cell,* 109**,** 145-148.

KLAUCK, T. M., FAUX, M. C., LABUDDA, K., LANGEBERG, L. K., JAKEN, S. & SCOTT, J. D. 1996. Coordination of three signaling enzymes by AKAP79, a mammalian scaffold protein. *Science,* 271**,** 1589-92.

KOIVUNEN, J., AALTONEN, V., KOSKELA, S., LEHENKARI, P., LAATO, M. & PELTONEN, J. 2004. Protein kinase C alpha/beta inhibitor Go6976 promotes formation of cell junctions and inhibits invasion of urinary bladder carcinoma cells. *Cancer Res,* 64**,** 5693-701.

KOIVUNEN, J., AALTONEN, V. & PELTONEN, J. 2006. Protein kinase C (PKC) family in cancer progression. *Cancer Lett,* 235**,** 1-10.

KOLCH, W., HEIDECKER, G., KOCHS, G., HUMMEL, R., VAHIDI, H., MISCHAK, H., FINKENZELLER, G., MARME, D. & RAPP, U. R. 1993. Protein kinase C alpha activates RAF-1 by direct phosphorylation. *Nature,* 364**,** 249-52.

KONTNY, E., ZIOLKOWSKA, M., RYZEWSKA, A. & MASLINSKI, W. 1999. Protein kinase c-dependent pathway is critical for the production of pro-inflammatory cytokines (TNF-alpha, IL-1beta, IL-6). *Cytokine,* 11**,** 839-48.

KOSAKA, C., SASAGURI, T., ISHIDA, A. & OGATA, J. 1996. Cell cycle arrest in the G2 phase induced by phorbol ester and diacylglycerol in vascular endothelial cells. *Am J Physiol,* 270**,** C170-8.

KRAFT, A. S., REEVES, J. A. & ASHENDEL, C. L. 1988. Differing modulation of protein kinase C by bryostatin 1 and phorbol esters in JB6 mouse epidermal cells. *J Biol Chem,* 263**,** 8437-42.

KRAFT, A. S., SMITH, J. B. & BERKOW, R. L. 1986. Bryostatin, an activator of the calcium phospholipid-dependent protein kinase, blocks phorbol ester-induced differentiation of human promyelocytic leukemia cells HL-60. *Proc Natl Acad Sci U S A,* 83**,** 1334-8.

KRAMER, I. M., VAN DER BEND, R. L., TOOL, A. T., VAN BLITTERSWIJK, W. J., ROOS, D. & VERHOEVEN, A. J. 1989. 1-O-hexadecyl-2-Q-methylglycerol, a novel inhibitor of protein kinase C, inhibits the respiratory burst in human neutrophils. *J Biol Chem,* 264**,** 5876-84.

KRAUSS, G. 2003a. *Intracellular Signal Transduction: the Protein Cascades of the MAP Kinase Pathways,* Wiley-VCH.

KRAUSS, G. 2003b. *Regulation of the Cell Cycle,* Wiley-VCH.

KRAUSS, G. 2003c. Regulation of the Cell Cycle. *Wiley-VCH.*

KRAUSS, G. 2003d. *Ser/Thr-specific Protein Kinases and Protein Phosphatases.,* Wiley-VCH.

KRUMHAAR, D. & HECKER, W. C. 1967. [126. Late results following surgery for diaphragmatic hernias and relaxations]. *Langenbecks Arch Chir,* 319**,** 749-50.

KYRIAKIS, J. M., APP, H., ZHANG, X. F., BANERJEE, P., BRAUTIGAN, D. L., RAPP, U. R. & AVRUCH, J. 1992. Raf-1 activates MAP kinase-kinase. *Nature,* 358**,** 417-21.

KYRIAKIS, J. M. & AVRUCH, J. 1996. Sounding the alarm: protein kinase cascades activated by stress and inflammation. *J Biol Chem,* 271**,** 24313-6.

KYRIAKIS, J. M., BANERJEE, P., NIKOLAKAKI, E., DAI, T., RUBIE, E. A., AHMAD, M. F., AVRUCH, J. & WOODGETT, J. R. 1994. The stress-activated protein kinase subfamily of c-Jun kinases. *Nature,* 369**,** 156-60.

KYRIAKIS, J. M., BRAUTIGAN, D. L., INGEBRITSEN, T. S. & AVRUCH, J. 1991. pp54 microtubule-associated protein-2 kinase requires both tyrosine and serine/threonine phosphorylation for activity. *J Biol Chem,* 266**,** 10043-6.

LA PORTA, C. A., TESSITORE, L. & COMOLLI, R. 1997. Changes in protein kinase C alpha, delta and in nuclear beta isoform expression in tumour and lung metastatic nodules induced by diethylnitrosamine in the rat. *Carcinogenesis,* 18**,** 715-9.

LANGE-CARTER, C. A., PLEIMAN, C. M., GARDNER, A. M., BLUMER, K. J. & JOHNSON, G. L. 1993. A divergence in the MAP kinase regulatory network defined by MEK kinase and Raf. *Science,* 260**,** 315-9.

LANGZAM, L., KOREN, R., GAL, R., KUGEL, V., PAZ, A., FARKAS, A. & SAMPSON, S. R. 2001. Patterns of protein kinase C isoenzyme expression in transitional cell carcinoma of bladder. Relation to degree of malignancy. *Am J Clin Pathol,* 116**,** 377-85.

LE GOOD, J. A., ZIEGLER, W. H., PAREKH, D. B., ALESSI, D. R., COHEN, P. & PARKER, P. J. 1998. Protein kinase C isotypes controlled by phosphoinositide 3-kinase through the protein kinase PDK1. *Science,* 281**,** 2042-5.

LE, T. T., GARDNER, J., HOANG-LE, D., SCHMIDT, C. W., MACDONALD, K. P., LAMBLEY, E., SCHRODER, W. A., OGBOURNE, S. M. & SUHRBIER, A. 2009. Immunostimulatory cancer chemotherapy using local ingenol-3-angelate and synergy with immunotherapies. *Vaccine,* 27**,** 3053-62.

LEA, I. A., JACKSON, M. A. & DUNNICK, J. K. 2009. Genetic pathways to colorectal cancer. *Mutat Res,* 670**,** 96-8.

LEE, J. W., SOUNG, Y. H., KIM, S. Y., NAM, H. K., PARK, W. S., NAM, S. W., KIM, M. S., SUN, D. I., LEE, Y. S., JANG, J. J., LEE, J. Y., YOO, N. J. & LEE, S. H. 2005. Somatic mutations of EGFR gene in squamous cell carcinoma of the head and neck. *Clin Cancer Res,* 11**,** 2879-82.

LEE, M. H. & YANG, H. Y. 2001. Negative regulators of cyclin-dependent kinases and their roles in cancers. *Cell Mol Life Sci,* 58**,** 1907-22.

LEFFELL, D. J. 2000. The scientific basis of skin cancer. *J Am Acad Dermatol,* 42**,** 18-22.

LI, L., SHUKLA, S., LEE, A., GARFIELD, S. H., MALONEY, D. J., AMBUDKAR, S. V. & YUSPA, S. H. 2010. The skin cancer chemotherapeutic agent ingenol-3-angelate (PEP005) is a substrate for the epidermal multidrug transporter (ABCB1) and targets tumor vasculature. *Cancer Research,* 70**,** 4509-19.

LI, Z., JIANG, Y., ULEVITCH, R. J. & HAN, J. 1996. The primary structure of p38 gamma: a new member of p38 group of MAP kinases. *Biochem Biophys Res Commun,* 228**,** 334-40.

LIN, A., MINDEN, A., MARTINETTO, H., CLARET, F. X., LANGE-CARTER, C., MERCURIO, F., JOHNSON, G. L. & KARIN, M. 1995. Identification of a dual specificity kinase that activates the Jun kinases and p38-Mpk2. *Science,* 268**,** 286-90.

LINDBERG, R. A., QUINN, A. M. & HUNTER, T. 1992. Dual-specificity protein kinases: will any hydroxyl do? *Trends Biochem Sci,* 17**,** 114-9.

LOCK, R. B. & STRIBINSKIENE, L. 1996. Dual modes of death induced by etoposide in human epithelial tumor cells allow Bcl-2 to inhibit apoptosis without affecting clonogenic survival. *Cancer Res,* 56**,** 4006-12.

LORENZO, P. S., BEHESHTI, M., PETTIT, G. R., STONE, J. C. & BLUMBERG, P. M. 2000. The guanine nucleotide exchange factor RasGRP is a high -affinity target for diacylglycerol and phorbol esters. *Molecular pharmacology,* 57**,** 840-6.

LORENZO, P. S., KUNG, J. W., BOTTORFF, D. A., GARFIELD, S. H., STONE, J. C. & BLUMBERG, P. M. 2001. Phorbol esters modulate the Ras exchange factor RasGRP3. *Cancer Research,* 61**,** 943-9.

LU, Z., LIU, D., HORNIA, A., DEVONISH, W., PAGANO, M. & FOSTER, D. A. 1998. Activation Of Protein Kinase C Triggers Its Ubiquitination And Degradation. *Mol Cell Biol,* 18**,** 839-45.

LUDWIG, S., ENGEL, K., HOFFMEYER, A., SITHANANDAM, G., NEUFELD, B., PALM, D., GAESTEL, M. & RAPP, U. R. 1996. 3pK, a novel mitogen-activated protein (MAP) kinase-activated protein kinase, is targeted by three MAP kinase pathways. *Mol Cell Biol,* 16**,** 6687-97.

LUNDQVIST-GUSTAFSSON, H. & BENGTSSON, T. 1999. Activation of the granule pool of the NADPH oxidase accelerates apoptosis in human neutrophils. *J Leukoc Biol,* 65**,** 196-204.

MACK, P. C., GANDARA, D. R., BOWEN, C., EDELMAN, M. J., PAGLIERONI, T., SCHNIER, J. B., GELMANN, E. P. & GUMERLOCK, P. H. 1999. RB status as a determinant of response to UCN-01 in non-small cell lung carcinoma. *Clin Cancer Res,* 5**,** 2596-604.

MAILLOUX, A., GRENET, K., BRUNEEL, A., BENETEAU-BURNAT, B., VAUBOURDOLLE, M. & BAUDIN, B. 2001. Anticancer drugs induce necrosis of human endothelial cells involving both oncosis and apoptosis. *Eur J Cell Biol,* 80**,** 442-9.

MAILLOUX, L. U. 2001. Hypertension in chronic renal failure and ESRD: prevalence, pathophysiology, and outcomes. *Semin Nephrol,* 21**,** 146-56.

MAJNO, G. & JORIS, I. 1995. Apoptosis, oncosis, and necrosis. An overview of cell death. *Am J Pathol,* 146**,** 3-15.

MALLYA, M., CAMPBELL, R. D. & AGUADO, B. 2002. Transcriptional analysis of a novel cluster of LY-6 family members in the human and mouse major histocompatibility complex: five genes with many splice forms. *Genomics,* 80**,** 113-23.

MARKS, F. & HECKER, E. 1967. Enzymatic preparation of 2-hydroxy-[4-14C]estrone. *Biochim Biophys Acta,* 144**,** 690-1.

MARSHALL, C. J. 1995. Specificity of receptor tyrosine kinase signaling: transient versus sustained extracellular signal-regulated kinase activation. *Cell,* 80**,** 179-85.

MARTINEZ-GIMENO, C., DIAZ-MECO, M. T., DOMINGUEZ, I. & MOSCAT, J. 1995. Alterations in levels of different protein kinase C isotypes and their influence on behavior of squamous cell carcinoma of the oral cavity: epsilon PKC, a novel prognostic factor for relapse and survival. *Head Neck,* 17**,** 516-25.

MASAI, H. & ARAI, K. 2002. Cdc7 kinase complex: a key regulator in the initiation of DNA replication. *J Cell Physiol,* 190**,** 287-96.

MASON, S. A., COZZI, S. J., PIERCE, C. J., PAVEY, S. J., PARSONS, P. G. & BOYLE, G. M. 2010. The induction of senescence-like growth arrest by protein kinase C-activating diterpene esters in solid tumor cells. *Invest New Drugs,* 28**,** 575-86.

MASUR, K., LANG, K., NIGGEMANN, B., ZANKER, K. S. & ENTSCHLADEN, F. 2001. High PKC*α* and low E-cadherin expression contribute to high migratory activity of colon carcinoma cells. *Mol Biol Cell,* 12**,** 1973-82.

MICHEL, C. I., HOLLEY, C. L., SCRUGGS, B. S., SIDHU, R., BROOKHEART, R. T., LISTENBERGER, L. L., BEHLKE, M. A., ORY, D. S. & SCHAFFER, J. E. 2011. Small nucleolar RNAs U32a, U33, and U35a are critical mediators of metabolic stress. *Cell Metab,* 14**,** 33-44.

MILLARD, S. S., YAN, J. S., NGUYEN, H., PAGANO, M., KIYOKAWA, H. & KOFF, A. 1997. Enhanced ribosomal association of p27(Kip1) mRNA is a mechanism contributing to accumulation during growth arrest. *J Biol Chem,* 272**,** 7093-8.

MILLER, A. J. & MIHM, M. C., JR. 2006. Melanoma. *N Engl J Med,* 355**,** 51-65.

MINDEN, A., LIN, A., MCMAHON, M., LANGE-CARTER, C., DERIJARD, B., DAVIS, R. J., JOHNSON, G. L. & KARIN, M. 1994. Differential activation of ERK and JNK mitogen-activated protein kinases by Raf-1 and MEKK. *Science,* 266**,** 1719-23.

MOCHLY-ROSEN, D. 1995. Localization of protein kinases by anchoring proteins: a theme in signal transduction. *Science,* 268**,** 247-51.

MOHAMMAD, R. M., KATATO, K., ALMATCHY, V. P., WALL, N., LIU, K. Z., SCHULTZ, C. P., MANTSCH, H. H., VARTERASIAN, M. & AL-KATIB, A. M. 1998a. Sequential treatment of human chronic lymphocytic leukemia with bryostatin 1 followed by 2-chlorodeoxyadenosine: preclinical studies. *Clin Cancer Res,* 4**,** 445-53.

MOHAMMAD, R. M., VARTERASIAN, M. L., ALMATCHY, V. P., HANNOUDI, G. N., PETTIT, G. R. & AL-KATIB, A. 1998b. Successful treatment of human chronic lymphocytic leukemia xenografts with combination biological agents auristatin PE and bryostatin 1. *Clin Cancer Res,* 4**,** 1337-43.

MORIGUCHI, T., KUROYANAGI, N., YAMAGUCHI, K., GOTOH, Y., IRIE, K., KANO, T., SHIRAKABE, K., MURO, Y., SHIBUYA, H., MATSUMOTO, K., NISHIDA, E. & HAGIWARA, M. 1996. A novel kinase cascade mediated by mitogen-activated protein kinase kinase 6 and MKK3. *J Biol Chem,* 271**,** 13675-9.

MORIGUCHI, T., TOYOSHIMA, F., MASUYAMA, N., HANAFUSA, H., GOTOH, Y. & NISHIDA, E. 1997. A novel SAPK/JNK kinase, MKK7, stimulated by TNFalpha and cellular stresses. *EMBO J,* 16**,** 7045-53.

MORITA, A. 2007. Tobacco smoke causes premature skin aging. *J Dermatol Sci,* 48**,** 169-75.

MORRISON, D. K. & CUTLER, R. E. 1997. The complexity of Raf-1 regulation. *Curr Opin Cell Biol,* 9**,** 174-9.

MORRISON, D. K., HEIDECKER, G., RAPP, U. R. & COPELAND, T. D. 1993. Identification of the major phosphorylation sites of the Raf-1 kinase. *J Biol Chem,* 268**,** 17309-16.

MOSER, B., CLARK-LEWIS, I., ZWAHLEN, R. & BAGGIOLINI, M. 1990. Neutrophil-activating properties of the melanoma growth-stimulatory activity. *The Journal of experimental medicine,* 171**,** 1797-802.

MUTTER, R. & WILLS, M. 2000. Chemistry and clinical biology of the bryostatins. *Bioorg Med Chem,* 8**,** 1841-60.

NAKAMURA, K., YOSHIKAWA, N., YAMAGUCHI, Y., KAGOTA, S., SHINOZUKA, K. & KUNITOMO, M. 2003. Effect of PKC412, an inhibitor of protein kinase C, on spontaneous metastatic model mice. *Anticancer Res,* 23**,** 1395-9.

NEBREDA, A. R., HILL, C., GOMEZ, N., COHEN, P. & HUNT, T. 1993. The protein kinase mos activates MAP kinase kinase in vitro and stimulates the MAP kinase pathway in mammalian somatic cells in vivo. *FEBS Lett,* 333**,** 183-7.

NEILL, G. W., GHALI, L. R., GREEN, J. L., IKRAM, M. S., PHILPOTT, M. P. & QUINN, A. G. 2003. Loss of protein kinase Calpha expression may enhance the tumorigenic potential of Gli1 in basal cell carcinoma. *Cancer Res,* 63**,** 4692-7.

NEWTON, A. C. 1993. Interaction of proteins with lipid headgroups: lessons from protein kinase C. *Annu Rev Biophys Biomol Struct,* 22**,** 1-25.

NEWTON, A. C. 1995. Protein Kinase C: Structure, Function, and Regulation. *The Journal of Biological Chemistry,* 270**,** 28495-28498.

NEWTON, A. C. 1997. Regulation of Protein kinase C. *Current Opinion in Cell Biology,* 9**,** 161-167.

NISHIZUKA, Y. 1984. The role of protein kinase C in cell surface signal transduction and tumour promotion. *Nature,* 308**,** 693-8.

NISHIZUKA, Y. 1989. The Albert Lasker Medical Awards. The family of protein kinase C for signal transduction. *JAMA,* 262**,** 1826-33.

NISHIZUKA, Y. 1992. Intracellular signaling by hydrolysis of phospholipids and activation of protein kinase C. *Science,* 258**,** 607-14.

NISHIZUKA, Y. 1995. Protein kinase C and lipid signaling for sustained cellular responses. *FASEB J,* 9**,** 484-96.

NISHIZUKA, Y. & NAKAMURA, S. 1995. Lipid mediators and protein kinase C for intracellular signalling. *Clin Exp Pharmacol Physiol Suppl,* 22**,** S202-3.

OANCEA, E. & MEYER, T. 1998. Protein kinase C as a molecular machine for decoding calcium and diacylglycerol signals. *Cell,* 95**,** 307-18.

OGBOURNE, S. M., SUHRBIER, A., JONES, B., COZZI, S. J., BOYLE, G. M., MORRIS, M., MCALPINE, D., JOHNS, J., SCOTT, T. M., SUTHERLAND, K. P., GARDNER, J. M.,

LE, T. T., LENARCZYK, A., AYLWARD, J. H. & PARSONS, P. G. 2004. Antitumor activity of 3-ingenyl angelate: plasma membrane and mitochondrial disruption and necrotic cell death. *Cancer Res,* 64**,** 2833-9.

OKA, M. & KIKKAWA, U. 2005. Protein Kinase C in Melanoma. *Cancer and Metastasis Reviews,* 24**,** 287-300.

OLSON, E. N., BURGESS, R. & STAUDINGER, J. 1993. Protein kinase C as a transducer of nuclear signals. *Cell Growth Differ,* 4**,** 699-705.

ONO, Y., FUJII, T., IGARASHI, K., KUNO, T., TANAKA, C., KIKKAWA, U. & NISHIZUKA, Y. 1989. Phorbol ester binding to protein kinase C requires a cysteine-rich zinc-finger-like sequence. *Proc Natl Acad Sci U S A,* 86**,** 4868-71.

PAK, Y., ENYEDY, I. J., VARADY, J., KUNG, J. W., LORENZO, P. S., BLUMBERG, P. M. & WANG, S. 2001. Structural basis of binding of high-affinity ligands to protein kinase C: prediction of the binding modes through a new molecular dynamics method and evaluation by site-directed mutagenesis. *Journal of medicinal chemistry,* 44**,** 1690-701.

PAWSON, T. 1995. Protein modules and signalling networks. *Nature,* 373**,** 573-80.

PERRY, C. W. & PHILLIPS, B. J. 2002. Quick Review: Breast Cancer. *The Internet Journal of Oncology.*

PETTIT, G. R., HERALD, C. L., DOUBEK, D. L., HERALD, D. L., ARNOLD, E. & CLARDY, J. 1982. Isolation and structure of bryostatin 1. *Journal of the American Chemical Society,* 104.

PFISTER, H. 2003. Chapter 8: Human papillomavirus and skin cancer. *J Natl Cancer Inst Monogr***,** 52-6.

PHARMA, L. 2010. *LEO Pharma's PEP005 Meets Primary Endpoint in Phase III Trial for Pre-Cancerous Skin Condition* [Online]. Available: http://www.leo-pharma.com/Home/LEO-Pharma/Media-Centre/News/News-2010/2010-feb-01-LEO-Pharma%E2%80%99s-PEP005-Meets-Primary-Endpoint-in-Phase-III-Trial-for-Pre-Cancerous-Skin-Condition.aspx [Accessed].

PICKERING, J. S., LUPTON, J. R. & CHAPKIN, R. S. 1995. Dietary fat, fiber, and carcinogen alter fecal diacylglycerol composition and mass. *Cancer Res,* 55**,** 2293-8.

PRICE, L. S. & COLLARD, J. G. 2001. Regulation of the cytoskeleton by Rho-family GTPases: implications for tumour cell invasion. *Semin Cancer Biol,* 11**,** 167-73.

PROPPER, D. J., MACAULAY, V., O'BYRNE, K. J., BRAYBROOKE, J. P., WILNER, S. M., GANESAN, T. S., TALBOT, D. C. & HARRIS, A. L. 1998. A phase II study of bryostatin 1 in metastatic malignant melanoma. *Br J Cancer,* 78**,** 1337-41.

QUINN, A. G., CAMPBELL, C., HEALY, E. & REES, J. L. 1994. Chromosome 9 allele loss occurs in both basal and squamous cell carcinomas of the skin. *J Invest Dermatol,* 102**,** 300-3.

QUINN, M. T. & GAUSS, K. A. 2004. Structure and regulation of the neutrophil respiratory burst oxidase: comparison with nonphagocyte oxidases. *J Leukoc Biol,* 76**,** 760-81.

RADY, P., SCINICARIELLO, F., WAGNER, R. F., JR. & TYRING, S. K. 1992. p53 mutations in basal cell carcinomas. *Cancer Res,* 52**,** 3804-6.

RAINGEAUD, J., GUPTA, S., ROGERS, J. S., DICKENS, M., HAN, J., ULEVITCH, R. J. & DAVIS, R. J. 1995. Pro-inflammatory cytokines and environmental stress cause p38 mitogen-activated protein kinase activation by dual phosphorylation on tyrosine and threonine. *J Biol Chem,* 270**,** 7420-6.

RAINGEAUD, J., WHITMARSH, A. J., BARRETT, T., DERIJARD, B. & DAVIS, R. J. 1996. MKK3- and MKK6-regulated gene expression is mediated by the p38 mitogen-activated protein kinase signal transduction pathway. *Mol Cell Biol,* 16**,** 1247-55.

RAMAN, M., CHEN, W. & COBB, M. H. 2007. Differential regulation and properties of MAPKs. *Oncogene,* 26**,** 3100-12.

REEVES, E. P., DEKKER, L. V., FORBES, L. V., WIENTJES, F. B., GROGAN, A., PAPPIN, D. J. & SEGAL, A. W. 1999. Direct interaction between p47phox and protein kinase C: evidence for targeting of protein kinase C by p47phox in neutrophils. *Biochem J,* 344 Pt 3**,** 859-66.

REPINE, J. E., WHITE, J. G., CLAWSON, C. C. & HOLMES, B. M. 1974. The influence of phorbol myristate acetate on oxygen consumption by polymorphonuclear leukocytes. *J Lab Clin Med,* 83**,** 911-20.

REUTHER, G. W. & DER, C. J. 2000. The Ras branch of small GTPases: Ras family members don't fall far from the tree. *Curr Opin Cell Biol,* 12**,** 157-65.

ROBERTS, O. L., HOLMES, K., MULLER, J., CROSS, D. A. & CROSS, M. J. 2009. ERK5 and the regulation of endothelial cell function. *Biochemical Society transactions,* 37**,** 1254-9.

ROBERTS, O. L., HOLMES, K., MULLER, J., CROSS, D. A. & CROSS, M. J. 2010. ERK5 is required for VEGF-mediated survival and tubular morphogenesis of primary human microvascular endothelial cells. *Journal of Cell Science,* 123**,** 3189-200.

ROBINSON, M. J. & COBB, M. H. 1997. Mitogen-activated protein kinase pathways. *Curr Opin Cell Biol,* 9**,** 180-6.

ROOSE, J. P., MOLLENAUER, M., GUPTA, V. A., STONE, J. & WEISS, A. 2005. A diacylglycerol-protein kinase C-RasGRP1 pathway directs Ras activation upon antigen receptor stimulation of T cells. *Molecular and Cellular Biology,* 25**,** 4426-41.

ROSENBAUM, S. E. & NILES, R. M. 1992. Regulation of protein kinase C gene expression by retinoic acid in B16 mouse melanoma cells. *Archives of biochemistry and biophysics,* 294**,** 123-9.

ROSENSTREICH, D. L. & MIZEL, S. B. 1979. Signal requirements for T lymphocyte activation. I. Replacement of macrophage function with phorbol myristic acetate. *J Immunol,* 123**,** 1749-54.

ROUSE, J., COHEN, P., TRIGON, S., MORANGE, M., ALONSO-LLAMAZARES, A., ZAMANILLO, D., HUNT, T. & NEBREDA, A. R. 1994. A novel kinase cascade triggered by stress and heat shock that stimulates MAPKAP kinase-2 and phosphorylation of the small heat shock proteins. *Cell,* 78**,** 1027-37.

RUSSELL, M., LANGE-CARTER, C. A. & JOHNSON, G. L. 1995. Direct interaction between Ras and the kinase domain of mitogen-activated protein kinase kinase kinase (MEKK1). *J Biol Chem,* 270**,** 11757-60.

RUSSO, A. A., JEFFREY, P. D., PATTEN, A. K., MASSAGUE, J. & PAVLETICH, N. P. 1996. Crystal structure of the p27Kip1 cyclin-dependent-kinase inhibitor bound to the cyclin A-Cdk2 complex. *Nature,* 382**,** 325-31.

SABAPATHY, K., HOCHEDLINGER, K., NAM, S. Y., BAUER, A., KARIN, M. & WAGNER, E. F. 2004. Distinct roles for JNK1 and JNK2 in regulating JNK activity and c-Jun-dependent cell proliferation. *Mol Cell,* 15**,** 713-25.

SANDO, J. J. & CHERTIHIN, O. I. 1996. Activation of protein kinase C by lysophosphatidic acid: dependence on composition of phospholipid vesicles. *Biochem J,* 317 (Pt 2)**,** 583-8.

SANO, M. & SCHNEIDER, M. D. 2003. Cyclins that don't cycle--cyclin T/cyclin-dependent kinase-9 determines cardiac muscle cell size. *Cell Cycle,* 2**,** 99-104.

SCHEFFZEK, K., AHMADIAN, M. R., KABSCH, W., WIESMULLER, L., LAUTWEIN, A., SCHMITZ, F. & WITTINGHOFER, A. 1997. The Ras-RasGAP complex: structural basis for GTPase activation and its loss in oncogenic Ras mutants. *Science,* 277**,** 333-8.

SCHLEIMER, R. P., GILLESPIE, E. & LICHTENSTEIN, L. M. 1981. Release of histamine from human leukocytes stimulated with the tumor-promoting phorbol diesters. I. Characterization of the response. *J Immunol,* 126**,** 570-4.

SCHUCHTER, L. M., ESA, A. H., MAY, S., LAULIS, M. K., PETTIT, G. R. & HESS, A. D. 1991. Successful treatment of murine melanoma with bryostatin 1. *Cancer Res,* 51**,** 682-7.

SCHUMACHER, C., CLARK-LEWIS, I., BAGGIOLINI, M. & MOSER, B. 1992. High- and low-affinity binding of GRO alpha and neutrophil-activating peptide 2 to interleukin 8 receptors on human neutrophils. *Proceedings of the National Academy of Sciences of the United States of America,* 89**,** 10542-6.

SEGAL, A. W. 2005. How neutrophils kill microbes. *Annu Rev Immunol,* 23**,** 197-223.

SEIDEL, M. G., KLINGER, M., FREISSMUTH, M. & HOLLER, C. 1999. Activation of mitogen-activated protein kinase by the A(2A)-adenosine receptor via a rap1-dependent and via a p21(ras)-dependent pathway. *J Biol Chem,* 274**,** 25833-41.

SEROVA, M., GHOUL, A., BENHADJI, K. A., FAIVRE, S., LE TOURNEAU, C., CVITKOVIC, E., LOKIEC, F., LORD, J., OGBOURNE, S. M., CALVO, F. & RAYMOND, E. 2008. Effects of protein kinase C modulation by PEP005, a novel ingenol angelate, on mitogen-activated protein kinase and phosphatidylinositol 3-kinase signaling in cancer cells. *Mol Cancer Ther,* 7**,** 915-22.

SEYNAEVE, C. M., STETLER-STEVENSON, M., SEBERS, S., KAUR, G., SAUSVILLE, E. A. & WORLAND, P. J. 1993a. Cell cycle arrest and growth inhibition by the protein kinase antagonist UCN-01 in human breast carcinoma cells. *Cancer Research,* 53**,** 2081-6.

SEYNAEVE, C. M., STETLER-STEVENSON, M., SEBERS, S., KAUR, G., SAUSVILLE, E. A. & WORLAND, P. J. 1993b. Cell cycle arrest and growth inhibition by the protein kinase antagonist UCN-01 in human breast carcinoma cells. *Cancer Res,* 53**,** 2081-6.

SHANMUGAM, M., KRETT, N. L., PETERS, C. A., MAIZELS, E. T., MURAD, F. M., KAWAKATSU, H., ROSEN, S. T. & HUNZICKER-DUNN, M. 1998. Association of PKC delta and active Src in PMA-treated MCF-7 human breast cancer cells. *Oncogene,* 16**,** 1649-54.

SHAUL, Y. D. & SEGER, R. 2006. ERK1c regulates Golgi fragmentation during mitosis. *J Cell Biol,* 172**,** 885-97.

SHERR, C. J. & ROBERTS, J. M. 1995. Inhibitors of mammalian G1 cyclin-dependent kinases. *Genes Dev,* 9**,** 1149-63.

SHIBUYA, E. K. & RUDERMAN, J. V. 1993. Mos induces the in vitro activation of mitogen-activated protein kinases in lysates of frog oocytes and mammalian somatic cells. *Mol Biol Cell,* 4**,** 781-90.

SILINSKY, E. M. & SEARL, T. J. 2003. Phorbol esters and neurotransmitter release: more than just protein kinase C? *Br J Pharmacol,* 138**,** 1191-201.

SILLER, G., GEBAUER, K., WELBURN, P., KATSAMAS, J. & OGBOURNE, S. M. 2009. PEP005 (ingenol mebutate) gel, a novel agent for the treatment of actinic keratosis: results of a randomized, double-blind, vehicle-controlled, multicentre, phase IIa study. *Australas J Dermatol,* 50**,** 16-22.

SILLER, G., ROSEN, R., FREEMAN, M., WELBURN, P., KATSAMAS, J. & OGBOURNE, S. M. 2010. PEP005 (ingenol mebutate) gel for the topical treatment of superficial basal cell carcinoma: results of a randomized phase IIa trial. *Australas J Dermatol,* 51**,** 99-105.

SIMONE, C. & GIORDANO, A. 2001. New insight in cdk9 function: from Tat to MyoD. *Front Biosci,* 6**,** D1073-82.

SKEEL, R. T. 2003. *Handbook of Cancer Chemotherapy*, Lippincott Williams & Wilkins.

SKLADANOWSKI, A. & KONOPA, J. 1993. Adriamycin and daunomycin induce programmed cell death (apoptosis) in tumour cells. *Biochem Pharmacol,* 46**,** 375-82.

SMALLWOOD, J. I. & MALAWISTA, S. E. 1992. Protein kinase C isoforms in human neutrophil cytoplasts. *Journal of Leukocyte Biology,* 51**,** 84-92.

SONG, X., LOPEZ-CAMPISTROUS, A., SUN, L., DOWER, N. A., KEDEI, N., YANG, J., KELSEY, J. S., LEWIN, N. E., ESCH, T. E., BLUMBERG, P. M. & STONE, J. C. 2013. RasGRPs are targets of the anti-cancer agent ingenol-3-angelate. *PLoS One,* 8**,** e72331.

SOSMAN, J. A., KIM, K. B., SCHUCHTER, L., GONZALEZ, R., PAVLICK, A. C., WEBER, J. S., MCARTHUR, G. A., HUTSON, T. E., MOSCHOS, S. J., FLAHERTY, K. T., HERSEY, P., KEFFORD, R., LAWRENCE, D., PUZANOV, I., LEWIS, K. D., AMARAVADI, R. K., CHMIELOWSKI, B., LAWRENCE, H. J., SHYR, Y., YE, F., LI, J., NOLOP, K. B., LEE, R. J., JOE, A. K. & RIBAS, A. 2012. Survival in BRAF V600-mutant advanced melanoma treated with vemurafenib. *The New England journal of medicine,* 366**,** 707-14.

STANLEY, E. R., BERG, K. L., EINSTEIN, D. B., LEE, P. S., PIXLEY, F. J., WANG, Y. & YEUNG, Y. G. 1997. Biology and action of colony--stimulating factor-1. *Molecular reproduction and development,* 46**,** 4-10.

STEINBERG, S. F. 2005. Protein Kinase C delta. *UCSD-Nature Molecule Pages.*

STIEGLER, P. & GIORDANO, A. 2001. The family of retinoblastoma proteins. *Crit Rev Eukaryot Gene Expr,* 11**,** 59-76.

STOKOE, D., CAMPBELL, D. G., NAKIELNY, S., HIDAKA, H., LEEVERS, S. J., MARSHALL, C. & COHEN, P. 1992. MAPKAP kinase-2; a novel protein kinase activated by mitogen-activated protein kinase. *EMBO J,* 11**,** 3985-94.

STONE, J. C. 2011. Regulation and Function of the RasGRP Family of Ras Activators in Blood Cells. *Genes & cancer,* 2**,** 320-34.

SUGDEN, P. H. & CLERK, A. 1998. Cellular mechanisms of cardiac hypertrophy. *Journal of molecular medicine,* 76**,** 725-46.

SUOMELA, S., CAO, L., BOWCOCK, A. & SAARIALHO-KERE, U. 2004. Interferon alpha-inducible protein 27 (IFI27) is upregulated in psoriatic skin and certain epithelial cancers. *The Journal of investigative dermatology,* 122**,** 717-21.

SUTTON, R. B., DAVLETOV, B. A., BERGHUIS, A. M., SUDHOF, T. C. & SPRANG, S. R. 1995. Structure of the first C2 domain of synaptotagmin I: a novel Ca2+/phospholipid-binding fold. *Cell,* 80**,** 929-38.

SZALLASI, Z., DENNING, M. F., SMITH, C. B., DLUGOSZ, A. A., YUSPA, S. H., PETTIT, G. R. & BLUMBERG, P. M. 1994. Bryostatin 1 protects protein kinase C-delta from down-regulation in mouse keratinocytes in parallel with its inhibition of phorbol ester-induced differentiation. *Mol Pharmacol,* 46**,** 840-50.

TAKAI, Y., KISHIMOTO, A., INOUE, M. & NISHIZUKA, Y. 1977. Studies on a cyclic nucleotide-independent protein kinase and its proenzyme in mammalian tissues. I. Purification and characterization of an active enzyme from bovine cerebellum. *J Biol Chem,* 252**,** 7603-9.

TAKAI, Y., KISHIMOTO, A., IWASA, Y., KAWAHARA, Y., MORI, T. & NISHIZUKA, Y. 1979. Calcium-dependent activation of a multifunctional protein kinase by membrane phospholipids. *J Biol Chem,* 254**,** 3692-5.

TAKAI, Y., SASAKI, T. & MATOZAKI, T. 2001. Small GTP-binding proteins. *Physiol Rev,* 81**,** 153-208.

TAN, Y., ROUSE, J., ZHANG, A., CARIATI, S., COHEN, P. & COMB, M. J. 1996. FGF and stress regulate CREB and ATF-1 via a pathway involving p38 MAP kinase and MAPKAP kinase-2. *EMBO J,* 15**,** 4629-42.

TANAKA, H., ONO, Y., NAKATA, S., SHINTANI, Y., SAKAKIBARA, N. & MORITA, A. 2007. Tobacco smoke extract induces premature skin aging in mouse. *J Dermatol Sci,* 46**,** 69-71.

TATEDA, K., MOORE, T. A., NEWSTEAD, M. W., TSAI, W. C., ZENG, X., DENG, J. C., CHEN, G., REDDY, R., YAMAGUCHI, K. & STANDIFORD, T. J. 2001. Chemokine-dependent neutrophil recruitment in a murine model of Legionella pneumonia: potential role of neutrophils as immunoregulatory cells. *Infection and immunity,* 69**,** 2017-24.

TECHNOLOGY, C. S. *MAP Kinase Signaling Resources* [Online]. Available: http://www.cellsignal.com/common/content/content.jsp?id=science-pathways-mapk [Accessed].

THE BREAST CANCER LINKAGE CONSORTIUM 1999. Cancer risks in BRCA2 mutation carriers. *Journal of the National Cancer Institute,* 91**,** 1310-1316.

THOMPSON, D., EASTON, D. F. & THE BREAST CANCER LINKAGE CONSORTIUM 2002. Cancer incidence in BRCA1 mutation carriers. *Journal of the National Cancer Institute* 94**,** 1358–1365.

THORBURN, J., XU, S. & THORBURN, A. 1997. MAP kinase- and Rho-dependent signals interact to regulate gene expression but not actin morphology in cardiac muscle cells. *EMBO J,* 16**,** 1888-900.

TOKER, A. 1998. Signaling through protein kinase C. *Front Biosci,* 3**,** D1134-47.

TOKER, A., MEYER, M., REDDY, K. K., FALCK, J. R., ANEJA, R., ANEJA, S., PARRA, A., BURNS, D. J., BALLAS, L. M. & CANTLEY, L. C. 1994. Activation of protein kinase C family members by the novel polyphosphoinositides PtdIns-3,4-P2 and PtdIns-3,4,5-P3. *J Biol Chem,* 269**,** 32358-67.

TOURNIER, C., HESS, P., YANG, D. D., XU, J., TURNER, T. K., NIMNUAL, A., BAR-SAGI, D., JONES, S. N., FLAVELL, R. A. & DAVIS, R. J. 2000. Requirement of JNK for stress-induced activation of the cytochrome c-mediated death pathway. *Science,* 288**,** 870-4.

TOURNIER, C., WHITMARSH, A. J., CAVANAGH, J., BARRETT, T. & DAVIS, R. J. 1997. Mitogen-activated protein kinase kinase 7 is an activator of the c-Jun NH2-terminal kinase. *Proc Natl Acad Sci U S A,* 94**,** 7337-42.

TOYOSHIMA, F., MORIGUCHI, T. & NISHIDA, E. 1997. Fas induces cytoplasmic apoptotic responses and activation of the MKK7-JNK/SAPK and MKK6-p38 pathways independent of CPP32-like proteases. *J Cell Biol,* 139**,** 1005-15.

TSAI, J. H., HSIEH, Y. S., KUO, S. J., CHEN, S. T., YU, S. Y., HUANG, C. Y., CHANG, A. C., WANG, Y. W., TSAI, M. T. & LIU, J. Y. 2000. Alteration in the expression of protein kinase C isoforms in human hepatocellular carcinoma. *Cancer Lett,* 161**,** 171-5.

TU, H., JACOBS, S. C., BORKOWSKI, A. & KYPRIANOU, N. 1996. Incidence of apoptosis and cell proliferation in prostate cancer: relationship with TGF-beta1 and bcl-2 expression. *Int J Cancer,* 69**,** 357-63.

UHLINGER, D. J., TYAGI, S. R., INGE, K. L. & LAMBETH, J. D. 1993. The respiratory burst oxidase of human neutrophils. Guanine nucleotides and arachidonate regulate the assembly of a multicomponent complex in a semirecombinant cell-free system. *The Journal of Biological Chemistry,* 268**,** 8624-31.

UNDEN, A. B., HOLMBERG, E., LUNDH-ROZELL, B., STAHLE-BACKDAHL, M., ZAPHIROPOULOS, P. G., TOFTGARD, R. & VORECHOVSKY, I. 1996. Mutations in the human homologue of Drosophila patched (PTCH) in basal cell carcinomas and the Gorlin syndrome: different in vivo mechanisms of PTCH inactivation. *Cancer Res,* 56**,** 4562-5.

VALVERDE, A. M., SINNETT-SMITH, J., VAN LINT, J. & ROZENGURT, E. 1994. Molecular cloning and characterization of protein kinase D: a target for diacylglycerol and phorbol esters with a distinctive catalytic domain. *Proc Natl Acad Sci U S A,* 91**,** 8572-6.

VARTERASIAN, M. L., MOHAMMAD, R. M., EILENDER, D. S., HULBURD, K., RODRIGUEZ, D. H., PEMBERTON, P. A., PLUDA, J. M., DAN, M. D., PETTIT, G. R., CHEN, B. D. & AL-KATIB, A. M. 1998. Phase I study of bryostatin 1 in patients with relapsed non-Hodgkin's lymphoma and chronic lymphocytic leukemia. *J Clin Oncol,* 16**,** 56-62.

VARTERASIAN, M. L., MOHAMMAD, R. M., SHURAFA, M. S., HULBURD, K., PEMBERTON, P. A., RODRIGUEZ, D. H., SPADONI, V., EILENDER, D. S., MURGO,

A., WALL, N., DAN, M. & AL-KATIB, A. M. 2000. Phase II trial of bryostatin 1 in patients with relapsed low-grade non-Hodgkin's lymphoma and chronic lymphocytic leukemia. *Clin Cancer Res,* 6**,** 825-8.

VOGELSTEIN, B., FEARON, E. R., HAMILTON, S. R., KERN, S. E., PREISINGER, A. C., LEPPERT, M., NAKAMURA, Y., WHITE, R., SMITS, A. M. & BOS, J. L. 1988. Genetic alterations during colorectal-tumor development. *N Engl J Med,* 319**,** 525-32.

VOSSLER, M. R., YAO, H., YORK, R. D., PAN, M. G., RIM, C. S. & STORK, P. J. 1997. cAMP activates MAP kinase and Elk-1 through a B-Raf- and Rap1-dependent pathway. *Cell,* 89**,** 73-82.

WALKER, P. R., SMITH, C., YOUDALE, T., LEBLANC, J., WHITFIELD, J. F. & SIKORSKA, M. 1991. Topoisomerase II-reactive chemotherapeutic drugs induce apoptosis in thymocytes. *Cancer Res,* 51**,** 1078-85.

WANG, X. S., DIENER, K., MANTHEY, C. L., WANG, S., ROSENZWEIG, B., BRAY, J., DELANEY, J., COLE, C. N., CHAN-HUI, P. Y., MANTLO, N., LICHENSTEIN, H. S., ZUKOWSKI, M. & YAO, Z. 1997. Molecular cloning and characterization of a novel p38 mitogen-activated protein kinase. *J Biol Chem,* 272**,** 23668-74.

WEICHERT, W., GEKELER, V., DENKERT, C., DIETEL, M. & HAUPTMANN, S. 2003. Protein kinase C isoform expression in ovarian carcinoma correlates with indicators of poor prognosis. *Int J Oncol,* 23**,** 633-9.

WEINBERG, R. A. 1995. The retinoblastoma protein and cell cycle control. *Cell,* 81**,** 323-30.

WEINBERG, R. A. 2007a. **pRb and Control of the Cell Cycle Clock**. ***Garland Science***.

WEINBERG, R. A. 2007b. *pRb and Control of the Cell Cycle Clock,* Garland Science.

WEN-SHENG, W. 2003. ERK signaling pathway is involved in p15INK4b/p16INK4a expression and HepG2 growth inhibition triggered by TPA and Saikosaponin a. *Oncogene,* 22**,** 955-63.

WESTLIN, W. F. & GIMBRONE, M. A., JR. 1993. Neutrophil-mediated damage to human vascular endothelium. Role of cytokine activation. *The American journal of pathology,* 142**,** 117-28.

WETSEL, W. C., KHAN, W. A., MERCHENTHALER, I., RIVERA, H., HALPERN, A. E., PHUNG, H. M., NEGRO-VILAR, A. & HANNUN, Y. A. 1992. Tissue and cellular distribution of the extended family of protein kinase C isoenzymes. *J Cell Biol,* 117**,** 121-33.

WHITMARSH, A. J., SHORE, P., SHARROCKS, A. D. & DAVIS, R. J. 1995. Integration of MAP kinase signal transduction pathways at the serum response element. *Science,* 269**,** 403-7.

WILLMORE-PAYNE, C., HOLDEN, J. A. & LAYFIELD, L. J. 2006. Detection of EGFR- and HER2-activating mutations in squamous cell carcinoma involving the head and neck. *Mod Pathol,* 19**,** 634-40.

WILLMORE-PAYNE, C., HOLDEN, J. A., TRIPP, S. & LAYFIELD, L. J. 2005. Human malignant melanoma: detection of BRAF- and c-kit-activating mutations by high-resolution amplicon melting analysis. *Hum Pathol,* 36**,** 486-93.

WOLPE, S. D., DAVATELIS, G., SHERRY, B., BEUTLER, B., HESSE, D. G., NGUYEN, H. T., MOLDAWER, L. L., NATHAN, C. F., LOWRY, S. F. & CERAMI, A. 1988. Macrophages secrete a novel heparin-binding protein with inflammatory and neutrophil chemokinetic properties. *The Journal of experimental medicine,* 167**,** 570-81.

WU, Z., WU, J., JACINTO, E. & KARIN, M. 1997. Molecular cloning and characterization of human JNKK2, a novel Jun NH2-terminal kinase-specific kinase. *Mol Cell Biol,* 17**,** 7407-16.

XU, S., ROBBINS, D. J., CHRISTERSON, L. B., ENGLISH, J. M., VANDERBILT, C. A. & COBB, M. H. 1996. Cloning of rat MEK kinase 1 cDNA reveals an endogenous membrane-associated 195-kDa protein with a large regulatory domain. *Proc Natl Acad Sci U S A,* 93**,** 5291-5.

YAO, Z., DIENER, K., WANG, X. S., ZUKOWSKI, M., MATSUMOTO, G., ZHOU, G., MO, R., SASAKI, T., NISHINA, H., HUI, C. C., TAN, T. H., WOODGETT, J. P. & PENNINGER, J. M. 1997. Activation of stress-activated protein kinases/c-Jun N-terminal protein kinases (SAPKs/JNKs) by a novel mitogen-activated protein kinase kinase. *J Biol Chem,* 272**,** 32378-83.

YEE, A. S., SHIH, H. H. & TEVOSIAN, S. G. 1998. New perspectives on retinoblastoma family functions in differentiation. *Front Biosci,* 3**,** D532-47.

YUNG, Y., YAO, Z., HANOCH, T. & SEGER, R. 2000. ERK1b, a 46-kDa ERK isoform that is differentially regulated by MEK. *J Biol Chem,* 275**,** 15799-808.

YUSPA, S. H., VIGUERA, C. & NIMS, R. 1979. Maintenance Of Human-Skin On Nude-Mice For Studies Of Chemical Carcinogenesis. *Cancer Letters,* 6**,** 301-310.

ZHANG, G., KAZANIETZ, M. G., BLUMBERG, P. M. & HURLEY, J. H. 1995. Crystal structure of the cys2 activator-binding domain of protein kinase C delta in complex with phorbol ester. *Cell,* 81**,** 917-24.

ZHENG, C. F. & GUAN, K. L. 1993. Cloning and characterization of two distinct human extracellular signal-regulated kinase activator kinases, MEK1 and MEK2. *J Biol Chem,* 268**,** 11435-9.

ZHOU, G., BAO, Z. Q. & DIXON, J. E. 1995. Components of a new human protein kinase signal transduction pathway. *J Biol Chem,* 270**,** 12665-9.

ZHOU, W., TAKUWA, N., KUMADA, M. & TAKUWA, Y. 1993. Protein kinase C-mediated bidirectional regulation of DNA synthesis, RB protein phosphorylation, and cyclin-dependent kinases in human vascular endothelial cells. *J Biol Chem,* 268**,** 23041-8.

ZHOU, W., TAKUWA, N., KUMADA, M. & TAKUWA, Y. 1994. E2F1, B-myb and selective members of cyclin/cdk subunits are targets for protein kinase C-mediated bimodal growth regulation in vascular endothelial cells. *Biochem Biophys Res Commun,* 199**,** 191-8.

ZIVKOVIC, M., POLJAK-BLAZI, M., EGGER, G., SUNJIC, S. B., SCHAUR, R. J. & ZARKOVIC, N. 2005. Oxidative burst and anticancer activities of rat neutrophils. *BioFactors,* 24**,** 305-12.

ZIVKOVIC, M., POLJAK-BLAZI, M., ZARKOVIC, K., MIHALJEVIC, D., SCHAUR, R. J. & ZARKOVIC, N. 2007. Oxidative burst of neutrophils against melanoma B16-F10. *Cancer Lett,* 246**,** 100-8.

ZOELLNER, H., HOFLER, M., BECKMANN, R., HUFNAGL, P., VANYEK, E., BIELEK, E., WOJTA, J., FABRY, A., LOCKIE, S. & BINDER, B. R. 1996. Serum albumin is a specific inhibitor of apoptosis in human endothelial cells. *J Cell Sci,* 109 (Pt 10)**,** 2571-80.

ZONG, W. X. & THOMPSON, C. B. 2006. Necrotic death as a cell fate. *Genes Dev,* 20**,** 1-15.

ZUCKER, M. B., TROLL, W. & BELMAN, S. 1974. TUMOR-PROMOTER PHORBOL ESTER (12-0-TETRADECANOYL-PHORBOL-13-ACETATE), A POTENT AGGREGATING AGENT FOR BLOOD-PLATELETS. *Journal of Cell Biology,* 60**,** 325-336.

ZWARTKRUIS, F. J., WOLTHUIS, R. M., NABBEN, N. M., FRANKE, B. & BOS, J. L. 1998. Extracellular signal-regulated activation of Rap1 fails to interfere in Ras effector signalling. *EMBO J,* 17**,** 5905-12.

Appendix

Appendix 1

MONITORING OF TUMOR-BEARING MICE:

The mice will be monitored by the following clinical assessment criteria for distress during the period of the experiment to determine whether the treatments described in this application (i.e., tumor burden and effects of drugs) are causing distress to the mice to a degree to where they should be euthanased.

Clinical scoring

Criteria	Grade 0	Grade 1	Grade 2
Weight loss	<10%	>10 to <25%	>25%
Posture	Normal	Hunching noted only at rest	Severe hunching impairs movement
Activity	Normal	Mild to moderately decreased	Stationary unless stimulated
Fur texture	Normal	Mild to moderate ruffling	Severe ruffling/poor grooming
Sunburn	Normal	Minor erythema	Major erythema with blistering

Scores for each parameter are summed to give a possible total of 8.

Mild: <3

Moderate: 3 to 6

Severe: >6

Additional criterion for euthanasing tumour-bearing mice

Total tumor volume/mouse = 1000 mm^3 (1ml).

Total tumor burden should be limited to 1 gm/mouse (e.g., Teicher et al, Anticancer Drug Development Guide, Humana Press, 1997, p91). The commonly-used literature method will be used to calculate volume:

Volume = A x b x b x 0.5, where A is the length and b is the measured breadth of the tumor lump (skin included, thus still an overestimate). (Teicher et al, ibid., p92). Mouse weight, area of local inflammation and tumor volume measured every second day for 2 weeks from initial treatment, then twice weekly for the last 2 weeks.

A look-up table will be used in the animal house (attached), to quickly calculate the total tumor burden and euthanase if necessary.

The mouse will be euthanased if the above score reaches 3 on the above cumulative criteria, or if the total tumour burden/mouse reaches the above dimensions.

Mouse Tumor Volume (cubic mm) (across = length in mm down = width in mm)

First read off the volume of each tumor, then add the individual volumes to obtain the total tumor burden.

	2	3	4	5	6	7	8	9	10	11	12	13	14	15	16	17	18	19	20
1	1	2	2	3	3	4	4	5	5	6	6	7	7	8	8	9	9	10	10
2	4	6	8	10	12	14	16	18	20	22	24	26	28	30	32	34	36	38	40
3		14	18	23	27	32	36	41	45	50	54	59	63	68	72	77	81	86	90
4			32	40	48	56	64	72	80	88	96	104	112	120	128	136	144	152	160
5				63	75	88	100	113	125	138	150	163	175	188	200	213	225	238	250
6					108	126	144	162	180	198	216	234	252	270	288	306	324	342	360
7						172	196	221	245	270	294	319	343	368	392	417	441	466	490
8							256	288	320	352	384	416	448	480	512	544	576	608	640
9								365	405	446	486	527	567	608	648	689	729	770	810
10									500	550	600	650	700	750	800	850	900	950	1000
11										666	726	787	847	908	968	1029	1089	1150	1210
12											864	936	1008	1080	1152	1224	1296	1368	1440

Table 1: Calculation chart titled "Monitoring of Tumor Bearing Mice" following clinical assessment criteris was used to measure the volume of tumors.

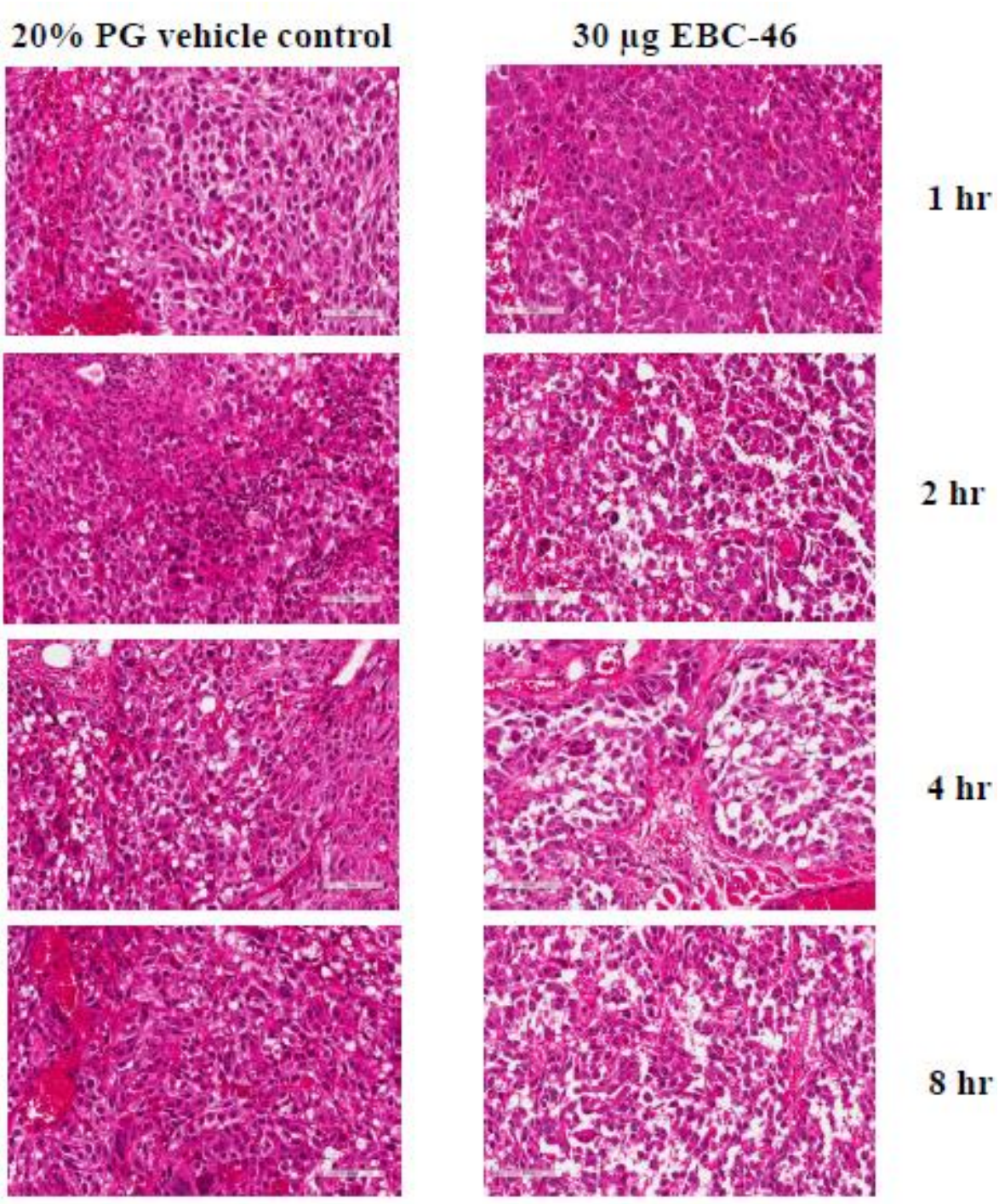

Figure 1: Sk-Mel-28 tumor sections stained with H&E for histological analysis where tumors were treated with 20% PG vehicle control or 30 µg of EBC-46 following treatment from 1 hr up to 7 days.

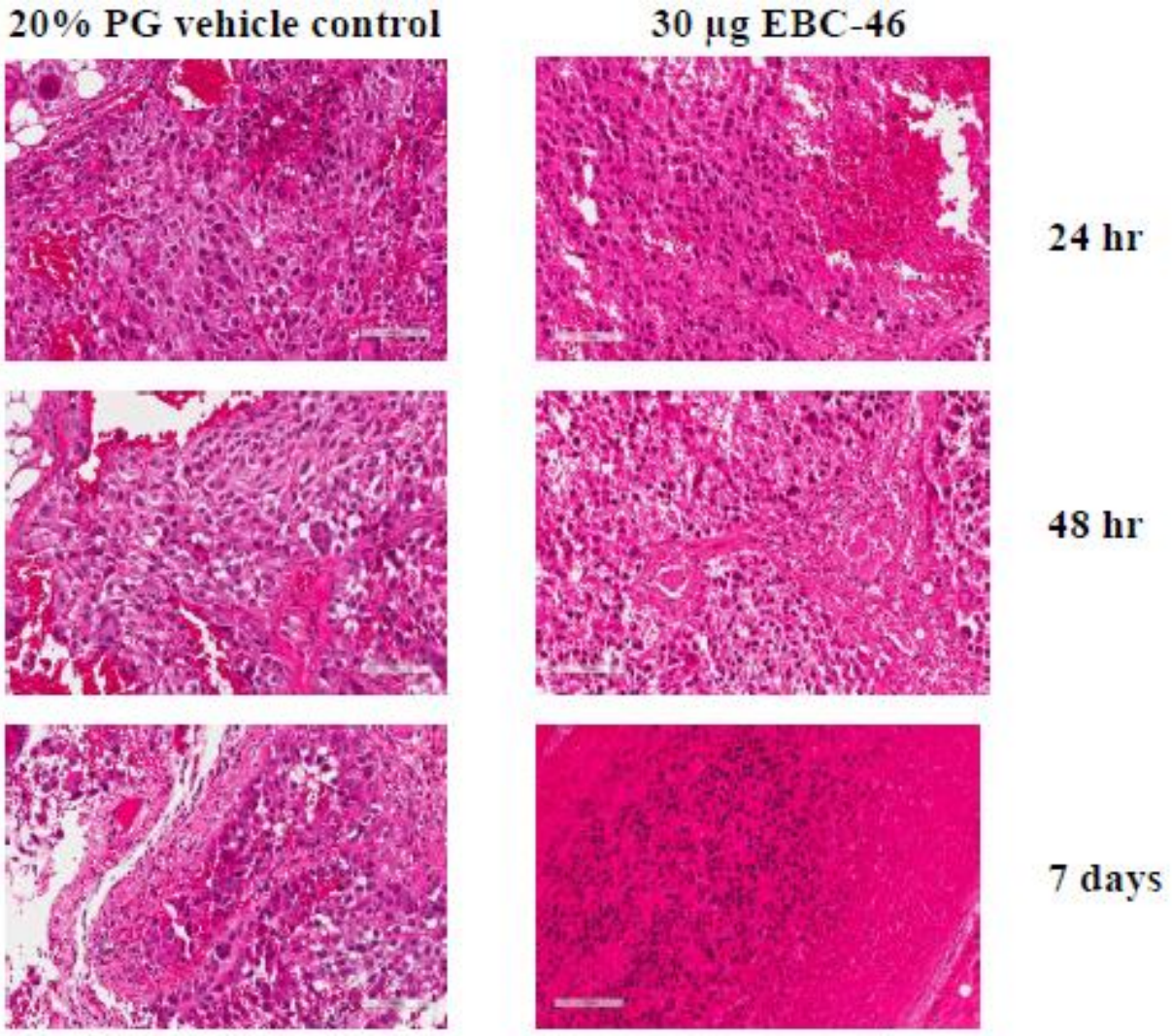

Figure 1 (contd.): Sk-Mel-28 tumor sections stained with H&E for histological analysis where tumors treated with 20% PG vehicle control or 30 µg of EBC-46 following treatment from 1 hr after up to 7 days.

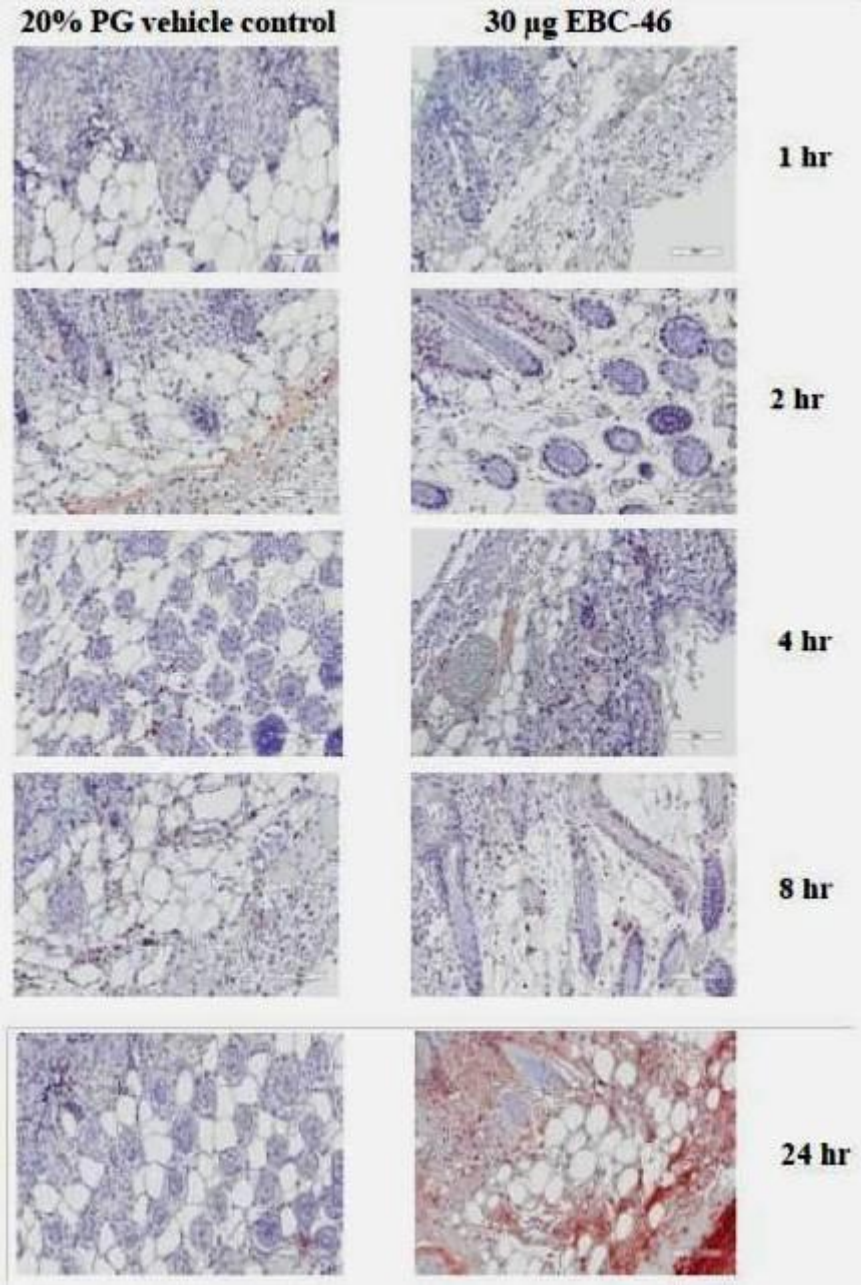

Figure 2: Normal skin sections stained with MPO for neutrophils where skin treated with 20% PG vehicle control or 30 µg of EBC-46 following treatment from 1 hr after up to 7 days

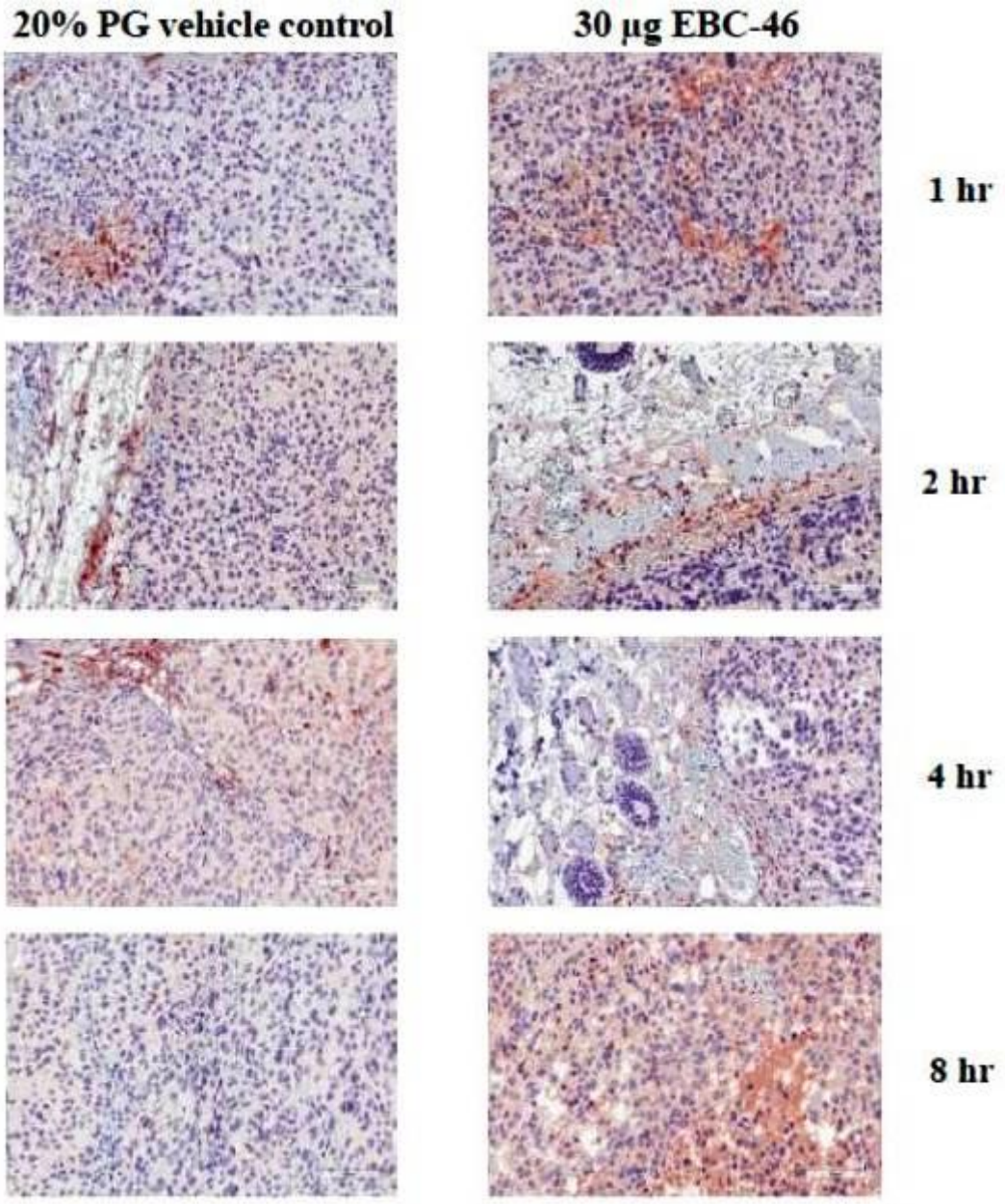

Figure 3: Sk-Mel-28 tumor sections stained with MPO for neutrophils where tumors were treated with 20% PG vehicle control or 30 µg of EBC-46 following treatment from 1 hr after up to 7 days.

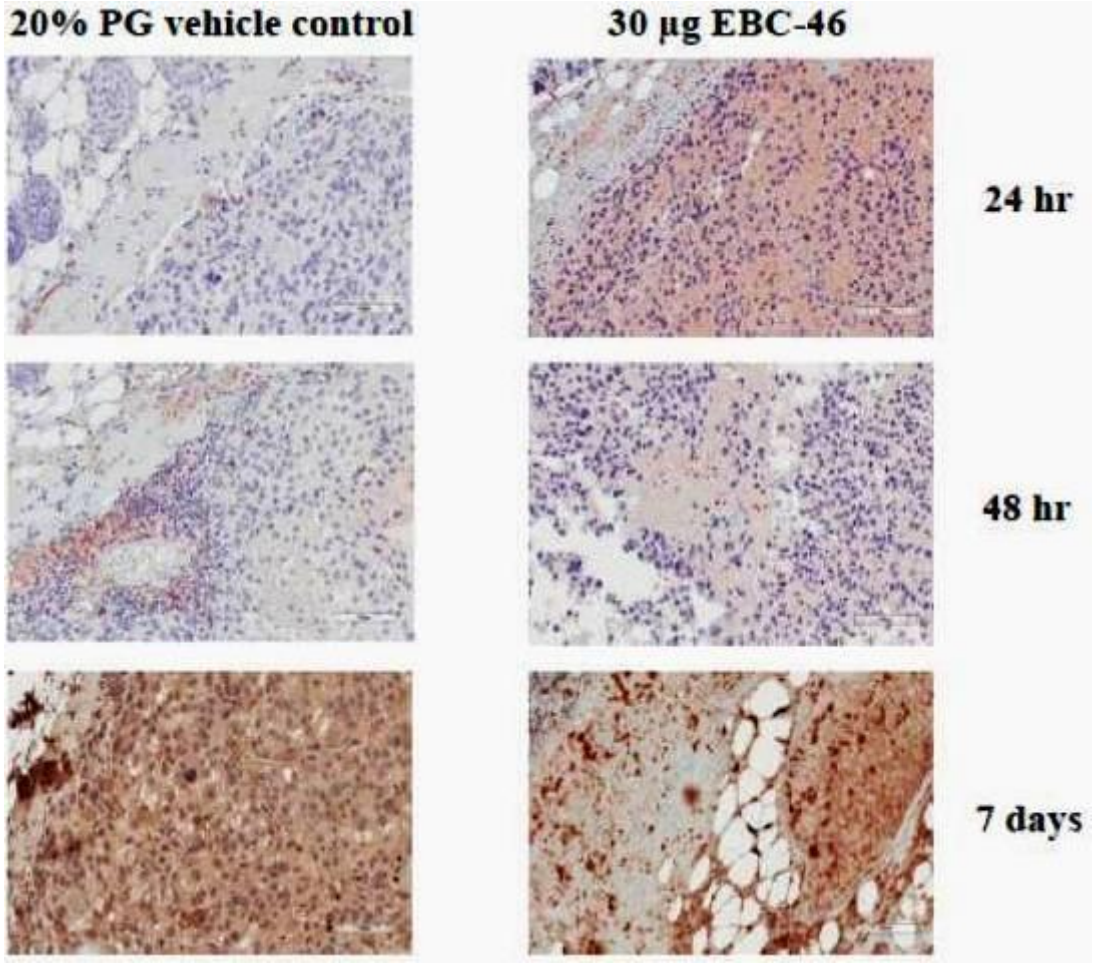

Figure 3 (contd.): Sk-Mel-28 tumor sections stained with MPO for neutrophils where tumors treated with 20% PG vehicle control or 30 µg of EBC-46 following treatment from 1 hr after up to 7 days.

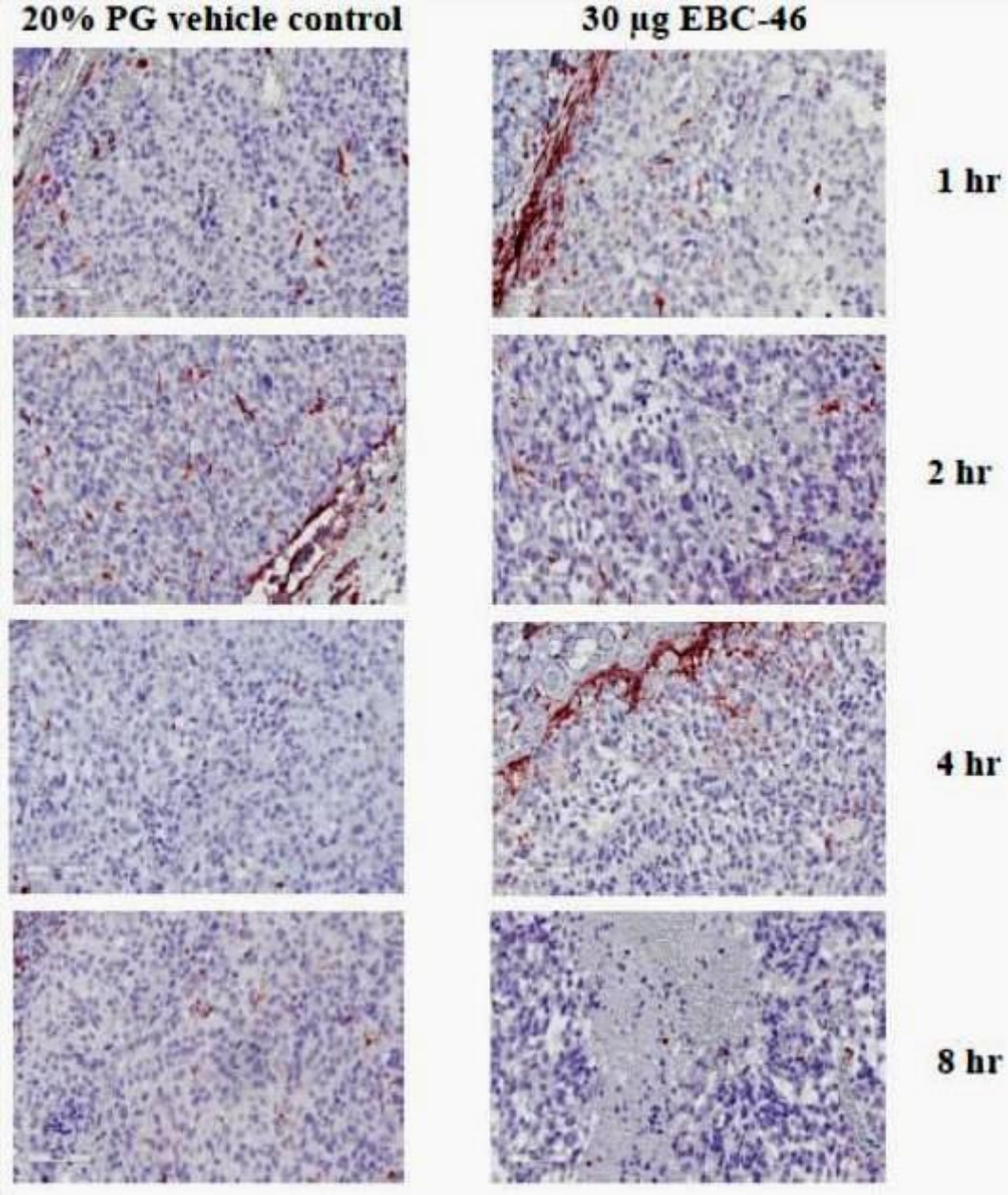

Figure 4: Sk-Mel-28 tumor sections stained with F4/80 for macrophages where tumors treated with 20% PG vehicle control or 30 µg of EBC-46 following treatment from 1 hr after up to 7 days

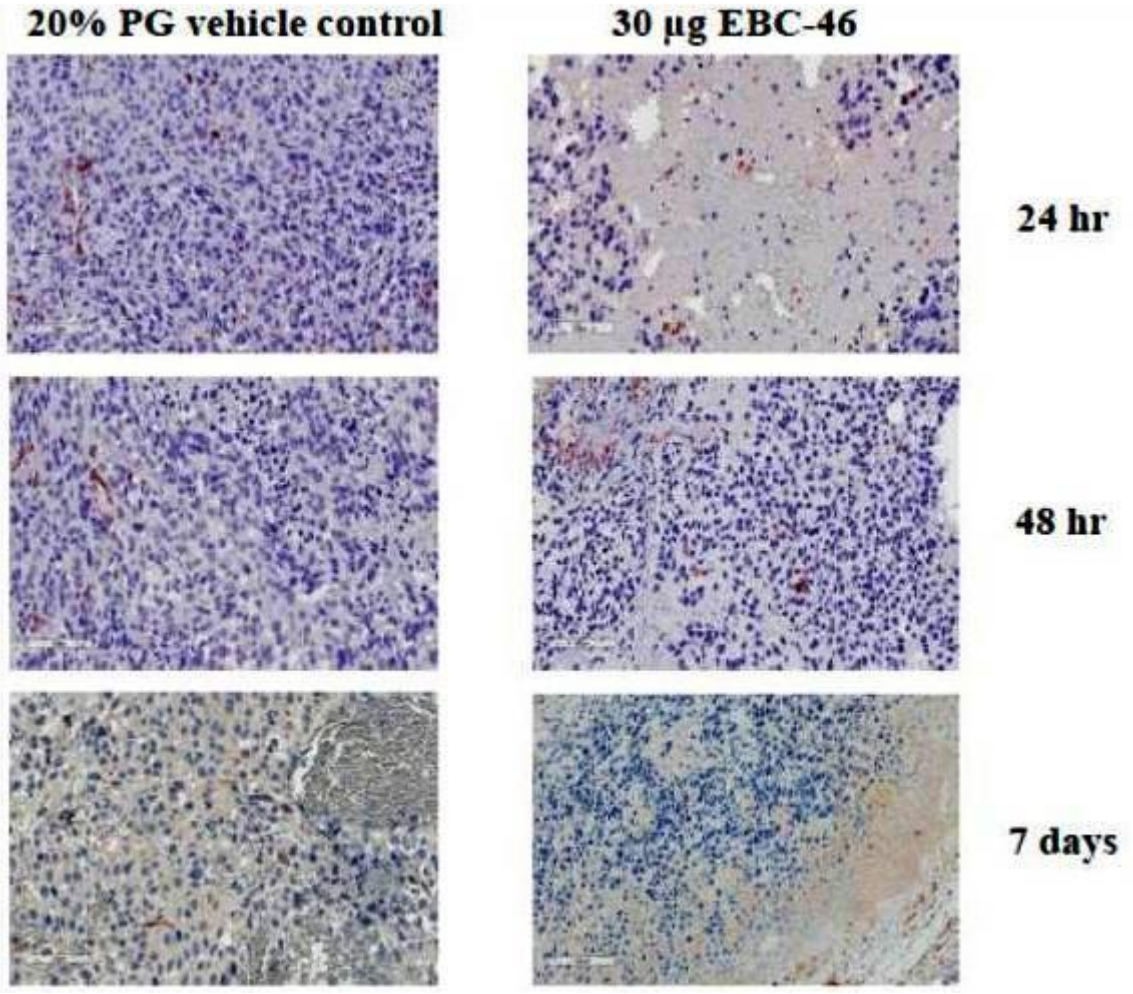

Figure 4 (contd.): Sk-Mel-28 tumor sections stained with F4/80 for macrophages where tumors treated with 20% PG vehicle control or 30 µg of EBC-46 following treatment from 1 hr after up to 7 days

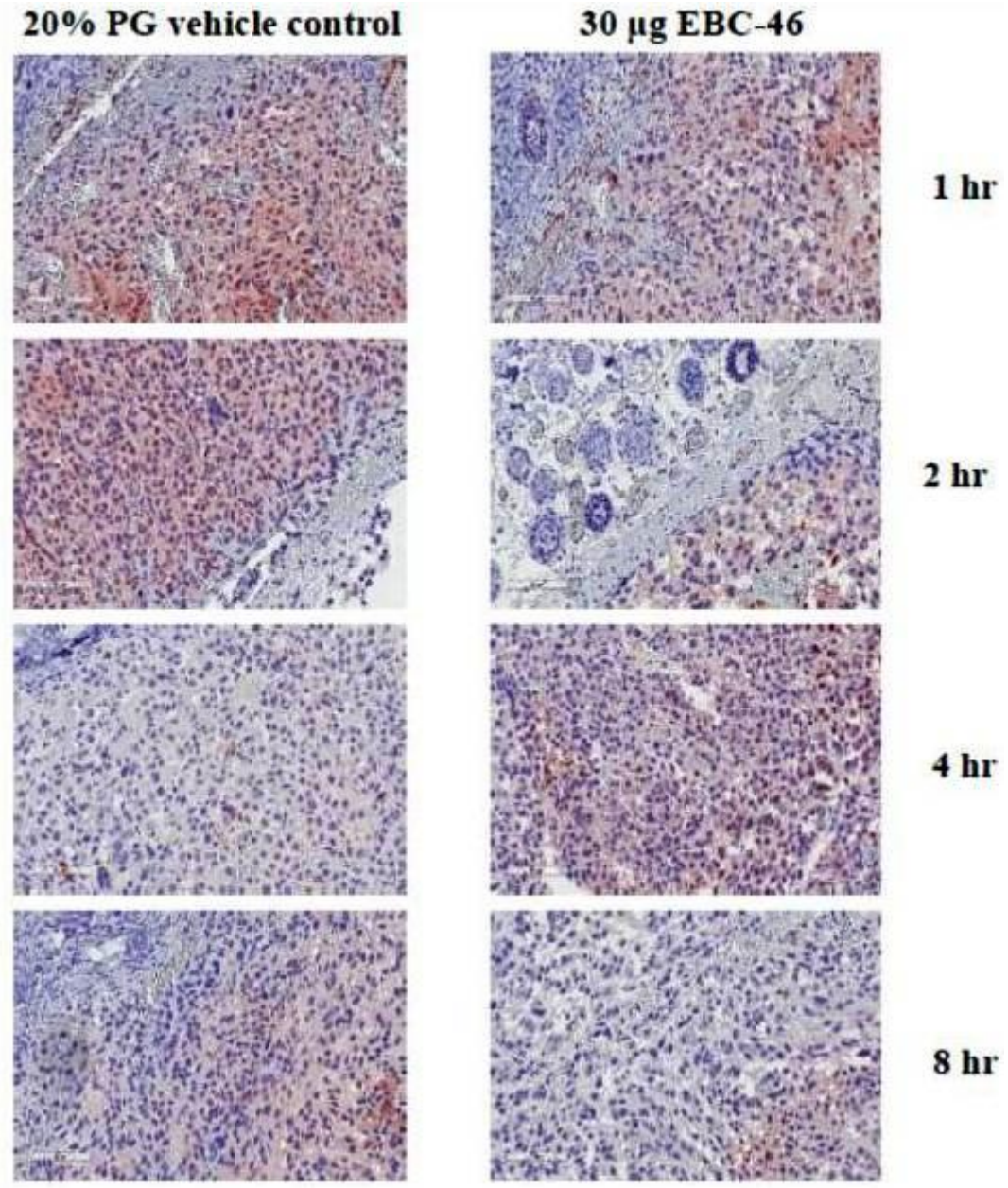

Figure 5: **Sk-Mel-28 tumor sections stained with CD-31 for endothelial cells where tumors treated with 20% PG vehicle control or 30 µg of EBC-46 following treatment from 1 hr after treatment up to 7 days.**

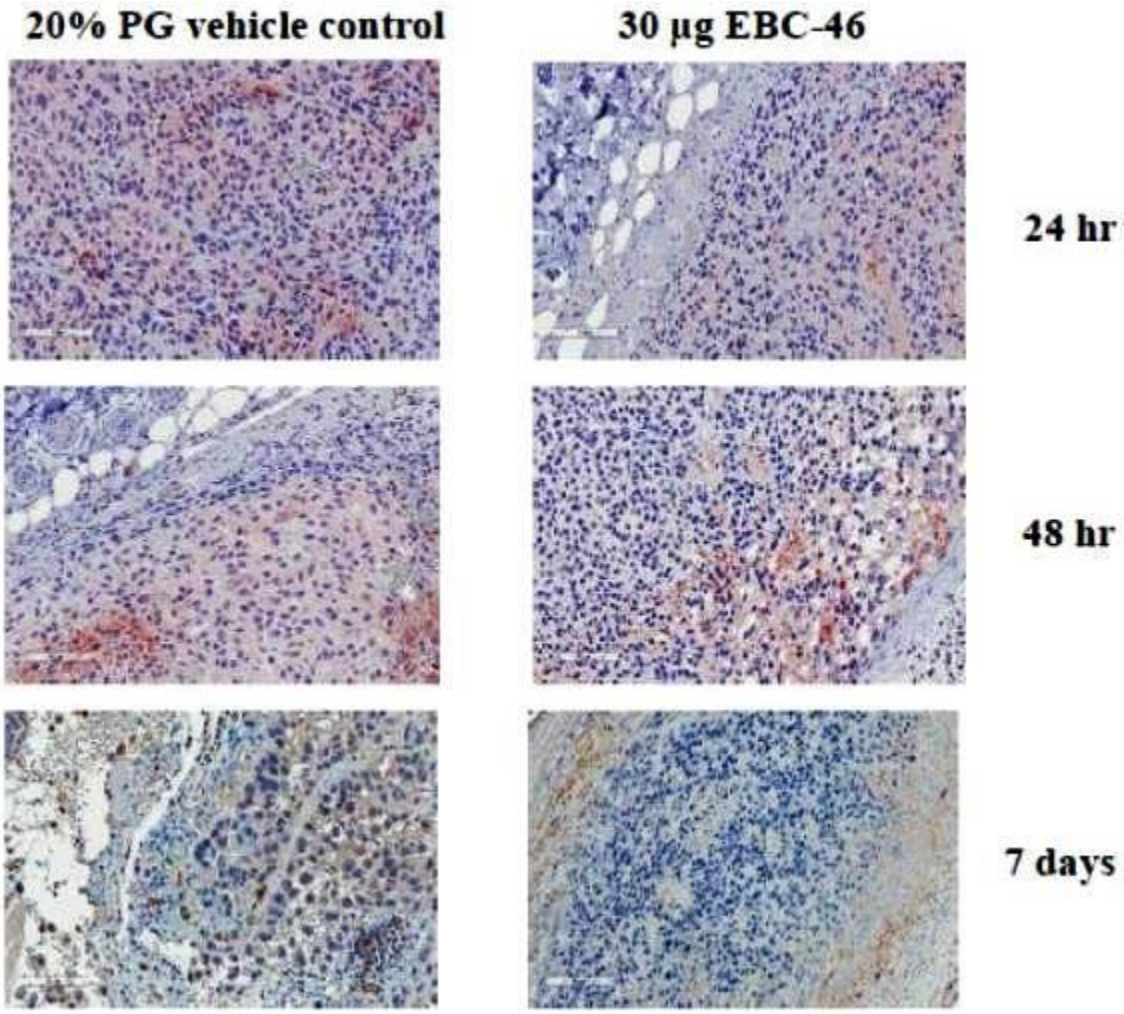

Figure 5 (contd.): Sk-Mel-28 tumor sections stained with CD-31 for endothelial cells where tumors treated with 20% PG vehicle control or 30 µg of EBC-46 following treatment from 1 hr after up to 7 days.

Appendix Table 1: Top twenty genes significantly UP-regulated following 1 hr treatment by 30 µg EBC-46 (compared to vehicle control 20% PG) in Sk-Mel-28 tumors as detected on HumanHT-12 v4 Illumina BeadChips.

ProbeID	p Value	Regulation	FC (abs)	Symbol	Definition
2510164	0.009	up	14.037	SNORD3A	Homo sapiens small nucleolar RNA, C/D box 3A (SNORD3A), small nucleolar RNA.
580161	0.009	up	12.791	SNORD3C	Homo sapiens small nucleolar RNA, C/D box 3C (SNORD3C), small nucleolar RNA.
380685	0.010	up	11.884	SNORD3D	Homo sapiens small nucleolar RNA, C/D box 3D (SNORD3D), small nucleolar RNA.
2750475	0.029	up	1.701	D4S234E	Homo sapiens DNA segment on chromosome 4 (unique) 234 expressed sequence (D4S234E), transcript variant 2, mRNA.
6290142	0.047	up	1.669	LOC100008589	Homo sapiens 28S ribosomal RNA (LOC100008589), non-coding RNA.
5310634	0.045	up	1.578	FASN	Homo sapiens fatty acid synthase (FASN), mRNA.
6840301	0.030	up	1.395	NT5DC2	Homo sapiens 5'-nucleotidase domain containing 2 (NT5DC2), mRNA.
6280504	0.040	up	1.374	LOC100008589	Homo sapiens 28S ribosomal RNA (LOC100008589), non-coding RNA.
840474	0.039	up	1.367	GSTZ1	Homo sapiens glutathione transferase zeta 1 (maleylacetoacetate isomerase) (GSTZ1), transcript variant 2, mRNA.
3850722	0.040	up	1.365	TMEM185B	Homo sapiens transmembrane protein 185B (pseudogene) (TMEM185B), non-coding RNA.
4050056	0.045	up	1.341	TBC1D16	Homo sapiens TBC1 domain family, member 16 (TBC1D16), mRNA.
3930356	0.028	up	1.319	SNX8	Homo sapiens sorting nexin 8 (SNX8), mRNA.
3940458	0.010	up	1.319	CRYL1	Homo sapiens crystallin, lambda 1 (CRYL1), mRNA.
4040605	0.010	up	1.310	PSEN2	Homo sapiens presenilin 2 (Alzheimer disease 4) (PSEN2), transcript variant 2, mRNA.
1030768	0.043	up	1.306	LDLRAP1	Homo sapiens low density lipoprotein receptor adaptor protein 1 (LDLRAP1), mRNA.
4780364	0.012	up	1.305	C11orf1	Homo sapiens chromosome 11 open reading frame 1 (C11orf1), mRNA.
7160161	0.029	up	1.305	S100A5	Homo sapiens S100 calcium binding protein A5 (S100A5), mRNA.
4610215	0.042	up	1.299	CTNNBIP1	Homo sapiens catenin, beta interacting protein 1 (CTNNBIP1), transcript variant 1, mRNA.
6590037	0.013	up	1.298	SLC20A2	Homo sapiens solute carrier family 20 (phosphate transporter), member 2 (SLC20A2), mRNA.
2900221	0.022	up	1.297	LRRC18	Homo sapiens leucine rich repeat containing 18 (LRRC18), mRNA.

Appendix Table 2: Top twenty genes significantly DOWN-regulated following 1 hr treatment by 30 µg EBC-46 (compared to vehicle control 20% PG) in Sk-Mel-28 tumors as detected on HumanHT-12 v4 Illumina BeadChips.

ProbeID	p Value	Regulation	FC (abs)	Symbol	Definition
4490176	0.010	down	3.067	RGS1	Homo sapiens regulator of G-protein signaling 1 (RGS1), mRNA.
7160239	0.038	down	2.896	FOSB	Homo sapiens FBJ murine osteosarcoma viral oncogene homolog B (FOSB), mRNA.
6400364	0.002	down	2.861	NR4A2	Homo sapiens nuclear receptor subfamily 4, group A, member 2 (NR4A2), transcript variant 1, mRNA.
6510367	0.000	down	2.742	JUN	Homo sapiens jun oncogene (JUN), mRNA.
650639	0.001	down	2.583	NR4A2	Homo sapiens nuclear receptor subfamily 4, group A, member 2 (NR4A2), transcript variant 1, mRNA.
3400019	0.010	down	2.576	RGS2	Homo sapiens regulator of G-protein signalling 2, 24kDa (RGS2), mRNA.
6860377	0.035	down	2.364	DUSP1	Homo sapiens dual specificity phosphatase 1 (DUSP1), mRNA.
3930605	0.034	down	2.323	CYR61	Homo sapiens cysteine-rich, angiogenic inducer, 61 (CYR61), mRNA.
4280017	0.009	down	2.036	FOS	Homo sapiens v-fos FBJ murine osteosarcoma viral oncogene homolog (FOS), mRNA.
3440138	0.034	down	1.844	CLK1	Homo sapiens CDC-like kinase 1 (CLK1), mRNA.
2900348	0.002	down	1.811	ZFP36	Homo sapiens zinc finger protein 36, C3H type, homolog (mouse) (ZFP36), mRNA.
240682	0.015	down	1.788	ANKRD37	Homo sapiens ankyrin repeat domain 37 (ANKRD37), mRNA.
5670465	0.011	down	1.775	ADM	Homo sapiens adrenomedullin (ADM), mRNA.
2810463	0.037	down	1.744	LOC729009	PREDICTED: Homo sapiens misc_RNA (LOC729009), miscRNA.
7400653	0.000	down	1.684	PFKFB4	Homo sapiens 6-phosphofructo-2-kinase/fructose-2,6-biphosphatase 4 (PFKFB4), mRNA.
50309	0.050	down	1.679	DPYSL4	Homo sapiens dihydropyrimidinase-like 4 (DPYSL4), mRNA.
4040097	0.046	down	1.605	KLF6	Homo sapiens Kruppel-like factor 6 (KLF6), transcript variant 2, mRNA.
1690121	0.017	down	1.602	CLK1	Homo sapiens CDC-like kinase 1 (CLK1), mRNA.
4730181	0.016	down	1.600	FTHL12	Homo sapiens ferritin, heavy polypeptide-like 12 (FTHL12) on chromosome 9.
5720039	0.003	down	1.598	CXCL1	Homo sapiens chemokine (C-X-C motif) ligand 1 (melanoma growth stimulating activity, alpha) (CXCL1), mRNA.

Appendix Table 3: Top twenty genes significantly UP-regulated following 2 hr treatment by 30 µg EBC-46 (compared to vehicle control 20% PG) in Sk-Mel-28 tumors as detected on HumanHT-12 v4 Illumina BeadChips.

ProbeID	p Value	Regulation	FC (abs)	Symbol	Definition
580161	0.010	up	28.295	SNORD3C	Homo sapiens small nucleolar RNA, C/D box 3C (SNORD3C), small nucleolar RNA.
380685	0.018	up	24.886	SNORD3D	Homo sapiens small nucleolar RNA, C/D box 3D (SNORD3D), small nucleolar RNA.
2510164	0.019	up	24.431	SNORD3A	Homo sapiens small nucleolar RNA, C/D box 3A (SNORD3A), small nucleolar RNA.
3780767	0.002	up	4.210	LOC100132564	PREDICTED: Homo sapiens hypothetical protein LOC100132564 (LOC100132564), mRNA.
3850168	0.036	up	2.059	LOC644936	Homo sapiens cytoplasmic beta-actin pseudogene (LOC644936), non-coding RNA.
4390564	0.003	up	1.951	NUCKS1	Homo sapiens nuclear casein kinase and cyclin-dependent kinase substrate 1 (NUCKS1), mRNA.
3060377	0.026	up	1.779	MFAP4	Homo sapiens microfibrillar-associated protein 4 (MFAP4), mRNA.
1850678	0.026	up	1.732	MCAM	Homo sapiens melanoma cell adhesion molecule (MCAM), mRNA.
2710286	0.043	up	1.716	LRP1	Homo sapiens low density lipoprotein-related protein 1 (alpha-2-macroglobulin receptor) (LRP1), mRNA.
7040019	0.045	up	1.710	PCSK2	Homo sapiens proprotein convertase subtilisin/kexin type 2 (PCSK2), mRNA.
2470719	0.048	up	1.709	RTN3	Homo sapiens reticulon 3 (RTN3), transcript variant 1, mRNA.
3930020	0.048	up	1.671	CTSF	Homo sapiens cathepsin F (CTSF), mRNA.
6940475	0.050	up	1.595	AKAP12	Homo sapiens A kinase (PRKA) anchor protein (gravin) 12 (AKAP12), transcript variant 1, mRNA.
4230292	0.028	up	1.594	CD109	Homo sapiens CD109 molecule (CD109), mRNA.
2000133	0.008	up	1.573	RNU12	Homo sapiens RNA, U12 small nuclear (RNU12) on chromosome X.
2940110	0.043	up	1.558	UHRF1	Homo sapiens ubiquitin-like with PHD and ring finger domains 1 (UHRF1), transcript variant 1, mRNA.
5260594	0.017	up	1.547	AHNAK2	Homo sapiens AHNAK nucleoprotein 2 (AHNAK2), mRNA.
60427	0.034	up	1.538	NUCB2	Homo sapiens nucleobindin 2 (NUCB2), mRNA.
4050554	0.028	up	1.524	NMI	Homo sapiens N-myc (and STAT) interactor (NMI), mRNA.
3450521	0.031	up	1.521	ECM1	Homo sapiens extracellular matrix protein 1 (ECM1), transcript variant 2, mRNA.

Appendix Table 4: Top twenty genes significantly DOWN-regulated following 2 hr treatment by 30 µg EBC-46 (compared to vehicle control 20% PG) in Sk-Mel-28 tumors as detected on HumanHT-12 v4 Illumina BeadChips.

ProbeID	p Value	Regulation	FC (abs)	Symbol	Definition
380327	0.019	down	2.002	LOC730820	PREDICTED: Homo sapiens similar to nuclear receptor binding factor 2 (LOC730820), mRNA.
2370193	0.039	down	1.801	RPS15A	Homo sapiens ribosomal protein S15a (RPS15A), transcript variant 2, mRNA.
130717	0.036	down	1.787	ARPC1B	Homo sapiens actin related protein 2/3 complex, subunit 1B, 41kDa (ARPC1B), mRNA.
5360646	0.032	down	1.750	PSMC4	Homo sapiens proteasome (prosome, macropain) 26S subunit, ATPase, 4 (PSMC4), transcript variant 1, mRNA.
430309	0.048	down	1.740	C6orf66	Homo sapiens chromosome 6 open reading frame 66 (C6orf66), mRNA.
7160239	0.045	down	1.725	FOSB	Homo sapiens FBJ murine osteosarcoma viral oncogene homolog B (FOSB), mRNA.
7040095	0.048	down	1.723	RPL17	Homo sapiens ribosomal protein L17 (RPL17), transcript variant 2, mRNA.
460193	0.014	down	1.673	MAD2L1BP	Homo sapiens MAD2L1 binding protein (MAD2L1BP), transcript variant 2, mRNA.
1470349	0.034	down	1.616	RPLP0	Homo sapiens ribosomal protein, large, P0 (RPLP0), transcript variant 2, mRNA.
130414	0.034	down	1.610	LOC730167	PREDICTED: Homo sapiens similar to protein tyrosine phosphatase 4a1, transcript variant 1 (LOC730167), mRNA.
5820133	0.034	down	1.607	AKIRIN1	Homo sapiens akirin 1 (AKIRIN1), mRNA.
3460553	0.036	down	1.604	LOC440055	PREDICTED: Homo sapiens similar to ribosomal protein S12 (LOC440055), mRNA.
3990497	0.002	down	1.588	SNORA61	Homo sapiens small nucleolar RNA, H/ACA box 61 (SNORA61), small nucleolar RNA.
2680706	0.034	down	1.569	PGAM1	Homo sapiens phosphoglycerate mutase 1 (brain) (PGAM1), mRNA.
5260717	0.038	down	1.569	SBDSP	Homo sapiens Shwachman-Bodian-Diamond syndrome pseudogene (SBDSP) on chromosome 7.
1230309	0.014	down	1.557	RPL26	Homo sapiens ribosomal protein L26 (RPL26), mRNA.
6220671	0.015	down	1.548	PLAUR	Homo sapiens plasminogen activator, urokinase receptor (PLAUR), transcript variant 2, mRNA.
1850458	0.039	down	1.546	SLC25A26	Homo sapiens solute carrier family 25, member 26 (SLC25A26), transcript variant 1, mRNA.
2120377	0.042	down	1.538	LOC100130561	PREDICTED: Homo sapiens similar to high-mobility group (nonhistone chromosomal) protein 1-like 10, transcript variant 2 (LOC100130561), mRNA.
3360608	0.049	down	1.533	RPS15A	Homo sapiens ribosomal protein S15a (RPS15A), transcript variant 1, mRNA.

Appendix Table 5: Top twenty genes significantly UP-regulated following 4 hr treatment by 30 µg TPA (compared to vehicle control 20% PG) in Sk-Mel-28 tumors as detected on HumanHT-12 v4 Illumina BeadChips.

ProbeID	p Value	Regulation	FC (abs)	Symbol	Definition
4540475	0.042	up	2.072	FABP5L2	PREDICTED: Homo sapiens fatty acid binding protein 5-like 2 (FABP5L2), mRNA.
580358	0.037	up	1.907	FABP5L2	PREDICTED: Homo sapiens fatty acid binding protein 5-like 2 (FABP5L2), mRNA.
5270021	0.030	up	1.844	UBE2E2	Homo sapiens ubiquitin-conjugating enzyme E2E 2 (UBC4/5 homolog, yeast) (UBE2E2), mRNA.
2630044	0.002	up	1.390	NRIP3	Homo sapiens nuclear receptor interacting protein 3 (NRIP3), mRNA.
6100301	0.040	up	1.367	CDC123	Homo sapiens cell division cycle 123 homolog (S. cerevisiae) (CDC123), mRNA.
3870255	0.021	up	1.347	PPPDE1	Homo sapiens PPPDE peptidase domain containing 1 (PPPDE1), mRNA.
6660709	0.016	up	1.338	TTC37	Homo sapiens tetratricopeptide repeat domain 37 (TTC37), mRNA.
630682	0.016	up	1.328	LOC642956	PREDICTED: Homo sapiens hypothetical LOC642956 (LOC642956), mRNA.
2060601	0.024	up	1.325	FABP5	Homo sapiens fatty acid binding protein 5 (psoriasis-associated) (FABP5), mRNA.
3990324	0.046	up	1.323	TANC1	Homo sapiens tetratricopeptide repeat, ankyrin repeat and coiled-coil containing 1 (TANC1), mRNA.
1770133	0.011	up	1.299	LOC389599	PREDICTED: Homo sapiens similar to amyotrophic lateral sclerosis 2 (juvenile) chromosome region, candidate 2 (LOC389599), mRNA.
6650079	0.032	up	1.289	C3orf14	Homo sapiens chromosome 3 open reading frame 14 (C3orf14), mRNA.
6980255	0.018	up	1.287	LEPROT	Homo sapiens leptin receptor overlapping transcript (LEPROT), mRNA.
2190189	0.021	up	1.283	NOP58	Homo sapiens NOP58 ribonucleoprotein homolog (yeast) (NOP58), mRNA.
6370538	0.022	up	1.276	WBSCR22	Homo sapiens Williams Beuren syndrome chromosome region 22 (WBSCR22), mRNA.
4010020	0.049	up	1.219	ELF1	Homo sapiens E74-like factor 1 (ets domain transcription factor) (ELF1), mRNA.
4860379	0.040	up	1.216	C5orf21	Homo sapiens chromosome 5 open reading frame 21 (C5orf21), mRNA.
4590521	0.009	up	1.207	NDUFA1	Homo sapiens NADH dehydrogenase (ubiquinone) 1 alpha subcomplex, 1, 7.5kDa (NDUFA1), nuclear gene encoding mitochondrial protein, mRNA.
1770021	0.038	up	1.193	LOC100130591	PREDICTED: Homo sapiens hypothetical protein LOC100130591 (LOC100130591), mRNA.
6550240	0.021	up	1.187	C1orf114	Homo sapiens chromosome 1 open reading frame 114 (C1orf114), mRNA.

Appendix Table 6: Top twenty genes significantly DOWN-regulated following 4 hr treatment by 30 µg TPA (compared to vehicle control 20% PG) in Sk-Mel-28 tumors as detected on HumanHT-12 v4 Illumina BeadChips.

ProbeID	p Value	Regulation	FC (abs)	Symbol	Definition
7040008	0.047	down	1.776	CD74	Homo sapiens CD74 molecule, major histocompatibility complex, class II invariant chain (CD74), transcript variant 2, mRNA.
4560047	0.049	down	1.720	CD74	Homo sapiens CD74 molecule, major histocompatibility complex, class II invariant chain (CD74), transcript variant 1, mRNA.
7560041	0.033	down	1.667	AXUD1	Homo sapiens AXIN1 up-regulated 1 (AXUD1), mRNA.
1190367	0.039	down	1.664	IER3	Homo sapiens immediate early response 3 (IER3), mRNA.
5390161	0.009	down	1.632	DUSP5	Homo sapiens dual specificity phosphatase 5 (DUSP5), mRNA.
1230767	0.040	down	1.568	IFITM2	Homo sapiens interferon induced transmembrane protein 2 (1-8D) (IFITM2), mRNA.
5420564	0.023	down	1.471	NFIL3	Homo sapiens nuclear factor, interleukin 3 regulated (NFIL3), mRNA.
5900725	0.010	down	1.431	PHLDA1	Homo sapiens pleckstrin homology-like domain, family A, member 1 (PHLDA1), mRNA.
3190148	0.010	down	1.374	DDIT4	Homo sapiens DNA-damage-inducible transcript 4 (DDIT4), mRNA.
1410079	0.043	down	1.342	CDC26	Homo sapiens cell division cycle 26 homolog (S. cerevisiae) (CDC26), mRNA.
4920164	0.013	down	1.298	SIK1	Homo sapiens salt-inducible kinase 1 (SIK1), mRNA.
1690678	0.038	down	1.298	SIK1	Homo sapiens salt-inducible kinase 1 (SIK1), mRNA.
5960196	0.041	down	1.281	MOGAT1	Homo sapiens monoacylglycerol O-acyltransferase 1 (MOGAT1), mRNA.
6590538	0.035	down	1.272	TF	Homo sapiens transferrin (TF), mRNA.
3400050	0.022	down	1.271	TBL3	Homo sapiens transducin (beta)-like 3 (TBL3), mRNA.
510678	0.025	down	1.252	LOC643009	PREDICTED: Homo sapiens similar to gamma-glutamyltransferase 2, transcript variant 2 (LOC643009), mRNA.
2340598	0.011	down	1.242	ANKRD54	Homo sapiens ankyrin repeat domain 54 (ANKRD54), mRNA.
10189	0.004	down	1.240	C19orf24	Homo sapiens chromosome 19 open reading frame 24 (C19orf24), mRNA.
1580521	0.043	down	1.237	RNF167	Homo sapiens ring finger protein 167 (RNF167), mRNA.
2760370	0.019	down	1.232	CALR	Homo sapiens calreticulin (CALR), mRNA.

Appendix Table 7: Top twenty genes significantly UP-regulated following 8 hr treatment by 30 µg TPA (compared to vehicle control 20% PG) in Sk-Mel-28 tumors as detected on HumanHT-12 v4 Illumina BeadChips.

ProbeID	p Value	Regulation	FC (abs)	Symbol	Definition
3870338	0.012	up	2.106	IFI44L	Homo sapiens interferon-induced protein 44-like (IFI44L), mRNA.
7320372	0.021	up	1.755	EOMES	Homo sapiens eomesodermin homolog (Xenopus laevis) (EOMES), mRNA.
6860747	0.036	up	1.616	THNSL1	Homo sapiens threonine synthase-like 1 (S. cerevisiae) (THNSL1), mRNA.
1440328	0.044	up	1.516	LOC100129848	PREDICTED: Homo sapiens hypothetical protein LOC100129848 (LOC100129848), mRNA.
1010307	0.007	up	1.501	ACER2	Homo sapiens alkaline ceramidase 2 (ACER2), mRNA.
2000148	0.020	up	1.490	IFIT1	Homo sapiens interferon-induced protein with tetratricopeptide repeats 1 (IFIT1), transcript variant 2, mRNA.
6860524	0.002	up	1.488	METTL3	Homo sapiens methyltransferase like 3 (METTL3), mRNA.
4640750	0.009	up	1.482	HIBCH	Homo sapiens 3-hydroxyisobutyryl-Coenzyme A hydrolase (HIBCH), nuclear gene encoding mitochondrial protein, transcript variant 2, mRNA.
2230452	0.042	up	1.475	MRPL11	Homo sapiens mitochondrial ribosomal protein L11 (MRPL11), nuclear gene encoding mitochondrial protein, transcript variant 3, mRNA.
3940411	0.033	up	1.473	MGC16169	Homo sapiens hypothetical protein MGC16169 (MGC16169), mRNA.
1990630	0.031	up	1.456	TRIB3	Homo sapiens tribbles homolog 3 (Drosophila) (TRIB3), mRNA.
6550288	0.038	up	1.441	KTELC1	Homo sapiens KTEL (Lys-Tyr-Glu-Leu) containing 1 (KTELC1), mRNA.
5810273	0.002	up	1.438	C5orf53	Homo sapiens chromosome 5 open reading frame 53 (C5orf53), mRNA.
2230201	0.049	up	1.436	TARBP1	Homo sapiens TAR (HIV-1) RNA binding protein 1 (TARBP1), mRNA.
2260477	0.002	up	1.423	PTGS2	Homo sapiens prostaglandin-endoperoxide synthase 2 (prostaglandin G/H synthase and cyclooxygenase) (PTGS2), mRNA.
5810681	0.018	up	1.422	ZMYM6	Homo sapiens zinc finger, MYM-type 6 (ZMYM6), mRNA.
1850619	0.027	up	1.417	LOC645203	PREDICTED: Homo sapiens similar to transmembrane protein 14C (LOC645203), mRNA.
2320707	0.003	up	1.415	RABL4	Homo sapiens RAB, member of RAS oncogene family-like 4 (RABL4), mRNA.
2690435	0.020	up	1.409	IFIT1	Homo sapiens interferon-induced protein with tetratricopeptide repeats 1 (IFIT1), transcript variant 2, mRNA.
2480398	0.013	up	1.399	FAM27L	Homo sapiens family with sequence similarity 27-like (FAM27L), mRNA.

Appendix Table 8: Top twenty genes significantly DOWN-regulated following 8 hr treatment by 30 µg TPA (compared to vehicle control 20% PG) in Sk-Mel-28 tumors as detected on HumanHT-12 v4 Illumina BeadChips.

ProbeID	p Value	Regulation	FC (abs)	Symbol	Definition
770743	0.043	down	1.800	MIR1978	Homo sapiens microRNA 1978 (MIR1978), microRNA.
670025	0.036	down	1.711	CORO1C	Homo sapiens coronin, actin binding protein, 1C (CORO1C), transcript variant 1, mRNA.
6200402	0.044	down	1.702	MT1A	Homo sapiens metallothionein 1A (MT1A), mRNA.
3610215	0.007	down	1.624	LOC100131866	PREDICTED: Homo sapiens misc_RNA (LOC100131866), miscRNA.
2470161	0.025	down	1.611	PLEKHF1	Homo sapiens pleckstrin homology domain containing, family F (with FYVE domain) member 1 (PLEKHF1), mRNA.
5290161	0.010	down	1.597	C17orf91	Homo sapiens chromosome 17 open reading frame 91 (C17orf91), transcript variant 2, mRNA.
3290037	0.013	down	1.592	DNAJC7	Homo sapiens DnaJ (Hsp40) homolog, subfamily C, member 7 (DNAJC7), mRNA.
1070373	0.046	down	1.550	SNX30	Homo sapiens sorting nexin family member 30 (SNX30), mRNA.
3170286	0.042	down	1.531	LOC647000	PREDICTED: Homo sapiens similar to tubulin, beta 5 (LOC647000), mRNA.
2940398	0.009	down	1.528	CDCA2	Homo sapiens cell division cycle associated 2 (CDCA2), mRNA.
6480332	0.006	down	1.503	C20orf117	Homo sapiens chromosome 20 open reading frame 117 (C20orf117), transcript variant 2, mRNA.
770561	0.001	down	1.474	C20orf108	Homo sapiens chromosome 20 open reading frame 108 (C20orf108), mRNA.
3520044	0.001	down	1.460	LOC100133866	PREDICTED: Homo sapiens similar to phosphodiesterase 4D interacting protein (myomegalin) (LOC100133866), mRNA.
4150053	0.011	down	1.460	YBX1	Homo sapiens Y box binding protein 1 (YBX1), mRNA.
6580039	0.011	down	1.453	PKM2	Homo sapiens pyruvate kinase, muscle (PKM2), transcript variant 1, mRNA.
3370703	0.038	down	1.449	FEN1	Homo sapiens flap structure-specific endonuclease 1 (FEN1), mRNA.
2470687	0.038	down	1.448	LOC645387	PREDICTED: Homo sapiens misc_RNA (LOC645387), miscRNA.
360114	0.032	down	1.447	CTXN1	Homo sapiens cortexin 1 (CTXN1), mRNA.
4290044	0.017	down	1.431	STRN4	Homo sapiens striatin, calmodulin binding protein 4 (STRN4), transcript variant 1, mRNA.
2450202	0.028	down	1.427	KIF3C	Homo sapiens kinesin family member 3C (KIF3C), mRNA.

Appendix Table 9: Top twenty genes significantly UP-regulated following 30 min treatment by EBC-46 (compared to TPA) in mice as detected on MouseRef-8 v2.0 BeadChips.

ProbeID	FC (abs)	Regulation	Symbol	Definition
5340064	15.849	up	Pvalb	Mus musculus parvalbumin (Pvalb), mRNA.
4860577	9.893	up	Actn3	Mus musculus actinin alpha 3 (Actn3), mRNA.
4250750	9.760	up	Pgam2	Mus musculus phosphoglycerate mutase 2 (Pgam2), mRNA.
1190347	8.393	up	Actn3	Mus musculus actinin alpha 3 (Actn3), mRNA.
1850100	7.269	up	Rpl3l	Mus musculus ribosomal protein L3-like (Rpl3l), mRNA.
1070397	7.047	up	Mybpc2	Mus musculus myosin binding protein C, fast-type (Mybpc2), mRNA.
4040435	6.581	up	Chchd10	Mus musculus coiled-coil-helix-coiled-coil-helix domain containing 10 (Chchd10), mRNA.
2260066	6.071	up	Tnni2	Mus musculus troponin I, skeletal, fast 2 (Tnni2), mRNA.
4290273	5.672	up	Ampd1	Mus musculus adenosine monophosphate deaminase 1 (isoform M) (Ampd1), mRNA. XM_921992
1240243	5.313	up	Pfkm	Mus musculus phosphofructokinase, muscle (Pfkm), mRNA.
2470356	5.262	up	Cox6a2	Mus musculus cytochrome c oxidase, subunit VI a, polypeptide 2 (Cox6a2), nuclear gene encoding mitochondrial protein, mRNA.
4860465	4.792	up	Ttn	Mus musculus titin (Ttn), transcript variant N2-B, mRNA.
6060523	4.733	up	Rtn2	Mus musculus reticulon 2 (Z-band associated protein) (Rtn2), transcript variant B, mRNA.
4250148	4.660	up	Tmod4	Mus musculus tropomodulin 4 (Tmod4), mRNA.
5690092	4.342	up	Ak1	Mus musculus adenylate kinase 1 (Ak1), mRNA.
3190689	4.194	up	Adssl1	Mus musculus adenylosuccinate synthetase like 1 (Adssl1), mRNA.
1780411	4.030	up	Des	Mus musculus desmin (Des), mRNA.
4810646	3.896	up	Eef1a2	Mus musculus eukaryotic translation elongation factor 1 alpha 2 (Eef1a2), mRNA.
2850398	3.884	up	Asb2	Mus musculus ankyrin repeat and SOCS box-containing 2 (Asb2), mRNA.
1770468	3.830	up	Adssl1	Mus musculus adenylosuccinate synthetase like 1 (Adssl1), mRNA.

Appendix Table 10: Top twenty genes significantly DOWN-regulated following 30 min treatment by EBC-46(compared to TPA) in mice as detected on MouseRef-8 v2.0 BeadChips.

ProbeID	FC (abs)	Regulation	Symbol	Definition
4830543	5.431	down	Ifi27	Mus musculus interferon, alpha-inducible protein 27 (Ifi27), mRNA.
5360370	5.276	down	OTTMUSG00000000971	Mus musculus predicted gene, OTTMUSG00000000971 (OTTMUSG00000000971), mRNA.
2480296	5.061	down	LOC100048554	PREDICTED: Mus musculus similar to monocyte chemoattractant protein-2 (MCP-2) (LOC100048554), mRNA.
7510243	4.325	down	C4b	Mus musculus complement component 4B (Childo blood group) (C4b), mRNA. XM_921663 XM_921673 XM_921676 XM_921678
7050538	4.015	down	Ccl9	Mus musculus chemokine (C-C motif) ligand 9 (Ccl9), mRNA.
4010082	3.722	down	Ctgf	Mus musculus connective tissue growth factor (Ctgf), mRNA.
4200341	3.172	down	Lbp	Mus musculus lipopolysaccharide binding protein (Lbp), mRNA.
3120465	3.132	down	Cstb	Mus musculus cystatin B (Cstb), mRNA.
4070348	3.113	down	Rpl3	Mus musculus ribosomal protein L3 (Rpl3), mRNA.
830369	3.081	down	Cyba	Mus musculus cytochrome b-245, alpha polypeptide (Cyba), mRNA.
2030465	3.057	down	1810064F22Rik	Mus musculus RIKEN cDNA 1810064F22 gene (1810064F22Rik), mRNA.
6770114	3.027	down	Trem2	Mus musculus triggering receptor expressed on myeloid cells 2 (Trem2), mRNA.
7330278	2.943	down	Lgals1	
4210196	2.891	down	Ednrb	Mus musculus endothelin receptor type B (Ednrb), mRNA.
6110204	2.851	down	Ctsk	Mus musculus cathepsin K (Ctsk), mRNA.
1940370	2.841	down	Tmsb4x	Mus musculus thymosin, beta 4, X chromosome (Tmsb4x), mRNA.
7380327	2.820	down	Slc12a5	Mus musculus solute carrier family 12, member 5 (Slc12a5), mRNA.
5080326	2.775	down	S100a6	Mus musculus S100 calcium binding protein A6 (calcyclin) (S100a6), mRNA.
2230544	2.723	down	Col3a1	Mus musculus collagen, type III, alpha 1 (Col3a1), mRNA.
3180543	2.714	down	Sdpr	Mus musculus serum deprivation response (Sdpr), mRNA.

Appendix Table 11: Top twenty genes significantly UP-regulated following 1 hr treatment by EBC-46 (compared to TPA) in mice as detected on MouseRef-8 v2.0 BeadChips.

ProbeID	FC (abs)	Regulation	Symbol	Definition
5360228	11.583	up	Lor	Mus musculus loricrin (Lor), mRNA.
2070593	7.035	up	Krt10	Mus musculus keratin 10 (Krt10), mRNA.
830333	7.009	up	Krtdap	Mus musculus keratinocyte differentiation associated protein (Krtdap), mRNA. XM_923930 XM_923934
3940682	5.266	up	Dmkn	Mus musculus dermokine (Dmkn), transcript variant 2, mRNA.
50521	5.023	up	Dmkn	Mus musculus dermokine (Dmkn), transcript variant 2, mRNA.
5270408	4.927	up	Lce1m	Mus musculus late cornified envelope 1M (Lce1m), mRNA.
1260358	4.775	up	Lce1b	Mus musculus late cornified envelope 1B (Lce1b), mRNA.
5550184	3.326	up	Calm4	Mus musculus calmodulin 4 (Calm4), mRNA.
5720450	3.323	up	Lce1d	Mus musculus late cornified envelope 1D (Lce1d), mRNA.
4780048	3.016	up	Lce1a2	Mus musculus late cornified envelope 1A2 (Lce1a2), mRNA.
1740424	2.966	up	Elovl4	Mus musculus elongation of very long chain fatty acids (FEN1/Elo2, SUR4/Elo3, yeast)-like 4 (Elovl4), mRNA.
6420356	2.907	up	Lce1c	Mus musculus late cornified envelope 1C (Lce1c), mRNA.
7150326	2.810	up	Krt5	Mus musculus keratin 5 (Krt5), mRNA.
6650730	2.722	up	Lce1a1	Mus musculus late cornified envelope 1A1 (Lce1a1), mRNA.
2510064	2.668	up	Col17a1	Mus musculus collagen, type XVII, alpha 1 (Col17a1), mRNA.
5670554	2.667	up	Crct1	Mus musculus cysteine-rich C-terminal 1 (Crct1), mRNA.
5260392	2.612	up	Asprv1	Mus musculus aspartic peptidase, retroviral-like 1 (Asprv1), mRNA.
4120463	2.520	up	Flg2	Mus musculus filaggrin family member 2 (Flg2), mRNA.
4480615	2.479	up	Sbsn	Mus musculus suprabasin (Sbsn), transcript variant 1, mRNA.
6200446	2.439	up	Klk8	Mus musculus kallikrein related-peptidase 8 (Klk8), mRNA.

Appendix Table 12: Top twenty genes significantly DOWN-regulated following 1 hr treatment by EBC-46 (compared to TPA) in mice as detected on MouseRef-8 v2.0 BeadChips.

ProbeID	FC (abs)	Regulation	Symbol	Definition
5340064	6.695	down	Pvalb	Mus musculus parvalbumin (Pvalb), mRNA.
5490528	5.882	down	Myh2	
3420110	5.692	down	Tnnc2	Mus musculus troponin C2, fast (Tnnc2), mRNA.
130349	5.472	down	Mylpf	Mus musculus myosin light chain, phosphorylatable, fast skeletal muscle (Mylpf), mRNA.
110707	4.476	down	Tnnt3	Mus musculus troponin T3, skeletal, fast (Tnnt3), mRNA.
1070397	4.080	down	Mybpc2	Mus musculus myosin binding protein C, fast-type (Mybpc2), mRNA.
2510053	3.743	down	Ckm	Mus musculus creatine kinase, muscle (Ckm), mRNA.
4040386	3.570	down	Hspb6	Mus musculus heat shock protein, alpha-crystallin-related, B6 (Hspb6), mRNA.
10639	3.404	down	Fhl1	Mus musculus four and a half LIM domains 1 (Fhl1), transcript variant 2, mRNA.
7150685	3.343	down	Tcap	Mus musculus titin-cap (Tcap), mRNA.
5550309	3.183	down	Fhl1	Mus musculus four and a half LIM domains 1 (Fhl1), transcript variant 1, mRNA.
1050678	3.154	down	Actn2	Mus musculus actinin alpha 2 (Actn2), mRNA.
1070088	2.793	down	Tpm2	Mus musculus tropomyosin 2, beta (Tpm2), mRNA.
1470154	2.792	down	Mb	Mus musculus myoglobin (Mb), mRNA.
4220474	2.765	down	Myh4	Mus musculus myosin, heavy polypeptide 4, skeletal muscle (Myh4), mRNA.
3990609	2.637	down	Nrap	Mus musculus nebulin-related anchoring protein (Nrap), transcript variant 1, mRNA.
4250750	2.546	down	Pgam2	Mus musculus phosphoglycerate mutase 2 (Pgam2), mRNA.
1110687	2.385	down	Ryr1	Mus musculus ryanodine receptor 1, skeletal muscle (Ryr1), mRNA.
2470133	2.368	down	Csrp3	Mus musculus cysteine and glycine-rich protein 3 (Csrp3), mRNA.
2470356	2.349	down	Cox6a2	Mus musculus cytochrome c oxidase, subunit VI a, polypeptide 2 (Cox6a2), nuclear gene encoding mitochondrial protein, mRNA.

Appendix Table 13: Top twenty genes significantly UP-regulated following 2 hr treatment by EBC-46 (compared to TPA) in mice as detected on MouseRef-8 v2.0 BeadChips.

ProbeID	FC (abs)	Regulation	Symbol	Definition
1470619	5.574	up	Krt14	Mus musculus keratin 14 (Krt14), mRNA.
5360228	2.831	up	Lor	Mus musculus loricrin (Lor), mRNA.
2070593	2.357	up	Krt10	Mus musculus keratin 10 (Krt10), mRNA.
3290240	2.096	up	Gpr34	Mus musculus G protein-coupled receptor 34 (Gpr34), mRNA.
2680072	2.085	up	Doxl2	Mus musculus diamine oxidase-like protein 2 (Doxl2), mRNA.
2510064	2.002	up	Col17a1	Mus musculus collagen, type XVII, alpha 1 (Col17a1), mRNA.

Appendix Table 14: Top twenty genes significantly DOWN-regulated following 2 hr treatment by EBC-46 (compared to TPA) in mice as detected on MouseRef-8 v2.0 BeadChips.

ProbeID	FC (abs)	Regulation	Symbol	Definition
4760356	2.006	down	Cat	Mus musculus catalase (Cat), mRNA.
830273	2.045	down	Ccl11	Mus musculus small chemokine (C-C motif) ligand 11 (Ccl11), mRNA.
5570435	2.269	down	Mup2	Mus musculus major urinary protein 2 (Mup2), transcript variant 1, mRNA.
160402	2.329	down	Ogn	Mus musculus osteoglycin (Ogn), mRNA.
1740008	4.281	down	Ptx3	

Appendix Table 15: Top twenty genes significantly UP-regulated following 4 hr treatment by EBC-46 (compared to TPA) in mice as detected on MouseRef-8 v2.0 BeadChips.

ProbeID	FC (abs)	Regulation	Symbol	Definition
3610082	12.110	up	Cxcl1	Mus musculus chemokine (C-X-C motif) ligand 1 (Cxcl1), mRNA.
1710193	10.742	up	Gja1	Mus musculus gap junction membrane channel protein alpha 1 (Gja1), mRNA.
1780341	10.015	up	Krt17	Mus musculus keratin 17 (Krt17), mRNA.
1470619	9.664	up	Krt14	Mus musculus keratin 14 (Krt14), mRNA.
2070593	8.638	up	Krt10	Mus musculus keratin 10 (Krt10), mRNA.
1780475	6.977	up	Defb6	Mus musculus defensin beta 6 (Defb6), mRNA.
6620008	6.092	up	Ly6g6c	Mus musculus lymphocyte antigen 6 complex, locus G6C (Ly6g6c), mRNA.
7040184	5.713	up	Lgals7	Mus musculus lectin, galactose binding, soluble 7 (Lgals7), mRNA.
3940138	4.989	up	Lypd3	Mus musculus Ly6/Plaur domain containing 3 (Lypd3), mRNA.
6620079	4.727	up	Egr1	Mus musculus early growth response 1 (Egr1), mRNA.
2490288	4.586	up	LOC100047935	PREDICTED: Mus musculus similar to ribosomal protein L5 (LOC100047935), misc RNA.
4830543	4.455	up	Ifi27	Mus musculus interferon, alpha-inducible protein 27 (Ifi27), mRNA.
4060504	4.214	up	Rpl36a	Mus musculus ribosomal protein L36a (Rpl36a), mRNA.
460682	4.121	up	2200001I15Rik	Mus musculus RIKEN cDNA 2200001I15 gene (2200001I15Rik), mRNA.
1190082	4.002	up	Eif3i	Mus musculus eukaryotic translation initiation factor 3, subunit I (Eif3i), mRNA.
6770754	3.856	up	Trim29	Mus musculus tripartite motif protein 29 (Trim29), mRNA.
5900504	3.810	up	Rpl34	Mus musculus ribosomal protein L34 (Rpl34), transcript variant 1, mRNA.
830333	3.806	up	Krtdap	Mus musculus keratinocyte differentiation associated protein (Krtdap), mRNA. XM_923930 XM_923934
4070348	3.659	up	Rpl3	Mus musculus ribosomal protein L3 (Rpl3), mRNA.
1850327	3.654	up	2900010M23Rik	Mus musculus RIKEN cDNA 2900010M23 gene (2900010M23Rik), mRNA.

Appendix Table 16: Top twenty genes significantly DOWN-regulated following 4 hr treatment by EBC-46 (compared to TPA) in mice as detected on MouseRef-8 v2.0 BeadChips.

ProbeID	FC (abs)	Regulation	Symbol	Definition
2230681	11.187	down	Arpc1a	Mus musculus actin related protein 2/3 complex, subunit 1A (Arpc1a), mRNA.
830240	8.816	down	Lyz2	Mus musculus lysozyme 2 (Lyz2), mRNA.
7400050	5.767	down	Bckdk	Mus musculus branched chain ketoacid dehydrogenase kinase (Bckdk), nuclear gene encoding mitochondrial protein, mRNA.
3460356	5.008	down	Pdia3	Mus musculus protein disulfide isomerase associated 3 (Pdia3), mRNA.
1170398	4.653	down	Med25	Mus musculus mediator of RNA polymerase II transcription, subunit 25 homolog (yeast) (Med25), mRNA.
2940678	4.544	down	Rtn4	Mus musculus reticulon 4 (Rtn4), transcript variant 1, mRNA.
4220753	4.510	down	Gnai2	Mus musculus guanine nucleotide binding protein, alpha inhibiting 2 (Gnai2), mRNA.
2470195	4.498	down	Pcbp1	Mus musculus poly(rC) binding protein 1 (Pcbp1), mRNA.
2060435	4.382	down	Sfrs5	Mus musculus splicing factor, arginine/serine-rich 5 (SRp40, HRS) (Sfrs5), transcript variant 2, mRNA.
6250022	4.374	down	Uba1	Mus musculus ubiquitin-like modifier activating enzyme 1 (Uba1), mRNA.
4490482	4.344	down	Sf1	Mus musculus splicing factor 1 (Sf1), mRNA. XM_979946 XM_979979
4050121	4.304	down	Rbpms	Mus musculus RNA binding protein gene with multiple splicing (Rbpms), transcript variant 3, mRNA.
6130692	4.296	down	Hnrpm	Mus musculus heterogeneous nuclear ribonucleoprotein M (Hnrpm), mRNA.
1260482	4.259	down	Sparc	Mus musculus secreted acidic cysteine rich glycoprotein (Sparc), mRNA.
3450072	4.234	down	Zmym3	Mus musculus zinc finger, MYM-type 3 (Zmym3), mRNA.
1570373	4.141	down	Csnk1e	Mus musculus casein kinase 1, epsilon (Csnk1e), mRNA.
6580376	4.048	down	Zfhx3	Mus musculus zinc finger homeobox 3 (Zfhx3), mRNA.
1450246	4.017	down	Trpc4ap	Mus musculus transient receptor potential cation channel, subfamily C, member 4 associated protein (Trpc4ap), mRNA.
510341	3.995	down	Rnf10	Mus musculus ring finger protein 10 (Rnf10), mRNA.
4760129	3.965	down	Camta2	Mus musculus calmodulin binding transcription activator 2 (Camta2), mRNA.

Appendix Table 17: Top twenty genes significantly UP-regulated following 8 hr treatment by EBC-46 (compared to TPA) in mice as detected on MouseRef-8 v2.0 BeadChips.

ProbeID	FC (abs)	Regulation	Symbol	Definition
3610082	20.710	up	Cxcl1	Mus musculus chemokine (C-X-C motif) ligand 1 (Cxcl1), mRNA.
2510053	14.251	up	Ckm	Mus musculus creatine kinase, muscle (Ckm), mRNA.
4220474	10.225	up	Myh4	Mus musculus myosin, heavy polypeptide 4, skeletal muscle (Myh4), mRNA.
3360270	9.740	up	Cox7a1	Mus musculus cytochrome c oxidase, subunit VIIa 1 (Cox7a1), mRNA.
3440615	9.616	up	Dscr1	
1230767	7.854	up	Thbd	Mus musculus thrombomodulin (Thbd), mRNA.
150544	7.030	up	Ankrd1	Mus musculus ankyrin repeat domain 1 (cardiac muscle) (Ankrd1), mRNA.
6180202	6.003	up	LOC100044702	PREDICTED: Mus musculus similar to LPS-induced CXC chemokine (LOC100044702), mRNA.
6940184	5.886	up	Ccl4	Mus musculus chemokine (C-C motif) ligand 4 (Ccl4), mRNA.
4120131	5.807	up	Pdk4	Mus musculus pyruvate dehydrogenase kinase, isoenzyme 4 (Pdk4), mRNA.
4220575	5.571	up	Dysfip1	Mus musculus dysferlin interacting protein 1 (Dysfip1), mRNA.
1780598	5.210	up	Ttn	
4860577	5.187	up	Actn3	Mus musculus actinin alpha 3 (Actn3), mRNA.
4860465	5.049	up	Ttn	Mus musculus titin (Ttn), transcript variant N2-B, mRNA.
4900438	4.978	up	Ppp1r3c	Mus musculus protein phosphatase 1, regulatory (inhibitor) subunit 3C (Ppp1r3c), mRNA.
870601	4.951	up	Myoz1	Mus musculus myozenin 1 (Myoz1), mRNA.
1850100	4.921	up	Rpl3l	Mus musculus ribosomal protein L3-like (Rpl3l), mRNA.
4290273	4.881	up	Ampd1	Mus musculus adenosine monophosphate deaminase 1 (isoform M) (Ampd1), mRNA. XM_921992
1190347	4.595	up	Actn3	Mus musculus actinin alpha 3 (Actn3), mRNA.
610671	4.464	up	Ampd1	Mus musculus adenosine monophosphate deaminase 1 (isoform M) (Ampd1), mRNA. XM_921992

Appendix Table 18: Top twenty genes significantly DOWN-regulated following 8 hr treatment by EBC-46 (compared to TPA) in mice as detected on MouseRef-8 v2.0 BeadChips.

ProbeID	FC (abs)	Regulation	Symbol	Definition
6280026	2.480	down	H2-K1	Mus musculus histocompatibility 2, K1, K region (H2-K1), mRNA.
5270408	2.253	down	Lce1m	Mus musculus late cornified envelope 1M (Lce1m), mRNA.
1050215	2.201	down	Smpd1	Mus musculus sphingomyelin phosphodiesterase 1, acid lysosomal (Smpd1), mRNA.
7650035	2.084	down	Serpinb12	Mus musculus serine (or cysteine) peptidase inhibitor, clade B (ovalbumin), member 12 (Serpinb12), mRNA.
6510653	2.083	down	Ap2a1	Mus musculus adaptor protein complex AP-2, alpha 1 subunit (Ap2a1), transcript variant 2, mRNA.
3460379	2.042	down	Arhgef2	Mus musculus rho/rac guanine nucleotide exchange factor (GEF) 2 (Arhgef2), mRNA.
2570747	2.041	down	Ube2k	Mus musculus ubiquitin-conjugating enzyme E2K (UBC1 homolog, yeast) (Ube2k), mRNA.
1820215	2.032	down	BC039093	

Appendix Table 19: Top twenty genes significantly UP-regulated following 30 min treatment by TPA (compared to EBC-46) in mice as detected on MouseRef-8 v2.0 BeadChips.

ProbeID	FC (abs)	Regulation	Symbol	Definition
460576	6.545	up	Fstl1	Mus musculus follistatin-like 1 (Fstl1), mRNA.
2100402	6.345	up	Bgn	Mus musculus biglycan (Bgn), mRNA.
6220026	6.112	up	Zfp36	Mus musculus zinc finger protein 36 (Zfp36), mRNA.
4570368	5.328	up	Errfi1	Mus musculus ERBB receptor feedback inhibitor 1 (Errfi1), mRNA.
7160603	5.121	up	Sepp1	Mus musculus selenoprotein P, plasma, 1 (Sepp1), transcript variant 1, mRNA.
5960497	4.385	up	Tgfbr2	Mus musculus transforming growth factor, beta receptor II (Tgfbr2), transcript variant 1, mRNA.
1400053	4.356	up	LOC100047583	PREDICTED: Mus musculus similar to apolipoprotein D (LOC100047583), mRNA.
270324	4.300	up	Tnc	Mus musculus tenascin C (Tnc), mRNA.
7210041	4.223	up	Col6a1	Mus musculus procollagen, type VI, alpha 1 (Col6a1), mRNA.
3170280	4.220	up	Col6a1	Mus musculus procollagen, type VI, alpha 1 (Col6a1), mRNA.
610414	4.177	up	Ctsa	Mus musculus cathepsin A (Ctsa), transcript variant 2, mRNA.
4150386	3.947	up	Col5a1	Mus musculus procollagen, type V, alpha 1 (Col5a1), mRNA.
6180544	3.870	up	Mmp3	Mus musculus matrix metallopeptidase 3 (Mmp3), mRNA.
580332	3.561	up	C1qb	Mus musculus complement component 1, q subcomponent, beta polypeptide (C1qb), mRNA.
1740112	3.515	up	Loxl1	Mus musculus lysyl oxidase-like 1 (Loxl1), mRNA.
6620079	3.510	up	Egr1	Mus musculus early growth response 1 (Egr1), mRNA.
3120014	3.429	up	Junb	Mus musculus Jun-B oncogene (Junb), mRNA.
4010292	3.393	up	Nid1	Mus musculus nidogen 1 (Nid1), mRNA.
6270600	3.385	up	Osm	Mus musculus oncostatin M (Osm), mRNA.
3520066	3.313	up	Mmp14	Mus musculus matrix metallopeptidase 14 (membrane-inserted) (Mmp14), mRNA.

Appendix Table 20: Top twenty genes significantly DOWN-regulated following 30 min treatment by TPA (compared to EBC-46) in mice as detected on MouseRef-8 v2.0 BeadChips.

ProbeID	FC (abs)	Regulation	Symbol	Definition
770086	3.070	down	Uqcr	Mus musculus ubiquinol-cytochrome c reductase (6.4kD) subunit (Uqcr), mRNA.
7210156	3.007	down	Ndufb8	Mus musculus NADH dehydrogenase (ubiquinone) 1 beta subcomplex 8 (Ndufb8), mRNA.
10598	3.006	down	Cxcl9	Mus musculus chemokine (C-X-C motif) ligand 9 (Cxcl9), mRNA.
5550543	2.741	down	2010107E04Rik	Mus musculus RIKEN cDNA 2010107E04 gene (2010107E04Rik), mRNA.
610392	2.703	down	Chchd1	Mus musculus coiled-coil-helix-coiled-coil-helix domain containing 1 (Chchd1), mRNA.
3140110	2.616	down	LOC100044779	PREDICTED: Mus musculus similar to prothymosin alpha (LOC100044779), misc RNA.
4120768	2.566	down	Dnaja1	Mus musculus DnaJ (Hsp40) homolog, subfamily A, member 1 (Dnaja1), mRNA.
5910475	2.488	down	Ndufs6	Mus musculus NADH dehydrogenase (ubiquinone) Fe-S protein 6 (Ndufs6), mRNA.
610746	2.470	down	Gjb6	Mus musculus gap junction protein, beta 6 (Gjb6), transcript variant 2, mRNA.
870382	2.361	down	1110020P15Rik	Mus musculus RIKEN cDNA 1110020P15 gene (1110020P15Rik), mRNA.
5290475	2.346	down	1110020P15Rik	Mus musculus RIKEN cDNA 1110020P15 gene (1110020P15Rik), mRNA.
1410068	2.339	down	LOC100048301	PREDICTED: Mus musculus similar to RNA Polymerase II subunit 14.5 kD (LOC100048301), mRNA.
290672	2.339	down	Pfn2	Mus musculus profilin 2 (Pfn2), mRNA.
1500707	2.338	down	Gcnt1	Mus musculus glucosaminyl (N-acetyl) transferase 1, core 2 (Gcnt1), mRNA.
830600	2.312	down	Nags	Mus musculus N-acetylglutamate synthase (Nags), transcript variant 2, mRNA.
940612	2.307	down	4930579E17Rik	
4070538	2.305	down	Timm8a1	Mus musculus translocase of inner mitochondrial membrane 8 homolog a1 (yeast) (Timm8a1), mRNA.
6650674	2.295	down	Gulo	Mus musculus gulonolactone (L-) oxidase (Gulo), mRNA.
3130324	2.295	down	2610109H07Rik	Mus musculus RIKEN cDNA 2610109H07 gene (2610109H07Rik), mRNA.
4900646	2.286	down	Tnni3k	Mus musculus TNNI3 interacting kinase (Tnni3k), mRNA.

Appendix Table 21: Top twenty genes significantly UP-regulated following 1 hr treatment by TPA (compared to EBC-46) in mice as detected on MouseRef-8 v2.0 BeadChips.

ProbeID	FC (abs)	Regulation	Symbol	Definition
3890274	40.195	up	Scd1	Mus musculus stearoyl-Coenzyme A desaturase 1 (Scd1), mRNA.
5570435	19.943	up	Mup2	Mus musculus major urinary protein 2 (Mup2), transcript variant 1, mRNA.
3800706	12.354	up	A030004J04Rik	Mus musculus RIKEN cDNA A030004J04 gene (A030004J04Rik), mRNA.
2490288	12.235	up	LOC100047935	PREDICTED: Mus musculus similar to ribosomal protein L5 (LOC100047935), misc RNA.
6940521	11.959	up	LOC100040592	PREDICTED: Mus musculus similar to Hmgcs1 protein, transcript variant 1, mRNA.
830632	11.782	up	Fcgr4	Mus musculus Fc receptor, IgG, low affinity IV (Fcgr4), mRNA.
2970612	9.306	up	Rps21	Mus musculus ribosomal protein S21 (Rps21), mRNA.
6270228	9.196	up	S100a3	Mus musculus S100 calcium binding protein A3 (S100a3), mRNA.
2710477	8.838	up	Rps24	Mus musculus ribosomal protein S24 (Rps24), transcript variant 1, mRNA.
5290475	8.458	up	1110020P15Rik	Mus musculus RIKEN cDNA 1110020P15 gene (1110020P15Rik), mRNA.
3060095	8.395	up	Krt71	Mus musculus keratin 71 (Krt71), mRNA.
1450333	8.383	up	Clec7a	Mus musculus C-type lectin domain family 7, member a (Clec7a), mRNA.
2510707	8.360	up	Rpl38	Mus musculus ribosomal protein L38 (Rpl38), transcript variant 1, mRNA.
2480296	8.316	up	LOC100048554	PREDICTED: Mus musculus similar to monocyte chemoattractant protein-2 (MCP-2) mRNA.
4200100	7.984	up	Dusp1	Mus musculus dual specificity phosphatase 1 (Dusp1), mRNA.
2230730	6.934	up	Gjb2	Mus musculus gap junction protein, beta 2 (Gjb2), mRNA.
1980288	6.634	up	Sumo1	Mus musculus SMT3 suppressor of mif two 3 homolog 1 (yeast) (Sumo1), mRNA.
1070762	6.617	up	Cox4i1	
2060561	6.573	up	Npm3	Mus musculus nucleoplasmin 3 (Npm3), mRNA.
2060326	6.571	up	Lamp2	

Appendix Table 22: Top twenty genes significantly DOWN-regulated following 1 hr treatment by TPA (compared to EBC-46) in mice as detected on MouseRef-8 v2.0 BeadChips.

ProbeID	FC (abs)	Regulation	Symbol	Definition
4780762	205.469	down	Ubb	Mus musculus ubiquitin B (Ubb), mRNA.
2690315	166.960	down	Rps14	Mus musculus ribosomal protein S14 (Rps14), mRNA.
110092	141.548	down	Gm1821	Mus musculus gene model 1821, (NCBI) (Gm1821), non-coding RNA. XM_899826
6350128	123.934	down	Rps12	Mus musculus ribosomal protein S12 (Rps12), mRNA.
7570762	122.270	down	EG668668	Mus musculus predicted gene, EG668668 (EG668668), mRNA.
2000398	116.611	down	Hba-a1	Mus musculus hemoglobin alpha, adult chain 1 (Hba-a1), mRNA.
1170372	98.762	down	Actb	Mus musculus actin, beta (Actb), mRNA.
540326	93.080	down	Rplp1	Mus musculus ribosomal protein, large, P1 (Rplp1), mRNA.
2260576	88.968	down	Tuba1b	Mus musculus tubulin, alpha 1B (Tuba1b), mRNA.
6840433	73.512	down	Npm1	Mus musculus nucleophosmin 1 (Npm1), mRNA.
360437	73.104	down	Maged2	Mus musculus melanoma antigen, family D, 2 (Maged2), mRNA.
1030484	71.317	down	Hnrpm	Mus musculus heterogeneous nuclear ribonucleoprotein M (Hnrpm), mRNA.
4900519	63.052	down	Sgk1	Mus musculus serum/glucocorticoid regulated kinase 1 (Sgk1), mRNA.
1580471	53.728	down	Atp5g3	Mus musculus ATP synthase, H+ transporting, mitochondrial F0 complex, subunit c (subunit 9), isoform 3 (Atp5g3), nuclear gene encoding mitochondrial protein, mRNA.
4060056	52.536	down	2310016E02Rik	Mus musculus RIKEN cDNA 2310016E02 gene (2310016E02Rik), transcript variant 1, mRNA.
3890626	51.641	down	Eef1g	Mus musculus eukaryotic translation elongation factor 1 gamma (Eef1g), mRNA.
1070224	40.546	down	Emp3	Mus musculus epithelial membrane protein 3 (Emp3), mRNA.
2370593	40.367	down	D4Ertd22e	Mus musculus DNA segment, Chr 4, ERATO Doi 22, expressed (D4Ertd22e), transcript variant 1, mRNA.
780093	33.011	down	Cox6b1	Mus musculus cytochrome c oxidase, subunit VIb polypeptide 1 (Cox6b1), mRNA.
4220670	31.871	down	Pcbp2	Mus musculus poly(rC) binding protein 2 (Pcbp2), mRNA.

Appendix Table 23: Top twenty genes significantly UP-regulated following 2 hr treatment by TPA (compared to EBC-46) in mice as detected on MouseRef-8 v2.0 BeadChips.

ProbeID	FC (abs)	Regulation	Symbol	Definition
2320491	226.756	up	Tmem176a	Mus musculus transmembrane protein 176A (Tmem176a), mRNA.
4050427	200.327	up	Tmem45a	Mus musculus transmembrane protein 45a (Tmem45a), mRNA.
4560372	173.990	up	Tmem50b	Mus musculus transmembrane protein 50B (Tmem50b), mRNA.
7610411	147.482	up	Frag1	Mus musculus FGF receptor activating protein 1 (Frag1), mRNA.
3800161	130.603	up	1700063I17Rik	Mus musculus RIKEN cDNA 1700063I17 gene (1700063I17Rik), mRNA.
3390424	128.561	up	Atg2a	Mus musculus ATG2 autophagy related 2 homolog A (S. cerevisiae) (Atg2a), mRNA.
4860132	110.497	up	Rufy3	Mus musculus RUN and FYVE domain containing 3 (Rufy3), mRNA.
1980202	96.246	up	Ttc30b	Mus musculus tetratricopeptide repeat domain 30B (Ttc30b), mRNA. XM_911984 XM_986297
3990152	94.715	up	Fsd1	Mus musculus fibronectin type 3 and SPRY domain-containing protein (Fsd1), mRNA.
6860278	92.165	up	Samhd1	Mus musculus SAM domain and HD domain, 1 (Samhd1), mRNA.
7610736	91.208	up	Zfp445	Mus musculus zinc finger protein 445 (Zfp445), mRNA.
540156	88.253	up	Chmp2a	Mus musculus chromatin modifying protein 2A (Chmp2a), mRNA.
3520382	82.188	up	Upp2	Mus musculus uridine phosphorylase 2 (Upp2), mRNA.
2710341	81.593	up	Nsg2	Mus musculus neuron specific gene family member 2 (Nsg2), mRNA.
3170136	78.898	up	A430083B19Rik	Mus musculus RIKEN cDNA A430083B19 gene (A430083B19Rik), mRNA.
7050193	72.038	up	Ly9	
3830390	70.808	up	Grik5	Mus musculus glutamate receptor, ionotropic, kainate 5 (gamma 2) (Grik5), mRNA.
4890056	63.200	up	Wdr4	Mus musculus WD repeat domain 4 (Wdr4), mRNA.
5050095	60.733	up	2310007F21Rik	Mus musculus RIKEN cDNA 2310007F21 gene (2310007F21Rik), mRNA.
6280477	59.576	up	Ifng	Mus musculus interferon gamma (Ifng), mRNA.

Appendix Table 24: Top twenty genes significantly DOWN-regulated following 2 hr treatment by TPA (compared to EBC-46) in mice as detected on MouseRef-8 v2.0 BeadChips.

ProbeID	FC (abs)	Regulation	Symbol	Definition
6350128	251.199	down	Rps12	Mus musculus ribosomal protein S12 (Rps12), mRNA.
4780762	219.573	down	Ubb	Mus musculus ubiquitin B (Ubb), mRNA.
2690315	191.865	down	Rps14	Mus musculus ribosomal protein S14 (Rps14), mRNA.
540326	163.775	down	Rplp1	Mus musculus ribosomal protein, large, P1 (Rplp1), mRNA.
110092	159.445	down	Gm1821	Mus musculus gene model 1821, (NCBI) (Gm1821), non-coding RNA. XM_899826
6420242	126.901	down	LOC100048187	PREDICTED: Mus musculus similar to ribosomal protein S27 (metallopanstimulin 1) (LOC100048187), mRNA.
7200097	113.634	down	LOC100039571	PREDICTED: Mus musculus similar to ribosomal protein L23a (LOC100039571), mRNA.
7570762	106.215	down	EG668668	Mus musculus predicted gene, EG668668 (EG668668), mRNA.
2000398	97.573	down	Hba-a1	Mus musculus hemoglobin alpha, adult chain 1 (Hba-a1), mRNA.
1170372	91.060	down	Actb	Mus musculus actin, beta (Actb), mRNA.
4060056	86.159	down	2310016E02Rik	Mus musculus RIKEN cDNA 2310016E02 gene (2310016E02Rik), transcript variant 1, mRNA.
6280541	83.213	down	Rps19	Mus musculus ribosomal protein S19 (Rps19), mRNA.
3890626	76.798	down	Eef1g	Mus musculus eukaryotic translation elongation factor 1 gamma (Eef1g), mRNA.
1580187	73.253	down	Mat2a	Mus musculus methionine adenosyltransferase II, alpha (Mat2a), mRNA.
6840433	73.088	down	Npm1	Mus musculus nucleophosmin 1 (Npm1), mRNA.
360437	71.852	down	Maged2	Mus musculus melanoma antigen, family D, 2 (Maged2), mRNA.
2030575	70.792	down	Ppia	Mus musculus peptidylprolyl isomerase A (Ppia), mRNA.
6520619	69.984	down	LOC100047998	PREDICTED: Mus musculus similar to ribosomal protein L37a (LOC100047998), mRNA.
5720609	66.005	down	Lyz	Mus musculus lysozyme (Lyz), mRNA.
1580471	62.044	down	Atp5g3	Mus musculus ATP synthase, H+ transporting, mitochondrial F0 complex, subunit c (subunit 9), isoform 3 (Atp5g3), nuclear gene encoding mitochondrial protein, mRNA.

Appendix Table 25: Top twenty genes significantly UP-regulated following 4 hr treatment by TPA (compared to EBC-46) in mice as detected on MouseRef-8 v2.0 BeadChips.

ProbeID	FC (abs)	Regulation	Symbol	Definition
3360608	8.740	up	Cfd	Mus musculus complement factor D (adipsin) (Cfd), mRNA.
1050678	3.439	up	Actn2	Mus musculus actinin alpha 2 (Actn2), mRNA.
4040386	2.881	up	Hspb6	Mus musculus heat shock protein, alpha-crystallin-related, B6 (Hspb6), mRNA.
6100612	2.642	up	Pde4dip	Mus musculus phosphodiesterase 4D interacting protein (myomegalin) (Pde4dip), transcript variant 1, mRNA.
3610296	2.554	up	Krtap16-3	Mus musculus keratin associated protein 16-3 (Krtap16-3), mRNA.
1780411	2.540	up	Des	Mus musculus desmin (Des), mRNA.
2510561	2.457	up	Myl4	Mus musculus myosin, light polypeptide 4 (Myl4), mRNA.
6860228	2.386	up	Myh1	Mus musculus myosin, heavy polypeptide 1, skeletal muscle, adult (Myh1), mRNA.
7150685	2.361	up	Tcap	Mus musculus titin-cap (Tcap), mRNA.
4810450	2.219	up	Adipoq	Mus musculus adiponectin, C1Q and collagen domain containing (Adipoq), mRNA.
4220364	2.214	up	Ryr1	Mus musculus ryanodine receptor 1, skeletal muscle (Ryr1), mRNA.
3990609	2.137	up	Nrap	Mus musculus nebulin-related anchoring protein (Nrap), transcript variant 1, mRNA.
5220279	2.094	up	Mt1	Mus musculus metallothionein 1 (Mt1), mRNA.
7510243	2.051	up	C4b	Mus musculus complement component 4B (Childo blood group) (C4b), mRNA. XM_921663 XM_921673 XM_921676 XM_921678
2470133	2.016	up	Csrp3	Mus musculus cysteine and glycine-rich protein 3 (Csrp3), mRNA.
6100403	2.016	up	8030451F13Rik	Mus musculus RIKEN cDNA 8030451F13 gene (8030451F13Rik), mRNA.
4490358	2.013	up	Bloc1s1	Mus musculus biogenesis of lysosome-related organelles complex-1, subunit 1 (Bloc1s1), mRNA.
3440615	2.012	up	Dscr1	
3120259	2.001	up	Rnf114	Mus musculus ring finger protein 114 (Rnf114), mRNA.

Appendix Table 26: Top twenty genes significantly DOWN-regulated following 4 hr treatment by TPA (compared to EBC-46) in mice as detected on MouseRef-8 v2.0 BeadChips.

ProbeID	FC (abs)	Regulation	Symbol	Definition
5050750	2.451	down	Med15	Mus musculus mediator complex subunit 15 (Med15), transcript variant 1, mRNA.
6180544	2.117	down	Mmp3	Mus musculus matrix metallopeptidase 3 (Mmp3), mRNA.
6580470	2.040	down	Mapk3	
510368	2.010	down	Fos	Mus musculus FBJ osteosarcoma oncogene (Fos), mRNA.

Appendix Table 27: Top twenty genes significantly UP-regulated following 8 hr treatment by TPA (compared to EBC-46) in mice as detected on MouseRef-8 v2.0 BeadChips.

ProbeID	FC (abs)	Regulation	Symbol	Definition
6060379	198.425	up	Cdc2a	Mus musculus cell division cycle 2 homolog A (S. pombe) (Cdc2a), mRNA.
7510736	177.471	up	Prl7a1	Mus musculus prolactin family 7, subfamily a, member 1 (Prl7a1), mRNA.
2680133	163.174	up	BC057371	Mus musculus cDNA sequence BC057371 (BC057371), mRNA.
3370246	139.275	up	Tmem110	Mus musculus transmembrane protein 110 (Tmem110), mRNA.
5860204	136.629	up	Og9x	
3290754	131.347	up	Jarid1c	
7400544	122.666	up	Tspyl1	Mus musculus testis-specific protein, Y-encoded-like 1 (Tspyl1), mRNA.
3310746	107.408	up	Ercc2	Mus musculus excision repair cross-complementing rodent repair deficiency, complementation group 2 (Ercc2), mRNA.
5390113	105.452	up	OTTMUSG000000 16790	Mus musculus predicted gene, OTTMUSG00000016790 (OTTMUSG00000016790), mRNA.
3400609	105.040	up	Lcmt1	Mus musculus leucine carboxyl methyltransferase 1 (Lcmt1), mRNA.
4670008	100.948	up	Mbd1	Mus musculus methyl-CpG binding domain protein 1 (Mbd1), mRNA.
4590615	90.688	up	Ccdc9	Mus musculus coiled-coil domain containing 9 (Ccdc9), mRNA.
3520300	87.946	up	Ncf1	Mus musculus neutrophil cytosolic factor 1 (Ncf1), mRNA.
2570538	82.011	up	LOC100047653	PREDICTED: Mus musculus hypothetical protein LOC100047653, transcript variant 2 (LOC100047653), mRNA.
1260301	67.610	up	Spint2	Mus musculus serine protease inhibitor, Kunitz type 2 (Spint2), transcript variant 1, mRNA.
3310484	60.909	up	Mterfd1	Mus musculus MTERF domain containing 1 (Mterfd1), mRNA.
1010204	58.736	up	Wwtr1	Mus musculus WW domain containing transcription regulator 1 (Wwtr1), mRNA.
7210736	57.206	up	Gipc1	Mus musculus GIPC PDZ domain containing family, member 1 (Gipc1), mRNA.
3830167	55.629	up	Trim60	Mus musculus tripartite motif-containing 60 (Trim60), mRNA.
2630348	54.816	up	Dnase1	Mus musculus deoxyribonuclease I (Dnase1), mRNA.

Appendix Table 28: Top twenty genes significantly DOWN-regulated following 8 hr treatment by TPA (compared to EBC-46) in mice as detected on MouseRef-8 v2.0 BeadChips.

ProbeID	FC (abs)	Regulation	Symbol	Definition
6350128	225.202	down	Rps12	Mus musculus ribosomal protein S12 (Rps12), mRNA.
4780762	200.248	down	Ubb	Mus musculus ubiquitin B (Ubb), mRNA.
540326	177.389	down	Rplp1	Mus musculus ribosomal protein, large, P1 (Rplp1), mRNA.
2690315	170.250	down	Rps14	Mus musculus ribosomal protein S14 (Rps14), mRNA.
110092	160.279	down	Gm1821	Mus musculus gene model 1821, (NCBI) (Gm1821), non-coding RNA. XM_899826
7570762	141.669	down	EG668668	Mus musculus predicted gene, EG668668 (EG668668), mRNA.
1170372	94.878	down	Actb	Mus musculus actin, beta (Actb), mRNA.
2000398	93.457	down	Hba-a1	Mus musculus hemoglobin alpha, adult chain 1 (Hba-a1), mRNA.
2260576	88.299	down	Tuba1b	Mus musculus tubulin, alpha 1B (Tuba1b), mRNA.
1580471	86.363	down	Atp5g3	Mus musculus ATP synthase, H+ transporting, mitochondrial F0 complex, subunit c (subunit 9), isoform 3 (Atp5g3), nuclear gene encoding mitochondrial protein, mRNA.
4060056	79.448	down	2310016E02Rik	Mus musculus RIKEN cDNA 2310016E02 gene (2310016E02Rik), transcript variant 1, mRNA.
6520619	77.653	down	LOC100047998	PREDICTED: Mus musculus similar to ribosomal protein L37a (LOC100047998), mRNA.
6420242	77.376	down	LOC100048187	PREDICTED: Mus musculus similar to ribosomal protein S27 (metallopanstimulin 1) (LOC100048187), mRNA.
360437	77.314	down	Maged2	Mus musculus melanoma antigen, family D, 2 (Maged2), mRNA.
6840433	73.169	down	Npm1	Mus musculus nucleophosmin 1 (Npm1), mRNA.
780093	63.526	down	Cox6b1	Mus musculus cytochrome c oxidase, subunit VIb polypeptide 1 (Cox6b1), mRNA.
7050300	61.216	down	Eif4a2	Mus musculus eukaryotic translation initiation factor 4A2 (Eif4a2), mRNA.
1470470	59.576	down	Serf2	Mus musculus small EDRK-rich factor 2 (Serf2), mRNA.
1580280	57.107	down	Fth1	Mus musculus ferritin heavy chain 1 (Fth1), mRNA.
6940014	50.841	down	Tmem147	Mus musculus transmembrane protein 147 (Tmem147), mRNA.

Appendix Table 29: Top twenty genes significantly UP-regulated in PBMCs following 4 hr treatment by 30 ng/ml of EBC-46 (compared to untreated PBMCs) as detected on HumanHT-12 v4 Illumina BeadChips.

ProbeID	FC (abs)	Regulation	Symbol	Definition
450762	2.388	up	FCGR2A	Homo sapiens Fc fragment of IgG, low affinity IIa, receptor (CD32) (FCGR2A), mRNA.
2190349	2.036	up	KCNJ15	Homo sapiens potassium inwardly-rectifying channel, subfamily J, member 15 (KCNJ15), transcript variant 3, mRNA.
3520398	2.090	up	IL28RA	Homo sapiens interleukin 28 receptor, alpha (interferon, lambda receptor) (IL28RA), transcript variant 1, mRNA.
990474	2.105	up	TAF9	Homo sapiens TAF9 RNA polymerase II, TATA box binding protein (TBP)-associated factor, 32kDa (TAF9), transcript variant 2, mRNA.
130181	2.822	up	ANKRD22	Homo sapiens ankyrin repeat domain 22 (ANKRD22), mRNA.
5570398	4.240	up	FCGR1C	Homo sapiens Fc fragment of IgG, high affinity Ic, receptor (CD64) (FCGR1C), mRNA.
5270132	2.053	up	CBLB	Homo sapiens Cas-Br-M (murine) ecotropic retroviral transforming sequence b (CBLB), mRNA.
1510364	3.203	up	GBP5	Homo sapiens guanylate binding protein 5 (GBP5), mRNA.
7040537	2.389	up	TAF9	Homo sapiens TAF9 RNA polymerase II, TATA box binding protein (TBP)-associated factor, 32kDa (TAF9), transcript variant 3, mRNA.
20010	2.106	up	CARS	Homo sapiens cysteinyl-tRNA synthetase (CARS), transcript variant 4, mRNA.
430630	2.034	up	HSPA9	Homo sapiens heat shock 70kDa protein 9 (mortalin) (HSPA9), nuclear gene encoding mitochondrial protein, mRNA.
3400722	2.126	up	C7orf57	Homo sapiens chromosome 7 open reading frame 57 (C7orf57), mRNA.
3420253	2.017	up	CSTF3	Homo sapiens cleavage stimulation factor, 3' pre-RNA, subunit 3, 77kDa (CSTF3), transcript variant 2, mRNA.
3440400	2.251	up	TMCC3	Homo sapiens transmembrane and coiled-coil domain family 3 (TMCC3), mRNA.
5700707	3.134	up	SPRED1	Homo sapiens sprouty-related, EVH1 domain containing 1 (SPRED1), mRNA.
1240528	2.511	up	IL1F5	Homo sapiens interleukin 1 family, member 5 (delta) (IL1F5), transcript variant 2, mRNA.
1030463	2.395	up	PROK2	Homo sapiens prokineticin 2 (PROK2), mRNA.
2970164	2.220	up	EDNRB	Homo sapiens endothelin receptor type B (EDNRB), transcript variant 1, mRNA.
3440735	2.025	up	C10orf141	Homo sapiens chromosome 10 open reading frame 141 (C10orf141), mRNA.
5220093	2.001	up	HAVCR2	Homo sapiens hepatitis A virus cellular receptor 2 (HAVCR2), mRNA.

Appendix Table 30: Top twenty genes significantly DOWN-regulated in PBMCs following 4 hr treatment by 30 ng/ml of EBC-46 (compared to untreated PBMCs) as detected on HumanHT-12 v4 Illumina BeadChips.

ProbeID	FC (abs)	Regulation	Symbol	Definition
5560193	3.194	down	BCAS4	Homo sapiens breast carcinoma amplified sequence 4 (BCAS4), transcript variant 1, mRNA.
6620392	3.187	down	LFNG	Homo sapiens LFNG O-fucosylpeptide 3-beta-N-acetylglucosaminyltransferase (LFNG), transcript variant 1, mRNA.
670711	3.140	down	PLCL2	Homo sapiens phospholipase C-like 2 (PLCL2), mRNA.
2450129	3.121	down	FLOT2	Homo sapiens flotillin 2 (FLOT2), mRNA.
3710647	3.030	down	MXD4	Homo sapiens MAX dimerization protein 4 (MXD4), mRNA.
3710685	2.941	down	CARD9	Homo sapiens caspase recruitment domain family, member 9 (CARD9), mRNA.
1470215	2.914	down	MAP3K8	Homo sapiens mitogen-activated protein kinase kinase kinase 8 (MAP3K8), mRNA.
3450201	2.836	down	FAM65B	Homo sapiens family with sequence similarity 65, member B (FAM65B), transcript variant 2, mRNA.
6330471	2.793	down	BLK	Homo sapiens B lymphoid tyrosine kinase (BLK), mRNA.
7200743	2.770	down	SLAMF6	Homo sapiens SLAM family member 6 (SLAMF6), mRNA.
1050672	2.712	down	CKAP2	Homo sapiens cytoskeleton associated protein 2 (CKAP2), transcript variant 2, mRNA.
5290239	2.707	down	XRCC6BP1	Homo sapiens XRCC6 binding protein 1 (XRCC6BP1), mRNA.
1170703	2.693	down	RCSD1	Homo sapiens RCSD domain containing 1 (RCSD1), mRNA.
1430717	2.669	down	BTN3A3	Homo sapiens butyrophilin, subfamily 3, member A3 (BTN3A3), transcript variant 2, mRNA.
3120292	2.668	down	FAM117B	Homo sapiens family with sequence similarity 117, member B (FAM117B), mRNA.
940152	2.632	down	MKNK2	Homo sapiens MAP kinase interacting serine/threonine kinase 2 (MKNK2), transcript variant 1, mRNA.
4830458	2.630	down	GMPPB	Homo sapiens GDP-mannose pyrophosphorylase B (GMPPB), transcript variant 2, mRNA.
6960215	2.627	down	PITPNM1	Homo sapiens phosphatidylinositol transfer protein, membrane-associated 1 (PITPNM1), mRNA.
2060411	2.605	down	LOC652616	PREDICTED: Homo sapiens similar to neutrophil cytosolic factor 1 (LOC652616), mRNA.
5900286	2.604	down	ZFP90	Homo sapiens zinc finger protein 90 homolog (mouse) (ZFP90), mRNA.

Appendix Table 31: Top twenty genes significantly UP-regulated in PBMCs following 24 hr treatment by 30 ng/ml of EBC-46 (compared to untreated PBMCs) as detected on HumanHT-12 v4 Illumina BeadChips.

ProbeID	FC (abs)	Regulation	Symbol	Definition
5960196	2.109	up	MOGAT1	Homo sapiens monoacylglycerol O-acyltransferase 1 (MOGAT1), mRNA.
520162	2.896	up	HPSE	Homo sapiens heparanase (HPSE), mRNA.
450674	2.403	up	C10orf128	PREDICTED: Homo sapiens chromosome 10 open reading frame 128, transcript variant 5 (C10orf128), mRNA.
2710746	2.385	up	BCAR1	Homo sapiens breast cancer anti-estrogen resistance 1 (BCAR1), mRNA.
5080131	2.116	up	MGST1	Homo sapiens microsomal glutathione S-transferase 1 (MGST1), transcript variant 1a, mRNA.
5690202	2.389	up	AKIRIN2	Homo sapiens akirin 2 (AKIRIN2), mRNA.
3940754	2.468	up	CD226	Homo sapiens CD226 molecule (CD226), mRNA.
6330270	6.610	up	GPC4	Homo sapiens glypican 4 (GPC4), mRNA.
7650689	2.636	up		ij82b05.y1 Human insulinoma Homo sapiens cDNA clone IMAGE: 5777984 5, mRNA sequence
4230672	2.077	up	LOC653496	PREDICTED: Homo sapiens similar to hypothetical gene supported by AK123662 (LOC653496), mRNA.
5720184	4.393	up	KLF10	Homo sapiens Kruppel-like factor 10 (KLF10), transcript variant 1, mRNA.
7150619	2.765	up	CSF1	Homo sapiens colony stimulating factor 1 (macrophage) (CSF1), transcript variant 1, mRNA.
510576	2.112	up	BCOR	Homo sapiens BCL6 co-repressor (BCOR), transcript variant 1, mRNA.
60102	2.114	up	MAPKAP1	Homo sapiens mitogen-activated protein kinase associated protein 1 (MAPKAP1), transcript variant 6, mRNA.
6400370	2.057	up	IL12RB1	Homo sapiens interleukin 12 receptor, beta 1 (IL12RB1), transcript variant 2, mRNA.
5260546	3.225	up	ADAM17	Homo sapiens ADAM metallopeptidase domain 17 (ADAM17), mRNA.
3420253	2.288	up	CSTF3	Homo sapiens cleavage stimulation factor, 3' pre-RNA, subunit 3, 77kDa (CSTF3), transcript variant 2, mRNA.
6450687	2.021	up	EXOSC7	Homo sapiens exosome component 7 (EXOSC7), mRNA.
7150551	2.742	up	MMP19	Homo sapiens matrix metallopeptidase 19 (MMP19), transcript variant 2, mRNA.
2970164	2.640	up	EDNRB	Homo sapiens endothelin receptor type B (EDNRB), transcript variant 1, mRNA.

Appendix Table 32: Top twenty genes significantly DOWN-regulated in PBMCs following 24 hr treatment by 30 ng/ml of EBC-46 (compared to untreated PBMCs) as detected on HumanHT-12 v4 Illumina BeadChips.

ProbeID	FC (abs)	Regulation	Symbol	Definition
2640619	2.931	down	ZNF91	Homo sapiens zinc finger protein 91 (ZNF91), mRNA.
7200240	2.731	down	ARHGAP4	Homo sapiens Rho GTPase activating protein 4 (ARHGAP4), mRNA.
1500189	2.686	down	CD81	Homo sapiens CD81 molecule (CD81), mRNA.
1410603	2.649	down	RAB3IP	Homo sapiens RAB3A interacting protein (rabin3) (RAB3IP), transcript variant A, mRNA.
6370576	2.639	down	TREM2	Homo sapiens triggering receptor expressed on myeloid cells 2 (TREM2), mRNA.
1940273	2.567	down	SGSM2	Homo sapiens small G protein signaling modulator 2 (SGSM2), transcript variant 1, mRNA.
6480095	2.543	down	SNX27	Homo sapiens sorting nexin family member 27 (SNX27), mRNA.
6220438	2.518	down	RPS6KA5	Homo sapiens ribosomal protein S6 kinase, 90kDa, polypeptide 5 (RPS6KA5), transcript variant 1, mRNA.
3290292	2.491	down	LAP3	Homo sapiens leucine aminopeptidase 3 (LAP3), mRNA.
940639	2.472	down	ERP27	Homo sapiens endoplasmic reticulum protein 27 kDa (ERP27), mRNA.
2710682	2.462	down	NQO2	Homo sapiens NAD(P)H dehydrogenase, quinone 2 (NQO2), mRNA.
3890689	2.418	down	CD247	Homo sapiens CD247 molecule (CD247), transcript variant 1, mRNA.
6960288	2.402	down		Homo sapiens cDNA FLJ36653 fis, clone UTERU2001176
240025	2.400	down	CNPY3	Homo sapiens canopy 3 homolog (zebrafish) (CNPY3), mRNA.
4120367	2.386	down	LPCAT2	Homo sapiens lysophosphatidylcholine acyltransferase 2 (LPCAT2), mRNA.
1070097	2.368	down	TPCN1	Homo sapiens two pore segment channel 1 (TPCN1), mRNA.
5050537	2.367	down	OPLAH	Homo sapiens 5-oxoprolinase (ATP-hydrolysing) (OPLAH), mRNA.
6660626	2.353	down	BRD3	Homo sapiens bromodomain containing 3 (BRD3), mRNA.
1980521	2.349	down	SLC44A2	Homo sapiens solute carrier family 44, member 2 (SLC44A2), mRNA.
130086	2.347	down	CYB561	Homo sapiens cytochrome b-561 (CYB561), transcript variant 1, mRNA.

Appendix Table 33: Top twenty genes significantly UP-regulated in PBMCs following 96 hr treatment by 30 ng/ml of EBC-46 (compared to untreated PBMCs) as detected on HumanHT-12 v4 Illumina BeadChips.

ProbeID	FC (abs)	Regulation	Symbol	Definition
1190064	3.911	up	UGT2B7	PREDICTED: Homo sapiens UDP glucuronosyltransferase 2 family, polypeptide B7 (UGT2B7), mRNA.
5420450	2.519	up	UGT2B7	PREDICTED: Homo sapiens UDP glucuronosyltransferase 2 family, polypeptide B7 (UGT2B7), mRNA.
4010491	2.906	up	CST6	PREDICTED: Homo sapiens cystatin E/M (CST6), mRNA.
3520092	2.064	up	BAX	Homo sapiens BCL2-associated X protein (BAX), transcript variant sigma, mRNA.
2510253	2.301	up	C10orf35	Homo sapiens chromosome 10 open reading frame 35 (C10orf35), mRNA.
130717	2.466	up	ARPC1B	Homo sapiens actin related protein 2/3 complex, subunit 1B, 41kDa (ARPC1B), mRNA.
510114	3.844	up	CCNB1IP1	Homo sapiens cyclin B1 interacting protein 1 (CCNB1IP1), transcript variant 3, mRNA.
6980167	2.340	up	C21orf121	Homo sapiens chromosome 21 open reading frame 121 (C21orf121), mRNA.
6510377	3.268	up	TNFRSF12A	Homo sapiens tumor necrosis factor receptor superfamily, member 12A (TNFRSF12A), mRNA.
7050064	4.389	up	RAMP1	Homo sapiens receptor (G protein-coupled) activity modifying protein 1 (RAMP1), mRNA.
5570139	3.435	up	QPCT	Homo sapiens glutaminyl-peptide cyclotransferase (QPCT), mRNA.
7550348	2.150	up	NUP188	Homo sapiens nucleoporin 188kDa (NUP188), mRNA.
1990196	2.067	up	DACT3	Homo sapiens dapper, antagonist of beta-catenin, homolog 3 (Xenopus laevis) (DACT3), mRNA.
2710575	6.069	up	CD69	Homo sapiens CD69 molecule (CD69), mRNA.
5420474	2.025	up	HSPBL2	Homo sapiens heat shock 27kDa protein-like 2 pseudogene (HSPBL2), non-coding RNA.
5570520	3.053	up	RRAD	Homo sapiens Ras-related associated with diabetes (RRAD), mRNA.
7200639	2.523	up	RRAD	Homo sapiens Ras-related associated with diabetes (RRAD), mRNA.
2940075	2.103	up	STRADB	Homo sapiens STE20-related kinase adaptor beta (STRADB), mRNA.
1990630	2.275	up	TRIB3	Homo sapiens tribbles homolog 3 (Drosophila) (TRIB3), mRNA.
1340039	2.072	up	TFPI	Homo sapiens tissue factor pathway inhibitor (lipoprotein-associated coagulation inhibitor) (TFPI), transcript variant 1, mRNA.

Appendix Table 34: Top twenty genes significantly DOWN-regulated in PBMCs following 96 hr treatment by 30 ng/ml of EBC-46 (compared to untreated PBMCs) as detected on HumanHT-12 v4 Illumina BeadChips.

ProbeID	FC (abs)	Regulation	Symbol	Definition
6370369	210.764	down	CD14	Homo sapiens CD14 molecule (CD14), transcript variant 2, mRNA.
4010296	171.783	down	RNASE1	Homo sapiens ribonuclease, RNase A family, 1 (pancreatic) (RNASE1), transcript variant 1, mRNA.
6660398	88.364	down	FCN1	Homo sapiens ficolin (collagen/fibrinogen domain containing) 1 (FCN1), mRNA.
1090307	58.509	down	RNASE1	Homo sapiens ribonuclease, RNase A family, 1 (pancreatic) (RNASE1), transcript variant 3, mRNA.
2260129	51.553	down	MS4A6A	Homo sapiens membrane-spanning 4-domains, subfamily A, member 6A (MS4A6A), transcript variant 2, mRNA.
2060121	49.915	down	FUCA1	Homo sapiens fucosidase, alpha-L- 1, tissue (FUCA1), mRNA.
5310402	42.935	down	FPR3	Homo sapiens formyl peptide receptor 3 (FPR3), mRNA.
4560129	34.977	down	LGMN	Homo sapiens legumain (LGMN), transcript variant 2, mRNA.
2470184	25.810	down	ADAMDEC1	Homo sapiens ADAM-like, decysin 1 (ADAMDEC1), mRNA.
6270553	23.977	down	CXCL10	Homo sapiens chemokine (C-X-C motif) ligand 10 (CXCL10), mRNA.
7560138	23.377	down	PMP22	Homo sapiens peripheral myelin protein 22 (PMP22), transcript variant 2, mRNA.
3180039	19.224	down	RGL1	Homo sapiens ral guanine nucleotide dissociation stimulator-like 1 (RGL1), mRNA.
6060484	17.002	down	MARCKS	Homo sapiens myristoylated alanine-rich protein kinase C substrate (MARCKS), mRNA.
1690056	13.284	down	LYZ	Homo sapiens lysozyme (renal amyloidosis) (LYZ), mRNA.
1510538	12.917	down	EPB41L3	Homo sapiens erythrocyte membrane protein band 4.1-like 3 (EPB41L3), mRNA.
3990433	11.953	down	ADAP2	Homo sapiens ArfGAP with dual PH domains 2 (ADAP2), mRNA.
2190717	11.363	down	IL18BP	Homo sapiens interleukin 18 binding protein (IL18BP), transcript variant A, mRNA.
2750685	10.402	down	LOC392437	PREDICTED: Homo sapiens misc_RNA (LOC392437), miscRNA.
6450543	9.526	down	CST3	Homo sapiens cystatin C (CST3), mRNA.
3390594	8.779	down	KLRD1	Homo sapiens killer cell lectin-like receptor subfamily D, member 1 (KLRD1), transcript variant 1, mRNA.

Appendix Table 35: Top twenty genes significantly UP-regulated in PBMCs following 4 hr treatment by 30 ng/ml of TPA (compared to untreated PBMCs) as detected on HumanHT-12 v4 Illumina BeadChips.

ProbeID	FC (abs)	Regulation	Symbol	Definition
6420520	2.547	up	CD40	Homo sapiens CD40 molecule, TNF receptor superfamily member 5 (CD40), transcript variant 1, mRNA.
5130397	2.235	up		602617110F1 NIH_MGC_79 Homo sapiens cDNA clone IMAGE:4730811 5, mRNA sequence
6290187	2.382	up	RCE1	Homo sapiens RCE1 homolog, prenyl protein peptidase (S. cerevisiae) (RCE1), transcript variant 2, mRNA.
6180445	2.466	up	LOC389286	Homo sapiens similar to FKSG62 (LOC389286), mRNA.
3800551	2.088	up	MICAL1	Homo sapiens microtubule associated monoxygenase, calponin and LIM domain containing 1 (MICAL1), mRNA.
7150176	2.328	up	MAT2A	Homo sapiens methionine adenosyltransferase II, alpha (MAT2A), mRNA.
1570273	2.045	up	NEDD4L	Homo sapiens neural precursor cell expressed, developmentally down-regulated 4-like (NEDD4L), mRNA.
670136	2.022	up	FLJ38717	Homo sapiens FLJ38717 protein (FLJ38717), mRNA.
3800482	2.802	up	MGC61598	PREDICTED: Homo sapiens similar to ankyrin-repeat protein Nrarp (MGC61598), mRNA.
4250537	2.071	up	DNAJB4	Homo sapiens DnaJ (Hsp40) homolog, subfamily B, member 4 (DNAJB4), mRNA.
5420528	2.131	up	DNAJB4	Homo sapiens DnaJ (Hsp40) homolog, subfamily B, member 4 (DNAJB4), mRNA.
2650349	2.539	up	C19orf48	Homo sapiens chromosome 19 open reading frame 48 (C19orf48), mRNA.
2850630	2.260	up	C19orf48	Homo sapiens chromosome 19 open reading frame 48 (C19orf48), mRNA.
7380368	2.010	up	WDR74	PREDICTED: Homo sapiens WD repeat domain 74 (WDR74), mRNA.
2190537	2.090	up	WDR74	PREDICTED: Homo sapiens WD repeat domain 74 (WDR74), mRNA.
2650020	2.008	up	PWWP2B	Homo sapiens PWWP domain containing 2B (PWWP2B), transcript variant 1, mRNA.
4590519	2.406	up	LOC100130332	PREDICTED: Homo sapiens similar to PRO2474 (LOC100130332), mRNA.
3440692	2.057	up	CHMP7	Homo sapiens CHMP family, member 7 (CHMP7), mRNA.
2370092	2.019	up	STXBP6	Homo sapiens syntaxin binding protein 6 (amisyn) (STXBP6), mRNA.
2060608	2.951	up		FNPARC07 FNP Homo sapiens cDNA, mRNA sequence

Appendix Table 36: Top twenty genes significantly DOWN-regulated in PBMCs following 4 hr treatment by 30 ng/ml of TPA (compared to untreated PBMCs)as detected on HumanHT-12 v4 Illumina BeadChips.

ProbeID	FC (abs)	Regulation	Symbol	Definition
1430280	7.064	down	CEBPA	Homo sapiens CCAAT/enhancer binding protein (C/EBP), alpha (CEBPA), mRNA.
50286	5.132	down	EEPD1	Homo sapiens endonuclease/exonuclease/phosphatase family domain containing 1 (EEPD1), mRNA.
4040162	5.000	down	MEF2C	Homo sapiens myocyte enhancer factor 2C (MEF2C), mRNA.
1440064	4.211	down		Homo sapiens cDNA FLJ44441 fis, clone UTERU2020242
1940021	4.098	down	GRN	Homo sapiens granulin (GRN), mRNA.
6420750	4.012	down	TLR2	Homo sapiens toll-like receptor 2 (TLR2), mRNA.
3390438	4.000	down	PLA2G7	Homo sapiens phospholipase A2, group VII (platelet-activating factor acetylhydrolase, plasma) (PLA2G7), mRNA.
2120053	3.953	down	CYP1B1	Homo sapiens cytochrome P450, family 1, subfamily B, polypeptide 1 (CYP1B1), mRNA.
580358	3.895	down	FABP5L2	PREDICTED: Homo sapiens fatty acid binding protein 5-like 2 (FABP5L2), mRNA.
4200343	3.881	down	CYFIP1	Homo sapiens cytoplasmic FMR1 interacting protein 1 (CYFIP1), transcript variant 2, mRNA.
6860482	3.865	down	HERC6	Homo sapiens hect domain and RLD 6 (HERC6), transcript variant 1, mRNA.
6380484	3.848	down	SERPINA1	Homo sapiens serpin peptidase inhibitor, clade A (alpha-1 antiproteinase, antitrypsin), member 1 (SERPINA1), transcript variant 3, mRNA.
520408	3.704	down	IFIT3	Homo sapiens interferon-induced protein with tetratricopeptide repeats 3 (IFIT3), mRNA.
1240152	3.695	down	CFD	Homo sapiens complement factor D (adipsin) (CFD), mRNA.
4610672	3.597	down	FLJ14213	Homo sapiens protor-2 (FLJ14213), mRNA.
1260228	3.579	down	CLEC5A	Homo sapiens C-type lectin domain family 5, member A (CLEC5A), mRNA.
1190739	3.520	down	ITPRIPL2	Homo sapiens inositol 1,4,5-triphosphate receptor interacting protein-like 2 (ITPRIPL2), mRNA.
6840184	3.512	down	GRN	Homo sapiens granulin (GRN), mRNA.
6400465	3.471	down	PTPN6	Homo sapiens protein tyrosine phosphatase, non-receptor type 6 (PTPN6), transcript variant 2, mRNA.
6060468	3.468	down	S100A8	Homo sapiens S100 calcium binding protein A8 (S100A8), mRNA.

Appendix Table 37: Top twenty genes significantly UP-regulated in PBMCs following 24 hr treatment by 30 ng/ml of TPA (compared to untreated PBMCs) as detected on HumanHT-12 v4 Illumina BeadChips.

ProbeID	FC (abs)	Regulation	Symbol	Definition
4230136	2.156	up	TCP1	Homo sapiens t-complex 1 (TCP1), transcript variant 1, mRNA.
6650692	2.223	up	ISOC2	Homo sapiens isochorismatase domain containing 2 (ISOC2), mRNA.
540717	2.210	up	LONP1	Homo sapiens lon peptidase 1, mitochondrial (LONP1), nuclear gene encoding mitochondrial protein, mRNA.
3800577	2.200	up	LOC642661	PREDICTED: Homo sapiens misc_RNA (LOC642661), miscRNA.
160537	2.148	up	FVT1	Homo sapiens follicular lymphoma variant translocation 1 (FVT1), mRNA.
3930132	2.203	up	TUBA3D	Homo sapiens tubulin, alpha 3d (TUBA3D), mRNA.
5270296	2.161	up	TFB2M	Homo sapiens transcription factor B2, mitochondrial (TFB2M), nuclear gene encoding mitochondrial protein, mRNA.
4060722	2.249	up	PHB2	Homo sapiens prohibitin 2 (PHB2), transcript variant 2, mRNA.
4830301	2.209	up	KAT2A	Homo sapiens K(lysine) acetyltransferase 2A (KAT2A), mRNA.
6450372	2.059	up	PDHA1	Homo sapiens pyruvate dehydrogenase (lipoamide) alpha 1 (PDHA1), mRNA.
2760332	2.016	up	SCARNA10	Homo sapiens small Cajal body-specific RNA 10 (SCARNA10), guide RNA.
7150176	2.051	up	MAT2A	Homo sapiens methionine adenosyltransferase II, alpha (MAT2A), mRNA.
6650176	2.204	up	TRMT11	Homo sapiens tRNA methyltransferase 11 homolog (S. cerevisiae) (TRMT11), mRNA.
1010630	2.318	up	NOP2	Homo sapiens NOP2 nucleolar protein homolog (yeast) (NOP2), transcript variant 1, mRNA.
6960538	2.275	up	NOP2	Homo sapiens NOP2 nucleolar protein homolog (yeast) (NOP2), transcript variant 1, mRNA.
4480341	2.741	up	DHCR24	Homo sapiens 24-dehydrocholesterol reductase (DHCR24), mRNA.
5310300	2.464	up	SFRS13A	Homo sapiens splicing factor, arginine/serine-rich 13A (SFRS13A), transcript variant 2, mRNA.
630709	2.548	up	ELOF1	Homo sapiens elongation factor 1 homolog (S. cerevisiae) (ELOF1), mRNA.
2650349	2.767	up	C19orf48	Homo sapiens chromosome 19 open reading frame 48 (C19orf48), mRNA.
2850630	2.540	up	C19orf48	Homo sapiens chromosome 19 open reading frame 48 (C19orf48), mRNA.

Appendix Table 38: Top twenty genes significantly DOWN-regulated in PBMCs following 24 hr treatment by 30 ng/ml of TPA (compared to untreated PBMCs) as detected on HumanHT-12 v4 Illumina BeadChips.

ProbeID	FC (abs)	Regulation	Symbol	Definition
3310538	7.616	down	CD36	Homo sapiens CD36 molecule (thrombospondin receptor) (CD36), transcript variant 3, mRNA.
2140136	6.465	down	EMR2	Homo sapiens egf-like module containing, mucin-like, hormone receptor-like 2 (EMR2), transcript variant 2, mRNA.
1010592	5.565	down	CD36	Homo sapiens CD36 molecule (thrombospondin receptor) (CD36), transcript variant 1, mRNA.
3290639	5.162	down	RAB7B	Homo sapiens RAB7B, member RAS oncogene family (RAB7B), mRNA.
6040324	4.072	down	SDCBP	Homo sapiens syndecan binding protein (syntenin) (SDCBP), transcript variant 2, mRNA.
1190739	3.851	down	ITPRIPL2	Homo sapiens inositol 1,4,5-triphosphate receptor interacting protein-like 2 (ITPRIPL2), mRNA.
6450092	3.803	down	C5AR1	Homo sapiens complement component 5a receptor 1 (C5AR1), mRNA.
3140364	3.636	down	PTPN12	Homo sapiens protein tyrosine phosphatase, non-receptor type 12 (PTPN12), mRNA.
7210170	3.512	down	DSE	Homo sapiens dermatan sulfate epimerase (DSE), transcript variant 1, mRNA.
2030687	3.484	down	C3orf59	Homo sapiens chromosome 3 open reading frame 59 (C3orf59), mRNA.
5490240	3.428	down	MAP1LC3A	Homo sapiens microtubule-associated protein 1 light chain 3 alpha (MAP1LC3A), transcript variant 2, mRNA.
3800463	3.274	down	SLC29A3	Homo sapiens solute carrier family 29 (nucleoside transporters), member 3 (SLC29A3), mRNA.
2480544	3.273	down	KCNMB1	Homo sapiens potassium large conductance calcium-activated channel, subfamily M, beta member 1 (KCNMB1), mRNA.
7040142	3.257	down	KYNU	Homo sapiens kynureninase (L-kynurenine hydrolase) (KYNU), transcript variant 2, mRNA.
7210253	3.125	down	LOC730415	PREDICTED: Homo sapiens hypothetical LOC730415, transcript variant 2 (LOC730415), mRNA.
1030333	3.108	down	CCL2	Homo sapiens chemokine (C-C motif) ligand 2 (CCL2), mRNA.
510079	3.072	down	HLA-DRB4	Homo sapiens major histocompatibility complex, class II, DR beta 4 (HLA-DRB4), mRNA.
3460685	3.041	down	KYNU	Homo sapiens kynureninase (L-kynurenine hydrolase) (KYNU), transcript variant 1, mRNA.
1400520	3.036	down	CNTNAP2	Homo sapiens contactin associated protein-like 2 (CNTNAP2), mRNA.
5900564	3.018	down	SLC16A6	Homo sapiens solute carrier family 16, member 6 (monocarboxylic acid transporter 7) (SLC16A6), mRNA.

Appendix Table 39: Top twenty genes significantly UP-regulated in PBMCs following 96 hr treatment by 30 ng/ml of TPA (compared to untreated PBMCs) as detected on HumanHT-12 v4 Illumina BeadChips.

ProbeID	FC (abs)	Regulation	Symbol	Definition
6650692	2.698	up	ISOC2	Homo sapiens isochorismatase domain containing 2 (ISOC2), mRNA.
4730168	2.556	up	SARS2	Homo sapiens seryl-tRNA synthetase 2, mitochondrial (SARS2), nuclear gene encoding mitochondrial protein, mRNA.
3420433	2.003	up	SHMT1	Homo sapiens serine hydroxymethyltransferase 1 (soluble) (SHMT1), transcript variant 1, mRNA.
2690528	2.126	up	SHMT1	Homo sapiens serine hydroxymethyltransferase 1 (soluble) (SHMT1), transcript variant 1, mRNA.
4060722	2.271	up	PHB2	Homo sapiens prohibitin 2 (PHB2), transcript variant 2, mRNA.
1660270	2.765	up	MTHFD1	Homo sapiens methylenetetrahydrofolate dehydrogenase (NADP+ dependent) 1, methenyltetrahydrofolate cyclohydrolase, formyltetrahydrofolate synthetase (MTHFD1), mRNA.
1110440	2.394	up	WDR77	Homo sapiens WD repeat domain 77 (WDR77), mRNA.
2760332	2.036	up	SCARNA10	Homo sapiens small Cajal body-specific RNA 10 (SCARNA10), guide RNA.
3290291	2.235	up	SLBP	Homo sapiens stem-loop binding protein (SLBP), mRNA.
2900692	3.323	up	GSG2	Homo sapiens germ cell associated 2 (haspin) (GSG2), mRNA.
610537	3.726	up	C21orf42	Homo sapiens chromosome 21 open reading frame 42 (C21orf42), mRNA.
7330338	2.411	up	DEPDC1B	Homo sapiens DEP domain containing 1B (DEPDC1B), mRNA.
1230730	2.005	up	SLC30A5	Homo sapiens solute carrier family 30 (zinc transporter), member 5 (SLC30A5), transcript variant 1, mRNA.
4810750	2.153	up	BEND4	Homo sapiens BEN domain containing 4 (BEND4), mRNA.
430100	2.098	up	XRCC6	Homo sapiens X-ray repair complementing defective repair in Chinese hamster cells 6 (XRCC6), mRNA.
6960538	2.106	up	NOP2	Homo sapiens NOP2 nucleolar protein homolog (yeast) (NOP2), transcript variant 1, mRNA.
1690392	2.543	up	HIST1H2BH	Homo sapiens histone cluster 1, H2bh (HIST1H2BH), mRNA.
4290259	2.251	up	CCDC51	Homo sapiens coiled-coil domain containing 51 (CCDC51), mRNA.
2650494	2.412	up	SMC2	Homo sapiens structural maintenance of chromosomes 2 (SMC2), transcript variant 1, mRNA.
6400647	2.053	up	EHD4	Homo sapiens EH-domain containing 4 (EHD4), mRNA.

Appendix Table 40: Top twenty genes significantly DOWN-regulated in PBMCs following 96 hr treatment by 30 ng/ml of TPA (compared to untreated PBMCs) as detected on HumanHT-12 v4 Illumina BeadChips

ProbeID	FC (abs)	Regulation	Symbol	Definition
7550358	5.134	down	NELL2	Homo sapiens NEL-like 2 (chicken) (NELL2), mRNA.
3850246	4.900	down	HOPX	Homo sapiens HOP homeobox (HOPX), transcript variant 3, mRNA.
2370438	4.606	down	A2M	Homo sapiens alpha-2-macroglobulin (A2M), mRNA.
4280017	4.375	down	FOS	Homo sapiens v-fos FBJ murine osteosarcoma viral oncogene homolog (FOS), mRNA.
840685	4.302	down	IL1B	Homo sapiens interleukin 1, beta (IL1B), mRNA.
2480092	4.165	down	CCL22	Homo sapiens chemokine (C-C motif) ligand 22 (CCL22), mRNA.
1990037	4.146	down	CHI3L1	Homo sapiens chitinase 3-like 1 (cartilage glycoprotein-39) (CHI3L1), mRNA.
4390450	4.109	down	SGK	Homo sapiens serum/glucocorticoid regulated kinase (SGK), mRNA.
3930537	3.930	down		Human T-cell receptor (V beta 4.1-variant, J beta 2.1, C beta 2) mRNA
1410209	3.855	down	SGK1	Homo sapiens serum/glucocorticoid regulated kinase 1 (SGK1), transcript variant 1, mRNA.
1710070	3.786	down	ITGAM	Homo sapiens integrin, alpha M (complement component 3 receptor 3 subunit) (ITGAM), transcript variant 2, mRNA.
1260086	3.748	down	ID2	Homo sapiens inhibitor of DNA binding 2, dominant negative helix-loop-helix protein (ID2), mRNA.
160242	3.625	down	C13orf15	Homo sapiens chromosome 13 open reading frame 15 (C13orf15), mRNA.
2030324	3.466	down	SGK1	Homo sapiens serum/glucocorticoid regulated kinase 1 (SGK1), transcript variant 1, mRNA.
2640192	3.449	down	BNIP3L	Homo sapiens BCL2/adenovirus E1B 19kDa interacting protein 3-like (BNIP3L), mRNA.
4490500	3.351	down	ITGAX	Homo sapiens integrin, alpha X (complement component 3 receptor 4 subunit) (ITGAX), mRNA.
2140382	3.287	down	PASK	Homo sapiens PAS domain containing serine/threonine kinase (PASK), mRNA.
4040653	3.276	down	LOC728855	Homo sapiens hypothetical LOC728855 (LOC728855), non-coding RNA.
1170671	3.244	down	CD3D	Homo sapiens CD3d molecule, delta (CD3-TCR complex) (CD3D), transcript variant 1, mRNA.
1710279	3.200	down	GZMM	Homo sapiens granzyme M (lymphocyte met-ase 1) (GZMM), mRNA.

Appendix Table 41: Upstream Regulator Analysis by IPA of Sk-Mel-28 tumor treated with EBC-46 (versus 20% PG) at 4 hr

Upstream Regulator	Molecule Type	Predicted Activation State	Activation z-score	p-value of overlap
miR-4717-3p (miRNAs w/seed CACAUGG)	mature microRNA	Inhibited	-6.536	4.35E-04
bexarotene	chemical drug		-0.653	4.35E-04
TGM2	enzyme	Activated	2.988	4.87E-04
miR-664-3p (and other miRNAs w/seed AUUCAUU)	mature microRNA	Inhibited	-4.587	6.75E-04
miR-4679 (miRNAs w/seed CUGUGAU)	mature microRNA	Inhibited	-5.88	7.20E-04
IFNA2	cytokine	Activated	3.032	1.48E-03
miR-4704-5p (miRNAs w/seed ACACUAG)	mature microRNA	Inhibited	-5.089	1.66E-03
miR-4501 (and other miRNAs w/seed AUGUGAC)	mature microRNA	Inhibited	-5.632	1.74E-03
15-LOX	group			1.86E-03
miR-4733-5p (miRNAs w/seed AUCCCAA)	mature microRNA	Inhibited	-5.97	1.91E-03
PAX8	transcription regulator	Activated	2.164	2.12E-03
NCAM1	other		1.067	2.45E-03
HOXB9	transcription regulator			3.22E-03
FADD	other	Activated	2.121	3.39E-03
IFNB1	cytokine	Activated	2.374	3.68E-03
miR-654-3p (and other miRNAs w/seed AUGUCUG)	mature microRNA	Inhibited	-5.384	3.70E-03
miR-1193 (miRNAs w/seed GGAUGGU)	mature microRNA	Inhibited	-5.897	4.00E-03
miR-640 (miRNAs w/seed UGAUCCA)	mature microRNA	Inhibited	-5.402	4.10E-03
KRAS	enzyme		0.544	4.57E-03
miR-582-3p (miRNAs w/seed AACUGGU)	mature microRNA	Inhibited	-5.862	4.65E-03
miR-4717-3p (miRNAs w/seed CACAUGG)	mature microRNA	Inhibited	-6.536	4.35E-04

Appendix Table 42: Upstream Regulator Analysis by IPA of Sk-Mel-28 tumor treated with EBC-46 (versus 20% PG) at 8 hr

Upstream Regulator	Molecule Type	Predicted Activation State	Activation z-score	p-value of overlap
spermidine	chemical - endogenous mammalian		1	3.35E-05
Gsk3	group		0.579	7.44E-05
miR-4277 (miRNAs w/seed CAGUUCU)	mature microRNA	Inhibited	-5.874	7.79E-05
ETS1	transcription regulator	Activated	2.598	1.05E-04
TNFSF14	cytokine		1.077	1.16E-04
CSF1	cytokine	Activated	3.236	1.63E-04
HDAC3	transcription regulator			2.03E-04
palmitic acid	chemical - endogenous mammalian		1.674	2.97E-04
green tea polyphenol	chemical drug		0.625	3.51E-04
miR-3651 (miRNAs w/seed AUAGCCC)	mature microRNA	Inhibited	-5.392	4.01E-04
GSK3B	kinase		-1.485	4.22E-04
11,12-epoxyeicosatrienoic acid	chemical - endogenous mammalian		0.2	5.19E-04
PDGF BB	complex	Activated	3.588	5.67E-04
PRKAR2B	kinase		-0.577	5.89E-04
prostaglandin E2	chemical - endogenous mammalian		0.965	6.21E-04
bezafibrate	chemical drug		1.601	6.29E-04
exenatide	biologic drug			6.62E-04
miR-1267 (miRNAs w/seed CUGUUGA)	mature microRNA	Inhibited	-5.018	7.14E-04
genistein	chemical drug		-0.011	7.47E-04
elastase	group			7.90E-04
spermidine	chemical - endogenous mammalian		1	3.35E-05

Appendix Table 43: Upstream Regulator Analysis by IPA of Sk-Mel-28 tumor treated with TPA (versus 20% PG) at 4 hr

Upstream Regulator	Molecule Type	Predicted Activation State	Activation z-score	p-value of overlap
BSCL2	other			2.46E-05
DAZ2	translation regulator			3.21E-04
EIF2S1	translation regulator			3.71E-04
glucosamine	chemical - endogenous mammalian		-1	5.73E-04
Immunoglobulin	complex		0.053	1.01E-03
IL5	cytokine	Activated	2.938	1.06E-03
miR-3688-3p (and other miRNAs w/seed AUGGAAA)	mature microRNA	Inhibited	-3.552	1.17E-03
1L-6-hydroxymethyl-chiro-inositol 2-(R)-2-O-methyl-3-O-octadecylcarbonate	chemical - kinase inhibitor			2.18E-03
estradiol valerate	chemical drug			2.18E-03
RLN1	other			2.18E-03
CEBPB	transcription regulator		1.937	2.67E-03
miR-3925-3p (miRNAs w/seed CUCCAGU)	mature microRNA	Inhibited	-3.921	2.74E-03
IL1B	cytokine	Activated	2.75	2.86E-03
OSMR	transmembrane receptor			2.89E-03
SU6656	chemical toxicant			3.32E-03
beta-estradiol	chemical - endogenous mammalian		0.606	4.91E-03
IRAK4	kinase			5.22E-03
NPPC	other			5.56E-03
ST3-Hel2A-2	chemical reagent			5.56E-03
dexmedetomidine	chemical drug			5.56E-03
BSCL2	other			2.46E-05

Appendix Table 44: Upstream Regulator Analysis by IPA of Sk-Mel-28 tumor treated with TPA (versus 20% PG) at 8 hr

Upstream Regulator	Molecule Type	Predicted Activation State	Activation z-score	p-value of overlap
miR-4709-5p (miRNAs w/seed CAACAGU)	mature microRNA	Inhibited	-6.574	6.74E-05
miR-516a-3p (and other miRNAs w/seed GCUUCCU)	mature microRNA	Inhibited	-7.648	4.62E-04
miR-421-3p (and other miRNAs w/seed UCAACAG)	mature microRNA	Inhibited	-7.973	6.13E-04
miR-4519 (miRNAs w/seed AGCAGUG)	mature microRNA	Inhibited	-6.915	7.54E-04
sildenafil	chemical drug		-1.237	8.14E-04
miR-4293 (miRNAs w/seed AGCCUGA)	mature microRNA	Inhibited	-6.998	8.49E-04
galactose	chemical - endogenous mammalian		1.067	1.09E-03
TWIST1	transcription regulator		0.896	1.69E-03
GnRH analog	biologic drug		0.977	1.70E-03
KRAS	enzyme		-0.273	1.98E-03
miR-1294 (miRNAs w/seed GUGAGGU)	mature microRNA	Inhibited	-6.785	2.28E-03
naproxen	chemical drug			2.33E-03
ANGPTL3	growth factor			2.58E-03
CRYAA	other			2.58E-03
dicumarol	chemical drug			2.58E-03
bumetanide	chemical drug			2.58E-03
acacetin	chemical - endogenous non-mammalian			2.58E-03
miR-5095 (and other miRNAs w/seed UACAGGC)	mature microRNA	Inhibited	-8.937	2.74E-03
miR-1976 (and other miRNAs w/seed CUCCUGC)	mature microRNA	Inhibited	-9.334	2.75E-03
miR-4755-3p (miRNAs w/seed GCCAGGC)	mature microRNA	Inhibited	-11.433	2.76E-03
miR-4709-5p (miRNAs w/seed CAACAGU)	mature microRNA	Inhibited	-6.574	6.74E-05